University of Southampton

Delineating the apoptotic mechanisms of an anti-CD19 immunotoxin used in combination with the anti-CD20 antibody rituximab against human B-lymphoma cells

Christine Jane Bryson

Doctor of Philosophy

Simon Flavell Leukaemia Research Unit

Division of Cancer Sciences

Faculty of Medicine, Health and Life Sciences

May 2004

UNIVERSITY OF SOUTHAMPTON

ABSTRACT

FACULTY OF MEDICINE, HEALTH AND LIFE SCIENCES
CANCER SCIENCES DIVISION

Doctor of Philosophy

DELINEATING THE APOPTOTIC MECHANISMS OF AN ANTI-CD19 IMMUNOTOXIN USED IN COMBINATION WITH THE ANTI-CD20 ANTIBODY RITUXIMAB AGAINST HUMAN B-LYMPHOMA CELLS

By Christine Jane Bryson

Anti-CD20 antibodies such as rituximab, have demonstrated anti-proliferative effects in vitro and therapeutic activity in B cell lymphoma patients. The anti-CD19 immunotoxin BU12-saporin has also been shown to have protein synthesis inhibition and anti-proliferative effects. In SCID-Ramos mice models, the combination of rituximab and BU12-saporin significantly increased long term disease free survival. This provides the rationale for further investigation to determine the pathways of protein synthesis inhibition and apoptosis involved, for possible future therapeutic use.

The aim was to determine the effect of rituximab and BU12-saporin individually and in combination on B lymphoma cell lines and determine the contribution of complement mediated mechanisms. In an in vitro protein synthesis inhibition assay, using Burkitt's lymphoma cells, the presence of rituximab caused a complement independent 5-fold additive decrease to the IC_{50} value of BU12-saporin. Two corroborative apoptosis assays confirmed that the functional effect of BU12-saporin and rituximab in combination was the induction of apoptosis. Statistical analysis showed exposure to rituximab and BU12-saporin in combination caused a significant additive, complement-independent increase to the sub G_0/G_1 population. Annexin V/PI staining of Ramos cells treated with rituximab and BU12-saporin showed significant additive complement independent increases to the early apoptotic and secondary necrotic cells, and significantly decreased the viable cell population.

This project also aimed to examine these events at the molecular level, including PARP cleavage, caspase activation, the effect of caspase inhibitors, the role of selected Bcl-2 family proteins and to determine the effectiveness of the combination against cells over expressing Bcl-2. Cleavage of the caspase substrate PARP was detected by western blot of Ramos cells exposed to rituximab and BU12-saporin. Caspase 3 and caspase 9 cleavage was detected but no caspase 8 cleavage was detected, except in late apoptotic cells. Addition of the peptide caspase inhibitor zVAD significantly reduced the number of apoptotic cells, and PARP and caspase 3 cleavage. Blocking TRAIL or FAS receptors did not reduce the level of PARP cleavage or caspase 3 cleavage. This suggested the mitochondrial rather than the death receptor pathway was involved in the induction of apoptosis by rituximab and BU12-saporin. No changes in the expression levels of selected Bcl-2 family proteins (Mcl-1, Bax, Bak, Bcl-2 or Bcl-X_L) were detected in response to the combination of rituximab and BU12-saporin. Over-expression of Bcl-X_L, but not Bcl-2, significantly protected Ramos cells from rituximab and BU12-saporin induced apoptosis by annexin V/PI staining, also no PARP or caspase 3 cleavage was detected in cells over expressing Bcl- X_L. These studies demonstrated that rituximab and BU12-saporin induced apoptosis in an additive and possibly synergistic manner, independent of complement, which involved caspases 3 and 9 and was not inhibited by Bcl-2 over-expression.

Contents

List of Figures

Chapter 1

Chapter 3

List of Tables

Chapter 1

Chapter 3

Chapter 4

Chapter 5

Chapter 6

Abbreviations

ADCC	Antibody dependent cell mediated cytotoxicity
AIF	Apoptosis inducing factor
APAF 1	Apoptosis protease activating factor 1
ATP	Adenosine triphosphate
BAPTA	1,2-bis(2-aminophenoxy)ethane N,N,N',N'-tetraacetic acid
CD	Cluster of differentiation
CDC	Complement dependent cytotoxicity
CDCC	Complement dependent cell mediated cytotoxicity
CHOP	Cyclophosphamide, doxorubicin, vincristine, prednisolone
CLL	Chronic lymphocytic leukaemia
CVP	Cyclophosphamide, vincristine, prednisolone
DAF	Decay accelerating factor
DED	Death effector domain
DEVD	Caspase 3 inhibitor, Asp-Glu-Val-Asp fluoromethylketone
DISC	Death inducing signal complex
DNA	Deoxyribose nucleic acid
DT	Diphtheria toxin
EF2	Elongation factor 2
EGTA	Ethylene glycol-bis(β-aminoethyl ether)
EGFR	Epidermal growth factor receptor
FADD	FAS associated protein with death domain
FAS	CD95/Apo-1
FCS	Foetal calf serum
FITC	Fluorescein isothiocyanate
FLICE	FADD like caspase (caspase 8)
FLIP	FLICE-inhibitory protein
GM-CSF	Granulocyte-macrophage colony stimulating factor
GPI	Glycophospatidyl insoitol
HI FCS	Heat inactivated foetal calf serum

HSP	Heat shock protein
IAP	Inhibitor of apoptosis protein
IC_{50}	Inhibition concentration (at which 50% inhibition is achieved)
IKB	Inhibitor of NK κB
IKK	Inhibitor of NK κB kinase
IL	Interleukin
ITAM	Immunoreceptor tyrosine based activation motif
I.V	Intra venous
JAK	Janus associated kinase
MAC	Membrane attack complex
MAPK	Mitogen activated protein kinase
MCP	Membrane co-factor protein (CD46)
MDR	Multi drug resistant
MHC	Major histocompatibility complex
NF-κB	Nuclear factor κB
NHL	Non Hodgkin's lymphoma
PAP	Pokeweed antiviral protein
PARP	Poly ADP-ribose polymerase
PCR	Polymerase chain reaction
PE	Pseudomonas exotoxin
PI	Propidium iodide
PI_3K	Phosphatidyl inositol 3 kinase
PSI	Protein synthesis inhibition
PTPC	permeability transition pore complex
RAIDD	Receptor interacting protein associated protein with death domain
RIP	Ribosome inactivating protein
RNA	Ribose nucleic acid
ROS	Reactive oxygen species
SAPK	Stress activated protein kinases
SCID	Severe combined immuno deficiency
SM-ase	Sphingomyelinase
STAT	Signal transducer and activator of transcription
TNF	Tumour necrosis factor
TRADD	TNF-1 receptor associated death domain

TRAIL	Tumour necrosis factor related apoptosis inducing ligand
VDAC	Voltage dependent anion channel
XIAP	X-linked inhibitor of apoptosis protein
zVAD	Pan-caspase inhibitor, benzyloxycarbonyl-Val-Ala-Asp-fluoromethylketone.

Acknowledgments

I would like to thank my supervisors David Flavell and Graham Packham.

Special thanks go to Bee Flavell and the staff of the Simon Flavell Leukaemia Research Unit, Amorel Noss, Sarah Field and Tony Carr.

This work was undertaken with the financial support of Leukaemia Busters.

Thanks also go to Exodus, Zoë Clitter and 6th Southampton South Guides and my parents for everything in between.

Chapter One

Introduction

1.1 Lymphoma

Cancers of the lymphatic system are described as lymphomas. Whereas leukaemias proliferate as single cells, lymphomas develop as solid tumours within a lymphoid tissue such as bone marrow, the thymus (both central lymphoid tissues) or the lymph nodes (peripheral lymphoid tissue, also including blood and spleen). As with all cancers the fine balance between cellular proliferation and death is disturbed, lymphomas involve the activation of proto-oncogenes and the disruption of tumour suppressor genes. Most lymphoid malignancies are derived from B lymphocytes at various stages of differentiation.

Lymphomas are broadly categorised as either Hodgkin's disease or non Hodgkin's lymphoma (NHL), although many similar but separate sub types of disease exist. Hodgkin's disease is diagnosed by the presence of characteristic Reed-Sternberg cells (large binucleate cells with prominent nucleoli). There are four subtypes of the disease and in total 1,400 new cases are diagnosed in the UK each year. (Statistics from the Lymphoma Association see references.) Hodgkin's disease can be successfully treated with radiotherapy and most cases are completely cured.

Around 8,000 new cases of non Hodgkin's lymphoma are report each year in Britain, accounting for approximately 2.4% of all new cancers registered per year (Evans and Hancock 2003). The disease is most common in North America and Western Europe, prevalence increases each year, rises with age and is 50% more comment in men than women (Chiu and Weisenburger 2003). There are many different sub types of non Hodgkin's lymphoma with different prognoses. Non Hodgkin's lymphoma cells are classified as high or low grade, depending on the frequency of cellular division, and named according to the appearance of cells. Non Hodgkin's lymphoma represents 2.6% of all cancer deaths (Evans and Hancock 2003).

The main mechanism of proto-oncogene activation in lymphoma is by chromosome translocation. Specific chromosome translocations are characteristic of sub types of nonn Hodgkin's lymphoma, the typical result is deregulated expression of a proto-oncogene. One exception is the translocation implicated in mucosa associated lymphoma tissue lymphoma (MALT) the t(11;18) translocation result in a gene fusion producing a chimeric protein (Chaganti *et al.*, 2000). The (t14;18) translocation implicated in 80 to 90% of follicular lymphomas results in the anti apoptotic Bcl-2 gene at chromosome band 18q21 translocated to the heavy chain region of the immuoglobin locus within chromosome band 14q32, leading to over expression of Bcl-2 and resistance to apoptosis (Sanchez-Beato *et al.*, 2002).

Lymphoma	**Translocation**	**Cases Affected**	**Proto-oncogene involved**	**Proto-oncogene function**
Follicular lymphoma	t(14;18)	80-90%	*Bcl2*	Negative regulation of apoptosis
	t(2;18)			
	t(18;22)			
Mantle cell lymphoma	t(11;14)	70%	*Bcl1*/ cyclin D1	G1/S cell cycle transition
MALT lymphoma	t(11;18)	50%	*AP12/MLT*	Anti-apoptotic? Gene fusion, chimeric protein formed.
	t(1;14)	Rare	*Bcl10*	Apoptosis inhibition via NF-κB
Diffuse large B-cell lymphoma	der(3)(q27)	35%	*Bcl6*	Transcription repressor; B-cell activation, cell cycle, apoptosis control, inflammation.
Burkitt's lymphoma	t(8;14)	80%	*c-myc*	Transcription factor regulating differentiation, metabolism, cell cycle and apoptosis control.
	t(2;8)	15%		
	t(8;22)	5%		

Table 1.1
Chromosome translocations in non Hodgkin's lymphoma. (Table adapted from Evans and Hancock 2003 and Sanchez-Beato *et al.*, 2002)

Burkitt's lymphoma is an uncommon but aggressive form of non Hodgkin's lymphoma, which is often associated with the cells infiltrating other organs such as the bowel or the meninges of the brain. With intensive and complex chemotherapy regimes long term survival is achieved in about 50% of cases. In the majority of Burkitt's lymphoma cases (approximately 75%), a chromosomal translocation of the c-myc region from chromosome 8 to the Ig heavy chain gene cluster on chromosome 14 is observed (Sanchez-Beato *et al.*, 2002). In the remaining cases c-myc is translocated to a position near the κ or λ light chain genes. c-Myc is a proto-oncogene encoding a transcription factor essential for mitosis.

This translocation may result in lymphoma as a consequence of constitutive over expression of c-myc due to the high activity of these regions (Chaganti *et al.*, 2000).

The most common low grade or indolent non Hodgkin's lymphomas are the follicular lymphomas, defined as a neoplasm of follicle centred B-cells (Reiser and Diehl 2002). Follicular lymphoma is slow growing and causes few early symptoms, first symptoms include enlarged lymph nodes, fevers, night sweats, and weight loss. Due to the slow growth of the disease and few symptoms, a high percentage of patients (80-85%) present with widespread, advanced disease (Chiu and Weisenburger 2003). The course of the disease usually follows several cycles of relapse and remission. Poor prognostic factors include, three or more extranodal disease sites (e.g. skin or gastrointestinal tract), aged over 60, disseminated disease, abdominal mass (>10cm), bone marrow involvement, transformation from low-grade or a previous poor response to treatment (Evans and Hancock 2003).

Treatments for non Hodgkin's lymphoma in routine use include radiotherapy, single agent and combination chemotherapy, purine analogues (e.g. fludarabine), biological or cytokine therapy (e.g. interferon), steroids, antibody therapy (e.g. rituximab) (Antibody therapy is discussed in detail in section 1.3.) Treatments in clinical trials include high dose therapy and stem cell transplantation, immuotoxins, anti-sense therapy, DNA vaccination, radiolabelled antibodies (e.g. tositumomab) and other antibodies (Evans and Hancock 2003). Some patients with advanced low grade follicular lymphoma with a low to moderate tumour burden are treated with a 'watch and wait' policy. Cytotoxic treatment is postponed until the disease progresses, trials have shown no difference in overall survival between patients treated aggressively and patients treated with watch and wait (Reiser and Diehl 2002).

First line treatment varies between centres, although alkylating agents are commonly used, most frequently chlorambucil or cyclophosphamide, side effects are few but include mild nausea or indigestion and depressed white blood cell count (Evans and Hancock 2003). Also combination chemotherapy can be used as a first line therapy, CVP (cyclophosphamide, vincristine, prednisolone) is used although there are more side effects. The response rate to first line treatment is 70% to 90% of people achieve remission for two to three years (Reiser and Diehl 2002).

If a prolonged remission was achieved in response to chlorambucil, often this course of treatment will be repeated for second line and subsequent treatments. Combination chemotherapy regimes are also commonly used, CHOP (cyclophosphamide, doxorubicin, vincristine, prednisolone). Purine analogues such as fludarabine and cladribine may also be used, given by IV injection side effects of these drugs include reduced platelet and white blood cell count. Remission rates of 70% to 80% are achieved in previously untreated lymphoma or 50% as a second line therapy (Reiser and Diehl 2002). Clinical trails combining purine analogues with anthracyclines (mitoxantrone) or alkylating agents (cyclophosphamide) improved event free survival but no evidence for improved overall survival has been shown.

Recombinant interferon has demonstrated activity against follicular lymphoma. The main side effect is mild to severe flu-like symptoms. Interferon may be combined with first line therapy or used as a maintenance therapy. Clinical trials with interferon combined with single alkylating agent chemotherapy showed no improvement, although in combination with an anthracycline regimen benefits were obtained (Reiser and Diehl 2002). Administration of interferon as a long term maintenance therapy in four out of five clinical trials found enhanced disease free survival in patients achieving a complete response to first line therapy (Reiser and Diehl 2002).

As all of the treatments are approximately equally effective, choice depends on previous responses to therapy, side effects and toxicity, convenience (number of hospital visits required) and the speed of response required (i.e. for severe symptoms, major organ involvement). In these cases a combination chemotherapy regime is usually appropriate as the response is fairly rapid. For follicular lymphoma, survival data has not improved for the last three decades. Clinical trials such as high dose chemotherapy and stem cell support, or purine analogues in combination with anthracyclines or alkylating drugs have shown increases in event free survival but no effect on long term overall survival. Current clinical trials focus on combinations of therapy, such as interferon and high dose chemotherapy.

1.2 Apoptosis

Apoptosis plays a physiological role during development, but also plays an essential role in the normal turnover of cells. A variety of pathological conditions result when changes to the rate of cell proliferation or death occur. During necrosis the cellular organelles swell, plasma membranes rupture and the cell contents leak out resulting in inflammation. A critical difference between apoptosis and necrosis is that apoptosis is energy dependent and may involve the synthesis of new proteins, whereas a necrotic cell suffers protein synthesis inhibition and energy supply failure. The pathways of apoptosis can be broadly spilt into several stages; an induction signalling event (of intracellular or extracellular origin), intracellular processing of this signal, activation of the cellular death effector mechanisms, which then cause the characteristic processes of programmed cell death. The morphological characteristics of apoptosis include, flipping of membrane phospholipids, chromatin condensation and DNA cleavage, cell shrinkage, membrane blebbing and the formation of apoptotic bodies for phagocytosis.

Signals from the extracellular environment are received via cell surface receptors. This type of signal can include specific death signals, or growth and survival signals (or lack of signals) from the extracellular environment. For example extracellular signals may include, UV radiation and oxidation damage or molecules such as, integrins, growth factors, cytokines (FAS, TNF-α), G-protein coupled receptors, toxins or small molecule anti-cancer drugs. Transduction and modulation of these death activator signals is then required. This may take the form of transcription factors, kinases, phosphatases or secondary messengers such as cAMP or changes to the intracellular calcium levels (Darzynkiewicz *et al.,* 1997). Intracellular signals may serve to activate or inhibit apoptosis. In a variety of cell types members of a family of proto-oncogenes have been shown to regulate apoptosis by inhibitory and activation effects. Through this wide variety of signalling mechanisms the main death effectors of the apoptotic response, are recruited and activated.

1.2.1 The extrinsic or death receptor pathway

The extrinsic pathway or the death receptor pathway of the induction of apoptosis is initiated by a ligand binding to a death receptor. Death receptors are characterised by an extracellular cysteine rich domain and an intracellular death domain. Binding of the ligand to the receptor results in trimerisation of the receptor and clustering of the receptors intracellular death domains, leading to the formation of the death inducing signal complex (DISC). Trimerisation of death domains leads to the recruitment of adaptor proteins, e.g. FADD or RAIDD, and subsequent binding and activation of caspase 8 and 10.

FAS (CD95/Apo-1) is a member of the TNF receptor super family, binding of FAS ligand causes the trimerisation of FAS, which via the trimer of death domains recruits and binds the adaptor protein FAS associated protein with death domain (FADD) (Wang and El-Deiry 2003). Pro-capsase 8 is then recruited and bound via the death effector domains (DED) of FADD and procaspase 8. Formation of DISC results in activation of the caspase cascade or the activation of Bid (discussed in the more detail section 1.2.2) leading to apoptosis. Caspase 8 shares homology with the caspase family and also contains a death domain to interact directly with FADD. At several stages FAS induced apoptosis can be blocked by FLICE-inhibitory protein (FLIP), by Bcl-2 (discussed in the more detail section 1.2.3) or the cytokine response modifier A (Crm A) (Dempsey *et al.*, 2003).

Another example of death receptor mediated induction of apoptosis is the TNF signalling pathway. On ligand binding the receptor trimerises and recruits the adaptor proteins TRADD, RIP and RAIDD and FADD (Wang and El-Deiry 2003). Activation of caspase 2 follows, which mediates the activation of downstream effector caspases and the induction of apoptosis. The TNF receptor can also modulate a survival signal, and is involved in regulation of growth signalling. NF-κB (nuclear factor-κB) is a collective name for inducible dimeric transcription factor composed for members of the Rel family of DNA binding proteins (Karin and Ben-Neriah 2000).

NF-κB is involved in the regulation of a large number of genes in response to stress such as infection or inflammation. NF-κB is sequestered to the cytoplasm by members of a family of inhibitor proteins, IκBs, which on binding NF-κB mask the nuclear localisation signal (Dempsey *et al.*, 2003). NF- κB is released via the phosphorylation, ubiquitination

and proteolytic degradation of IκB in response to a variety of extracellular stimuli including pro-inflammatory cytokines such as TNK-α and interleukin 1 (Karin and Ben-Neriah 2000). In the survival pathway mediated by TNF receptor, rapid serine phosphorylation mediated by the IKK kinases causes IκB phosphorylated at ser-32 and ser-36, to release NF-κB which translocates to the nucleus binds where it binds κB promoter regions and initiates transcription of cell survival and anti apoptotic proteins (Karin and Ben-Neriah 2000).

1.2.2 The intrinsic or mitochondrial pathway

DNA damage by UV radiation, oxidation damage, cytotoxic drugs, neurotoxins or activation of tumour suppressors (p53) and oncogenes result in apoptosis induced via the intrinsic pathway. The intrinsic pathway of apoptosis is induced by increased mitochondrial membrane permeabilisation resulting in a reduction of mitochondrial transmembrane potential. The outer membrane becomes permeable to proteins and releases soluble inter membrane proteins, including cytochrome c, apoptosis inducing factor (AIF) and Smac/diablo (second mitochondrial derived activator of caspase; direct IAP (inhibitor of apoptosis protein) binding protein with low pI). Smac/diablo released from the mitochondria blocks the IAPs, which normally interact with caspase 9 to inhibit apoptosis. Once in the cytosol these proteins activate caspases or caspase independent mechanisms of apoptosis. AIF activates a DNase, endonuclease G, has been shown to have a role in caspase independent apoptosis. Endonuclease G is regulated by heat shock proteins 70 (HSP70), also known to inhibit the apoptosome (see below).

Cytochrome C released from the mitochondria complexes with apoptosis protease activating factor 1 (Apaf 1) in the presence of dATP to form the apoptosome. Activated Apaf-1 binds pro-caspase 9 which is proteolytically activated, which in turn cleaves caspase 3 and caspase 6, resulting in the caspase cascade. Apaf 1 recruits pro-caspase 9 via the caspase recruitment domain (CARD). The activated apoptosome is a stable complex, which remains intact during apoptosis and shows high levels of enzymatic activity. Currently the only known function of the apoptosome is the activation of pro-caspase 9, the exact structure of the apoptosome also remains to be determined. Molecular weights have been reported between 700-1400kDa. The apoptotic inhibitors Bcl-2 and Bcl-X_L inhibit apoptosis by preventing the release of cytochrome C from the

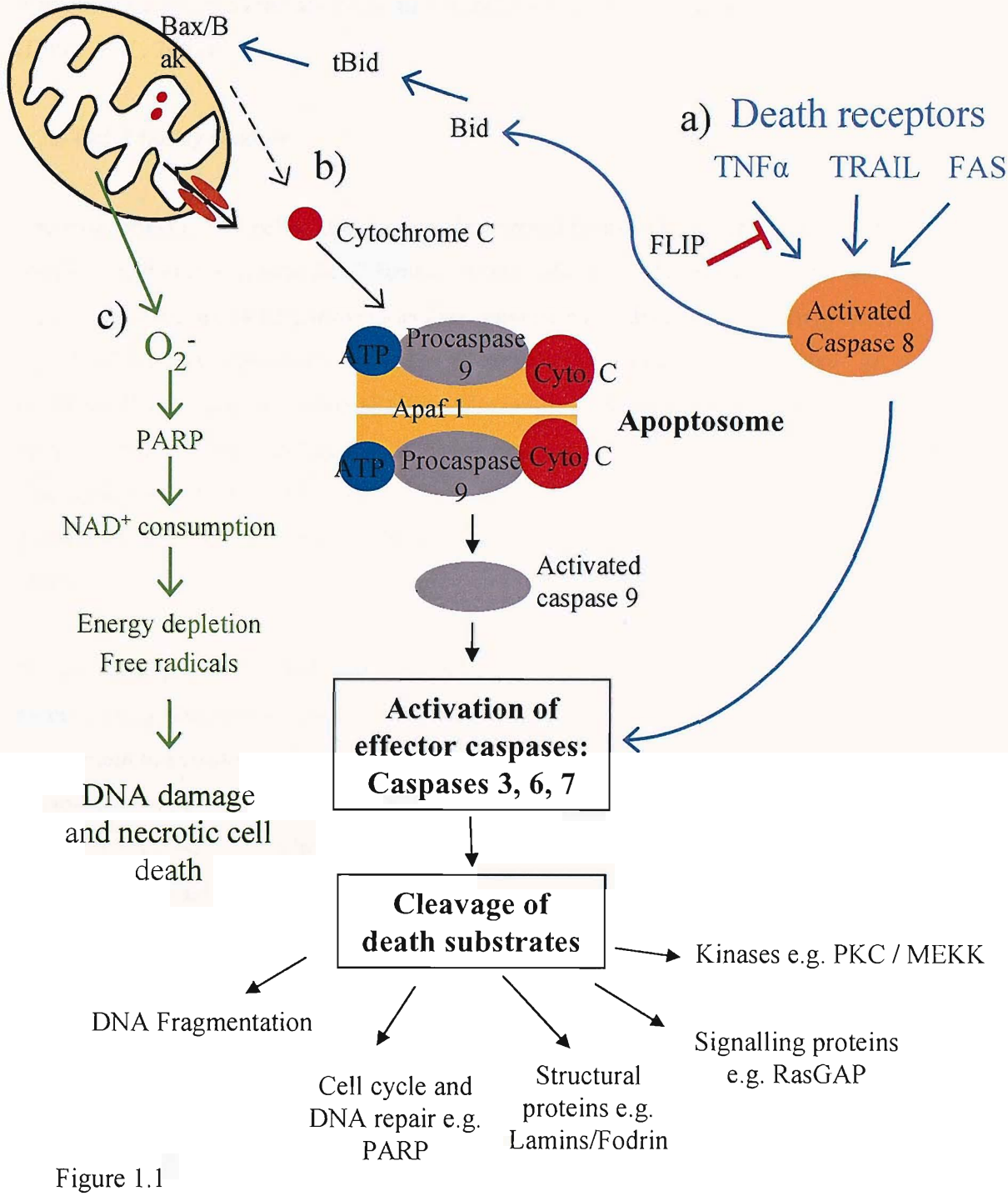

Figure 1.1
Overview of selected signalling pathways involved in the induction of apoptosis and necrosis. Pathway a) represents the death receptor pathway, caspase 8 is activated in response to receptors with a death domain leading to downstream effector caspase activation. Cleavage of Bid results in positive feedback to the mitochondrial pathway. Pathway b) represents the mitochondrial stress pathway, the release of cytochrome c results in the formation of the apoptosome and downstream caspase activation. Pathway c) represents necrotic death due to high levels of oxidative stress leading to PARP activation, activated PARP leads to structural DNA changes resulting in the consumption of NAD^+, leading to ATP depletion and necrotic cell death.

mitochondria, whereas the apoptotic promoter Bax triggers the release of cytochrome C (Dales *et al.*, 2001).

1.2.3 Bcl-2 family proteins

The susceptibility of a cell to apoptosis is determined by the relative abundance of pro-apoptotic and anti-apoptotic Bcl-2 family proteins. Bcl-2 family proteins are central regulators of the apoptotic pathways as they regulate many diverse survival and death signals. Bcl-2 family proteins are characterised by the presence of one or more of the 4 identified Bcl-2 homology domains (BH). The family is divided into two classes, anti-apoptotic members such as Bcl-2 and Bcl-X_L, and pro-apoptotic members such as Bax and Bak, and a large group of BH3 only death proteins. Since the discovery of Bcl-2 over 20 pro and anti apoptotic members of the Bcl-2 family have been identified (Baliga *et al.*, 2002).

Pro-apoptotic proteins include Bax, Bad, Bid, and Bak. Some pro-apoptotic Bcl-2 family members (e.g. Bax) translocate from the cytosol to the mitochondria, undergo a conformational change and insert into the mitochondrial membrane forming a multimer complex within the membrane which disrupts mitochondrial membrane permeability. As well as the release of cytochrome c, increased mitochondrial membrane permeability reduces mitochondrial transmembrane potential causing a decrease in ATP production and the generation of ROS.

Anti-apoptotic members of the Bcl-2 family of proteins include Bcl-2, Bcl-X_L and Mcl-1. Anti-apoptotic proteins protect the integrity of the mitochondria by preventing cytochrome c release and the formation of the apoptosome. Some anti-apoptotic members of the Bcl-2 family function by inhibiting the translocation and homodimerisation of the pro-apoptotic Bcl-2 family members. Bcl-2 forms a heterodimer with Bax, preventing Bax disrupting mitochondrial membrane permeability.

Bcl-2, a 26kDa protein localised to the ER and mitochondrial membrane, is an anti-apoptotic member of the family proposed to have a role in maintaining membrane potential and preventing the release of cytochrome C (Brenner *et al.*, 1999). Over expression of Bcl-2 has been linked to a variety of different malignancies including bowel,

breast, lung, and skin cancers (Baliga *et al.*, 2002). Expression of Bcl-2 confers a survival advantage by blocking apoptosis induced by a variety of signals at the mitochondrial level by maintaining the permeability transition pore in a closed position.

The pro-survival proteins Bcl-2, Mcl-1 and Bcl-X_L contain 3 or 4 BH domains, and are normally localised to the mitochondrial or nuclear membrane or the ER (Baliga *et al.*, 2002). These BH domains have no associated enzymatic activity, but mediate the interaction with other Bcl-2 family protein members. BH1–BH3 form a hydrophobic groove which is stabilised by BH4 by burying exposed hydrophobic residues. Heterodimers and homodimers of Bcl-2 family proteins form via binding of the hydrophobic groove, in general the ratio of pro and anti apoptotic members of the family available is thought to determine cell fate e.g Bak binding of the BH3 domain of Bcl-X_L is thought to be critical in regulating the anti apoptotic activity of Bcl-X_L.

Mcl-1 is widely expressed and is an essential survival molecule for B-cell lymphoma. Over expression of Mcl-1 promotes lymphomagenesis in the mouse although the role in human B-cell lymphoma is unclear (Zhou et al., 2001). Bcl-X_L and Mcl-1 are known to associate with the outer mitochondrial membrane and may help maintain the integrity of the mitochondrial membranes. Unlike Bcl-2 and Bcl-X_L, Mcl-1 is cleaved by caspases to a death promoting molecule during apoptosis (Michels *et al.*, 2004). Mcl-1 cleavage is likely to play an important role in the regulation of apoptosis, caspase mediated cleavage of Mcl-1 reduces the levels of the survival molecule, generates a cell killing protein and stimulates further caspase action via a positive feedback loop. This suggests Mcl-1 cleavage may have a role as a novel anti-cancer strategy. (Michels et al., 2004).

In cell free systems Bcl-2 must be associated with the mitochondria to prevent cytochrome c release (Kluck *et al.*, 1997). The main function of Bcl-2 family proteins is to directly regulate the mitochondrial membrane permeability and thus control the release of pro apoptotic factors from the inter-membrane space. These include, cytochrome C, heat shock protein 60, smac/diablo and HtrA2/Omi (involved in caspase activation by the inhibition of IAPs) (Tsujimoto 2003). Pro-apoptotic members of the Bcl-2 family contain BH3 death domains which are know to bind the BH3 binding pocket of Bcl-2 and Bcl-X_L to form heterodimers which block the survival promoting activity of Bcl-2 and Bcl-X_L.

BH3 only proteins (including Bid, Bim, Bmf and Bad) are normally localised to the cytosol or cytoskeleton but are translocated on the induction of apoptosis to the mitochondrial where they are able to bind to and regulate other Bcl-2 protein family members. When stimulated these BH3 only proteins are modified by various mechanisms, translocate to the mitochondria and result in increased mitochondrial membrane permeability. Bad is normally sequestered in the cytosol, on stimulation, Bad is dephosphorylated, released and translocates to the mitochondria. Bim and Bmf are normally bound to the micotubules and actin filaments of the cytoskeleton via dynein and myosin motor complexes (Tsujimoto 2003).

Bid is a BH3 only protein constitutively expressed in the cytoplasm, cleavage by caspase 8 or granzyme B forms truncated Bid (tBid). The conformation change of Bax and the insertion of Bax into the outer mitochondrial membrane is facilitated by tBid, promoting the induction of apoptosis (Tsujimoto 2003). tBid may exert it's effects by several mechanisms, including transiently binding Bax (Wei *et al.*, 2001), tBid may also inhibit an inhibitor of Bax multimer formation in the membrane itself (Roucou *et al.*, 2002), or by affecting the membrane directly (tBid is known to bind cardiolipin, Lutter *et al.*, 2000). Although the exact mechanism of action of tBid on Bax is unknown, tBid is also involved in caspase independent apoptosis, shown to release endonuclease G from the mitochondrial and implicated in FAS mediated apoptosis (Zimmerman *et al.*, 2001).

In vitro evidence has been shown to suggest Bcl-2 family proteins form channels in the phospholipid membrane which may be involved directly in the release of cytochrome C. Bcl-X_L has structural similarities to diphtheria toxin which is thought able to form ion or protein channels. This structure also resembles Bax, which differs by one helical region although has an opposing function (Suzuki *et al.*, 2000). Bid also shares a structural similarity although the BH3 region is the only region of sequence similarity. Channels are formed by these proteins (Bcl-X_L, Bax, and tBid) in synthetic lipid vesicles, with different properties possible accounting for their differing functional roles (Schlesinger *et al.*, 1997).

No evidence has been reported to show these channels are formed *in vivo*. It is unclear whether pores are actually formed by Bcl-X_L and other Bcl-2 family members or whether pores are formed by an interaction with the permeability transition pore complex (PTPC)

(Gottlieb 2000). An association between Bax and the voltage dependent anion channel of mitochondria (VDAC) has been shown, Bax and VDAC may be involved in the release of cytochrome c, as in liposomes a large pore is formed (Shimizu et al., 2000). Bcl-X_L has a functional role in closing the Bax /VDAC voltage dependent anion channel (Baliga *et al.*, 2002).

In the worm *C.elegans* regulation of caspase activity (CED 3) occurs via Bcl-2 family proteins (CED 9) binding to the homologue of Apaf-1 (CED 4) inhibiting the activation of initiator caspases. The direct regulation of caspase activation by Bcl-2 family proteins in mammalian apoptosis by Bcl-2 interacting directly with Apaf 1 has been reported by several groups (Hu *et al.*, 1998 and Pan *et al.*, 1998). Although conversely, Apaf-1 has been reported not to co-localise or immunoprecipitate with Bcl-2 or Bcl-X_L or bind other anti-apoptotic members of the Bcl-2 family (Hausmann *et al.*, 2000). This evidence suggests this form of regulation is unlikely in mammalian apoptosis, although does not rule out interaction with an as yet unidentified alternative CED-4 like adaptor protein.

Over expression of Bcl-2 is implicated in 85% of NHL cases by a gene rearrangement (the t(14;18) translocation), which also confers a resistance to FAS mediated apoptosis. The t(14;18) translocation in B-cell follicular lymphomas results in the constitutive over expression of Bcl-2, as the *bcl-2* gene is repositioned next to the constitutively expressed immunoglobin heavy chain gene promoting cell survival and inhibiting apoptosis. Remission following therapy can be followed at a molecular level by conversion to t(14;18) negativity, measured by PCR (Piro *et al.*, 1999).

Deregulation of Bcl-2 family protein expression is not only implicated in malignancies, but influences the cellular response to treatment as an inability to induce apoptosis contributes to resistance. High Bcl-2/Bax ratios indicate drug resistance in B-CLL cells (Pepper *et al.*, 1999). Novel strategies have been developed to combat Bcl-2 over expression and sensitise cells to apoptosis. These include the *bcl-2* antisense oligonucleotide G3139, which has been shown to be effective and have low toxicity in phase I clinical trials in non Hodgkin's lymphoma patients (Cotter *et al.*, 1999). Currently all trans retinoic acid is used in combination with anti-cancer drugs to down regulate Bcl-2 expression. Microtubule drugs targeting drugs such as paclitaxel are also used as one of

their down stream effects is the phosphorylation of Bcl-2 which inhibits it's anti apoptotic effects (Wang *et al.*, 1999).

1.2.4 Caspases

Protease inhibitors of different specificities have been shown to inhibit apoptosis suggesting the involvement of several classes of protease in apoptosis. Of particular interest are the caspases (cysteine aspartate proteases), calpains (calcium activated neutral proteases, activated by increased Ca^{2+} levels) and other proteases which are activated by proteolytic cleavage. Caspases are a family of cysteine aspartate proteases known to cleave and activate other members of the caspase family resulting in the proteolytic caspase cascade which activates specific enzymes and cleaves caspase substrates inducing apoptosis and cell death. Caspases cleave and inactivate proteins that protect cells from apoptosis Bcl-2, Bcl-X_L and ICAD (inhibitor of a nuclease responsible for DNA degradation) and also cleave structural proteins e.g. lamins and actin (Dales *et al.*, 2001). In mice, caspase defects result in partial inhibition of apoptosis, suggesting caspases play a non-redundant role as effectors of apoptosis (Dales *et al.*, 2001).

A hallmark in the induction of apoptosis is cleavage of the caspase substrate poly (ADP-ribose) polymerase (PARP), a nuclear repair enzyme involved in DNA repair and modification. Caspase 3 acts to cleave death substrates such as PARP (Mack *et al.*, 2000). Bcl-2 and Bcl-X_L and other proteins which promote survival, are cleaved by caspases (Dales *et al.*, 2001). IAPs (inhibitors of apoptotic proteins) inhibit mature active caspases. Members of the IAP family include XIAP (X-linked inhibitor of apoptosis protein), c-IAP-1, c-IAP-2 and survivin (Zimmerman *et al.*, 2001).

Inactive pro-enzyme forms of caspases are present in all nucleated cells (Mack *et al.*, 2000). Pro-enzymes contain an NH_2 terminal pro-domain, consisting of a large and a small subunit. Proteolytic cleavage (either by other proteases or autoprocessing) results in a mature caspase composed of two large and two small subunits (Dales *et al.*, 2001). Initiator caspases contain long pro-domains and effector caspases short pro-domains. Initiator caspases, such as caspases 2, 9, 8 and 10 are activated by a pro-apoptotic cleavage to initiate and convey an apoptotic signal. Effector caspases, such as caspases 3, 6, and 7

are downstream effectors which once activated by other caspases, cleave nuclear and cytoskeletal proteins inducing apoptosis (Gottlieb 2000).

Casapse 2 is involved in positive and negative regulation of apoptosis, two splice variants exist, a long form which induces apoptosis and a short form which inhibits apoptosis. Caspase 8, also an initiator caspase, is recruited via FADD to the CD95/FAS death inducing signal complex to play an important role in the induction of death receptor mediated apoptosis. Caspase 8 shares homology with the caspase family and also contains a death domain to interact directly with FADD. Caspase 8 activates downstream effector caspases such as pro-caspases 3, 6, and 7.

Caspase 3, often referred to as the central executioner caspase, plays a critical role in the induction of apoptosis. Caspase 3 is responsible for the cleavage of PARP and other substrates. Caspase 3 is activated by caspase 8, 6 and granzyme B. Caspase 3 activates pro-caspases 6 and 9. Caspase 7, an effector caspase which translocates to the mitochondria on activation is responsible for the morphological changes associated with apoptosis. Activation of caspases 3 and 7 can be blocked by IAP proteins. Caspase 10 has a role in embryonic development, it contains two death effector domains and can cleave pro-caspase3 (Gottlieb 2000).

cFLIP is a regulator of caspase activation, FLICE inhibitory protein binds to the DED of FADD inhibiting the recruitment and activation of caspase 8. At least 5 different IAPs inhibit apoptosis in cell culture, XIAP has the broadest and strongest activity, IAP1 and IAP2 are anti-apoptotic proteins that inhibit caspases 3, 7 and 9 (Zimmermann et al., 2001). All mammalian IAPs contain three conserved sequence motifs named BIR, except survivin which contains only one (Zimmermann et al., 2001). Serpin expressed in NK cells and cytoxic T cells, is an inhibitor of granzyme B, a serine protease capable of direct caspase activation which can also cleave some caspase substrates (Kitada *et al.,* 2002).

1.2.5 Alternative signalling pathways implicated in the induction of apoptosis

Hydrolysis of membrane sphingomyelin (localised to the outer plasma membrane leaflet), by three isoforms of a phopholipase C like enzyme sphinomyelinase (SMase), in response to stress, UV or ionising radiation produces ceramide, a secondary messenger. Ceramide

by the activation of downstream kinase pathways has been linked with the initiation of cellular differentiation, proliferation and the induction of apoptosis (via acid-SMase) (Kinloch *et al.,* 1999). An intracellular kinase implicated in mediating apoptosis and survival is phosphatidyl inositol-3-kinase (PI_3K). After binding an activated protein tyrosine receptor, the activated form of PI_3K, via phospholipase C, hydrolyses phosphatidylinositol 4,5 bisphosphate resulting in the production of diacyl glycerol, inositol triphosphate releasing the secondary messenger Ca^{2+} and activating protein kinase C.

Protein kinase B, Akt, is a growth factor regulated serine / threonine kinase which functions to promote cell survival via two distinct pathways. Activated Akt promotes survival by phosphorylation of pro-apoptotic kinases, caspases, Bcl-2 family members and transcription factors (Kinloch *et al.,* 1999). Phosphorylation of Bad prevents binding to Bcl-X_L, thus promoting the anti-apoptotic function of Bcl-X_L. Akt activates IKK leading to NF-κB activation also promoting cell survival (Kitada *et al.,* 2002).

Another cascade system involved in processing death signals (also implicated in triggering cell proliferation and differentiation) are the mitogen activated protein kinases (MAPK). MAP kinases are serine/ threonine kinases which require dual phosphorylation to respond to extracellular signals. One known activator is ceramide. The equilibrium between the SAPK (stress activated protein kinases) and MAPK cascades has been implicated in the induction of apoptosis (Kinloch *et al.,* 1999). The activation of death receptors is associated with the activation of JNK MAP kinase signalling, which has a role in regulating gene expression and the phosphorylation of a pro-and anti- apoptotic proteins.

1.2.6 Apoptosis and Cancer

Apoptosis has a role in controlling cell number in many developmental and physiological settings. Deregulation of apoptosis is linked to cancer as apoptosis is impaired in many human tumours. Resistance to apoptosis induced by chemotherapy also accounts for a high proportion of treatment failures. The therapeutic potential for specifically induced, controlled cell death is vast. Many studies have attempted to specifically induce apoptosis, examples of targets include Bcl-2 family proteins, intracellular protein inhibitors of apoptosis (e.g. IAPs) or the FAS or TRAIL receptors. Attempts have also been made to

indirectly induce apoptosis, via protein kinases / phosphatases, transcription factors, cell surface receptors or proteasome inhibition (Hu and Kavanagh 2003). Most of these approaches are still in pre-clinical developments due to problems such as resistance and low efficacy.

Alterations to p53 are the most common forms of human cancer. p53 functions as a transcription regulator regulating genes involved in DNA repair, cell cycle arrest and apoptosis. p53 is also known to have a role in several critical pathways of regulation of apoptosis e.g. the expression of Bax, and p53 can trigger expression of FAS receptor. Loss of p53 results in genomic instability, diminished cell cycle and impaired apoptosis. A new therapeutic designed to combat cancer derived from mutations in p53 is ONYX015. ONYX015 is an adenovirus selectively modified to lethally replicate in cells containing p53 mutations. ONYX015 carries a loss of function mutation and has no effect on normal cells, and is currently in several clinical trials (Cohen *et al.*, 2001).

Antisense approaches have been used to reduce the expression of a wide variety of anti-apoptotic genes (e.g. Bcl-2, G3139 previously discussed see section 1.2.3). Common problems are encountered in antisense therapy in specificity and ensuring delivery of DNA to every tumour cell *in vivo*. Inducers of apoptosis are commonly targetted in cancer therapy, the intrinsic and extrinsic pathway can be activated separately although the more successful strategies appear to target cell death machinery or protein kinases, transcription factors and proteasomes.

EGFR (epidermal growth factor receptor) is frequently over expressed in human cancers. Activation of EFGR tyrosine kinase is involved in proliferation, invasion, metastasis and angiogenesis. Gefitinab is a EGFR tyrosine kinase inhibitor that blocks signalling pathways responsible for proliferation invasion and survival of cancer cells. Gefitinab is currently being tested in phase I and II trials in solid tumour (Los *et al.*, 2003).

Monoclonal antibodies are increasingly being used to identify and target specific cellular populations by targeting characteristically expressed surface proteins. The CD (cluster of differentiation) antigens present on lymphocytes are ideal for this as they are highly specific and easily accessible. Once identified, these populations can be specifically targeted for death by conjugation of the antibody to small molecule drugs, toxins or

radionuclides. Genetic engineering can enhance specificity, reduce toxicity (humanised antibodies) and the half life of the antibody can be increased (White *et al.*, 2001), and thus improve therapeutic potential.

Trastuzumab (Herceptin) was approved for use in patients with metastatic breast cancer the USA in 1998. It is a genetically engineered anti-HER2 antibody that inhibits proliferation of HER2 over expressing cells *in vitro*. Over expression of HER2 is detected in 25 to 30% of patients and is associated with aggressive tumour growth. In a phase III randomised trial, patients treated with chemotherapy in combination with trastuzumab, compared to patients treated with chemotherapy alone showed significantly improved overall survival (45% compared to 29%), time to progression and duration of response and one year survival rate (von Mehren *et al.*, 2003). Side effects included chills, fever, nausea, and vomiting but were generally first-infusion related.

Recombinant forms of TNFα and FAS ligand are effective inducers of apoptosis, studies in animals have also shown TRAIL potentiates the effects of chemotherapy. TRAIL-R1 monoclonal antibody is specific for R1 on haematopoietic cancer cells. Preclinical experiments have shown TRAIL-R1 induces apoptosis in human breast, colon, and uterine cancers. Although TRAIL preferentially induces apoptosis in tumour cells apoptosis, potential problems include damage to normal cells as damage to normal hepatocytes has been reported (Jo *et al.*, 2000).

CD52 is a 21-28kDa cell surface GPI linked glycoprotein recognised by Campath antibodies. Although, the functions of CD52 are unknown, it is abundantly expressed on normal and malignant cells. Campath has been evaluated in trials against chronic lymphocytic leukaemia and non Hodgkin's lymphoma. Campath offers significant improvements over conventional chemotherapy, although overall response rates above 42% have not been reported and responses were short in duration (von Mehren *et al.*, 2003) suggesting Campath may be most effective in combinaiton and additional strategies are still required

Monoclonal antibodies have initially shown striking effects *in vitro*, although many potential problems have been encountered. These include the immunogenicity of foreign antibodies which limits the number of treatments a patient can safely receive. Limited

numbers of effectors cells may be present at the tumour site, or the tumour microenvironment may be immunosuppressive, many tumours secrete molecules to down regulate immune response (Holland and Zlotnik 1993). Antigen may shed into the circulation and any heterogeneity of antigen expression reduces the amount of antibody bound to the target (Jain and Baxter 1988). Antibody may not reach the tumour target due to disordered tumour vasculature and increased hydrostatic pressure (von Mehren *et al.*, 2003). Despite these issues, with continual improvements being made to antibody based therapies, pre-clinical and clinical data has shown a role for antibody based therapies in the treatment of cancer.

1.3 CD20 and Rituximab

CD20 is a 33-37 kDa phosphoprotein encoded by 8 exons on chromosome 1, expressed on 95% of normal and neoplastic B-cells until differentiation to IgM or IgD positive mature B-cells, but not stem cells (Grillo-Lopez *et al.,* 1999). Mice carrying a CD20 gene disruption do not show a specific phenotype nor were any major effects on the differentiation and function of B lymphocytes detected, (surface markers, antigen receptors signalling, proliferative responses or calcium uptake) (O'Keefe *et al.,* 1998). CD20 is a good target for immunotherapy as it does not shed, modulate or internalise on binding. CD20 also does not circulate as free antigen.

Based on the structural motif of four transmembrane regions with internal amino and carboxy termini (Shan *et al.,* 1998), a function as a membrane transporter, or as a Ca^{2+} channel involved in activation proliferation and differentiation of B-cells was proposed (Tedder *et al.,* 1994). In activated B-cells and B-cell lines, CD20 is heavily phosphorylated at cytoplasmic serine and threonine residues by protein kinase C, and calcium/calmodulin dependent protein kinase II, following mitogen stimulation of B-cells. CD20 signalling is associated with the activation of the src family kinases, lck, fyn suggesting an involvement for CD20 signalling in cell cycle regulation (figure 1.2) (Shan *et al.,* 2000).

Rituximab, (IDEC-C2B8, MabThera) a chimeric anti CD20 antibody containing human IgG1 Fc and κ constant regions and murine variable regions, induces remission of low-grade B-cell follicular lymphoma. Healthy B-cells are regenerated from stem cells within 9-12 months of therapy. Most normal and malignant cells are cleared following the first infusion of rituximab. The half life of a fourth infusion is 189.9 hours, whereas the first infusion has a half life of 68.1 hours, rituximab can be detected in patient sera between 3 to 6 months following treatment.

1.3.1 Clinical trials

B-cell depletion is observed with a 57% overall response rate, (statistics from rituximab prescribing information, Roche April 2001.) Although less than 40% of patients show a long term effect (Czuczman 1999b). A phase II study from the German Hodgkin

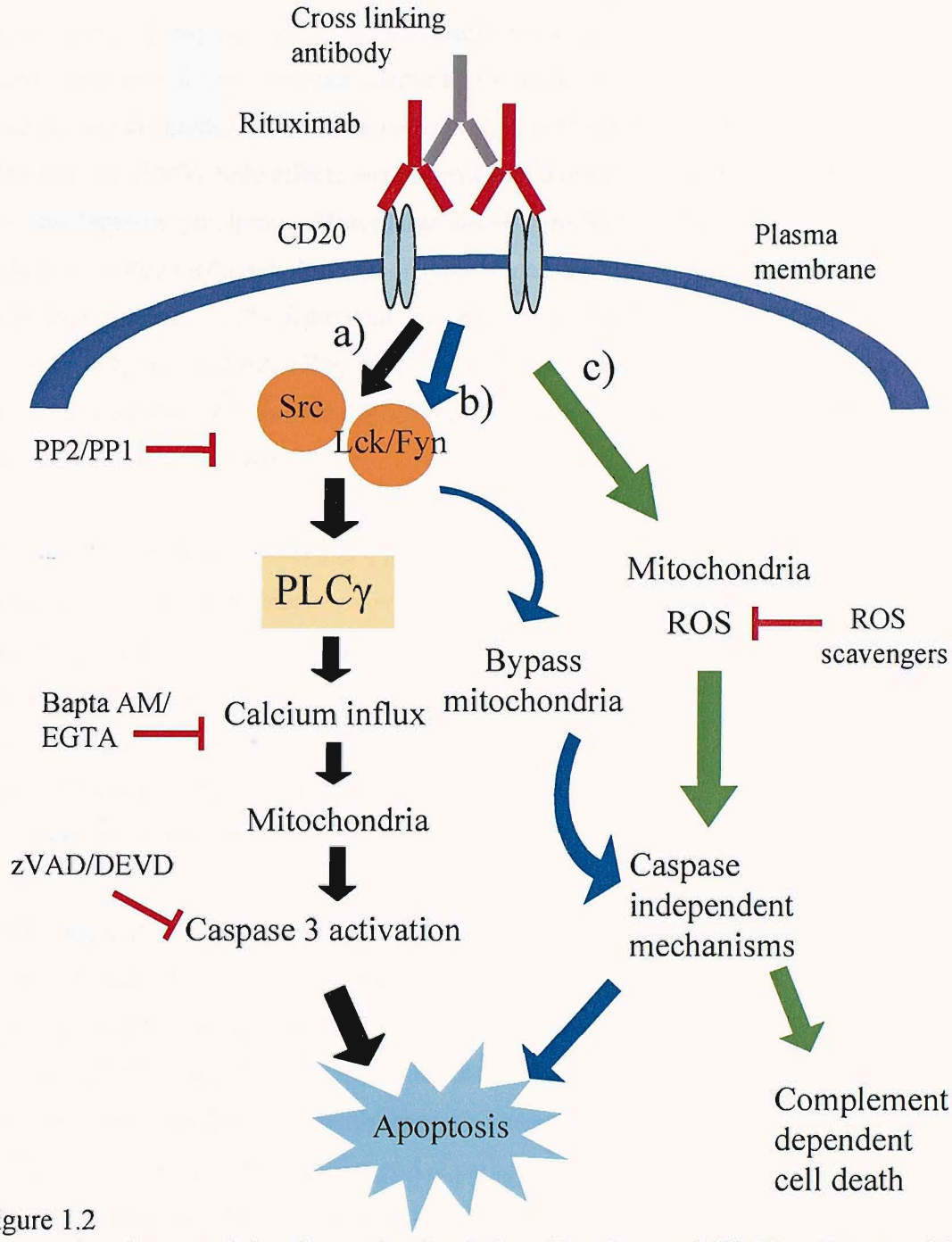

Figure 1.2

Proposed pathways of signal transduction induced by clustered CD20 antigen resulting in human Ramos B-cell apoptosis/cell death. a) Pathway denoted by black arrows: Clustering of bound CD20 by a secondary antibody results in src family protein tyrosine kinase activity, which is required for PLC-γ tyrosine phosphorylation, mobilization of intracellular calcium and caspase activation. Treatment with specific src family kinase inhibitors (PP1 or PP2), a calcium chelator (BAPTA) or caspase inhibitor (DEVD), prevented CD20 induced apoptosis (red arrows) (Hofmeister *et al* 2000). b) Pathway denoted by blue arrows: Clustering of bound CD20 by a secondary antibody results in src family protein tyrosine kinase activity although loss of mitochondrial membrane potential and caspase activation were not essential, (van der Kolk *et al* 2002, Chan *et al* 2003). c) Pathway denoted by green arrows: Clustering of bound CD20 resulted in no src family kinase activity, reactive oxygen species (ROS) were detected and could be inhibited by ROS scavengers, a complement dependent, caspase independent mechanism of cell death was described (Bellosillo *et al* 2001). Part of this figure was re-drawn from Hofmeister *et al* 2000.

lymphoma study group reported an 86% overall response rate in CD20 positive Hodgkin lymphoma patients at first or higher relapse to 4 weekly infusions of rituximab at 375mg/m^2 and the median duration of response had not been reached at 20+ months (Rehwald *et al.,* 2003). Side effects were transient and mild to moderate grade. In more aggressive types of lymphoma, diffuse large B-cell lymphoma (DLBCL), mantle cell lymphoma or other medium to high grade lymphomas, a phase II clinical trial showed an overall response rate of 31%. Rituximab was administered as 8 or 7 weekly infusions. The most commonly reported side effect was mild infusion syndrome (19%) associated with the first infusion and the median time to progression was 246 days in the 17 responding patients (Coiffer *et al.,* 1998).

In vivo experiments have shown that a patient's response to small molecule cytotoxic drugs can be augmented by treatment with the combination of a cytotoxic drug regime and rituximab. Increased cell death has been shown using combinations of rituximab and small molecule cytotoxic drugs such as CHOP chemotherapy in patients with low grade or follicular B-cell non Hodgkin's lymphoma (Czuczman *et al.,* 1999a). The overall response rate was 95%, with 55% of patients achieving complete remission, median time to progression was not reached by 29+ months (Czuczman 1999b).

The advantage of using rituximab against malignant cells over expressing Bcl-2 has been proven in clinical trials. In a study conducted on elderly patients with previously untreated DLBCL showed the overall response rate to rituximab and CHOP was 76% compared to 63% with CHOP alone (Coiffer *et al.,* 2002). Re-analysis of this study showed rituximab and CHOP chemotherapy significantly improved event free survival in Bcl-2 positive DLBCL patients compared to Bcl-2 negative patients (58%±10% versus 32%±10%, p = 0.001) (Mounier *et al.,* 2003). Conversion of patients with low grade or follicular non Hodgkin's B-cell lymphoma from Bcl-2 positive to Bcl-2 negative (detected by PCR) on treatment with rituximab suggests a role for rituximab in the clearing of residual disease (Czuczman *et al.,* 1999b).

1.3.2 *In vitro* sensitisation experiments

Sensitisation experiments *in vitro* showed that exposure to rituximab sensitised the lymphoma cell line DHL-4 to the effects of plant (ricin) and bacterial toxins (diphtheria)

(Demidem *et al.*, 1997). Sensitisation to a panel of cytotoxic drugs, including doxorubicin and cisplatin but not etopsoide was also achieved. Inhibition of cell proliferation and cell death was observed, but only a fraction of the cells observed entered apoptosis. The mechanism of sensitisation was proposed to be the down regulation of the *MDR-1* or *Bcl-2* genes (Demidem *et al.*, 1997).

Retinoids (e.g. fenretinide) have proven synergistic effects used in combination with rituximab in Ramos, Raji and Daudi Burkitt's lymphoma cell lines (Shan *et al.*, 2001). Apoptosis induced by retinoic acid derivatives is thought to be mediated by the binding for the nuclear retinoid receptor and transcription activation. A supra-additive increase in apoptosis by annexin V/PI staining of 24% ($p = 0.009$) was reported compared to expected levels. Direct synergistic anti-proliferative and apoptotic effects also have been reported with glucocortcoids and rituximab in combination against B-NHL cell lines (Rose *et al.*, 2002). Supra-additive effects were observed in annexin V/PI (viable population) and PI staining experiments, effects were independent of Bcl-2 over expression. The mechanism of synergy was proposed to be a result of cell cycle arrest and apoptosis and did not involve changes to Bax, Bcl-X_L, Bad, p53 and c-myc expression (Rose *et al.*, 2002).

Rituximab sensitised a panel of B NHL cell lines to the effects of paclitaxel (inhibits mictotubule depolymerisation), gemcitabine (pyrimidine analogue) and vinorelbine (vinca alkaloid analogue) (Emmanouilides *et al.*, 2002). Treatment of Ramos or 2H7 cells with the combination of paclitaxel and rituximab resulted in the formation of tBid and activation of caspases 9, 7, and 3, and PARP cleavage (Jazirehi *et al.*, 2003). Sensitisation was achieved through modification of apoptotic gene products rituximab treatment alone resulted in Bcl-X_L down regulation and apaf1 up regulation, whilst paclitaxel results in down regulation of Bcl-X_L, survivin, cIAP-1, and up regulation of Bad and Apaf1 (Emmanouilides *et al.*, 2003).

In combination with cisplatin against cisplatin resistant 2H7 cells, rituximab inhibited expression of Bcl-2 resulting in apoptosis via mitochondrial-dependent caspase activation. Treatment with the combination resulted in cytochrome c release, mitochondrial membrane depolarisation, caspase 3 and 9 activation and the generation of reactive oxygen species, neither rituximab or cisplatin treatment alone was sufficient to induce

apoptosis. With the combination decreased Apaf-1, cIAP-1, cIAP-2 and XIAP expression was observed (Alas *et al.*, 2002).

1.3.3 Rituximab and the role of complement mediated mechanisms

The cytotoxic mechanism of action of rituximab is unclear, much conflicting evidence has been reported in determining the mechanism. The heterogeneity of the responses to rituximab, both *in vitro* and *in vivo*, suggest a variety of mechanisms are involved. Mechanisms of action investigated have included complement dependent cytotoxicity (CDC), antibody–dependent cell mediated cytotoxicity (ADCC) and complement dependent cellular cytotoxicity (CDCC) and signalling causing the direct induction of apoptosis.

Originally the depletion of anti-CD20 bound B-cells was thought to be due to phagocytosis by macrophages and natural killer cells (ADCC). This mechanism is still supported by several groups (Flieger *et al.*, 2000, Voso *et al.*, 2002). Strong evidence for the involvement of the main effectors of ADCC, CD56 positive natural killer cells and CD14 positive monocytes has been shown in freshly isolated normal and B-cell chronic lymphocytic leukaemia (CLL) (Voso *et al.*, 2002). Cytotoxicity was also enhanced by the myeloid growth factor, granulocyte macrophage colony stimulating factor GM CSF (Voso *et al.*, 2002), suggesting cytokines such as IL2, IL12, G-CSF and GM-CSF may improve NK and macrophage function enhancing the cytotoxic action of rituximab. This provides the rationale for the use of rituximab in combination with cytokines e.g. IL12 (Ansell *et al.*, 2003).

Evidence for ADCC was also shown in a mature B-cell line ARH-77, resistant to complement mediated death, which was effectively killed by a bispecific antibody for CD20 and FCα-receptor 1 (CD89) (Stockmeyer *et al.*, 2000). Expressed on macrophages and neutrophils, FCα-receptor 1 recruits neutrophils as effector cells. The cytotoxicity of the bispecific antibody was also shown to be enhanced by the cytokines GM-CSF and G-CSF (Stockmeyer *et al.*, 2000). Additionally short term exposure to IL-2 or long term expansion of NK cells was shown to significantly improve rituximab mediated ADCC in a selection of freshly isolated leukaemic cells (shown to be more resistant to rituximab than cell lines) (Golay *et al.*, 2003). Although, another study showed only moderate

enhancement of rituximab induced ADCC by IL2 and no enhancement with IL12, IFN- and GM-CSF in the Daudi cell line (Flieger *et al.,* 2000). Flieger proposed these observations to be a cell line specific phenomenon (Flieger *et al.,* 2000).

CDC mediated mechanisms involve C1q binding to a target leading to the activation of the complement cascade and formation of the membrane attack complex (MAC) formed by polymerisation of C9 molecules, catalysed by C5b-8. CDCC mediated mechanisms involved C1q binding to Fc regions of antibodies bound to target antigens. Phagocytosis and cytotoxic killing by macrophages and polymorphonulcear leukocytes is activated by deposits of C3b, iC3b, C1q and C4b, and also chemotactic and cell activating anaphylatoxins such as C5a. Rituximab was found to activate CDC strongly, and ADCC or CDCC relatively ineffectively, and only 8% of Raji cells underwent apoptosis (Harjunpaa *et al.,* 2000). CDC was strongly enhanced by neutralisation of CD59 (which prevents MAC formation by inhibiting polymerisation of C9 molecules), CDC was weakly effected by neutralisation of CD46 (membrane co-factor protein, cofactor in the enzymatic degradation of C3b and C4b) and also weakly affected by CD55 (DAF inhibit C3/C5 convertase which controls activation of C3) (Harjunpaa *et al.,* 2000).

Golay and co workers recently reported that CDC and ADCC were the major mechanisms involved in rituximab mediated cell death in 4 follicular lymphoma and a Burkitt's lymphoma cell line (Golay *et al.,* 2000). In freshly isolated CLL cells, CDC was subsequently reported to be a more important mechanism than ADCC (Golay *et al.,* 2001a). CD55 was found to be the most important complement regulatory protein, followed by CD59, in contrast to the work reported by Harjunpaa (Golay *et al.,* 2000, Harjunpaa *et al.,* 2000). The level of CD20 expression was reported to determine the extent of lysis, although playing an important role in regulating CDC, CD55 and CD59 expression levels could not be used to predict the level of response to rituximab (Golay *et al.,* 2001a and b).

A panel of freshly isolated NHL cells were shown be equally sensitive to ADCC, CDCC and apoptosis, but differentially lysed by CDC (Manches *et al.,* 2003). In the same report follicular lymphomas were found to be particularly sensitive to CDC, and the expression level of CD20 and complement regulatory protein expression (CD46, CD55, and CD59) could predict sensitivity to CDC (Manches *et al.,* 2003). Reported radioimmunoassays

have shown deposits of C3b breakdown products (C3bi), (500 000 molecules per cell) co localised with bound rituximab (Kennedy *et al.*, 2003). Killing of Raji cells was significantly enhanced with an anti-C3bi antibody. C3bi deposits increased. Kennedy and co workers proposed that the C3bi is bound to the bound rituximab enhancing interactions with cells bearing Fc receptor and complement receptors (Kennedy *et al.*, 2003).

1.3.4 Rituximab and apoptosis

The ability of anti CD20 antibodies to induce apoptosis distinguishes them from most other anti-lymphoma antibodies (Glennie *et al.*, 2003). Cross linking CD20 by a secondary antibody or cells bearing Fc receptor, has been shown to up regulate the morphological changes characteristic of apoptosis, significant increases to the sub G_0/G_1 population of cells stained with propidium iodide on cross linking CD20 have also been observed (Pedersen *et al.*, 2002). Some of the characteristic signalling events that have been observed on cross linking CD20 include; up-regulation of protein tyrosine kinase activity, phospholipase C activity, calcium influx, activation of caspase 3 and cleavage of caspase substrates (figure 1.2) (Hofmeister *et al.*, 2000).

Clustering of CD20 is thought to cause the up-regulation of signalling pathways (Shan *et al.*, 1998). Cross linking of rituximab on freshly isolated CLL cells, resulted in strong and sustained phosphorylation of the 3 mitogen activated protein (MAP) kinases, c-Jun N terminal kinase, extracellular-signal related kinase and p38 (Pederson *et al.*, 2002). Rituximab (weakly) and B1 were shown to induce apoptosis without cross linking although other murine anti-CD20 antibodies (2H7 and 1F5) were shown to require cross linking for apoptosis (Hofmeister *et al.*, 2000, Cardarelli *et al.*, 2001). Extensive cross linking has been shown to up-regulate expression of the pro-apoptotic protein Bax, promoting the induction of apoptosis (Mathas *et al.*, 2000).

Evidence to support the direct induction of apoptosis by CD20 ligation includes successful inhibition of the kinases lck and fyn by pyrazolapyrimidine (PP2) and use of the calcium chelators EGTA and BAPTA, to inhibit apoptosis (Hofmeister *et al.*, 2000, Shan *et al.*, 1998). Cleavage of death substrates e.g. PARP and SP1 induced by anti-CD20, can be inhibited by inhibition of caspase 3 (Mathas *et al.*, 2000). Caspase 9, caspase 3 and PARP cleavage was shown, but not caspase 8 suggesting the induction of apoptosis

predominantly via cytochrome C release from the mitochondria (Byrd *et al.*, 2002). Reported work with caspase inhibitors has shown mixed results. DEVD has been shown to inhibit the apoptotic activity of homodimers of rituximab (Ghetie *et al.*, 2001). Bellosillo reports addition of the pan caspase inhibitor zVAD has no effect on the viability of cells treated with rituximab (Bellosillo *et al.*, 2001), although Shan reports zVAD inhibits DNA fragmentation induced by rituximab (Shan *et al.*, 2000).

In contrast to these results, caspase independent mechanisms of apoptosis have been also proposed. One mechanism proposed suggests the induction of apoptosis by the generation of reactive oxygen species (ROS) in a caspase independent process that involved mitochondrial membrane depolarization (Bellosillo *et al.*, 2001). Complement dependent cell death was observed which could be inhibited by ROS scavengers specific to O_2^- ions. ROS are known to have a role in signal transduction and been linked to apoptotic cell death, although also have toxic cellular effects and undergo enzymatic conversion to hydroxyl ions and hydrogen peroxide (Fiers *et al.*, 1999). The mechanism of cell death is thought to be caspase independent as no PARP cleavage or caspase 3 activation was detected and no response was observed to the caspase inhibitor zVAD (Bellosillo *et al.*, 2001).

A caspase independent cell death, also independent of lipid raft formation has also been proposed (discussed in more detail in section 1.3.5) (Chan *et al.*, 2003). CD20 induced cell death in Ramos cells has been shown to bypass mitochondria and caspase activation (van der Kolk *et al.*, 2002). Rituximab induced cell death involving loss of mitochondrial membrane potential, release of cytochrome c and activation of caspases 9 and 3, but did not depend on these events. zVAD blocked caspase 9 and 3 activation, PARP cleavage and DNA fragmentation but did not block apoptosis as measured by annexin V/PI staining. Bcl-2 over expression blocked loss of mitochondrial membrane potential, release of cytochrome but did not prevent rituximab induced cell death (van der Kolk *et al.*, 2002). These reports suggest several mechanisms may be operative.

It has also been proposed that rituximab may exert its effect by modifying the cytokine production of the cell (Alas *et al.*, 2001a). For example, the anti apoptotic cytokines IL6, IL10 and TNFα and IL10 have a modulatory role in the activation and proliferation of B

lymphocytes. In response to rituximab down regulation of IL10 and Bcl-2 has been observed, but no effects were observed on the expression of proteins such as bad, Bcl-X_L, p53, Bax and c-myc. Rituximab causes down regulation of the anti-apoptotic factor IL10 by disruption of autocrine/paracrine signalling loops, and subsequent inactivation of signal transducer and activation of transcription 3 (STAT3) activity (JAK/STAT pathway) resulting in Bcl-2 down regulation (Alas *et al.*, 2001b) and up-regulation of the pro-apoptotic protein Bax (Mathas *et al.*, 2000). Down regulation of the anti apoptotic proteins XIAP and mcl-1 was also shown, suggesting effecting the cytokine production of the cell is possible mechanism for the sensitisation effects of rituximab to chemotherapeutic drugs (Alas *et al.*, 2001a).

1.3.5 Lipid rafts and redistribution of CD20 within the lipid membrane

Binding of CD20 causes the redistribution of CD20 within the membrane to form lipid rafts, patches, or microdomains. These areas, rich in cholesterol and sphingolipids, form a platform for transmembrane signalling involving kinase activity (Deans *et al.*, 1998). CD20 signalling transduction has previously shown associations with src family tyrosine kinases (Shan *et al.*, 1998). The ability of CD20 antibodies to mediated CDC may be linked to the ability of the antibody to redistribute into lipid rafts after binding CD20. Rituximab and 1F5 recruit complement well and redistribute within the membrane but B1 is unable to translocate without hyper cross linking and also induces lower levels of CDC (Cragg *et al.*, 2003). Redistribution of CD20 makes raft sphingolipid and the src regulator Cbp/PAG (Csk binding protein/phosphoprotein associated with gylcosphingolipid-enriched microdomain) more resistant to detergents and raft associated Lyn kinase is down regulated. GPI linked complement regulatory protein CD55 is rendered hypersensitive to phospholipases C and D on CD20 accumulation, but the overall lipid content, signalling and surface proteins remain unmodified (Semac *et al.*, 2003). CD20 induced cell death independent of redistribution into membrane rafts has also been reported (Chan *et al.*, 2003).

The formation of clusters is possibly more important than dimerization to the up-regulation of signalling effects observed. (Hofmeister *et al.*, 2000). Although homodimers of anti CD19, CD20, CD21 and CD22 formed by two heterobifunctional cross linkers and a thioester bond have been shown to inhibit proliferation. Results from DNA analysis

show a reduced percentage in S phase and arrest in G_0/G_1 phase (Ghetie *et al.*, 1997). This result could be either due to a slower dissociation constant or increased signalling due to cross linking. These results were not observed by monomers alone.

1.3.6 Signalling pathway similarities

Several possible pathways of CD20 signalling have been proposed. The most well defined pathway has been proposed by Hofmeister and involves signalling via src family protein tyrosine kinase activation, followed by subsequent PLCγ tyrosine phosphorylation, the mobilization of intracellular calcium and caspase 3 activation (Hofmeister *et al.*, 2000). The main criticism of this mechanism is it is unclear how CD20 promotes these events without an immunoreceptor tyrosine-based activation motif (ITAM) and src kinase activity has not been detected in some reports (Bellosillo *et al.*, 2001). CD20 signalling shows a similarity to MHCII signalling, as MHC class II migrates to microdomains enriched in src kinases. Experiments suggest clustering rather than dimerization upregulates CD20 signalling, suggesting clustering accelerates recruitment of other elements involved in signalling (Hofmeister *et al.*, 2000).

Evidence also suggests a link between CD20 and B-cell receptor (BCR) signalling as both are involved in signalling similar cell cycle transition. BCR and CD20 co-localise after receptor ligation and rapidly dissociate before BCR internalisation (Petrie and Deans 2002). CD20 mediated apoptosis is associated with the src family PTKs Lyn, Fyn and Lck which are also activated BCR activation. Comparing the early response genes *c-myc* and *Berg 36* by northern blot, similar kinetics were observed during BCR and CD20 signalling. Extensive similarities to B-cell receptor induced apoptosis are also seen by the involvement of MAPK p44/p42 previously shown to mediate BCR induced apoptosis which is also dependent on phospholipase C activation (Mathas *et al.*, 2000).

Evidence to illustrating differences between BCR signalling and CD20 mediated signalling has also been reported. Ramos cells resistant to BCR mediated signalling were shown not to be resistant to CD20 and over expression of Bcl-2 prevented BCR signalling but not CD20 meidated signalling, suggesting different pathways (van der Kolk *et al.*, 2002). BCR signalling is known to involve the RAS/Raf-1/MAPK/ERK kinase signalling

pathway, it will be important to determine the role of this pathway in CD20 signalling in further studies (Mathas *et al.,* 2000).

1.4 Protein toxins and ribosome inactivating proteins

Plant toxins exist as holotoxins, consisting of a catalytic A chain disulphide bonded to a B chain that binds to the cell surface e.g. ricin, or hemitoxins, consisting of the catalytic A chain alone e.g. pokeweed anti-viral protein (Pennell *et al.*, 2002). Bacterial toxins *Pseudomonas* exotoxin (PE) and diphtheria toxin (DT) are single chain proteins with catalytic, translocation and cell binding domains which are processed post translationally into two polypeptide chains with inter-chain disulphide bonds (Thrush *et al.*, 1996). Ribosome inactivating proteins are a sub group of single chain plant toxins, including pokeweed antiviral protein, saporin and gelonin. Bacterial toxins PE and DT inhibit protein synthesis by inactivating elongation factor 2 (EF-2) by ADP ribosylation (Houchins 2000).

Source of toxin	Mechanism of action	Toxin Form	Examples
Plant toxins	N-glycosidase for 28S rRNA	Single chain (RIPs)	Pokeweed anti-viral protein, saporin, gelonin, momoridin, trichosanthin, barley toxin
		Double chain	Abrin, ricin, modeccin, viscumin
Bacterial toxins	ADP ribosylation of EF-2	Double chain (post translation modification)	Diphtheria toxin, *Pseudomonas* exotoxin
Fungal toxins	Ribonuclease of 28S rRNA	Single chain (RIPs)	α-sarcin, restrictocin

Table 1.2
The forms and mechanisms of toxins used in the preparation of immunotoxins. (Table adapted from Thrush *et al.*, 1996 and Jimenez and Vazquez 1985.)

The ricin A chain consists of a polypeptide chain of 265 amino acids, the B chain consists of 260 amino acids with four internal disulphide bonds linking eight cysteine residues. The two chains are joined by a disulphide bond between cysteine at position 257 of the A chain and a cysteine residue at position 4 in the B chain (Jimenez and Vazquez 1985). The B chain is involved in binding target glycoproteins and glycolipids with terminal galactose residues on the cell surface and triggering endocytosis (Fu et al., 1996).

Ribosome inactivating proteins may be found in different parts of a plant (roots, leaves, seeds and sap) at concentrations ranging from a few micrograms to hundreds of

milligrams per 100g of plant material prepared (Barbieri and Stirpe 1982). Saporin, a plentiful, safe to prepare but potent ribosome inactivating protein is extracted from the seeds of the soapwort plant *Saponaria officinalis* (up to 7% of total seed protein). Saporin (29.5kDa) is extremely resistant to denaturation and proteolysis, is not gylcosylated and does not contain lectin domains which are involved in non specific binding (Santanche *et al.*, 1997). As a type I single chain protein, saporin requires chemical conjugation to form an immunotoxin as alone the toxin is not internalised efficiently. Saporin, like ricin causes the irreversible inhibition of protein synthesis by the depurination of ribosomal RNA by cleaving the N-glycosidic bond at the A_{4324} position of the 28S RNA subunit, rendering it unable to bind elongation factors (Endo *et al.*, 1988a).

Different types of endocytic mechanisms have been shown to be involved in the endocytosis of protein toxins, the most well characterised mechanism of which is endocytosis via clathrin coated pits. Clathrin independent mechanisms include caveolae and macropinocytosis. Caveolae are small invaginated plasma membrane domains enriched in cholesterol and glycosphingolipids (Sandvig and van Deurs 2002a). Macropinocytosis requires phosphatidyl inositol 3-kinase and the actin cytoskeleton and involves the formation of macropinosomes by the closure of irregular ruffles at the plasma membrane (Sandvig and van Deurs 2002a).

Diphtheria toxin appears to be internalised almost exclusively by clathrin coated pits, via binding to the heparin-binding epidermal growth factor precursor (Lord and Roberts 1998). *Pseudomonas* exotoxin which binds the low density lipoprotein receptor related protein also appears to mostly use clathrin dependent mechanism of endocytosis (Sandvig and van Deurs 2002a). Several mechanisms appear to be simultaneously involved in the endocytosis of ricin. Clathrin dependent uptake of gold-conjugated ricin was observed by morphological studies (Sandvig *et al.*, 1991). Over expression of the protein dynamin, which inhibits uptake from clathrin coated pits, does not inhibit the endocytosis of ricin, suggesting a role for clathrin independent mechanisms. Depletion of membrane cholesterol by drugs such as nystatin which blocks uptake via caveolae, suggests caveolae are not the clathrin independent pathways of endocytosis involved in ricin uptake (Lord and Roberts 1998).

A group of protein toxins including diphtheria, anthrax and tetanus toxins are able to translocate from the endosomes into the cytoplasm. The low pH of the endosome induces a conformational change in the B chain, enabling it to insert into the endosomal membrane and form, or contribute to the formation of, a pore through which the A chain is able to pass (Sandvig and van Deurs 2002a). This mechanism relies on the low pH of the endosome, treating cells with drugs to increase the pH results in the failure of toxin translocation. Lower extra cellular pH allows diphtheria toxin to directly cross the plasma membrane (Lord and Roberts 1998).

Toxins which are unable to translocate from the endosomes include ricin and *Pseudomonas* exotoxin. From the endosomes, ricin may be recycled back to the plasma membrane, degraded within the lysosomes, or be trafficked to the *trans*-Golgi apparatus (figure 1.3). Toxins such as ricin and Shiga toxin employ more than one mechanism of transport to the trans-Golgi network to avoid the late endosomes (Sandvig and van Deurs 2002a). The range of molecules bound by ricin also suggests a number of transport mechanisms may be operative. Transport of ricin from the early endosomes to the Golgi, occurs via a Rab7 and a Rab9 independent pathway, a well characterised pathway normally involved in the transport of mannose 6 phosphate receptors and also independent of Rab11 which is involved in Shiga toxin transport (Sandvig and van Deurs 2002b). Transport of ricin to the Golgi is regulated by signalling within the cell, molecules such a calmodulin antagonists and cAMP are known to affect the passage of ricin from the endosomes.

After transport to the Golgi, protein toxins can be transported in a retrograde manner to the endoplasmic reticulum (ER). In the case of *Pseudomonas* exotoxin, a KDEL-like sequence acts as an ER retention sequence and transport to the ER occurs via COPI coated vesicles (Sandvig and van Deurs 2002a). Transport of ricin to the ER is thought to occur via binding to a recycling galactosylated component (Lord and Roberts 1998). Blocking the two galactose binding sites of ricin B chain inhibits the toxicity of ricin (Lord and Roberts 1998).

Within the ER, resident chaperones and enzymes are involved in the reduction of the internal disulphide bonds to prepare the A chain for transport into the cytoplasm by the Sec61p complex (Wesche *et al.,* 1999). Normally involved in the transport of newly

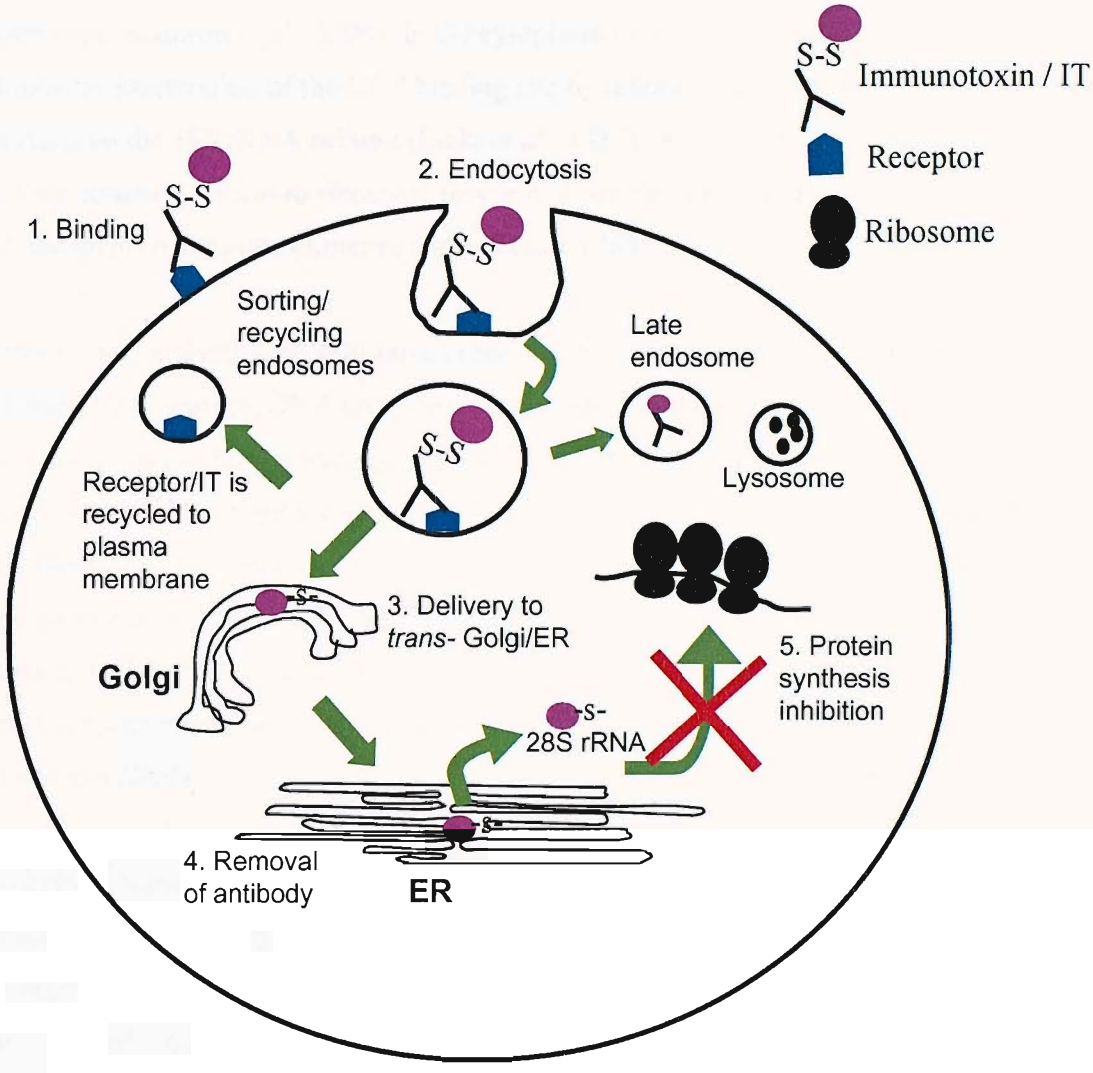

Figure 1.3
Entry and trafficking routes within the cell for an immunotoxin containing a plant toxin. Bound immunotoxins (1) containing plant toxins are endocyotosed possibly by several mechanisms (2) and delivered to the endosomes. Internalised immunotoxins may be recycled back to the membrane and the receptor recycled, or travel though the late endosomes and be degraded in the lysosomes or traffick to the *trans*-Golgi apparatus (3) and translocate to the cytosol via the ER (4). Protein synthesis inhibition (5) occurs by preventing the association of elongation factor (EF)1 and 2 to the 60S ribosomal subunit by removing the base adenine A_{4324} in the 28S ribosome subunit. (Figure adapted from Kreitman 1999 and Thrush *et al* 1996.)

synthesised proteins from the cytoplasm to the ER, the Sec61p complex is also involved in the return transport of misfolded proteins etc. to be ubiquitinylated for degradation in the proteosomes (Simpson *et al.*, 1999). In the cytoplasm ricin causes protein synthesis inhibition by inactivation of the EF-2 binding site by release of a single adenine residue from A_{4324} on the 28S rRNA subunit (Endo *et al.*, 1987). A_{4324} is involved in forming a stem loop structure critical to ribosome function. A single ricin A chain can inactivate 1500 ribosomes per minute (Jimenez and Vazquez 1985).

The ribosome inactivating protein saporin has also been reported to release adenine from RNA from other sources, DNA and poly(A), without co-factors (Barbieri *et al.*, 1996). Four specific sites of DNA cleavage by saporin and dianthin were observed in super coiled plasmids and also degraded the single strand of DNA from an M13 phage (Roncuzzi *et al.*, 1996). Generally these regions can be described as A and T rich regions (Roncuzzi *et al.*, 1996). In human derived cell lines, saporin has also been shown to induce caspase activation, PARP cleavage and some of the morphological changes associated with apoptosis, for example DNA laddering (Bolognesi *et al.*, 1996, Keppler-Hafkemeyer *et al.*, 1998 and 2000).

It has been proposed that the DNase activity of ribosome inactivating proteins is due to the presence of contaminating nucleases (Day *et al.*, 1998). The DNase activity of saporin is not thought to be due to contamination as the ribosome inactivating protein was from a highly purified source, enzyme activity was still present at low protein concentrations, and saporin showed DNase activity against herring sperm DNA, unlike other nucleases (Barbieri *et al.*, 1996).

1.5 Immunotoxins

Immunotoxins are hybrid molecules consisting of cell type specific ligands linked (genetically or by chemical conjugation) to plant or bacterial toxins. The most common ligands used to deliver a toxin to a cell are monoclonal antibodies. A molecular ribbon diagram of a typical immunotoxin is shown in figure 1.4. Advances in monoclonal antibody technology have allowed more specific targeting to cellular sub types, e.g. an antigen expressed at high levels on a tumour cell, which also allows targeting to resting cells unlike standard chemotherapy agents. Molecules used for targeting can include growth factors, cytokines, cell surface or soluble receptors. Bacterial toxins are particularly suitable for the construction of fusion proteins, whereas plant toxins are usually chemically conjugated to an antibody.

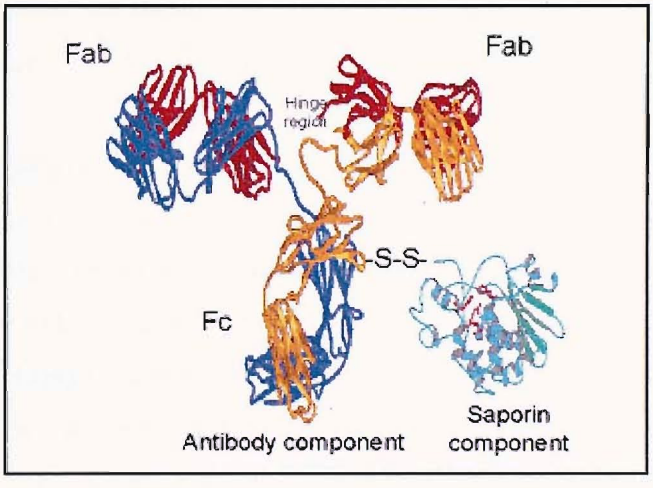

Figure 1.4
Molecular ribbon diagram of a typical immunotoxin showing an antibody chemically conjugated by a disulphide bonding to a molecule of saporin toxin.

Current drugs and radiation treatments are only semi selective for malignant cells and have side effects due to non specific toxicity. Immunotoxins have no bystander effects, surrounding cells are unaffected as the immunotoxin binds the cell expressing the target antigen and is internalised. Translocation occurs as the immunotoxin binds an antigen,

which is endocytosed via clathrin dependent or clathrin independent mechanisms and the receptor is recycled (Fitzgerald 1996) (figure 1.4). Cytosolic processing occurs to the carbonyl portion through the endocytic compartments as for free toxin (*trans*-Golgi, ER and lysosomes) (see section 1.4.). The disulphide linker is reduced inside the cell, producing free toxin, resulting in an RNA N-glycosidase in the case of an immunotoxin containing plant toxins (Bolognesi *et al.,* 1996). The RNA N-glycosidase catalyses the hydrolysis of the N-glycosidic bond at adenine 4324 on the 28S subunit of ribosomal RNA preventing the association of EF1 and EF2 with the 60s rRNA subunit resulting in protein synthesis inhibition (Endo *et al.,* 1987).

Lymphoid surface antigens are good targets for antibody mediated drug targeting as they have restricted, specific expression and are easily accessible. The ideal target must have a high binding affinity ($<10^{-8}$M) and be present at a high density on the cell surface on the target tissue and not cross react with healthy tissue or circulate as free antigen. Higher affinities are not so effective as they form a barrier on at edge of the tumour reducing percolation (Pennell *et al.,* 2002).

The individual characteristic behaviour of an antigen on binding is critical to its efficacy as a targeting molecule. Good target antigens must show selective expression and internalise on binding, antigens that are not internalised are often targeted by radioisotopes to enhance bystander killing (Pennell *et al.,* 2002). Antigen must also be accessible and not shed. The ability to selectively eliminate neoplastic B-cells by inducing apoptosis and also to target chemo resistant residual disease offers a significant advantage over conventional chemotherapy (Bolognesi *et al.,* 1998). Perhaps the most effective immunotoxins contain catalytic toxins, such as ribosome inactivating proteins, due to their extreme toxicity.

Anti-CD22, (CD22, a 135kDa cell surface marker of mature B-cells), conjugated toxins have proven useful at removing chemo resistant residual disease. By conjugation to either saporin, momordin, or PAP-s, anti-CD22 efficiently blocked protein synthesis in all CD22 positive cell lines (Bolognesi *et al.,* 1998). Whole antibody-toxin conjugates have limited use in treatment of solid tumours due to accessibility, recombinant single chain Fv fragments in this case show more potential. Although intact antibodies show greater

longevity, stability and higher potency making tumours that proliferate as singles cells, such as leukaemias, ideal targets (Reinherz *et al.*, 1986).

Genetically linked immunotoxins are preferable to chemical conjugation due to homogeneity within the population, ease of production and possibilities for further genetic engineering to enhance efficacy (Pennell *et al.*, 2002). Immunotoxins are limited by their inherent immunogenicity, toxicity and instability (Pennell *et al.*, 2002). Single chain/toxin fusion proteins of fully human origin are preferable, due to their stable and non immunogenic nature, single chain immunotoxins are cleaved by intracellular proteases at a specific cleavage site once internalised.

Patients treated with immunotoxins of non-human origin may also develop human anti-mouse antibody (HAMA) and human anti-toxin antibody (HATA) responses. HAMA responses can be reduced by using Fv fragments or humanised antibodies. The only way to combat HATA responses once they have developed is to change toxin. Total nodal irradiation or immunosuppression with cyclophosphamide or other agents may also be used during immunotoxin therapy to maximise efficacy of the treatment (Fitzgerald 1996). Alternatively recombinant growth factors, especially cytokines or soluble receptors maybe less immunogenic (Thrush *et al.*, 1996).

The major dose limiting toxicity associated with immunotoxin therapy is vascular leak syndrome. Vascular leak syndrome involves the extravasation of fluid and proteins from the vasculature, resulting in interstitial oedema and organ failure. Symptoms begin 3-4 days after the initiation of immunotoxin or interleukin-2 therapy and may become dose limiting within 5-10 days. Most symptoms disappear within 2 weeks, whilst some take longer to resolve (Baluna and Vitetta 1997).

Morphological changes to endothelial cells suggest cell-cell and cell-matrix interactions and the activation of inflammatory responses may be involved in vascular leak syndrome (Baluna and Vitetta 1997). Immunotoxins may bind directly to the endothelium to cause direct damage, or may activate leucocytes, induce inflammatory cascades thus causing indirect endothelial damage. TNF-α has been implicated in vascular leak syndrome induced by ricin (Baluna *et al.*, 1996). The effects of TNF-α include G protein coupled

activation of phospholipase, generation of reactive oxygen species and damage to DNA by endonucleases (Polunovsky *et al.*, 1994).

Vascular leak syndrome induced by ricin containing immunotoxins is thought to be a result of endothelial cell damage. A structural motif shared by toxins, some ribosome inactivating proteins and interleukin 2, which induce vascular leak syndrome, has been identified; (x)Asp(y) where (x) could b Leu, Ile, Gly or Val, and (y) Val, Leu, Ser (Baluna *et al.*, 1999). It has been proposed ricin damages endothelial cells by disrupting integrins, as viral disintegrins contain the same motif (Baluna *et al.*, 2000).

Ricin A chain contains the motif Leu^{74} Asp^{75} Val^{76} Asp^{75} which is partially exposed in folded ricin A chain and is critical for endothelial cell damage (Baluna *et al.*, 2000). Mutations in the Leu^{74} Asp^{75} Val^{76} motif reduced the activity of ricin (by protein synthesis inhibition assay) although this motif is not involved in the active site of ricin, but thought to be involved in internalization, intracellular routing or stability of ricin (Smallshaw *et al.*, 2003). Mutating the residues surrounding the Leu^{74}, Asp^{75}, Val^{76} motif Asn^{97} in the folded ricin A chain resulted in a toxin that could be administered to mice at a five fold greater dosage than native ricin, and also did not cause pulmonary vascular leak in a mouse model (Smallshaw *et al.*, 2003).

This motif may also be responsible for the induction of apoptosis. Deletion of the Leu^{74} Asp^{75} Val^{76} motif resulted in reduced apoptotic cell death detected by annexin V binding and no caspase 3 activation (Baluna *et al.*, 2000). Saporin contains two motifs that could be described as similar to the vascular leak syndrome motif described by Baluna and co-workers, although with no similarity of position (shown in figure 1.5). By sequence alignment of saporin and ricin A chain by conserved residues, the essential residue for vascular leak syndrome in ricin A chain Asp^{75} (determined by Baluna *et al.*, 2000) is not conserved in saporin, the equivalent residue is Lys^{67}. A conserved aspartic acid residue is present in the toxin momordin at a position equivalent to the critical Asp^{75} residue in ricin A chain (Savino *et al.*, 2000).

It is unclear whether protein synthesis inhibition ultimately leads to apoptosis or whether protein synthesis inhibition and apoptosis are separate events induced by different parts of the toxin molecule. In ricin, Vitetta's group suggest that apoptosis and protein synthesis

inhibition are two separate mechanisms mediated by separate active sites including the Leu^{74} Asp^{75} Val^{76} motif of ricin A chain (Baluna *et al.*, 2000, Smallshaw *et al.*, 2003). Olmo and co-workers suggest that the apoptotic effects of the ribosome inactivating protein α-sarcin occur as downstream effects of protein synthesis inhibition as a result of 28S rRNA cleavage (Olmo *et al.*, 2001).

Superimposing the crystal structures of ricin and saporin have shown that corresponding to ricin; Try^{72} Tyr^{120} Glu^{176} Arg^{179} and Trp^{208} constitute the active site of saporin. (Savino *et al.*, 2000). Subsequently Tyr^{16} Tyr^{72} Arg^{179} have been found to be essential for RNA glycosidase activity whereas Tyr^{120} and Glu^{176} can be partially dispensed with, and Tyr^{72} Tyr^{120} Glu^{176} Arg^{179} Trp^{208} are essential for the DNase activity of saporin (Bagga *et al.*, 2003). Although two residues are implicated in both RNA glycosidase activity and DNase activity, Bagga showed saporin has two independent catalytic activities, for complete cytotoxicity both activities are required.

In theory one molecule of toxin delivered intracellularly will be lethal (Yamaizumi *et al.*, 1978), although in practice it may take between 10 to 1000 (Thrush *et al.*, 1996, Kreitman and Pastan 1998). Potential problems can be divided into three types; problems with delivery of the toxin, problems due to failure of killing mechanisms, and problems associated with toxicity. Delivery of the toxin to the cell may be inefficient due to bulky tumour mass, binding affinity of the target, non-specific binding and shedding or modulation of the target antigen. Cell death may be inefficient due to failure of the patient's own effector cell mechanisms or due to populations of cells negative for expression of the target antigen. Once inside a cell, the toxin may be unable to escape the cells natural defence mechanisms, the lysosomes, where a toxin will be degraded (Thrush *et al.*, 1996).

Toxins are stable, survive temperature extremes and fairly resistant to proteolytic degradation by serum reductases making them ideal. To enhance their potency efforts concentrate on improving affinity and specificity of targeting, modifying linkages, and facilitating retention time and translocation. Phage and ribosome display techniques to allow the selection of stable antigen specific single chain Fv fragments by genotype and phenotype (Pennell *et al.*, 2002).

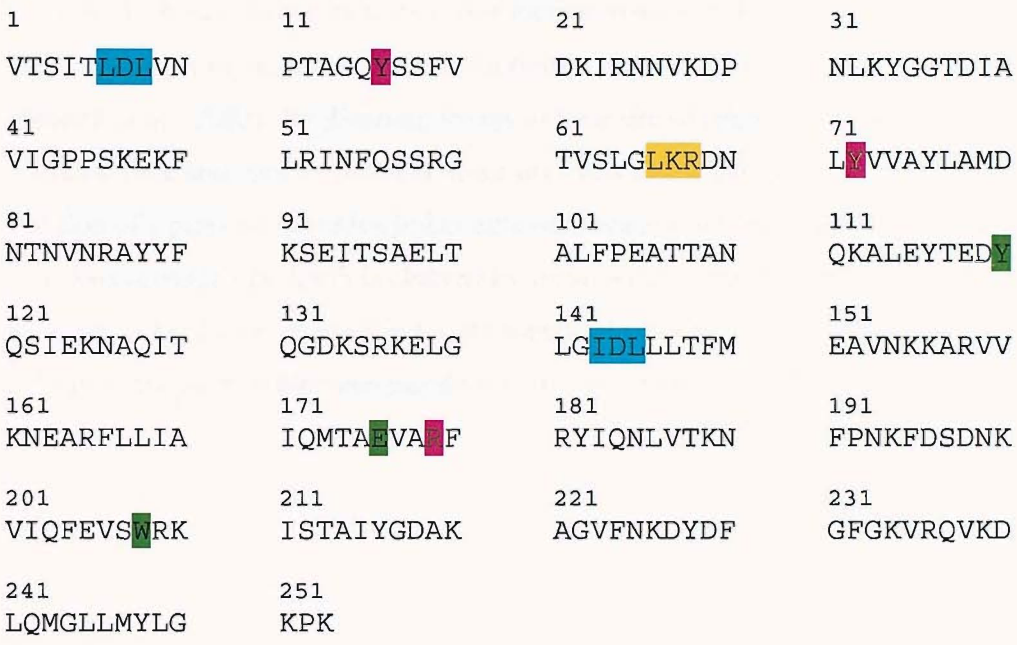

Figure 1.5
Amino acid sequence of saporin-6 taken from Di Maro *et al.*, 2001 and Savino *et al.*, 2000. Amino acids highlighted pink represent essential amino acids for RNA glycosidase activity Tyr^{16}, Tyr^{72}, Arg^{179} (Bagga *et al.*, 2003). Amino acids in green text or highlighted green represent residues essential for the DNase activity of saporin; Tyr^{72}, Tyr^{120}, Glu^{176}, Arg^{179}, Trp^{208} (Bagga *et al.*, 2003). Amino acids highlighted blue represent possible vascular leak syndrome motifs within the saporin sequence (according to the motif proposed by Baluna *et al.*, 2000). Amino acids highlighted yellow show a site in the saporin sequence corresponding to the vascular leak syndrome motif in ricin A chain, based on sequence alignment of conserved residues (Savino *et al.*, 2000).

The addition of organelle specific targeting sequences, such as KDEL, the ER retention sequence to RNase based immunotoxins increased toxicity four-fold, and the addition of the Golgi targeting sequence (YQRL) to ricin enhanced its translocation and cytotoxicity (Pennell *et al.,* 2002). By directing toxins to their site of release into the cytoplasm, the retention time and concentration at these sites was increased. Also in fusion proteins, the addition of a protease sensitive linker enhances release of free toxin into the cytoplasm. In vivo *Pseudomonas* exotoxin is cleaved by furin; a furin sensitive linker was engineered between an Fv fragment specific for the transferrin receptor and the ribosome inactivating protein restrictocin, which enhanced toxicity 2 to 20 fold (Goyal *et al.,* 2000).

1.6 CD19 and BU12-saporin

Expressed on all populations of B-cells throughout development until plasma cell differentiation, CD19 shows strong signalling activity and functions as a general regulator of B-cell antigen-receptor induced signalling thresholds (Tedder *et al.*, 2002). CD19 is a 95kDa glycoprotein member of the immunoglobin super family containing a cytoplasmic domain critical for signalling. In mouse development, expression of CD19 is tightly regulated as over expression results in a predisposition to auto immunity (Tedder *et al.*, 2002). Transgenic mice over expressing CD19 produce auto-antibodies, show elevated humoural immune responses and are hyper-responsive to transmembrane signals (Sato *et al.*, 1995). CD19 deficient mice are hypo-responsive to transmembrane signalling and produce weak immune responses (Sato *et al.*, 1995).

CD19 is also involved in signalling via B-cell receptor engagement and the CD19/CD21/CD81/Leu 13 signal transduction complex. CD19 functions as an adapter protein for the amplification of Src family tyrosine kinase activity. CD19 undergoes phosphorylation by Lyn after B-cell receptor ligation, resulting in the amplified Lyn kinase activity, which facilitates interaction with Vav and the p85 subunit of phosphatidylinositol 3 kinase (Myers *et al.*, 1995, Yazawa *et al.*, 2003). Co-ligation of CD19 and B-cell receptor results in downstream signalling events including changes to intracellular calcium levels which have been shown to lower the threshold for B-cell activation and regulate mitogen activated protein kinase activation and proliferation (Tedder *et al.*, 2002).

Anti-CD19 antibodies showed some initial success in treating patients with B-cell lymphoma (Heckman *et al.*, 1991). *In vitro* different anti-CD19 antibodies have shown varied effects. For example, HD37, 4G7 and BU12 but not B43 have shown anti tumour effects against Daudi cell tumours in SCID mice (Ghetie *et al.*, 1992). Anti-CD19 antibodies inhibited the entry of tonsilar B-cells into S-phase by inhibition of DNA synthesis (Rigley and Callard 1991). Inhibition of DNA, RNA and protein synthesis resulting cell cycle arrest by anti-CD19 antibodies HD37, 4G7 and BU12 requires cross linking and is dependent on the affinity of the antibody (Ghetie *et al.*, 1994). Cross linking CD19 in B-cell lymphoma cell lines significantly decreased the percentage of cells in S-

phase of the cell cycle, by inducing cell cycle arrest at G_1 or G_2/M phase (Ghetie *et al.*, 1994).

CD19 is a good target for immunotoxins as it is expressed at a high level in a homogeneous manner and is internalised on binding. Anti-CD19 immunotoxins containing deglycosylated ricin A chain have been shown to be effective to a variable degree against non Hodgkin's lymphoma *in vitro* and *in vivo* (Grossbard *et al.*, 1992, Herrrera *et al.*, 2003). The immunotoxin BU12-saporin has been shown to induce protein synthesis inhibition in a dose dependent manner in CD19 positive cell lines (Flavell *et al.*, 1995b), whereas BU12 antibody alone had virtually no effect on protein synthesis inhibition in Nalm 6 cells (Flavell *et al.*, 1995b).

In vivo, treatment with BU12-saporin significantly prolonged the life of SCID mice with Nalm-6 leukaemia (log rank analysis $p = 0.0007$) (Flavell *et al.*, 1995b). SCID/Nalm-6 mice treated with saporin and BU12 antibody also showed increased survival compared to PBS treated controls (log rank analysis $p = 0.004$) (Flavell *et al.*, 1995b). The activity of unconjugated saporin and BU12 antibody treatment suggests some non-specific toxic effects of saporin and/or anti-proliferation effects of BU12 antibody are apparent. However, treatment with the conjugated immunotoxin significantly increased survival compared to mice treated with BU12 antibody and saporin ($p = 0.05$) (Flavell *et al.*, 1995b).

1.7 Additivity of therapeutic effects

Successful treatment with an immunotoxin requires all malignant cells to be targeted to remove all possibility of future growth. Any viable cells remaining will lead to relapse. Heterogeneity of antigen expression within the lymphoma population may compromise this therapeutic approach as cells with low antigen expression or antigen negative cells will not receive toxin. Targeting multiple antigens combats heterogeneity of antigen expression, therefore improving the probability of attacking the whole of a specific population allowing clearance of minimal residual disease.

Two immunotoxins, targeted to CD19 and CD38, have been used successfully in combination in SCID/Ramos mice (Flavell *et al.*, 1995a). The combination of immunotoxins was found to significantly prolong survival compared to either immunotoxin used alone (Flavell *et al.*, 1995a). This approach also has the advantage of delivering more molecules of toxin to cells which are both CD19 and CD38 positive. These results observed were not due to the effect of immunotoxin plus antibody, although responses to combinations of BU12 antibody and CD38 immunotoxin reported vary (Ghetie *et al.*, 1992).

Ricin A chain containing immunotoxins specific for CD19 and CD22 were also shown to be more effective in combination against Nalm 6 proliferation in SCID mice (Herrera *et al.*, 2003). Combinations of immunotoxins specific for CD80 and CD86, containing a variety of ribosome inactivating proteins (gelonin, saporin and bouganin) have been shown to induce apoptosis and protein synthesis inhibition in Raji cells and the Hodgkin lymphoma cell line L428 (Bolognesi *et al.*, 2000). However, used in combination these anti-CD80 and anti-CD86 immunotoxins did not show additive cytotoxic effects (Bolognesi *et al.*, 2000).

Immunotoxins and antibodies proven individually effective have been used in combination to augment the responses. Anti-CD19 and anti-CD22 immunotoxins have been used in combination with anti-CD20 antibodies (rituximab and 1F5 antibody) and have been shown to have a significantly improved therapeutic effect over either modality used alone (Flavell *et al.*, 2000b). A significant augmentation of therapeutic effect is observed with combinations of rituximab and BU12-saporin. *In vitro* these combinations

have shown to have anti-proliferative effects and inhibit protein synthesis (Flavell *et al.*, 2000b). *In vivo* SCID/Ramos mice treated with a combination of either murine anti-CD20 antibody, 1F5, or rituximab and BU12-saporin showed a significant improvement in survival.

A wide variety of cytotoxic mechanisms of action for rituximab have been proposed (see section 1.3). Variation also exists between responses to rituximab and BU12-saporin reported in *in vitro* and *in vivo* studies (Flavell *et al.*, 2001). This suggests a variety of mechanisms are involved in cell killing in different systems and models. Initial experiments suggested the involvement of a complement mediated mechanism in rituximab and BU12-saporin induced cell killing (Flavell *et al.*, 2000b). Complement fixation by rituximab resulting in membrane damage may leave targets cells more vulnerable to immunotoxin action (Flavell *et al.*, 2000b). Also, the extent of lymphoma apoptosis was significantly reduced in de-complemented serum, whereas natural killer cell depletion with cobra venom or anti asialo GM1 antiserum did not affect the outcome (Flavell *et al.*, 2001). Direct cell signalling via the CD20 molecule was also proposed to be important (Flavell *et al.*, 2001).

The therapeutic effect of combination of rituximab and BU12-saporin observed in preliminary experiments appears to be additive. This provides the rationale for exploring the *in vitro* cytotoxic mechanisms of this effect, for possible therapeutic use in humans. Previous reports suggest the mechanisms employed by the combination in cell death include, complement, protein synthesis inhibition and apoptosis. Anti-CD19 antibodies may inhibit cellular proliferation (Ghetie *et al.*, 1994), ribosome inactivating proteins such as saporin induce protein synthesis inhibition and have also shown DNAse activity leading to apoptosis (Bolognesi *et al.*, 1996), rituximab mediated cell death may involved complement (Golay et al., 2000) or direct signalling and the induction of apoptosis (Shan *et al.*, 1998). The relative contribution of protein synthesis inhibition and apoptosis to the overall effect of the combination remains to be determined.

1.8 Aims and overview

The combination of immunotoxins and antibodies are a promising approach to treat malignancies. Clinical trails have shown mixed responses, to improve response rates a clearer understanding of the factors effecting cytotoxicity is required. This suggests further *in vitro* study of the mechanisms and pathways involved is warranted to improve the efficacy of these therapeutics *in vivo*.

The aim of the first experimental chapter was to determine the effect of rituximab and BU12-saporin individually and in combination on Ramos cells and other B-cell lymphoma cells lines. This was addressed using proteins synthesis inhibition assays, propidium iodide (PI) staining and combined annexin V/PI staining to determine the extent of protein synthesis inhibition and apoptosis. The effect of alternative anti-CD20 antibodies and alternative known protein synthesis inhibitors in combination was also investigated.

The aim of the second chapter was to determine the contribution of complement in the protein synthesis inhibition and apoptotic effects of rituximab and BU12-saporin detected in chapter one. The statistical significance of complement mediated mechanisms was determined using experimental technique employed in chapter one. Experiments were carried out in heat inactivated FCS and statistical analysis carried out.

Chapters 5 and 6 begin to examine the effects of rituximab and BU12-saporin at the molecular level. The aim of chapter 5 was to determine the extent of PARP cleavage, caspase activation and the effect of caspase inhibitors on Ramos cells exposed to rituximab and BU12-saporin. This was addressed by a series of western blots probed for PARP cleavage, caspase 3, 8 and 9 cleavage conducted in the presence and absence of caspase inhibitors. Experiments were also carried out with the FAS and TRAIL receptor inhibitors to make an initial determination of the pathways involved in apoptosis induced by rituximab and BU12-saporin.

The aim of the final experimental chapter was to determine the role of selected Bcl-2 family proteins in rituximab and BU12-saporin induced apoptosis and determine the effectiveness of rituximab and BU12-saporin against cells over expressing Bcl-2. Investigations were carried out by western blotting to determine any change in expression

of selected Bcl-2 family proteins in response to rituximab and BU12-saporin. Ramos cells lines over expressing Bcl-2 and Bcl-X_L were also employed in protein synthesis assays, apoptosis assays and western blotting to determine if over expression of either of these molecules could protect cells against the apoptotic effects of rituximab and BU12-saporin, thus reducing their therapeutic potential.

Chapter Two

Materials and Methods

Unless otherwise stated all chemicals and reagents were purchased from BDH, VWR Poole Dorset, UK.

2.1 General buffers and solutions

Phosphate buffered saline (PBS) pH 7.4

10mM	Na_2HPO_4
2mM	KH_2PO_4
150mM	NaCl
2.5mM	KCL

Tris buffered saline (TBS) pH 7.4

25mM	Tris
150mM	NaCl
2.5mM	KCL

2.2 Cell Culture

Reagents and Cell lines

RPMI 1640 (Sigma-Aldrich, Dorset, UK)
Foetal calf serum optimised for hybridomas (Perbio, Cheshire, UK)
Sodium pyruvate, 100mM (Sigma-Aldrich, Dorset, UK)
L-Glutamine, 200mM (Sigma-Aldrich, Dorset, UK)

75cm^3 vented cap tissue culture flasks (Bibby Sterilin, Staffordshire, UK)

Ramos	Burkitt's lymphoma, CD19 and CD20 positive. (Klein *et al.*, 1975)
Nalm 6	Acute lymphoblastic pre-B cell, CD19 positive. (Hurwitz *et al.*, 1979)
Namalwa	Burkitt's lymphoma, CD19 and CD20 positive. (Nadkarni *et al.*, 1969)
Raji	Burkitt's lymphoma, CD19 and CD20 positive. (Pulvertaft *et al.*, 1964)
Daudi	Burkitt's lymphoma, CD19 and CD20 positive. (Klein *et al.*, 1968)

Methods

Cells were cultured in RPMI 1640 medium (antibiotic free) containing 10% foetal calf serum and 1mM sodium pyruvate and 2mM glutamine (here after referred to as R10 medium). Cells were maintained in the logarithmic growth phase by passage at regulate intervals in 75cm^3 vented cap tissue culture flasks at 37°C in a humidified atmosphere of 5% carbon dioxide. Cell densities were determined using 0.4% (w/v) trypan blue in PBS (see material and methods section 2.1), filter sterilised and enumerated by haemocytometer.

Experiments carried out in de-complemented media were carried out in RMPI 1640 supplemented with 1mM sodium pyruvate and 2mM glutamine and 10% foetal calf serum which had been heat inactivated by incubation at 56°C in a water bath for 30 minutes (here after referred to as HI FCS). Cells were washed 3 times in RPMI before transfer to medium containing HI FCS.

2.3 Saporin and BU12 production and immunotoxin conjugation

Saporin production

The seeds of the soapwort plant, *Saponaria Officinalis* were obtained from Chiltern Seeds, Cumbria, UK. The SO6 isoform of saporin was extract using a previously published method (Stirpe *et al.*, 1983). Briefly, the crude extract was purified to homogeneity by

cation exchange chromatography on carboxymethyl-sepharose (Sigma Aldrich, Dorset, UK) with a sodium chloride gradient followed by gel filtration on a Sephacryl-S200HR column (Sigma Aldrich, Dorset, UK). The product gave a single band by SDS-PAGE of 29,500Da and was immunoreactive by ELISA to both polyclonal and monoclonal saporin anti-sera.

Antibody production

The anti-CD19 antibody, BU12, was produced as previously described (Flavell *et al.*, 1995b). Briefly, a CD19 antibody producing hybridoma clone was produced by immunisation of two BALB/c mice with the Burkitt's lymphoma cell line EB4. Immune spleen cells from these animals were fused with the mouse X63 AG8 653 plasmacytoma cell line and the resulting hybridomas screened and selected. BU12 hybridoma cells were cultured in an Acusyst R hollows fibre bioreactor system (Endotronics, Minneapolis, MN, USA) as per manufacturers' instructions. Supernatants containing antibody were harvested periodically and subject to ammonium sulphate precipitation to produce a crude extract, anion exchange chromatography on DEAE sepharose and sephacryl S200HR gel filtration (Sigma Aldrich, Dorset, UK). Purified antibody gave a band of 160 000Da by SDS PAGE and the specificity of the antibody was confirmed by flow cytometry

Immunotoxin conjugation

The immunotoxin BU12-saporin was constructed as previously described (Flavell *et al.*, 1995b) by conjugating BU12 antibody to saporin using the heterobifunctional cross-linking reagent N-succinimidyl 3-(2- pyridyldithio) propionate (SPDP) (Pharmacia, Milton Keynes,UK) from a method described by Thorpe (Thorpe *et al.*, 1985). producing a non-hindered disulphide bond. Free antibody was removed by carboxymethyl sepharose cation exchange columns (Sigma Aldrich, Dorset, UK). Purified BU12-saporin was dialysed into PBS pH 7.2, filter sterilised by 0.2μm filter and frozen in aliquots at -80°C.

2.4 Protein Synthesis Inhibition Assay

Reagents and Materials

R10 medium
96 well microtitre plates, flat bottomed (Bibby Sterilin, Staffordshire, UK)
^{3}H-Leucine, 50μCi diluted into PBS (ICN, Hampshire, UK)
Glass fibre filter mat (Perkin Elmer, Cambridge, UK)
Opti-fluor O scintillation fluid (Perkin Elmer, Cambridge, UK)
Cell harvester (Skatron Instruments)
Scintillation counter (Perkin Elmer, Cambridge, UK)
Pico vials, 4ml (Perkin Elmer, Cambridge, UK)

Method

PSI assays were carried out in penicillin (100IU/ml) and streptomycin (100μg/ml) supplemented R10 media. Dilutions of immunotoxin, cytotoxic drug or other reagent under test were prepared in R10 media at double final required concentration. 100μl of each dilution prepared, or media alone for control wells, was aliquoted in triplicate into a 96 well flat bottomed microtitre plate. Cells were washed twice in RPMI 1640 (1500rpm, 5 minutes) and resuspended in R10 media at a concentration of $5x10^{5}$ cells/ml. 100μl of this cell suspension was introduced to each well ($5x10^{4}$ cells/well). The plate was then incubated for 48 hours at 37°C in a humidified atmosphere of 5% carbon dioxide.

After 48 hours the plate was pulsed with 1μCi ^{3}H-leucine per well and incubated for a further 16 hours (overnight) at 37°C in a humidified atmosphere of 5% carbon dioxide. The contents of the wells were harvested onto glass fibre filters using a Skatron cell harvester and allowed to dry for 1 hour at 37°C. The amount of ^{3}H-leucine incorporated into the harvested cells was determined by scintillation count. The harvested cells on glass fibre discs were placed in 4ml scintillation tubes with 1ml of Opti-fluor-O scintillation fluid and counted using a Packard scintillation counter in. Results obtained (dpm) were expressed as a percentage of ^{3}H-leucine uptake compared to control cells.

The amount of leucine incorporated into treated cells was normalised as a percentage ^{3}H-leucine incorporation of an untreated control. Each 96 well plate contained up to 12 wells of untreated control cells from which a mean average untreated control cell ^{3}H-leucine incorporation was calculated. For example, the untreated control Ramos cells from the experiment shown in figure 3.2 gave the following counts (dpm):

27225.96
30536.71
25316.88
29063.56
30507.34

Giving a mean average = 28530.09

Ramos cells treated with BU12-saporin alone at $1x10^{-9}$M gave a count of 13849.66dpm.

As a percentage of the untreated controls: (13849.66 / 28530.09) x 100 = 48.5%. This calculation was carried out for each of the triplicates and the mean and standard deviation determined.

For the cells treated with the combination of rituximab and BU12-saporin, values were normalised with respect to control cells treated with rituximab alone. Taking figure 3.2 as an example, the average ^{3}H-leucine incorporation for the rituximab alone treated cells was determined to be 18476.69dpm. Ramos cells treated with BU12-saporin at $1x10^{-9}$M and rituximab at 10μg/ml gave a count of 5449.47dpm.

Thus: (5449.47 / 18476.69) x 100 = 29.5%

This calculation was carried out for each of the triplicates and the mean and standard deviation determined.

2.5 Propidium Iodide (PI) Staining

Reagents

Coulter DNA-prep reagent kit (Beckman Coulter, Buckinghamshire, UK)

Lysis buffer

PI staining solution

Method

The amount of DNA in a cell can be detected indirectly by staining with propidium iodide (PI). From the amount of DNA in a cell the proportion of cells in each stage of the cell cycle can be determined. Cells with less the normal DNA content (the sub G0/G1 population) suggests the cells maybe undergoing the DNA fragmentation and blebbing processes of early apoptosis. Cells with this abnormally low amount of DNA can not successfully continue through the cell cycle.

The method carried out as described in the manufacturers' instructions. Briefly, cell samples were washed twice in PBS (1500rpm for 5 minutes), and resuspended in 1ml PBS to a final concentration of $5x10^5$cells per flow tube. In a flow tube, 50µl of lysis buffer was added to 50µl of cells resuspended in PBS. Staining solution (1ml) was then added and the samples incubated for 15 minutes.

Reading was carried out on an Epics XL flow cytometer (Beckman Coulter, Buckinghamshire, UK). PI fluoresces at 620nm and is detected by this system using FL3. The protocol was set up to plot forward and side scatter, FL3 versus the aux channel (set to FL3), and single parameter histogram plots of FL3 and FL3 log.

2.6 Annexin V/PI staining

Reagents and Materials

Immunotech Annexin V/PI staining kit: (Beckman Coulter, Buckinghamshire, UK)

Propidium iodide (250μg/ml)

Annexin V-FITC conjugate (25μg/ml)

Binding buffer concentrate (x10)

Method

The method carried out as described in the manufacturers' instructions. Briefly, cell samples were washed twice in ice cold PBS (1500rpm, 5 minutes). In a flow tube, $5x10^5$ cells were resuspended in 100μl of binding buffer (freshly diluted from the stock). PI (5μl) and 1μl of annexin FITC conjugate were added, mixed, and incubated on ice in the dark for 15 minutes, and made up to a final volume of 500μl with binding buffer before reading.

A protocol was set up to the read the samples using an excitation light of 488nm, detecting at 518nm for the annexin FITC conjugate (FL1). Log plots of FL1 (annexin FITC) versus FL3 (PI) were set up as well as forward scatter and side scatter plots and single parameter FL1 and FL3 plots.

2.7 Western blotting

Reagents and Materials

Bradford protein dye reagent (Sigma Aldrich, Dorset, UK)
Bio-Rad mini-Protean 3 electrophoresis and blotting system (Bio-Rad, Hertfordshire, UK)
Pre-cast ready gels 15 well 4-15% Tris-HCL (Bio-Rad, Hertfordshire, UK)
Red sample loading buffer (NEB, Hertfordshire, UK)
Broad range markers, prestained (NEB, Hertfordshire, UK)

Protran 0.45μm nitrocellulose membrane (Schleicher and Schuell, Leicestershire, UK)

Chromatography paper 3mm (Whatman, Kent, UK)

Supersignal reagent (Perbio, Cheshire, UK)

Anti-PARP (1:1000)	(Catalogue number 4338-MC, R&D systems, Oxford, UK)
Anti-Bax (1:500)	(Catalogue number sc-493, Santa Cruz Biotechnology, Heidelberg, Germany)
Anti-Bak (1:500)	(Catalogue number sc-1035, Santa Cruz Biotechnology Heidelberg, Germany)
Anti-Bcl-2 (1:400)	(Catalogue number 554202, BD Pharmingen, Oxfordshire, UK)
Anti-Bcl-X_L (1:1000)	(Catalogue number AF800, R&D systems, Oxford, UK)
Anti-Mcl-1 (1:400)	(Catalogue number sc-819, Santa Cruz Biotechnology Heidelberg, Germany)
Anti-ß-tubulin (1:500)	(Catalogue number T5293 Sigma Aldrich, Dorset, UK)
Anti-PCNA (1:1000)	(From G.K.Packham, Cancer Sciences Division, University of Southampton)
Anti-caspase 3 (1:1000)	(Catalogue number 9662, Cell Signaling, Hertfordshire, UK)
Anti-caspase 8 (1:1000)	(Catalogue number 551242, BD Pharmingen, Oxford, UK)
Anti-caspase 9 (1:1000)	(Catalogue number 9502, Cell Signaling, Hertfordshire, UK)

Peroxidase conjugated goat anti-rabbit immunoglobins (Dako, Cambridgeshire, UK)

Peroxidase conjugated rabbit anti-mouse immunoglobins (Dako, Cambridgeshire, UK)

Peroxidase conjugated rabbit anti-goat immunoglobins (Dako, Cambridgeshire, UK)

Buffers

RIPA extraction buffer (5x)

- 0.75M NaCl
- 5% NP 40
- 2.5% Deoxycholate (Sigma Aldrich, Dorset, UK)
- 0.5% SDS
- 0.25M Tris (pH 8.0)
- 1% Mammalian protease inhibitor cocktail (Sigma)

CHAPS extraction buffer (5x)

50mM Pipes/NaOH (Sigma Aldrich, Dorset, UK)

2mM EDTA

0.1% CHAPS

5mM DTT

1% Mammalian protease inhibitor cocktail (Sigma)

Electrophoresis running buffer (10x)

200mM Tris (pH 8.3)

250mM Glycine

0.1% SDS

Transfer buffer

1x Electrophoresis running buffer

25% Ethanol(Fisher, Leicestershire, UK)

Blot washing buffer (T-TBS)

1x TBS (see methods and material 2.1)

0.1% Tween-20 (Sigma Aldrich, Dorset, UK)

Blocking Buffer / Antibody diluent

1x Blot washing buffer

5% Dried milk power

(For PARP blots in place of TBS in the blot washing buffer and the blocking buffer PBS was substituted.)

Method

Preparation of cellular lysates

After exposure to the appropriate drug for the selected time period cells were washed twice in ice cold PBS, the pellets dried and snap frozen and stored at -80°C until use.

An NP40 based extraction technique (RIPA buffer) was used for all the antibodies described except anti-caspases 3, 8, and 9 for which the CHAPS extraction buffer and procedure was used.

RIPA extraction

Dry pellets were resuspended with 100µl RIPA extraction buffer (1x) supplemented with 1% mammalian protease inhibitor cocktail on day of use, (or proportionally less RIPA buffer if the cell pellets appeared small.) Pellets were incubated on ice for 15 mins and centrifuged for 5 mins, 12,000 rpm at 4°C. The supernatant was removed to fresh microcentrifuge tubes (approximately 90µl).

CHAPS extraction

For CHAPS the extraction procedure, dry cell pellets were resuspended in 50ul of CHAPS buffer (1x) supplemented with 1% mammalian protease inhibitor cocktail on day of use. Three freeze thaw cycles were carried out. The samples were then centrifuged for 5 mins, 12,000 rpm at 4°C and supernatant (approximately 45µl) was removed to fresh microcentrifuge tubes

Concentration determination

The protein concentration of samples was determined by Bradford assay. Bradford reagent was used at a dilution of 1in 4 in a 96 well plate format assay (200µl per well) and samples read on a plate reader at 595nm. Samples were diluted to fall within the linear range of 0.1 to 1.4mg/ml of protein if appropriate. Protein concentrations were determined from a BSA standard curve.

Sample preparation and SDS-PAGE

The gel was fitted into the running tank and the inner reservoir was filled completely with 1x running buffer and the comb removed. The outer reservoir was filled with running buffer. Samples were prepared for loading in 5µl of 3x SDS sample buffer containing 1/10 DTT with 20µg of sample was loaded in 10µl (final volume 15µl). The samples were loaded using gel loading tips and the gel run at 30mamps for 90 minutes and checked regularly.

Electrotransfer

The gel was removed from the tank and the plates separated by forcing apart. The wells and thicken edge were cut off and discarded to prevent trapping air bubbles and allow the gel to lie as flat as possible. A corner of the gel was cut off for reference. The gel, two pieces of sponge padding, four pieces of 3mm filter paper, and one piece of nitrocellulose membrane cut to size (9cm x 6cm) were soaked in transfer buffer.

The blotting chamber was opened and one piece of soaked sponge was placed on the negative (black) side. This was followed by two pieces of soaked filter paper and then the gel. The nitrocellulose membrane was then placed on top, followed by two more soaked pieces of filter paper and smoothed between each layer to remove air bubbles. Finally, the second soaked sponge was placed on the top and the blotting chamber closed. The blotting chamber was inserted into the tank and covered with blotting buffer. This was run cooled with an ice block, for 60 minutes at 100volts.

Probing the blot

All subsequent steps are performed with shaking and blots were not permitted to dry out. The membrane was blocked in a shallow tray for 30 minutes with blocking buffer. Blots were then washed three times each for 5 minutes with an excess of T-TBS. The membrane was incubated with the primary antibody at a dilution of 1:1000 (unless otherwise stated) in antibody diluent overnight at 4°C. (Except for PARP blots for which steps were carried out at room temperature.) Blots were then washed three times for 5 minutes with an excess of T-TBS at room temperature. The secondary antibody (HRP conjugate) was diluted

1:5000 into antibody diluent and incubated with the membrane at room temperature for 1 hour. The membrane was washed a further three times for 5 minutes with an excess of T-TBS at room temperature. Supersignal reagent was prepared by adding equal quantities of reagents A and B, as according to the manufactures' instructions. The blot was covered thinly with supersignal solution for 2-5 minutes and then removed. The blot was covered tightly with cling film for detection of bands on a Rio-Rad chemiluminescent imager, using Quantity One software (Rio-Rad, Hertfordshire, UK).

Density analysis was carried out on QuantiScan software (Biosoft, UK) from original tif files. Density is expressed in arbitrary units or as a percentage of the full length species detected (e.g. cleaved PARP and uncleaved PARP is expressed as a ratio of the total density).

2.8 Caspase inhibitors

Reagents and Materials

z-VAD-fmk Caspase 3 inhibitor (Catalogue number 627610, Calbiochem, Nottingham, U.K)
z-DEVD- fmk Caspase 3 inhibitor (Catalogue number 264155, Calbiochem, Nottingham, U.K)

Method

Caspase inhibitors were reconstituted in DMSO at 50mM for use at a final concentration of 50μM. Inhibitors were added to samples at the same time as rituximab or BU12-saporin as appropriate and the preparation of samples carried out as detailed in section 2.6 and 2.7.

2.9 FAS and TRAIL receptor blocking agents

Reagents and Materials

Anti-FAS antibody, clone ZB4. Stock solution 1mg/lml, final concentration 500ng/ml. (Catalogue number 05-338, Upstate cell signalling solutions, Milton Keynes, UK)
TRAIL -R1:Fc DR4 Recombinant human proteins. Stock solution 1mg/lml, final concentration 2μg/ml. (Alexis Biochemicals, Nottingham, UK)

Method

Cells were pre-incubated with the FAS or TRAIL blocking reagents for 1 hour at 37°C in a humidified atmosphere of 5% carbon dioxide before exposure to rituximab or BU12-saporin as appropriate and western blotting carried out as detailed in section 2.7.

2.10 Statistical analysis

Statistical analysis was carried out on SPSS statistical software (LEAD technologies) using independent t tests or one way ANOVA analysis functions, as appropriate, using a confidence interval of 95% ($p = 0.05$). Two-sample student's t-tests were performed testing the hypothesis that means from two samples were equal. Levene's test was used to accept ($p > 0.05$) or reject ($p < 0.05$) (heteroscedastic t-test) the assumption of equal variances of both ranges of data. The One-Way ANOVA procedure produces a one-way analysis of variance for a quantitative dependent variable by a single factor (independent) variable. Analysis of variance is used to test the hypothesis that several means are equal. This technique is an extension of the two-sample t test.

Chapter Three

Analysis of protein synthesis inhibition and the induction of apoptosis in lymphoma cell lines exposed to rituximab and BU12-saporin

3.1 Introduction

The immunotoxin BU12-saporin contains the ribosome inactivating protein (RIP) saporin chemically coupled to an anti-CD19 antibody. BU12-saporin delivers saporin to B cells expressing CD19. Saporin is a single chain, type one ribosome inactivating protein believed to cause cell death by protein synthesis inhibition (Ferreras *et al.*, 1993). Saporin disrupts binding of the 28S ribosomal subunit by hydrolysis of the N-glycosidic bond at adenine 4324, causing irreversible inhibition of protein synthesis (Thrush *et al.*, 1996). It has been proposed that ribosome inactivating proteins cause cell death via protein synthesis inhibition and the direct induction of apoptosis (Bergamashchi *et al.*, 1996, Bolognesi *et al.*, 1996). This is supported by evidence from Keppler-Hafkemeyer *et al.*, (1998), who show that immunotoxins containing *Pseudomonas* exotoxin (PE) induce cell death involving caspase activation and PARP cleavage. The DNA fragmentation activity of saporin was confirmed recently (Bagga *et al.*, 2003). The residues Tyr^{72}, Tyr^{120}, Glu^{176}, Arg^{179}, Trp^{208} were found to be essential for DNA fragmentation, two of which ($Tyr^{72}$and Arg^{179}) were also found to be critical for the RNA N-glycosidase activity of saporin (Bagga *et al.*, 2003).

Rituximab (IDEC-C2B8, Mabthera) is a chimeric anti-CD20 antibody containing human IgG1 Fc regions and murine variable regions, which induces remission of low-grade B cell follicular lymphoma. The cytotoxic mechanism of action of rituximab is unclear, it was originally thought to be dependent on ADCC, but is also thought to be dependent on complement mediated mechanisms and the induction of apoptosis via direct cell signalling pathways (Shan *et al.*, 1998, Hofmeister *et al.*, 2000, Harjunpaa *et al.*, 2000). Evidence has been presented to support a variety of mechanisms of apoptosis induction, including caspase dependent mechanisms involving cytochrome c, changes to intracellular calcium levels, src family kinases, MAP kinases, Bcl-2 expression levels and modified cytokine

production (Alas *et al.*, 2001a). The conflicting evidence available suggests that a variety of mechanisms may be operative in rituximab induced cell death.

The effect of rituximab has been shown to be enhanced by a wide variety of drugs. Clinical benefit has been observed with rituximab used in combination with CHOP chemotherapy regimes (Czuczman et al., 1999). The overall response rate was 95%, with 55% of patients achieving complete remission (Czuczman 1999b). *In vitro* rituximab has been shown to have synergistic effects in combination with retinoids and glucocorticoids (Shan *et al.*, 2001, Rose *et al.*, 2002). Combinations of antibodies and immunotoxins have also been investigated. Rituximab in combination with an anti-CD22 ricin containing immunotoxin has shown a 1,000 fold increase in potency (Ghetie *et al.*, 2001). BU12-saporin has been used in combination with anti-CD7 and anti-CD38 saporin containing immunotoxins (Flavell *et al.*, 1995). An alternative anti-CD19 ricin containing immunotoxin has also shown increased survival in Nalm 6-SCID mice used in combination with a CD22 ricin immunotoxin (Herrera *et al.*, 2003).

Sensitisation experiments *in vitro* showed exposure to rituximab sensitised lymphoma cells to the effects of plant (ricin) and bacterial toxins (diphtheria) (Demidem *et al.*, 1997). Sensitisation by rituximab to a panel of cytotoxic drugs, including doxorubicin and cisplatin but not etopsoide was also achieved. Inhibition of cell proliferation and cell death was observed, but only a fraction of the cells observed entered apoptosis. One potential mechanism that has been proposed to account for rituximab mediated sensitisation is the down regulation of the anti apoptotic proteins gp170 (multi drug resistance protein 1) or Bcl-2 (Demidem *et al.*, 1997).

This hypothesis has been developed further to suggest that the sensitisation effects of rituximab maybe due to modified cytokine production by the cell (Alas *et al.*, 2001a). Rituximab causes down regulation of the anti-apoptotic factor interleukin (IL)10 by disruption of autocrine/paracrine signalling loops, and subsequent inactivation of signal transducer and activation of transcription 3 (STAT3) activity (JAK/STAT pathway) resulting in Bcl-2 down regulation (Alas *et al.*, 2001b). Down regulation of the anti apoptotic proteins XIAP and Mcl-1 was also demonstrated, suggesting another possible mechanism for the sensitisation effects of rituximab to chemotherapeutic drugs.

Co-operative therapeutic effects between rituximab and BU12-saporin were initially demonstrated in a SCID mouse model of B-cell lymphoma (Flavell et al., 2000a). SCID mice injected with Ramos cells (CD19 and CD20 positive) treated with the combination of rituximab and BU12-saporin showed significantly prolonged survival compared to either single therapy used alone (Flavell et al., 2000a). Initial experiments suggested a major role for a complement dependent mechanism, although direct cell signalling and apoptosis mechanisms were also proposed (Flavell et al., 2000b).

To determine if the effects observed in SCID mice are due to additive effects of the combination of rituximab and BU12-saporin *in vitro* investigation of the effects of the combination was required, also the ability of BU12-saporin to induce apoptosis needed to be determined. This chapter describes *in vitro* apoptosis assays carried out on several lymphoma cell lines to determine if the combination of rituximab and BU12-saporin induced a greater degree of apoptosis. The techniques used measure some of the characteristics of apoptosis, namely DNA fragmentation and the exposure of phosphatidyl serine on the external plasma membrane.

3.2 Results

3.2.1 Cell surface CD19 and CD20 expression on Ramos and Nalm 6 cells

Ramos and Nalm 6 cells were stained for single colour flow cytometry analysis to determine the expression level of CD19 and CD20 on the cell surface. The binding characteristics of rituximab, 1F5 and BU12 antibody by Ramos and Nalm 6 cells are shown in figure 3.1. The mean fluorescence intensity, (mean channel number) and standard deviation are shown for three independent repeats of the experiment. Both cell lines are CD19 positive (MFI Ramos 39.6 ±6.9, Nalm 6 51.0 ±20.2) and CD7 negative (MFI Ramos 2.2 ±0.7, Nalm 6 2.9 ±2.1) determined by BU12 antibody binding and the control HB2 antibody, binding detected by an appropriate secondary FITC conjugated antibody. Ramos cells are CD20 positive as determined by rituximab (MFI 202.9 ±38) and 1F5 binding (MFI 110.7 ±4.5). Rituximab and 1F5 did not bind to Nalm 6 cells.

Antibody (antigen)	Mean Fluorescent Intensity (MFI±SD)	
	Ramos	Nalm 6
Rituximab (CD20)	202.9 (±38)	2.4 (±0.4)
1F5 (CD20)	110.7 (±4.5)	2.1 (±0.1)
HB2 (CD7)	2.2 (±0.7)	2.9 (±2.1)
BU12 (CD19)	39.6 (±6.9)	51 (±20.2)

Table 3.1
Mean fluorescence intensity (arbitrary units) for rituximab, 1F5 and BU12 antibody binding on Ramos and Nalm 6 cells determined by indirect single colour staining flow cytometry. Standard deviations are shown for three independent repeats of the experiment.

3.2.2 Protein synthesis inhibition in Ramos cells by rituximab and BU12-saporin

To determine whether rituximab augments the dose dependent protein synthesis inhibition response of BU12-saporin, protein synthesis inhibition (PSI) assays were carried out. Lymphoma cell lines were exposed to dilutions of BU12-saporin in the presence and absence of rituximab on 96 well plates. Plates were then pulsed with ^{3}H-leucine for 16 hours and the cells harvested onto glass fibre disks. The amount of ^{3}H-leucine

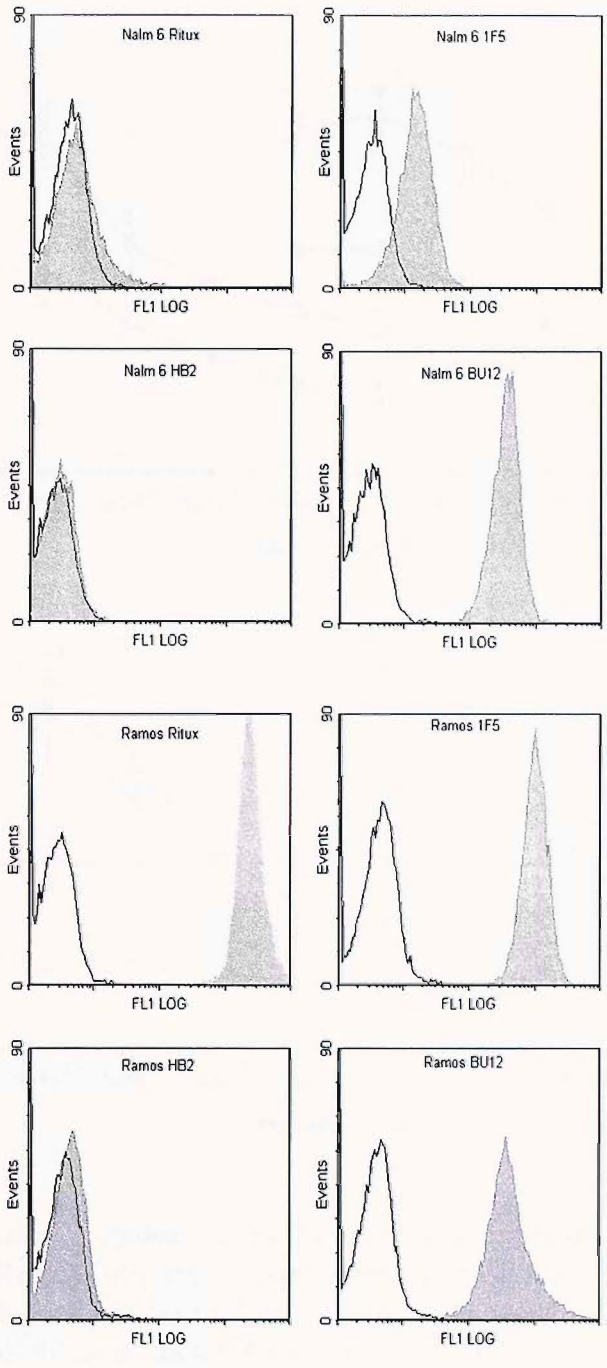

Figure 3.1
Flow cytometry profiles for Ramos and Nalm6 cells stained for CD19 (BU12) and CD20 (rituximab or 1F5) expression. Unstained controls are shown as open peaks. Cells were incubated with saturating concentrations HB2, rituximab, 1F5 and BU12 antibody (at 10µg/ml, 4°C) for one hour and read on an Epics XL flow cytometer (Beckman Coulter.) Data shown is representative of three identical repeats

a)

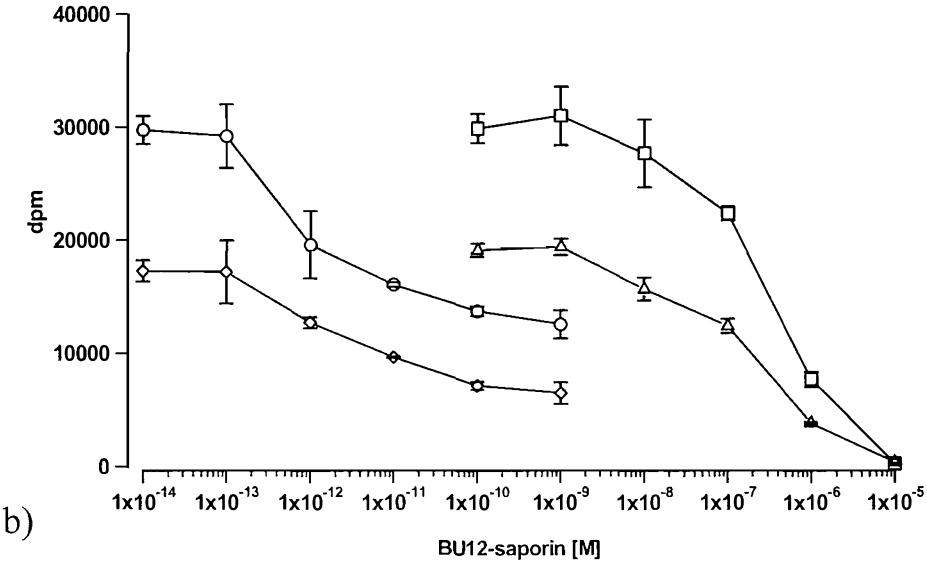

b)

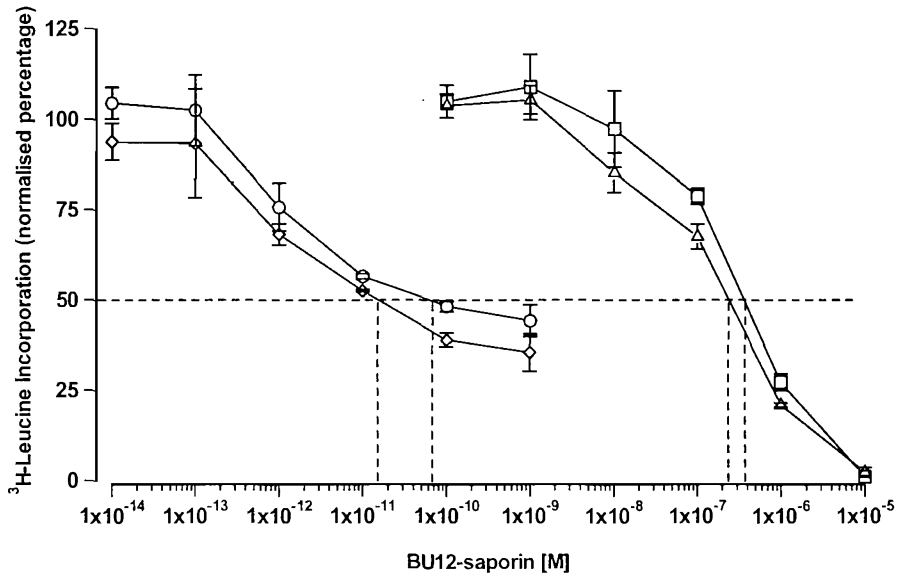

Figure 3.2

Representative dose response curves from a protein synthesis inhibition (PSI) assay carried out on Ramos cells. BU12-saporin or saporin alone was titrated in the presence and absence of rituximab at 10μg/ml. Cells were exposed to the drug combinations for 48 hours then pulsed with 1μCi 3H-leucine for 16 hours and harvested. Saporin alone (□), saporin with rituximab (△), BU12-saporin alone (○) and BU12-saporin with rituximab (◇) are shown. Points represent the mean of triplicate cultures, bars represent the standard deviation Sd(n-1) between triplicates. Data is representative of 5 identical repeats of this assay. Figure 3.2a shows raw data as decays per minute, figure 3.2b represents normalised data expressed as a percentage of ^{3}H-leucine incorporation by control cells or uptake by cells treated with rituximab alone.

incorporated into cellular proteins, thus the amount of protein synthesis was determined by scintillation counting (figure 3.2). The unconjugated RIP saporin was also titrated in the presence and absence of rituximab. Data are shown as a percentage of ^{3}H-leucine incorporation by untreated control cells, or for the titration of BU12-saporin carried out in the presence of rituximab, data is expressed as a percentage of ^{3}H-leucine incorporation by control cells treated with rituximab alone. This method of presenting data shows any additive effects caused by a combination of therapeutics. IC_{50} values were determined for each reagent and set of conditions under test (for full details of calculation see methods and materials 2.4).

Titration of BU12-saporin and saporin alone in a ^{3}H-leucine incorporation assay showed dose dependent protein synthesis inhibition in Ramos cells (figure 3.2 shows representative data from 6 independent repeats). Cells were exposed to BU12-saporin ($1x10^{-9}$M to $1x10^{-14}$M), and saporin ($1x10^{-5}$M to $1x10^{-10}$M), in the presence and absence of rituximab (10μg/ml). The results showed the IC_{50} value for Ramos cells exposed to BU12-saporin was $7x10^{-11}$M, and the IC_{50} value for cells treated with saporin alone was $4x10^{-7}$M (figure 3.2). The combination of BU12-saporin and rituximab decreased the IC_{50} to $1.5x10^{-11}$M, and the combination of saporin and rituximab gave an IC_{50} value of $2x10^{-7}$M. A mathematical mean average from the 6 repeats of this experiment gave an IC_{50} for BU12-saporin of $1.2x10^{-10}$M ($\pm 4.9x10^{-11}$) the IC_{50} for cells exposed to rituximab and BU12-saporin was $1.8x10^{-11}$M ($\pm 2x10^{-11}$).

On addition of rituximab to cells treated with saporin alone a 1 to 2 fold increase in potency was observed as shown by the decrease in the IC_{50} value. A similar effect was observed when BU12-saporin was titrated in combination with rituximab. With the combination of BU12-saporin and rituximab the augmentation effect was approximately a 5 (±2.6) fold increase in potency. The increase in potency on addition of rituximab was determined for each of the 6 independent repeats and an average determined from these values. This value has been quoted rather than the difference between the two mathematical means (although larger) as this does not represent the PSI data as accurately.

3.2.3 Rituximab and BU12-saporin induce DNA fragmentation in Ramos cells

To determine if the augmentation effects observed between rituximab and BU12-saporin in the PSI assay were due to increased levels apoptosis induced by the combination DNA fragmentation assays were carried out. Cells in culture were exposed to the antibody or immunotoxin individually or in combination for a period of 72 hours during which samples of cells were taken and stained with PI at three time points (24, 48 and 72 hours). Ramos cells were exposed to rituximab (10μg/ml), 1F5 antibody (10μg/ml) and BU12-saporin (10μg/ml) individually, and the combinations of rituximab or 1F5 antibody with BU12-saporin. Cells were also exposed to the constituent components of the immunotoxin, unconjugated BU12 antibody and saporin (at equimolar concentrations to BU12-saproin), to determine their contribution relative to the overall effect of BU12-saproin.

A single parameter FL3 histogram was used to determine the proportion of cells present in each stage of the cell cycle (representative raw data from one of three independent experiments is shown in figure 3.3). The fluorescence intensity, thus the amount of DNA increases across the x-axis. Cells with a normal diploid DNA content of 2N appear in the first peak, designated region A. These cells maybe described as in G_1 or G_0 resting phase. Cells in S phase, undergoing DNA synthesis, have an increasing amount of DNA and appear in region B. Region C contains cells with a DNA content of 4N therefore in G_2 or mitosis phase and are preparing to divide. Cells with less than the normal DNA content of 2N appear in region D. These cells are described as the sub G_0/G_1 population and are considered to be the results of DNA fragmentation and apoptosis.

Three independent repeats of the experiment were carried out, these data are summarised in histogram form in figure 3.4. The increase to the sub G_0/G_1 population caused by rituximab, 1F5 or saporin alone was approximately equal over the three time points. BU12 antibody has a greater initial effect at 24 hours, but this was not sustained at the later time points. Across the three time points the combination of saporin and rituximab and the combination of BU12 antibody and rituximab caused little change to the size of the sub G_0/G_1 population. BU12-saporin alone and in combination with rituximab and 1F5, at 48 and 72 hours, caused additive increases to the sub G_0/G_1 population over the three time points. This suggests it took longer for BU12-saporin to under go the processes of

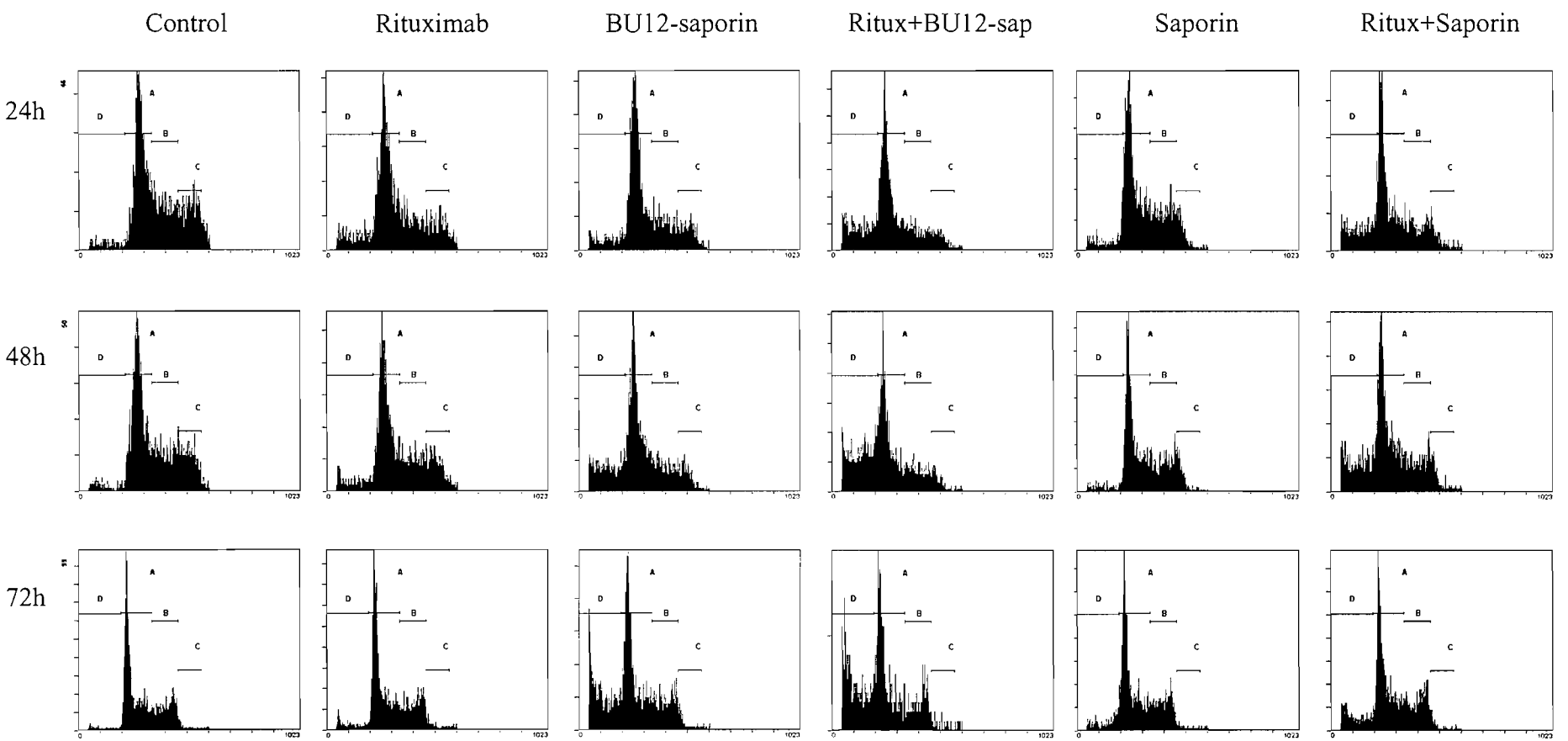

Figure 3.3 For full legend see page 88

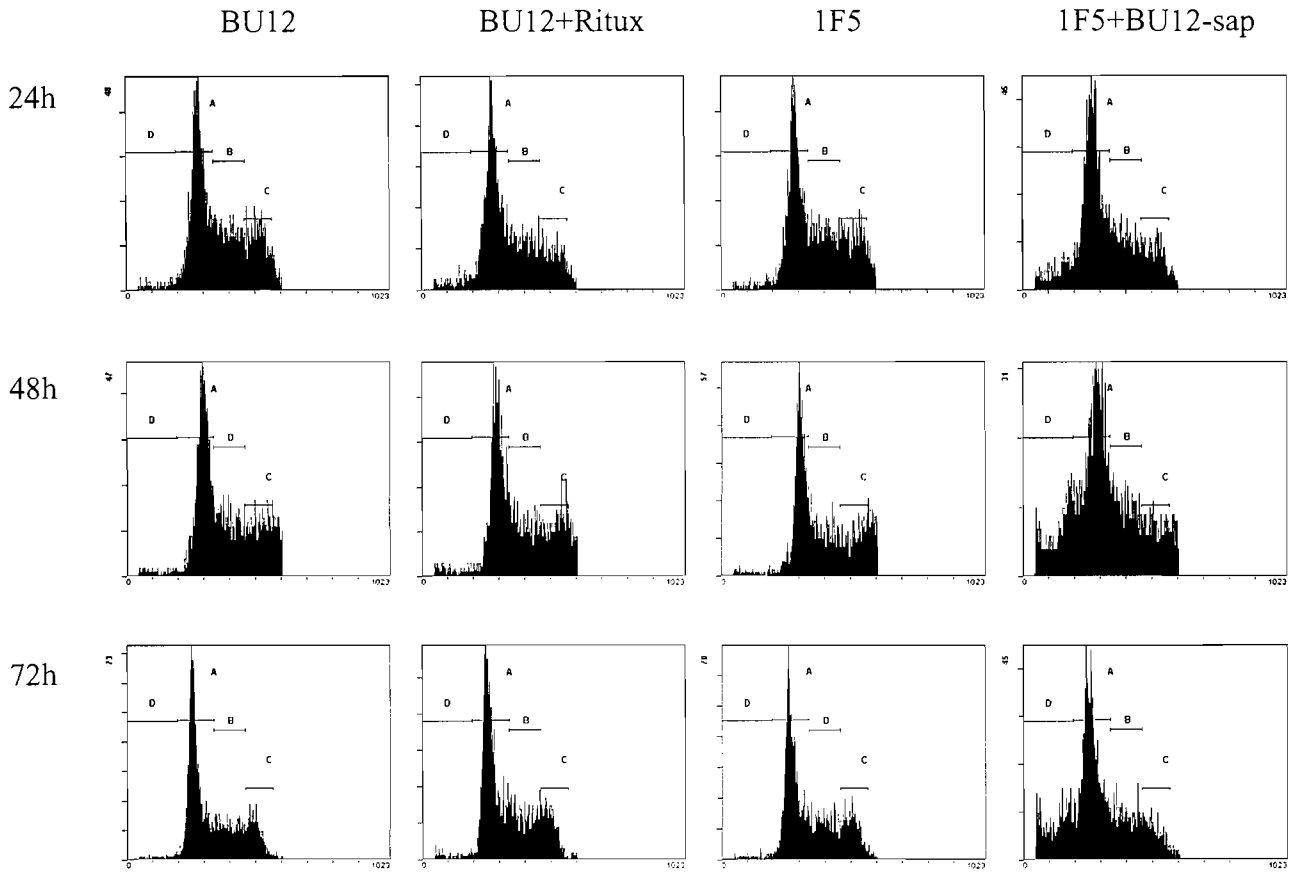

Figure 3.3
Cell cycle analysis by propidium iodide staining of Ramos cells exposed to rituximab, BU12-saporin, 1F5 antibody (all at 10μg/ml), saporin and BU12 antibody (at equimolar concentration to that present in BU12-saporin) individually and in combination and stained at 24, 48 and 72 hours. Histograms represent the amount of DNA present in the cell, gate A represent cells in G0/G1 phase, gate B, cells in S or M phase, gate C represents cells in G2 or early M phase and gate D represents the sub G0/G1 population.

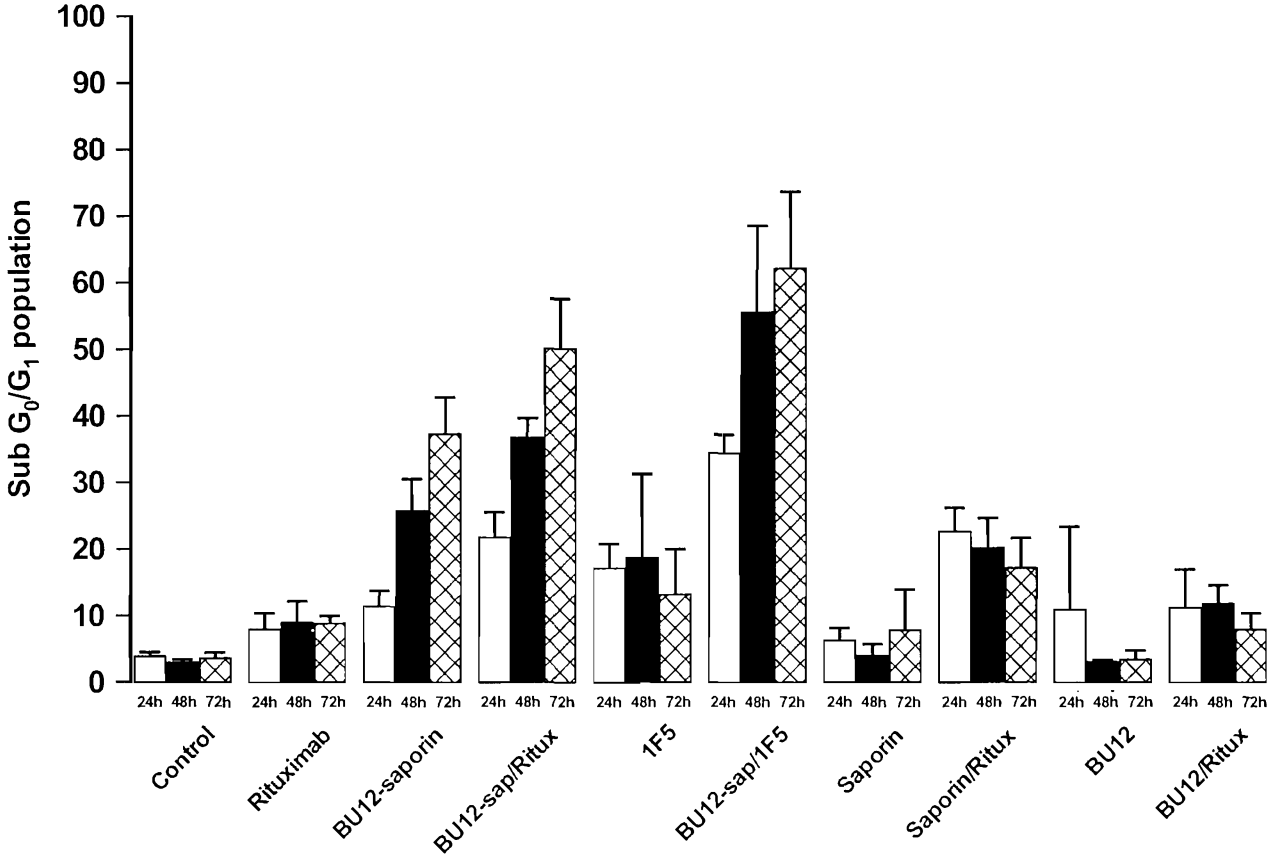

Figure 3.4
Percentage of apoptotic cells (sub G_0/G_1 population by PI stain) after treatment with rituximab (10μg/ml), BU12-saporin (10μg/ml), 1F5 murine anti-CD20(10μg/ml), saporin and BU12 antibody (at equimolar concentrations) individually and in combinations. Staining was carried out at 24(■), 48 (□) and 72 (▨) hours post exposure. Bars represent the mean and standard error of 6 replicate experiments.

internalisation, compared to the direct induction of apoptosis via cellular signalling events. But the effects of the immunotoxin by internalisation appear to be cumulative as the sub G_0/G_1 population rises over the three time points.

3.2.4 Statistical analysis of DNA fragmentation data

Independent t tests were carried out on the PI staining data to determine if effect of an antibody or immunotoxin on the sub G_0/G_1 population was significant compared to the effect on the sub G_0/G_1 population of the same antibody or immunotoxin used in combination (table 3.2). The effect of the combination of rituximab and BU12-saporin on the sub G_0/G_1 population was highly significant compared to the effect of rituximab alone at all three time points (24h $p = 0.006$, 48h $p = 0.0004$, 72h $p = 0.001$), and significant compared to the effect of BU12-saporin alone at two of the three time points (24h $p = 0.016$, 48h $p = 0.028$). The effect of the alternative anti-CD20 antibody, 1F5, on the sub G_0/G_1 population was significant compared to its effect in combination with BU12-saporin at all time points (24h $p = 0.003$, 48h $p = 0.024$, 72h $p = 0.003$). Inversely the effect of BU12-saporin in comparison to the effect of 1F5 and BU12-saporin in combination was also significant at all time points (table 3.2).

The combination of unconjugated BU12 antibody and rituximab does not have a significant effect ($p > 0.05$) on the sub G_0/G_1 population at any time point compared to rituximab exposure alone. Inversely the effect of the combination of rituximab and BU12 antibody compared to the effect of BU12 antibody alone was significant at two time points (48h $p = 0.006$, 72h $p = 0.051$, table 3.2). This shows the effect of BU12 antibody alone on the sub G_0/G_1 population was minimal, rituximab was required for the observed increase to the sub G_0/G_1 population.

Analysis of the combination of saporin and rituximab showed that compared to rituximab alone the combination of saporin and rituximab caused a significant increase to the sub G_0/G_1 population at all three time points (24h $p = 0.011$, 48h $p= 0.025$, 72h 0.036, table 3.2). Inversely, the effect of saporin on the sub G_0/G_1 population compared to the effect of the combination of rituximab and saporin was significant at two time points (24h p =

Independent t test for equality of means			
Samples under comparison		Time point	Significance at p=0.05
Rituximab	BU12-saporin + rituximab	**24h**	**0.006**
		48h	**0.0004**
		72h	**0.001**
BU12-saporin	BU12-saporin + rituximab	**24h**	**0.016**
		48h	**0.028**
		72h	0.076
1F5	BU12-saporin + 1F5	**24h**	**0.003**
		48h	**0.024**
		72h	**0.003**
BU12-saporin	BU12-saporin + 1F5	**24h**	**0.0004**
		48h	**0.020**
		72h	**0.028**
Saporin	Saporin + rituximab	**24h**	**0.006**
		48h	**0.004**
		72h	0.098
Rituximab	Saporin + rituximab	**24h**	**0.011**
		48h	**0.025**
		72h	**0.036**
BU12 antibody	Rituximab + BU12 antibody	24h	0.966
		48h	**0.006**
		72h	**0.051**
Rituximab	Rituximab + BU12 antibody	24h	0.416
		48h	0.310
		72h	0.604

Table 3.2
Summary of independent t tests carried out to determine the effect of individual antibodies and immunotoxins compared to their effect in combination by PI staining. Data is from figure 3.4 samples treated in active FCS only, bold text represents significant values at p=0.05. * Equal variances not assumed (Levene's test.)

0.006, 48h p = 0.004). This also showed that saporin alone is a more potent inducer of DNA fragmentation than BU12 antibody.

The DNA fragmentation data showed rituximab and BU12-saporin induce significantly more apoptosis in combination than either used alone. The effect of the combination of rituximab and BU12-saporin by PI staining maybe described as additive as the obtained sub G_0/G_1 population was slightly large than a theoretical sub G_0/G_1 population determined by the sum of the effects of BU12-saporin and rituximab. The effect of unconjugated BU12 antibody and saporin was minimal, some augmentation effects are observed with rituximab but these effects were not significant. The alternative murine anti-CD20 antibody 1F5 induced more DNA fragmentation than rituximab alone and also has an additive effect in combination with BU12-saporin.

3.2.5 Rituximab and BU12-saporin induce phosphatidyl serine exposure in Ramos cells

An alternative apoptosis assay, annexin V/PI staining was carried out to investigate further the apoptotic effects of BU12-saporin and investigate the augmentation effects of the combination of rituximab and BU12-saporin. Cells were exposed to rituximab, BU12-saporin and the combination of rituximab and BU12-saporin at three time points (24, 48 and 72 hours). Cells were also exposed to the constituent modalities of the immunotoxin. The quadrant plots from a one annexin V/PI staining experiment (representative of six independent experiments carried out) are shown in figure 3.5. PI staining is shown on the y axis and annexin V staining on the x axis. Cells in quadrant 3 are viable, these cells stain PI and annexin V negative. Quadrant 2 contains the PI positive and annexin positive cells; these dead cells are described as late apoptotic and secondary necrotic. Early apoptotic cells will stain annexin V positive, but PI negative (quadrant 4). Dead cells which stain PI positive have lost membrane integrity and are described as primary necrotic (quadrant 1), these cells have not been included in statistical analysis.

Cells in the secondary necrotic quadrant (staining annexin V and PI positive) were observed to separate into two sub-populations (figure 3.5). This was particularly apparent in rituximab and BU12-saporin treated cells at the later time points. The two sub-

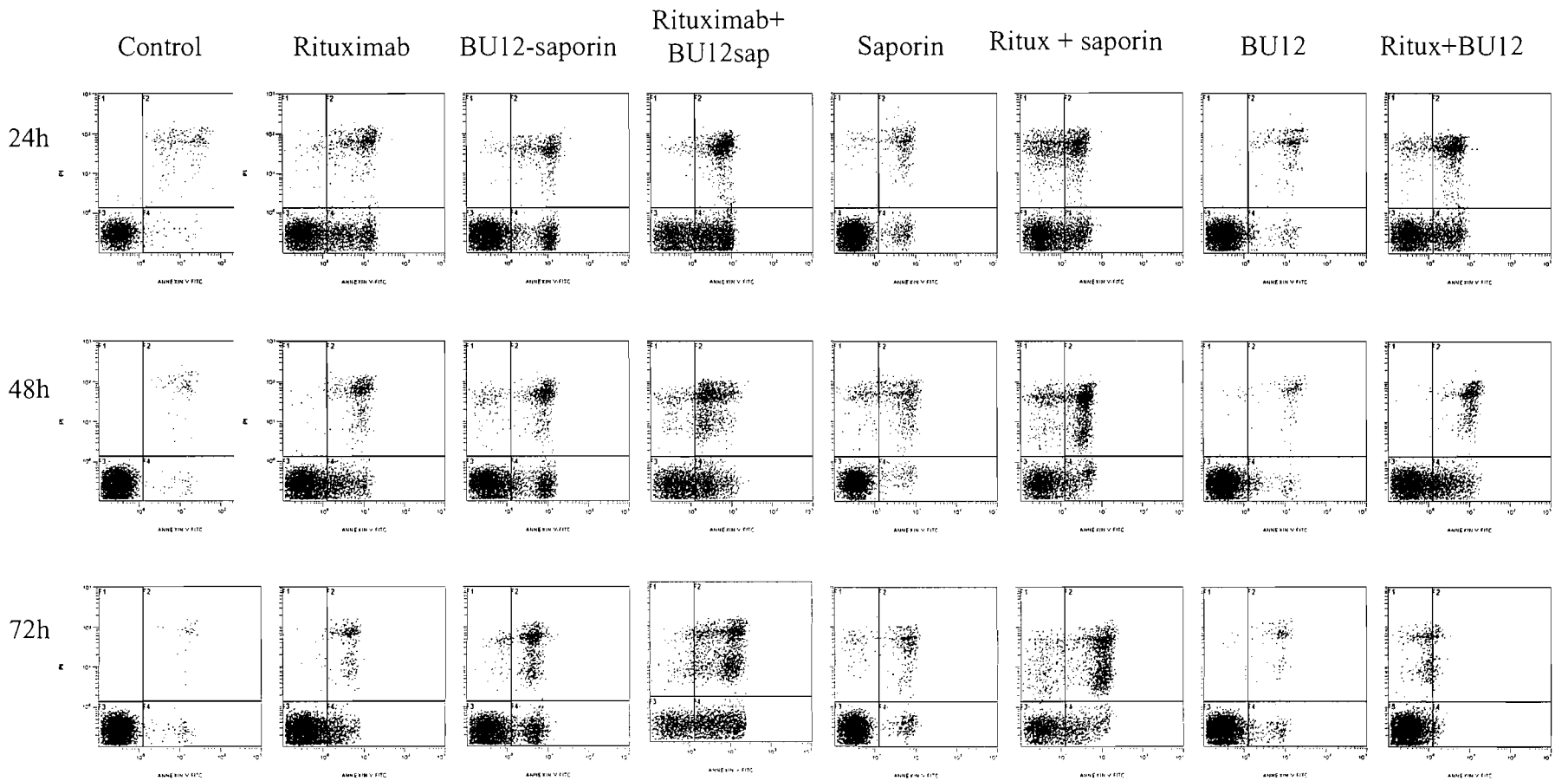

Figure 3.5

Raw data showing annexin V/PI staining of Ramos cells exposed to rituximab, BU12-saporin, (at 10μg/ml), saporin and BU12 antibody (at equimolar concentration to that present in BU12-saporin) individually and in combination and stained at 24, 48 and 72 hours. Annexin staining is shown on the x axis and PI staining on the y-axis. Quadrant 1 contains PI positive primary necrotic cells, quadrant 2, PI and annexin positive secondary necrotic cells, quadrant 3 viable cells and quadrant 4 PI negative annexin positive early apoptotic cells.

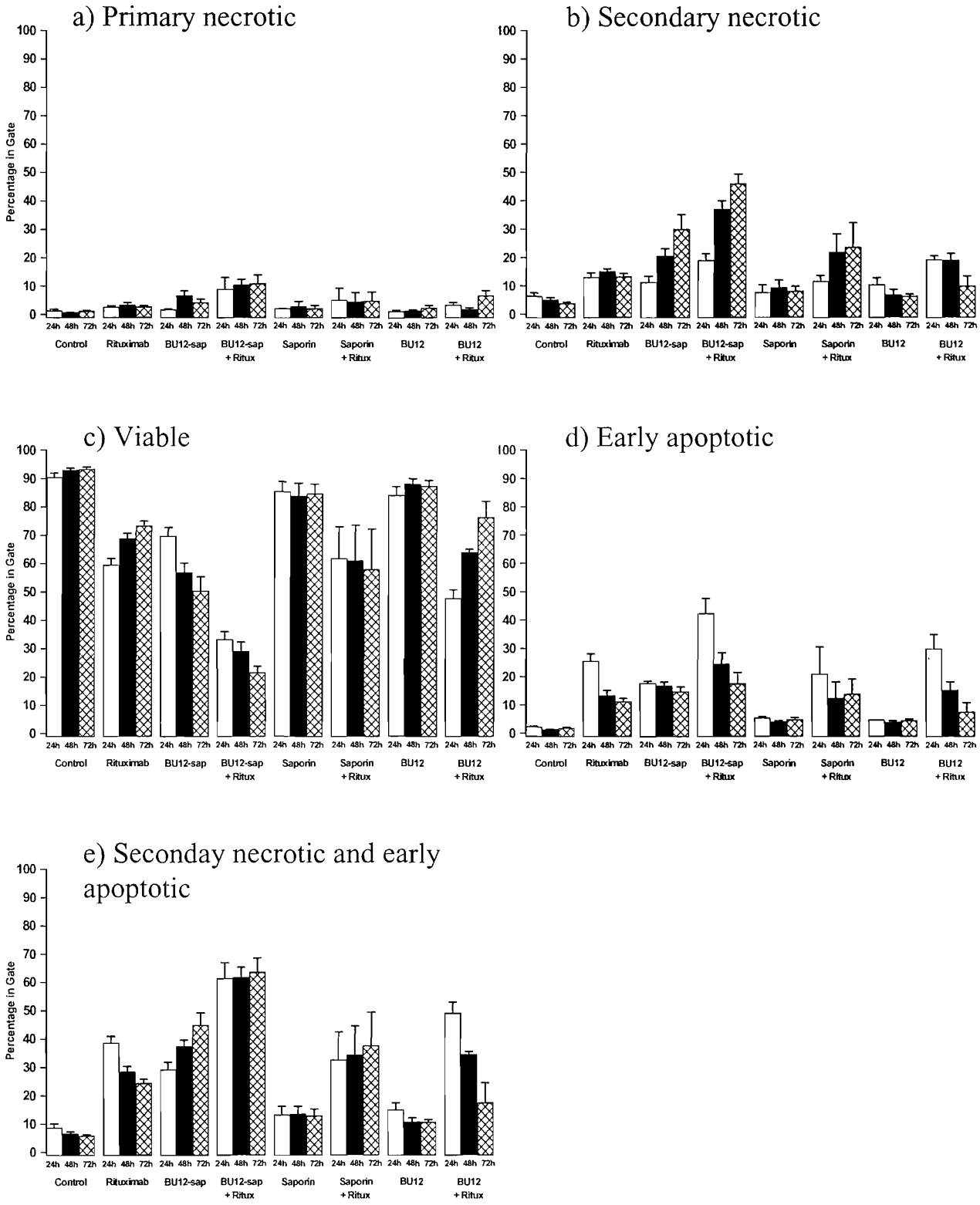

Figure 3.6

Summary of annexin V/ PI staining in Ramos cells exposed to rituximab at 10μg/ml, BU12-saporin at 10μg/ml, saporin and BU12 antibody (at equimolar concentrations) individually and in combination. Staining was carried out at 24(■), 48 (□) and 72 (▨) hours post exposure. Histograms represent the percentage of the cellular population determined to be; primary necrotic (PI positive) figure 3.6a, secondary necrotic (PI and annexin positive) figure 3.6b, viable (PI and annexin negative) figure 3.6c, and early apoptotic (annexin positive) figure 3.6d. Figure 3.6e represents the sum of the secondary necrotic and early apoptotic populations. Bars represent the mean and standard error of 6 replicate experiments.

populations are thought to represent cells in the later stages of apoptosis and truly secondary necrotic cells which had begun to lose membrane integrity and cell structure, thus staining more heavily with PI forming the second sub-population. These data presented in histogram form are shown in figure 3.6. A summary of the primary necrotic cells (annexin negative, PI positive) is shown in 3.6a, figure 3.6b shows secondary necrotic cells (annexin and PI positive), viable cells (annexin and PI negative) are shown in 3.6c and early apoptotic cells (annexin positive and PI negative are shown in 3.6d. Figure 3.6e shows the sum of the secondary necrotic and early apoptotic cells.

The population of primary necrotic cells for a successfully stained sample would be expected to be less than 10%. Larger primary necrotic populations are observed if samples were stressed in during preparation or staining, or if the population includes cells which have been dead for a longer period. Increases to the primary necrotic population were seen at 72h for cells treated with BU12-saporin and the combination of rituximab and BU12-saporin. Otherwise, the primary necrotic data falls with this range (<10%) suggesting adequate staining was achieved. The summary of the secondary necrotic cells (figure 3.6b) showed a consistent secondary necrotic population of 25% for cells treated with rituximab. Treatment of cells with BU12-saporin showed a consistent gradual increase to the secondary necrotic population. Cells treated with the combination of rituximab and BU12-saporin showed a secondary necrotic population characteristic of the BU12-saporin alone treated cells, with an overall increase attributable to the contribution of rituximab.

A significant decrease in the viable cell population is observed in all treated samples (figure 3.6c). Treatment with rituximab caused an initial drop in the viable population to approximately 60%, the population then increased over the next 48 hours. This showed the rituximab treated population was still able to replicate. An inverse trend was observed with BU12-saporin exposure, with subsequent decreases in the viable proportion of the population observed to 50% at 72 hours. BU12-saporin and rituximab treated cells showed an initial large decrease in viability to 30%, which decreased by a further 20% over the next 48 hours.

The early apoptotic population (annexin positive only) of untreated control cells was less than 5% (figure 3.6d). Treatment with rituximab showed an initial peak of early apoptotic cells, which stabilised at 48 and 72 hours to 10%, whereas treatment with BU12-saporin

showed a consistent early apoptotic population of approximately 20% at all three time points. Treatment with the combination of rituximab and BU12-saporin showed a pattern of apoptotic cells similar to that obtained for rituximab alone treated cells. An initial peak was observed, reaching 45% early apoptotic cells. Figure 3.6e shows the sum of the secondary necrotic and early apoptotic cells, which confirms rituximab treatment alone is unable to prevent further proliferation as the proportion of dead and apoptotic cells decreased. Treatment with BU12-saporin alone or in combination was potent enough to prevent further proliferation as the proportion of dead and apoptotic cells was constant or rising.

Exposing cells to the toxin saporin alone caused little increase to the secondary necrotic and early apoptotic population above the control, only a slight decrease was observed in the viable population (figure 3.6b,c,d). Saporin used in combination with rituximab was more effective, a further decrease was observed to the viable cells and the number of cells observed entering early apoptosis increased (figure 3.6c,d). Treatment with BU12 antibody alone was less effective than treatment with saporin alone. A slight decrease to the viable population was observed and only marginally more cells were observed entering early apoptosis and secondary necrosis (figure 3.6a-e). The combination of BU12 antibody and rituximab had a similar efficacy to the combination of saporin and rituximab, a larger decrease to the viable population was noted but similar numbers were recorded in the secondary necrotic and early apoptotic populations. The combination of rituximab and BU12 antibody was unable to prevent the viable proportion of cells increasing, whereas the combination of saporin and rituximab showed a constant viable population (figure 3.6c).

3.2.6 Statistical analysis of Annexin V/PI staining data

Independent t tests were carried out to compare to the effect of an antibody or immunotoxin to its effect used in combination for each population of annexin V/PI stained cells (table 3.3). Significance was observed in all of the stained populations (i.e. secondary necrotic, viable, early apoptotic and the combined secondary necrotic and early apoptotic) results were also significant comparing either rituximab or BU12-saporin alone to their

Samples under comparison		Time point	Significance at p=0.05			
			Secondary necrotic cells	Viable cells	Early apoptotic cells	secondary apoptotic + early apoptotic
Rituximab	BU12-saporin + rituximab	24h	0.067	**$3.6x10^{-5}$**	**0.019**	**0.004**
		48h	**0.0003***	**$1.3x10^{-6}$**	**0.028**	**$1.2x10^{-5}$**
		72h	**$5.2x10^{-6}$**	**$5.6x10^{-9}$**	0.187*	**0.0003***
BU12-saporin	BU12-saporin + rituximab	24h	**0.042**	**5.8x10-6**	**0.006***	**0.0004**
		48h	**0.002**	**0.0002**	0.567	0.772
		72h	**0.030**	**0.0005**	0.560*	**0.020**
Rituximab	Saporin + rituximab	24h	0.636	0.851*	0.552	0.449
		48h	0.186	0.603*	0.849	0.633*
		72h	0.349*	0.397*	0.510	0.380*
Saporin	Saporin + rituximab	24h	0.316	0.117	0.252*	0.136
		48h	0.156	0.161	0.222	0.177*
		72h	0.154	0.144	0.167	0.111
Rituximab	BU12 antibody + rituximab	24h	**0.043**	**0.025**	0.432	**0.051**
		48h	0.123	0.150	0.584	0.079
		72h	0.325	0.527	0.252	0.221
BU12 antibody	BU12 antibody rituximab	24h	**0.038**	**0.001**	**0.041***	**0.002**
		48h	**0.017**	**0.0005**	**0.018**	**0.0003**
		72h	0.386	0.146	0.425	0.398

Table 3.3
Summary of independent t tests carried out to determine the effect of individual antibodies and immunotoxins compared to their effect in combination by annexin V/PI staining. Data is from figure 3.6 samples treated in active FCS only, bold text represents significant values at p=0.05. * Equal variances not assumed (Levene's test.)

effect in combination. The early apoptotic population showed significance at the earlier time points but this disappears as the early apoptotic cells entered apoptosis and became late apoptotic and entered the secondary necrotic quadrant after 24 hours. Comparing the actual effect of the combination to a theoretical addition of the effect of rituximab and BU12-saporin, the effect of the combination on the viable cells can be described as additive. The early apoptotic population obtained after combination treatment was additive at 24 hours, and the secondary necrotic population was additive at 48 and 72 hours.

Compared to the effect of either the toxin saporin or rituximab the effect of the combination of saporin and rituximab was not significant (at $p = 0.05$) on any of the stained populations (secondary necrotic, viable, early apoptotic and the combined secondary necrotic and early apoptotic). This contrasts with the DNA fragmentation data, were saporin was found to be more effective than BU12 at increasing the sub G_0/G_1 population. The combination of the two antibodies rituximab and BU12 showed some significance at the earlier time points, particularly the secondary necrotic (24h $p = 0.038$, 48h $p = 0.017$, table 3.3) and viable cells (24h $p = 0.001$, $p = 0.0005$ table 3.4). Suggesting the combination of antibodies was more effective at inducing apoptosis than the combination containing the toxin saporin alone.

Therefore, by annexin V/PI staining rituximab and BU12-saporin caused significantly higher levels of apoptosis than either rituximab or BU12-saporin alone in an additive manner. The reduction in the proportion of viable cells with the combination was highly significant compared to rituximab or BU12-saporin alone. The combination of BU12 antibody and rituximab has shown some slightly significant effects, the combination of rituximab and saporin was not significantly effective.

3.2.7 Augmentation effects with alternative CD20 antibodies and protein synthesis inhibitors

To determine if an augmentation effect such as that observed with rituximab and BU12-saporin occurs between other known inhibitors of protein synthesis and other anti-CD20 antibodies experiments were carried out with cycloheximide and 1F5. Cycloheximide is a

known inhibitor of protein synthesis, via inhibition of peptidyl transferase of the larger 60S ribosomal subunit (Farber *et al.*, 1973). 1F5 is an alternative murine anti-CD20 antibody. Titrations of cycloheximide carried out on Ramos cells in the presence and absence of rituximab (figure 3.7) showed no augmentation or additivity of effect in the raw and normalised PSI data. At all three concentrations of rituximab (1, 10, and 50μg/ml) no augmentation effects were observed (figure 3.7), the IC_{50} values obtained for cycloheximide remained constant at $6x10^{-7}$M.

Annexin V/PI staining was carried out with the alternative murine CD20 antibody 1F5 in combination with BU12-saporin to determine if alternative CD20 antibodies also had an augmentation effect with BU12-saporin. A histogram summary of the stained populations is shown in figure 3.8. Cells were treated with rituximab, BU12-saporin and 1F5 alone and in combination (10μg/ml) at three time points, 24, 48 and 72 hours. The antibody 1F5 alone reduced the viable population more than rituximab alone, although neither antibody alone was able to prevent proliferation as over the three time points the numbers of viable cells treated with either antibody are observed to increase (figure 3.8c). The immunotoxin BU12-saporin alone was able to prevent further proliferation, over the three time points the percentage of viable cells decreased. The combination of 1F5 and BU12-saporin reduced viability to less than 10% whereas the combination of rituximab and BU12-saporin reduced viability to approximately 20%.

The early apoptotic populations are shown in figure 3.8d, cells treated with rituximab showed a peak of early apoptotic cells at 24 hours, apparent in cells treated with rituximab alone and in combination with BU12-saporin. After 24 hours the size of the early apoptotic population decreased as the secondary necrotic population grew. Treating cells with BU12-saporin resulted in a similar early apoptotic population (between 20%) at all three time points. Treating cells with 1F5 showed only a slightly greater proportion of early apoptotic cells than untreated control cells. This suggested that either 1F5 induced apoptosis earlier than 24 hours, or that 1F5 induced cell death by a different mechanism. It is interesting to note that the percentage of early apoptotic cells in 1F5 and BU12-saporin treated cells is lower than for BU12-saporin alone treated cells.

The proportion of secondary necrotic cells treated with 1F5 alone decreased over the time course due to the proliferation occurring within the sample (as discussed previously.) This

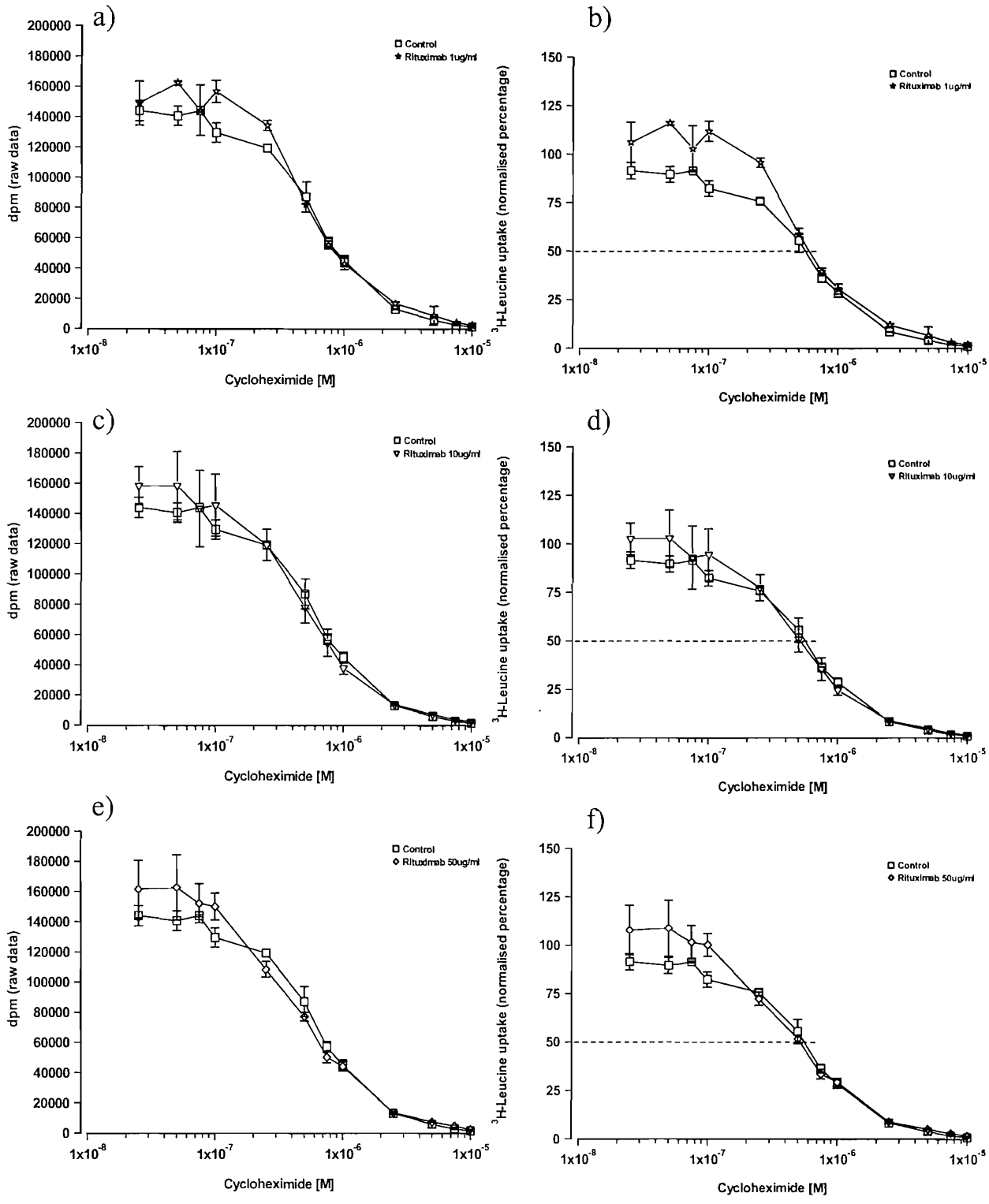

Figure 3.7

Dose response curves from a PSI assay showing the effect of cycloheximide titrated in the presence and absence of rituximab. Cells were exposed to the drug combinations for 24 hours then pulsed with 1μCi 3H-leucine for 16 hours and harvested. Cycloheximide alone (□), and rituximab at 1μg/ml (☆), 10μg/ml (▽) and 50μg/ml (◇) are shown. Points represent the mean of triplicate cultures, error bars represent the standard deviation Sd(n-1) between triplicates. Figures 3.7a, 3.7c and 3.7e show raw data as decays per minute, figures 3.7b, 3.7d and 3.7f represents normalised data expressed as a percentage of ^{3}H-leucine uptake by control cells or uptake by cells treated with rituximab alone.

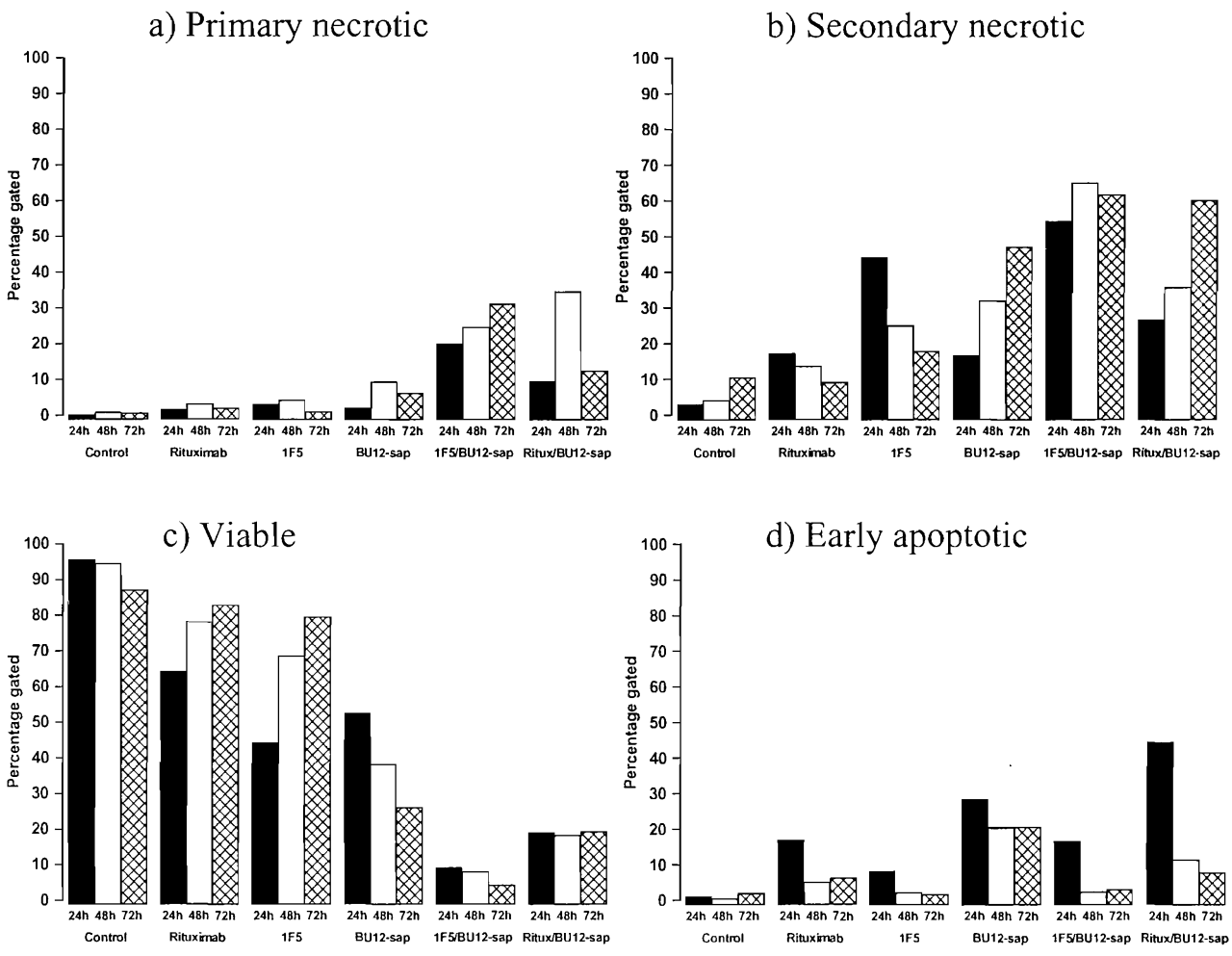

Figure 3.8
Annexin V/ PI staining of Ramos cells exposed to rituximab at 10ug/ml, 1F5 murine CD20 antibody 10ug/ml and BU12-saporin at 10ug/ml individually and in combination. Histograms represent the percentage of the cellular population determined to be; primary necrotic (PI positive) figure 3.8a, secondary necrotic (PI and annexin positive) figure 3.8b, viable (PI and annexin negative) figure 3.8c, and early apoptotic (annexin positive) figure 3.8d. Staining was carried out at 24(□), 48 (■) and 72 (▨) hours post exposure.

observation was also consistent for rituximab treated cells (figure 3.8b). Cells treated with the immunotoxin showed an increased secondary necrotic population. Treatment with BU12-saporin in combination with either anti-CD20 antibody resulted in a secondary necrotic population of 60%. The combination of 1F5 and BU12-saporin reached 60% after 24 hours, but with rituximab and BU12-saporin 60% was not reached until 72 hours. Increases to the secondary necrotic population above 60% have not been observed probably due to extremely damaged cells staining PI positive and moving into the primary necrotic gate (figure 3.8a).

In summary, no augmentation effects were observed with rituximab and cycloheximide in a PSI assay. The alternative murine anti-CD20 antibody 1F5 reduced viability and increased the secondary necrotic population without increasing the early apoptotic population by annexin V/PI staining.

3.2.8 Exposure of alternative lymphoma cell lines to rituximab and BU12-saporin

A panel of alternative lymphoma cell lines was treated with BU12-saporin and rituximab to gauge the range of response to BU12-saporin alone and in combination with rituximab in other cell lines. The alternative cell lines used, like Ramos, are derived from Burkitts lymphoma and are CD19 and CD20 positive (see chapter two for full details of cell lines used.) Titrations of BU12-saporin in the absence and presence of rituximab in PSI assays carried out on Daudi, Raji and Namalwa cells showed similarities to the behaviour of Ramos cells (figure 3.9.)

The sensitivity of these alternative cell lines to the immunotoxin BU12-saporin alone varied between the cell lines and also between identical repeats of the experiment. Raji cells were the least sensitive to BU12-saporin, showing an IC_{50} of $2x10^{-7}M$ (figure 3.9d), whereas Daudi and Namalwa cells had an IC_{50} of $8x10^{-10}M$ and $2x10^{-10}M$ respectively (figures 3.9b and f). Ramos cells were the most sensitive overall, although the sensitivity is subject to some variation between experiments. No standard deviations are shown for the IC_{50}s determined due to these wide variations.

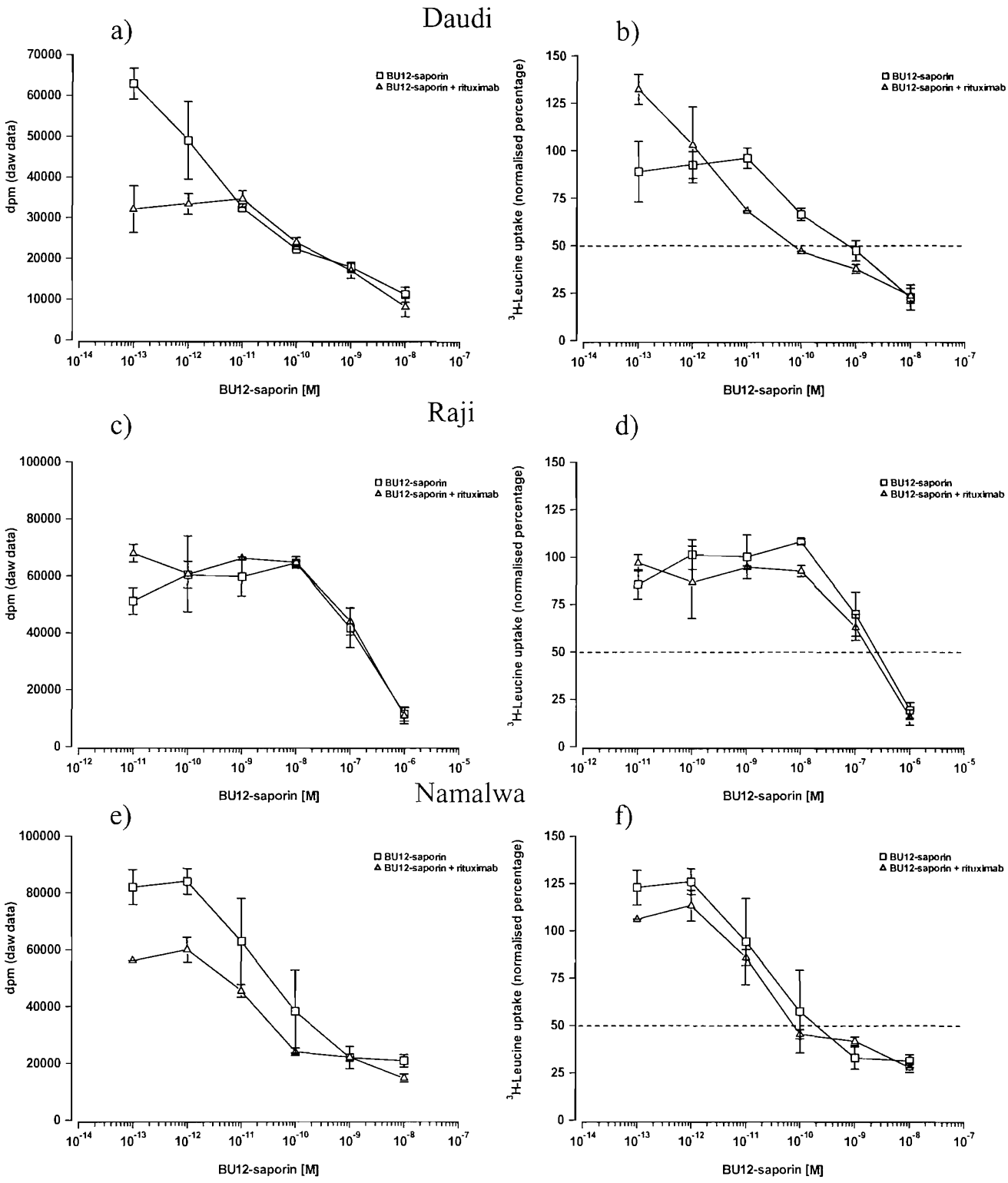

Figure 3.9

Dose response curves from a PSI assay carried out on Daudi, Raji and Namalwa cells. BU12-saporin was titrated in the presence and absence of rituximab at 10µg/ml. Cells were exposed to the drug combinations for 48 hours then pulsed with 1 µCi 3H-leucine for 16 hours and harvested. Symbols represent BU12-saporin alone (□) and BU12-saporin with rituximab (△). Points represent the mean of triplicate cultures, error bars represent the standard deviation Sd(n-1) between triplicates. Figures 3.9a, 3.9c and 3.9e show raw data as decays per minute, figures 3.9b, 3.9d and 3.9f represents normalised data expressed as a percentage of ^{3}H-leucine uptake by control cells or uptake by cells treated with rituximab alone.

The addition of rituximab to BU12-saporin treated Daudi and Raji cells was not apparent in the raw (dpm) leucine incorporation data, in Namalwa cells leucine incorporation was decreased several fold by the addition of rituximab (figure 3.9e). In the plots of normalised data (figure 3.9 b,d,f) an augmentation effect was observed on the addition of rituximab to the BU12-saporin titrations in three cell lines. Daudi cells show a pronounced augmentation of 1 log increase in potency on addition of rituximab. The augmentation effect in Raji cells was minor, approximately 1 fold, equal to the augmentation effect observed between saporin and rituximab in Ramos cells. In Namalwa cells the augmentation was similar to that observed between BU12-saporin and rituximab in Ramos cells, in this experiment approximately 4 fold. Some caution is attached to these observations as an augmentation effect was not observed in the raw data for Daudi and Raji cells, suggesting a discrepancy between control and rituximab treated control cell leucine incorporation.

3.2.9 DNA fragmentation in lymphoma cells lines treated with rituximab and BU12-saporin

To investigate further the DNA fragmentation effects of the combination of rituximab and BU12-saporin in alternative lymphoma cell lines, PI staining of Raji, Namalwa and Daudi cells treated with rituximab and BU12-saporin at 48 and 72 hours post exposure was carried out. The percentage of the population in the sub G_0/G_1 phase of the cell cycle was recorded from three independent repeats of the experiment for each of the four cell lines. Figure 3.10 shows the percentage of cells determined to be in the sub G_0/G_1 stage of the cell cycle from a single parameter FL3 histogram of PI stained cells.

Rituximab alone has little effect above the control in causing the induction of DNA fragmentation (figure 3.10). This result was reflected in all the cells lines shown. BU12-saporin used alone caused the sub G_0/G_1 population, in all four cell lines, to increase to 30% of the whole population. The effect of the combination of rituximab and BU12-saporin on the sub G_0/G_1 population is variable. In Ramos cells the effect of the combination appears additive, the combination appears to have minimal effects on Raji

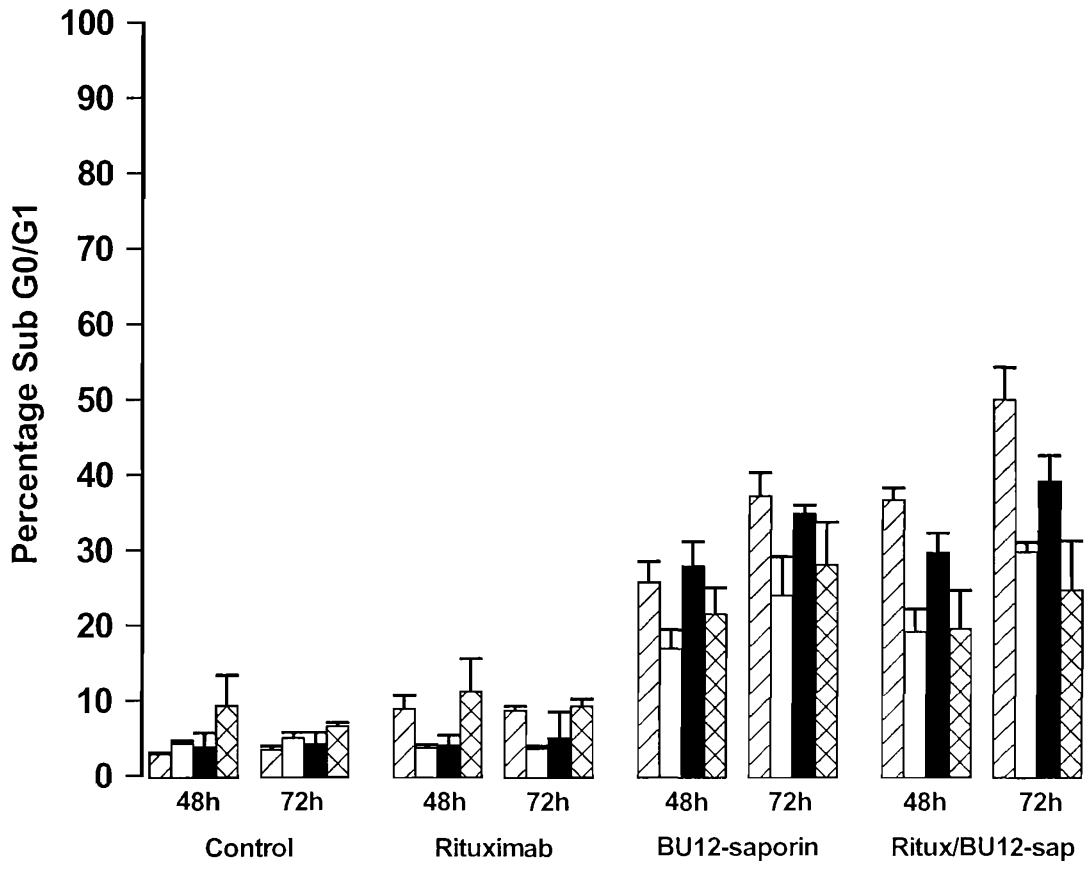

Figure 3.10
Percentage of apoptotic (sub G_0/G_1 population) Ramos (▨), Raji (□), Namalwa (■), and Daudi (▩) cells following treatment with rituximab (10μg/ml), BU12-saporin (10 μg/ml) individually and in combinations. PI staining was carried out 48 and 72 hours following treatment. Bars represent the mean of the percentage of the population determined to be in the sub G_0/G_1 stage of the cell cycle. Error bars represent the positive standard error between triplicates.

and Namalwa cells. With the combination, Daudi cells appear to show a decreased sub G_0/G_1 population.

3.2.10 Statistical analysis of DNA fragmentation data

To determine if each of the cell types behave in a statistically similar way to exposure to rituximab and BU12-saporin statistical analysis of these data (figure 3.10) by ANOVA was carried out. Statistical analysis by one way ANOVA showed the behaviour of the alternative lymphoma cell lines after individual rituximab and BU12-saporin exposure to be similar but the cell lines responded differently to the combination (table 3.4). Analysis showed that the effect of either rituximab or BU12-saporin alone on the sub G_0/G_1 population was not significantly different between the four cells lines, i.e. rituximab or BU12-saporin used alone had similar effects on Ramos, Raji, Namalwa and Daudi cells. If rituximab and BU12-saporin were used in combination there was a significant difference between the sub G_0/G_1 populations for the four cell lines (48h $p = 0.016$, at 72h $p = 0.015$). This showed the effect of the combination of rituximab and BU12-saporin was not similar in the four cell lines tested. This is due to the increased sub G_0/G_1 population in combination treated Ramos cells and the reduced effect on Daudi cells.

Comparison of treated Ramos, Raji, Namalwa, and Daudi cells	Time Point	F factor	Significance at $p = 0.05$
Control	48h	1.600	0.264
	72h	1.918	0.205
Rituximab	48h	2.193	0.167
	72h	2.246	0.160
BU12-saporin	48h	2.482	0.135
	72h	2.083	0.181
Combination	48h	**6.423**	**0.016**
	72h	**6.593**	**0.015**

Table 3.6
Summary of statistical analysis by one way ANOVA for the sub G_0/G_1 population of cells determined by PI staining Ramos, Raji, Namalwa and Daudi cells treated with rituximab at 10μg/ml and BU12-saporin. Data represents three independent experiments carried out on each cell line at 48 and 72 hours post exposure. Significant results at $p = 0.05$ are denoted by bold text.

3.2.11 Annexin V/PI staining of rituximab and BU12-saporin treated Nalm 6 cells

Annexin V/PI staining was carried out on Nalm 6 cells to compare the effect of the combination of rituximab and BU12-saporin on a CD20 negative cells line. Ramos and Nalm 6 cells treated with rituximab and BU12-saporin individually and in combination show clear differences between the two cells lines by annexin V/PI staining. These data presented in histogram form in figure 3.11, show the primary necrotic, secondary necrotic, viable and early apoptotic populations of Ramos and Nalm 6 cells at 24, 48, and 72h post exposure to rituximab, BU12-saporin and cisplatin. The primary necrotic populations are under 10%, suggesting staining is efficient and the cells have not been unduly stressed during the staining process (figure 3.11a).

Examining the viable population (figure 3.11c) showed marked differences between the Ramos and Nalm 6 cells lines. Ramos cells treated with rituximab alone show approximately a 10% decrease in viability, in comparison the Nalm 6 cells show a reduction in viability equal to untreated control cells. The effect of BU12-saporin on the two cell lines was also different even though CD19 expression from on the two cell lines would appear to be similar (figure 3.11). Ramos cells appear to be slightly more sensitive to BU12-saporin than Nalm 6 cells. Combination treatment reduces the viability of Ramos cells to 20% by 72h compared to Nalm 6 cells whereas viability of combination treated cells reflects the effect of BU12-saporin alone. These differences were attributed to the absence of CD20 expression on Nalm 6 cells. It is also noted that viability of Nalm 6 cells was reduced earlier than the viability of Ramos cells by cisplatin.

These observations are reflected in the early apoptotic populations shown in figure 3.11d. Rituximab alone had no effect on the early apoptotic population of Nalm 6 cells, and BU12-saporin appeared to have a slightly stronger effect on the early apoptotic population in Ramos than Nalm 6 cells (figure 3.11d). The effect of the combination on Ramos cells appeared to be additive and in Nalm 6 reflect the effect of BU12-saporin used alone. The levels of BU12-saporin treated early apoptotic cells decreased over the time period. This was due to the cells entering the latter stages of apoptosis and entering the secondary necrotic quadrant. The secondary necrotic populations confer that rituximab has an effect on Nalm 6 cells comparable to untreated control cells. The effect of the combination of rituximab and BU12-saporin had the observed effect of BU12-saporin alone. In Nalm 6

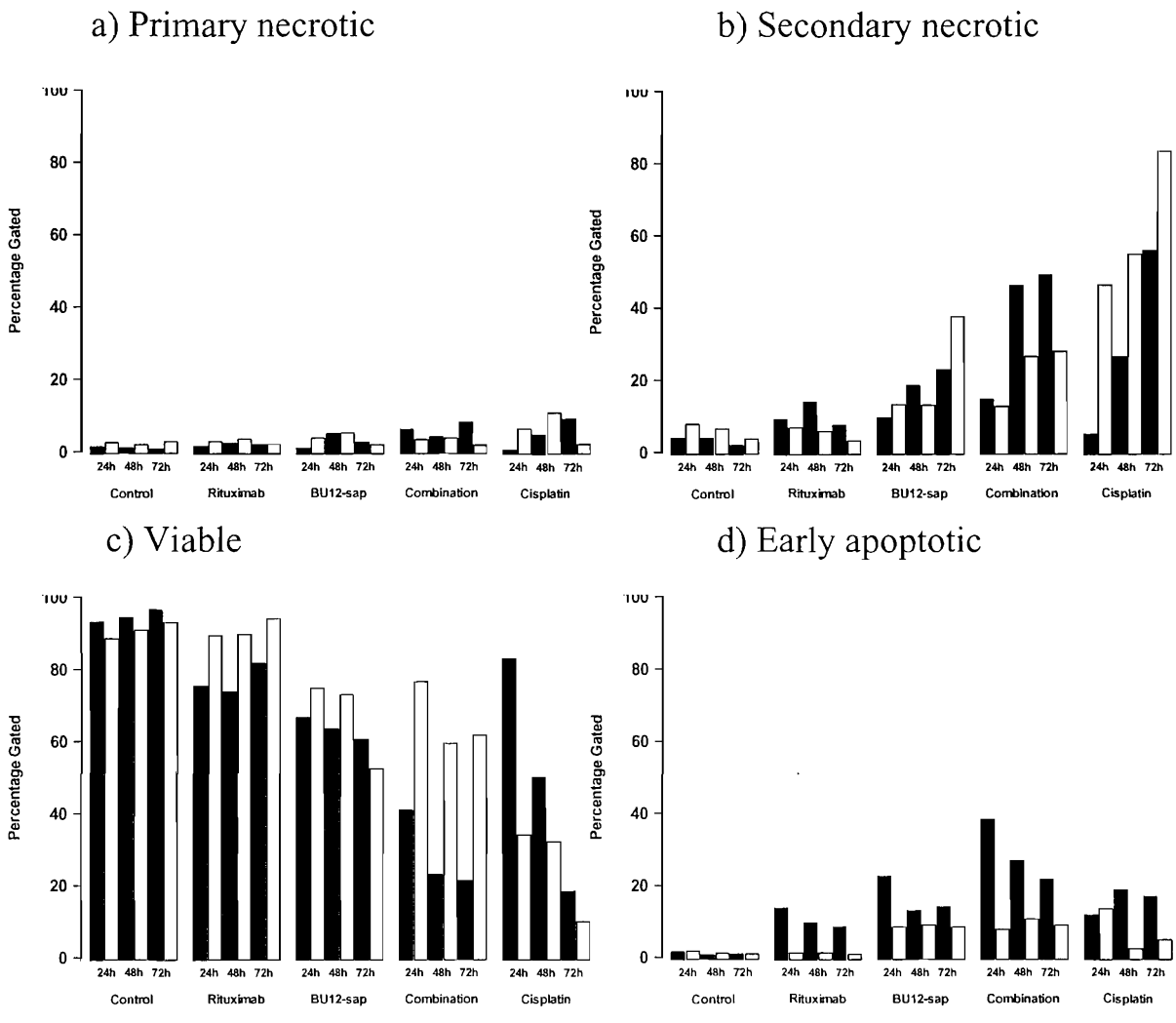

Figure 3.11
Annexin V/ PI staining of Ramos and Nalm6 cells exposed to rituximab (10μg/ml), BU12-saporin (10μg/ml) individually and in combination and cisplatin (1μg/ml). Staining of Ramos cells (■) and Nalm6 cells (□) was carried out at 24, 48 and 72 hours post exposure. Histograms represent the percentage of the cellular population determined to be; primary necrotic (PI positive) figure 3.11a, secondary necrotic (PI and annexin positive) figure 3.11b, viable (PI and annexin negative) figure 3.11c, and early apoptotic (annexin positive) figure 3.11d.

cells at 48h and 72h, reduced numbers of early apoptotic cells and increased secondary necrotic populations were observed probably due to the quicker effect cisplatin appears to have on Nalm 6 than Ramos cells.

3.3 Discussion

These studies were undertaken to determine the effect of rituximab on the protein synthesis inhibition and apoptosis inducing capacity of BU12-saporin. The combination of rituximab and BU12-saporin was shown to augment PSI in a ^{3}H-leucine incorporation assay in a variety of lymphoma cell lines. Rituximab and BU12-saporin were shown to induce DNA fragmentation and the combination of rituximab and BU12-saporin shown to significantly increase the sub G_0/G_1 population in an additive manner. By annexin V/PI staining the combination of rituximab and BU12-saporin has shown significant increases to the early apoptotic populations and highly significant decreases to the viable population.

Immunophenotyping experiments showed the Ramos and Nalm 6 cell lines used in this chapter are both CD19 positive and CD7 negative. Ramos cells are CD20 positive and stain with both rituximab and 1F5, whilst Nalm 6 cells are CD20 negative, no staining was observed with rituximab and a small amount of non-specific staining was observed with 1F5. Ramos cells expressed CD19 and CD20 at high levels, although there was little heterogeneity in CD20 expression, the level of CD19 expression was lower and expression was variable within the population (broader peak, figure 3.1). This may explain some of the variability in response observed to BU12-saporin.

3.3.1 Protein synthesis inhibition by rituximab and BU12-saporin

In a ^{3}H-leucine uptake assay (figure 3.2) saporin and BU12-saporin were shown to cause protein synthesis inhibition in a dose dependent manner. The immunotoxin BU12-saporin was over 3-logs more potent than the toxin saporin alone. Exposing Ramos cells to rituximab in combination with BU12-saporin, or exposing cells to the combination of rituximab and saporin caused increased levels of protein synthesis inhibition in cells. In the raw PSI assay data (figure 3.2a), decreased levels of ^{3}H-leucine incorporation were observed in combination with rituximab.

This effect is illustrated by a decreased IC_{50} values obtained from the normalised data (figure 3.2b, data are shown as a percentage of uptake by untreated control cells or cells treated with rituximab alone), in the case of saporin from $3x10^{-7}$M to $2x10^{-7}$M, the increase in potency on combination with rituximab is approximately 1-fold. For BU12-saporin the effect of the addition of rituximab was approximately, a 5-fold increase in potency as represented by a decreased IC_{50} value, a change from $7x10^{-11}$M to $1.5x10^{-11}$M was observed. Normalising these data suggested that this was an additive effect due to the combination of rituximab and BU12-saporin. These data are consistent with previous published observations (Flavell *et al.*, 2000b).

An alternative anti-CD30 saporin containing immunotoxin has been previously reported in a similar PSI assay to have an IC_{50} of $3.2x10^{-13}$M in the Hodgkin's lymphoma cell line L540. In this report an IC_{50} for saporin alone was determined to be $4.0x10^{-9}$M (Bolognesi *et al.*, 1996). These reported IC_{50} values show an increased potency compared to BU12-saporin IC_{50} demonstrated here (although BU12-saporin has not been tested on L540 cells). The increase in activity between the unconjugated toxin and the immunotoxin is similar in both cases, between 3 to 4 logs. Saporin containing immunotoxins have been shown previously to be more efficient at inhibiting protein synthesis than momordin and PAP-S containing immunotoxins directed at CD22 (Bolognesi *et al.*, 1998).

3.3.2 Cell cycle analysis and DNA fragmentation

Cell cycle analysis carried out by PI staining showed the combination of BU12-saporin and rituximab caused a significant increase to the sub G_0/G_1 population in an additive manner (figure 3.4). This effect was significant compared to the effect of BU12-saporin alone or the effect of rituximab alone. From these data the onset of DNA fragmentation and the induction of apoptosis could be inferred. Additional experiments have excluded any substantial effects from the constituent immunotoxin components, BU12 antibody and saporin toxin. Comparing the effect of an antibody or toxin in combination with its effect alone showed the relative contribution of the modality to the effect of the combination (table 3.2). The increase in the sub G_0/G_1 population when cells were treated with the combination of rituximab and BU12-saporin is significant compared to either rituximab or

BU12-saporin used alone. (Except for BU12-saporin compared to the combination ($p = 0.076$) at 72h). 1F5 antibody and BU12-saporin used in combination showed a significant improvement in comparison to the use of either 1F5 antibody or BU12-saporin alone. 1F5 antibody has previously been shown to be less effective than rituximab in causing the induction of apoptosis (Shan *et al.*, 2000), these data showed 1F5 antibody to be more effective than rituximab, alone and in combination with BU12-saporin.

Previously rituximab alone has been shown to induce apoptosis and cause a significant increase in the sub G_0/G_1 population (Ghetie *et al.*, 1992, Demidem *et al.*, 1997). Saporin containing immunotoxins directed against CD30 and CD22 have previously been shown to induce DNA fragmentation (Bolognesi *et al.*, 1996 and 1998).Other work has shown saporin is able to induce chromatin condensation, nuclear fragmentation and blebbing and significant increases to the sub G_0/G_1 population (Bergamaschi *et al.*, 1996, Bagga *et al.*, 2003). These effects were 2-3 logs more effective in saporin conjugated to an antibody, which is confirmed in the results described here for BU12-saporin.

Independent t-test comparisons on these data have confirmed the statistical significance of using the combination of BU12-saporin and rituximab, compared to either rituximab or BU12-saporin. This suggested that, as with exposure to the combination of BU12-saporin and rituximab in the protein synthesis inhibition assay, the effect of the combination can be described as additive. This additivity of effect of using rituximab and BU12-saporin at saturating concentrations suggests that BU12-saporin and rituximab maybe causing cell death by separate mechanisms.

A technical issue should be noted here regarding the PI data shown in this chapter. The gates determining the sub G_0/G_1 population and other stages of the cell cycle have been allocated by eye rather than by algorithm. Where the sub G_0/G_1 population is a separate peak this is not a problem, in some cases the sub G_0/G_1 population forms a shoulder or shift to the G_0/G_1 population peak. Assigning a percentage to a population like this is more difficult and open to interpretation. Interpretation of the percentage of a population with less than the normal DNA content also does not allow of the origin of the DNA fragments to be taken into consideration. Thus a few cells may fragment into many pieces or a large number of cells into a few slightly smaller pieces. PI staining data presented here is a good

indication that DNA fragmentation is occurring although these results may not accurately represent the proportion of the population undergoing apoptosis.

3.3.3 Annexin V/PI staining of Ramos cells exposed to rituximab and BU12-saporin

The combined annexin V/PI staining technique has been used successfully to distinguish between cells undergoing different stages of apoptotic or necrotic death. Cells exposed to combinations of rituximab and BU12-saporin consistently showed significantly decreased viability and significantly increased numbers of cells entering necrosis and apoptosis in an additive manner, compared to control cells or cells exposed to the constituent parts of the immunotoxins i.e. saporin or BU12 antibody, or either modality alone.

The technique of using combined annexin V/PI staining accurately represents the proportion of culture entering the early stages of apoptosis. Cells are observed to shift from the early apoptotic to secondary necrotic quadrants as they enter the later stages of apoptosis. A more accurate picture of the cell undergoing death processes can therefore be obtained by adding the secondary necrotic population and early apoptotic populations. This suggests approximately 60% of the population was under going death processes on treatment with the combination of rituximab and BU12-saporin. It is suspected the peaks of primary necrotic cells appearing after treatment with the combination in the latter stages of the experiment (figure 3.6) are not due to failed staining, but due to cells in a late stage of death and starting to disintegrate as the secondary necrotic population was not seen to rise above 60%.

T-tests were carried out to determine the contribution of an antibody or toxin compared to the effect of the antibody or toxin in combination by annexin V/PI staining are shown in table 3.3. Comparisons are shown for the secondary necrotic, viable, early apoptotic and the sum of the secondary necrotic and early apoptotic populations. The use of rituximab and BU12-saporin in combination was significant in all cellular populations (secondary necrotic, viable, early apoptotic and the sum of the secondary necrotic and early apoptotic) compared to the effect of either rituximab or BU12-saporin alone. This suggests BU12-saporin and rituximab work in an additive manner. As both reagents are at saturating

concentrations this suggests BU12-saporin and rituximab may cause cell death via separate mechanisms.

For the combination of rituximab and BU12-saporin compared to the effect of rituximab alone two points do not appear to show statistical significance (table 3.3). Significance was not observed at 24 hours in the secondary necrotic population, possibly due to the time required for the internalisation of BU12-saporin. The second suggests the number of early apoptotic cells in the combination of BU12-saporin and rituximab were not significant compared to BU12-saporin alone at 72 hours. This phenomenon is also apparent in the inverse comparison, comparing the effect of BU12-saporin to the effect of rituximab and BU12-saporin in combination. This was probably due to the number of early apoptotic cells decreasing by 72 hours, as these cells become secondary necrotic as they lose membrane integrity and become PI positive.

Saporin containing immunotoxins have previously been shown to cause apoptosis by annexin V/PI staining in T cells (Tazzari *et al.*, 2001). Rituximab alone or with a cross linking secondary antibody has been shown by many authors to induce apoptosis by annexin V staining (Hofmeister *et al.*, 2000, Pedersen *et al.*, 2002). It has also been reported that rituximab is only able to induce apoptosis detectable by annexin V staining in the presence of normal human sera (Bellosillo *et al.*, 2001), or an augmented apoptotic response with rituximab used in combination with retinoids or glucocorticoid (Shan *et al.*, 2001, Rose *et al.*, 2002).

The patterns of significance comparing the effects of BU12 antibody and saporin used alone and in combination, by annexin V/PI stain suggest that saporin was less effective than BU12 antibody. The effect of the combination of saporin and rituximab was not significant by annexin V/PI staining (table 3.3), whereas the combination of saporin and rituximab (by PI staining) caused significant increases to the sub G_0/G_1 population (table 3.2). This difference may have been due to the effect of saporin on the fundamentally different cellular properties these two techniques are assessing. Or these differences may have been due to variations in the samples stained in each technique although this is unlikely with six replicates of each carried out. The combination of rituximab and BU12 antibody is significant compared to BU12 antibody alone (secondary necrotic and viable cells, table 3.3). In both sets of data, (annexin V/PI and PI) the effect of the combination

of BU12-saporin and rituximab was significant compared to either used alone. The combination of BU12 antibody and rituximab was surprisingly significant at several points in both experiments. BU12 antibody was ineffective alone, suggesting the significant points are due to the action of rituximab in the combination samples.

Whilst comparing the PI and annexin V/PI staining data it must be taken in to consideration that external exposure of phosphatidyl serine is an earlier event in the induction of apoptosis than DNA fragmentation, although both types of experiment have been carried out over the same time course. Several problems with the annexin V/PI staining technique have been observed. A variable level of annexin staining has been observed between different batches of annexin V/FITC conjugate. This artificially increases the amount of primary necrotic and viable cells, as cells do not shift across into right hand quadrants and register annexin positive.

The annexin V/PI staining technique is known to be very sensitive and slight accidental changes to conditions or stress caused by manipulation of samples during staining can cause large artificial primary necrotic peaks. Differing sensitivities to rituximab and BU12-saporin have also been observed in the results presented in this chapter. This may be due cellular changes due to passages or due to the technique. Together these two observations may partially explain the large standard errors (figure 3.6), which in turn detracts from any statistical analysis. In an attempt to minimise these effects 6 replicates of staining experiments were carried out.

It has been reported that annexin V staining of tumour cells does not reflect clinical out come with *in vivo* exposure to rituximab (Weng *et al.*, 2002). In NHL cells from pre treated patients, apoptotic populations did not vary between non-responders and complete responders. Combined annexin V and $DiOC_6$ staining showed mitochondrial integrity, suggesting the mechanism of apoptosis induction is not mitochondrial (Weng *et al.*, 2002). This suggests the results shown here may not ultimately reflect clinical outcome. In attempt to counteract this corroborative PI and PSI assays are also shown and further molecular apoptosis analysis has also been carried out by western blotting.

3.3.4 The effect of alternative anti-CD20 antibodies and protein synthesis inhibitors

The effect of alternative CD20 antibodies and alternative protein synthesis inhibitors was analysed for augmentation effects by PSI. No augmentation was observed when cycloheximide was titrated in the presence and absence of rituximab at three different concentrations (figure 3.7). Cycloheximide is a known inhibitor of protein synthesis (Farber *et al.*, 1973) but also implicated in the induction of apoptosis via a FADD dependent mechanism (Tang *et al.*, 1999). This does not immediately suggest why an augmentation effect is not apparent.

The antibody 1F5 alone and in combination had a greater effect at reducing the viable population and increasing the secondary necrotic population than rituximab (figure 3.8), but has no effect on the apoptotic population. This shows the mechanism of action of the alternative CD20 antibody, 1F5 only includes apoptosis as a minor contribution. Taken together these results showed with an alternative protein synthesis inhibitor, rituximab does not cause increased levels of protein synthesis inhibition, and an alternative anti-CD20 antibody used in combination with BU12-saporin does not increase the size of apoptotic populations observed.

3.3.5 Alternative lymphoma cell lines and the induction of apoptosis

PSI assays carried out on alternative lymphoma cell lines expressing both CD19 and CD20 illustrate the augmentation effect observed when rituximab and BU12-saporin are used in combination is not unique to Ramos cells (figure 3.9). The Raji cell line appeared to be the least sensitive to BU12-saporin, the addition of rituximab gives a 1 fold increase to the potency of BU12-saporin. A 2 to 3 fold augmentation effect is observed in Namalwa cells. Daudi cells showed the largest effect, a 10 fold increase in potency was observed with rituximab.

The different cell lines showed different levels of sensitivity to BU12-saporin although sensitivity to BU12-saporin was not proportional to the magnitude of augmentation observed with rituximab. The augmentation effect was apparent in the raw data for

Namalwa cells (figure 3.9e) and the original Ramos cells (figure 3.2a), but only apparent in the normalised data for Raji and Daudi cells (figure 3.9b and d). This disparity between raw and normalised data suggests that this observation should be treated with caution. An alternative anti-CD22 saporin containing immunotoxin in a similar PSI assay has been shown on Raji and Daudi cells to give IC_{50} values of $1.02x10^{-12}$M and $5.37x10^{-12}$M respectively (Bolognesi *et al.*, 1998).

PI staining in the alternative cell lines show rituximab and BU12-saporin used individually have statistically the same effect on Raji, Ramos, Daudi and Namalwa cells (table 3.4). The effect of the combination on the different cell lines tested was significantly different by one way ANOVA (24h $p = 0.016$, 48h $p = 0.015$). This significant results was probably due to the sub G_0/G_1 population in combination treated Ramos cells being greater than in the other cell lines tested and the apparent insensitivity of Daudi cells to the combination of rituximab and BU12-saporin. By PSI assay Daudi cells showed the greatest augmentation using the combination of rituximab and BU12-saporin. Analysis by PI staining suggests Daudi cells undergo the least DNA fragmentation after exposure to rituximab and BU12-saporin, compared to other lymphoma cell lines.

In this experiment rituximab alone had little effect, probably due to the absence of a secondary cross linking antibody which has been shown to significantly improve DNA fragmentation in cells treated with rituximab alone (Shan *et al.*, 2000) or in combination with cisplatin (Alas *et al.*, 2001a). Saporin alone, and an anti-CD30 or an anti-CD22 saporin containing immunotoxins have previously been shown to induce time dependent increases to the sub G_0/G_1 population by PI staining (Bolognesi *et al.*, 1996 and 1998). Maximal increase was observed by 72 hours.

Combined annexin V/PI staining of rituximab and BU12-saporin treated Ramos and Nalm 6 cells showed the effect of the combination to induce apoptosis was dependent on CD20 expression which is absent in Nalm 6 cells (figure 3.11). The effect of the combination was equivalent to the effect of BU12-saporin alone. Nalm 6 cells are slightly less sensitive to BU12-saporin than Ramos cells although figure 3.1 shows the expression levels of CD19 are similar. Nalm 6 cells are also more sensitive to cisplatin than Ramos cells. There is no proposed explanation for this observation.

3.4 Conclusions

The work described in this chapter has shown rituximab significantly enhanced the protein synthesis and apoptosis inducing effects of BU12-saporin. By PSI assay, the combination showed a 5 fold increase in potency. The effect of the combination by PI staining was a significant increase to the sub G_0/G_1 population in an additive manner, significant compared to the effect of rituximab or BU12-saporin used alone. Annexin V/PI staining of combination treated cells showed a significant increase to the early apoptotic population and a highly significant decrease to the viable population, again the effect was additive and significant compared to either rituximab or BU12-saporin used alone.

The augmentation effect of rituximab and BU12-saporin was additive, an alternative PS inhibitor and rituximab and BU12-saporin and an alternative anti-CD20 antibody failed to show the same augmentation effects and increased apoptosis observed with rituximab and BU12-saporin. The most pronounced effects are observed in Ramos cells, but the effect was not limited to Ramos cells, illustrated by PSI assays and DNA fragmentation analysis in Daudi, Raji and Namalwa cells.

Chapter Four

The role of complement mediated mechanisms in the induction of apoptosis and protein synthesis inhibition in Ramos cells exposed to rituximab and BU12-saporin

4.1 Introduction

A significant augmentation effect between rituximab and BU12-saporin has been demonstrated in PSI assays, DNA fragmentation and annexin V/PI staining in a variety of lymphoma B cell lines (chapter 3). Rituximab has previously been shown *in vivo* to sensitise patients to CHOP chemotherapy regimes (Czuczman 1999). *In vitro* sensitisation effects have been observed with cisplatin (Alas *et al.*, 2002), glucocorticoids (Rose *et al.*, 2002), doxorubicine, TNF-α and also the bacterial toxin diptheria and the plant toxin ricin (Demidem *et al.*, 2000). By annexin V/PI staining supra-additive effects have been demonstrated between rituximab and retinoids, 24% more apoptotic cells were recorded than theoretically expected with the combination (Shan *et al.*, 2001). Synergistic effects have also been observed with rituximab and an anti-CD22 ricin containing immunotoxin, where homodimers of rituximab outperformed monomers (Ghetie *et al.*, 2001).

A variety of mechanisms have been proposed to be active in rituximab induced cell killing, including antibody dependent cell mediated cytotoxicity (ADCC), the direct induction of apoptosis and complement mediated mechanisms (Shan *et al.*, 1998, Hofmeister *et al.*, 2000, Harjunpaa *et al.*, 2000). The induction of apoptosis is strongly implicated, although complement dependent mechanisms are also thought to be involved. Originally the depletion of B cells by rituximab was thought to be due to phagocytosis by macrophages and natural killer cells (ADCC), although many authors still support this mechanism (Voso *et al.*, 2002). In isolated chronic lymphocytic leukaemia cells (CLL), Golay reported that complement dependent cytotoxicity (CDC) is a more efficient mechanism than ADCC (Golay *et al.*, 2000). The complement dependent cytotoxic response can be enhanced by inhibition of the complement regulatory proteins CD55 and CD59, and to a lesser extent by CD55 (DAF) and CD46 (MCP) (Harjunpaa *et al.*, 2000).

The level of CD20 expression is an important factor, although expression levels of CD55 and CD59 can not be used to predict the level of response to rituximab.

Activation of the terminal pathway of complement results in the formation of the membrane attack complex (MAC) leading to insertion into the cell membrane, recent evidence also suggests activation of the terminal pathway of complement can result in apoptosis (Nauta *et al.*, 2002). Reactive oxygen species (ROS) are known to have a role in the induction of necrosis and apoptotic cell death (Fiers *et al.*, 1999). A complement mediated cell death (caspase independent) involving the generation of ROS has been reported in response to rituximab (Bellosillo *et al.*, 2001). The mechanism proposed suggests a complement dependent induction of the mitochondrial pathway of apoptosis by the generation of ROS, which could be inhibited by ROS scavengers specific to O_2^- ions.

The action of an anti-CD7 saporin containing immunotoxin has previously been shown to involve ADCC (Flavell *et al.*, 1998). Although rituximab alone performed relatively poorly in an *in vitro* ADCC assay, *in vivo* exposure of SCID-Ramos mice to rituximab and BU12-saporin suggested the involvement of a complement mediated mechanism (Flavell *et al.*, 2000a). The extent of lymphoma cell apoptosis was significantly reduced in de-complemented serum, whereas natural killer cell depletion with cobra venom or anti-asialo GM1 antiserum did not decrease survival further, suggesting a complement dependent mechanism (Flavell *et al.*, 2001). Complement fixation by rituximab resulting in membrane damage was originally proposed to leave targets cells more vulnerable to immunotoxin action (Flavell *et al.*, 2000b).

This chapter describes experiments carried out to determine the relative contributions of complement dependent mechanisms (CDC), and the role of complement in the induction of apoptosis by rituximab and BU12-saporin. To determine the role and relative contribution of complement mediated mechanisms simultaneous protein synthesis inhibition assays, PI staining, and combined annexin/PI staining experiments were carried out in media containing active and heat inactivated foetal calf serum (HI FCS) i.e. de-complemented media, and statistical analyses carried out.

4.2 Results

4.2.1 The role of CDC in protein synthesis inhibition by rituximab and BU12-saporin

To determine any complement mediated contribution to the protein synthesis inhibition effects of rituximab and BU12-saporin observed in chapter 3, PSI assays were carried out in parallel in normal foetal calf serum (FCS) and in de-complemented media (i.e. heat inactivated foetal calf serum, HI FCS). A titration of BU12-saporin was carried out in the presence and absence of rituximab and the incorporation of ^{3}H-leucine by Ramos cells was determined. The unconjugated toxin saporin was also titrated in the presence and absence of rituximab.

Titrations of rituximab, saporin and BU12-saporin against Ramos cells in a PSI assay show similar results when the experiment is carried out in either active or HI FCS (figure 4.1). The normalised data show HI FCS does not effect leucine incorporation by cells treated with BU12-saporin or saporin in the presence or absence of rituximab (figure 4.1). Data show in figure 4.1 b and d have been normalised and are expressed as a percentage of control cell ^{3}H-leucine incorporation. Control cells were either untreated or treated with rituximab alone to normalise the effect of rituximab (see methods and materials section 2.4 for details).

The raw data (figure 4.1a and 4.1c) showed increased leucine incorporation in the cells treated in HI FCS compared to cells treated in active FCS. This is particularly apparent in cells exposed to saporin. No apparent explanation can be proposed for this observation. This observation is not reflected in the normalised data, suggesting this is not a significant effect as untreated control cells also show increased leucine incorporation in HI FCS compared to FCS. There is a slight, minor difference between IC_{50} values obtained comparing cells exposed to rituximab and BU12-saporin in normal and HI FCS. Taken together these results suggest, in this case, rituximab does not fix bovine complement and there is no complement mediated contribution to the protein synthesis inhibitory effect of rituximab and BU12-saporin.

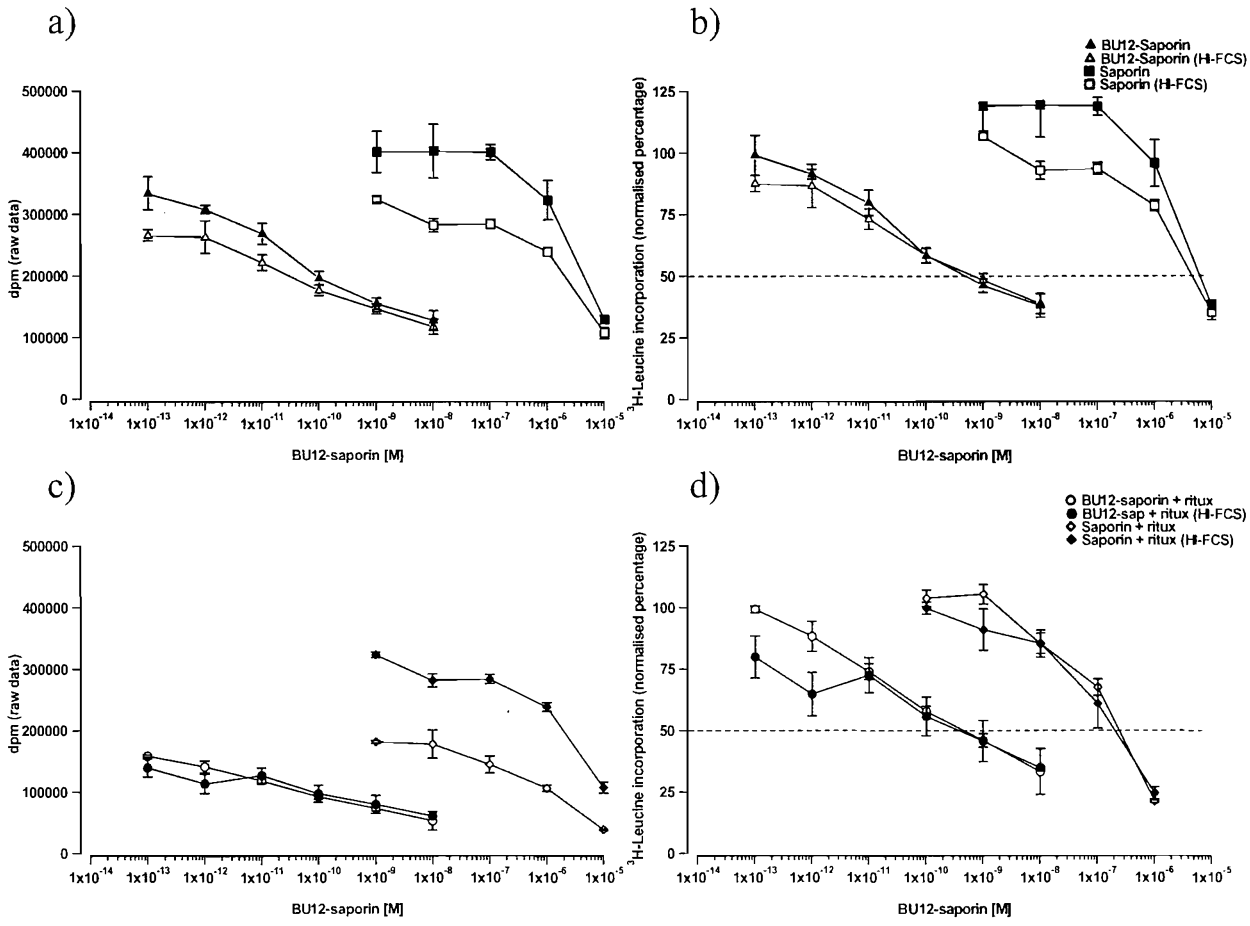

Figure 4.1
Dose response curves showing the effect of HI FCS on a titration of BU12-saporin and saporin in the presence and absence of rituximab (at 10μg/ml) in a Ramos cell protein synthesis inhibition assay. Saporin (□), BU12-saporin (△), saporin and rituximab (◇), and BU12-saporin and rituximab (○), are shown. Solid symbols represent the PSI assay carried out in HI FCS. Figures 4.1a and 4.1c show raw data as counts (dpm), figures 4.1b and 4.1d show normalised data (uptake as a percentage of control cell uptake or uptake by cells treated with rituximab alone, for details of calculation see section 2.4.) Points represent the mean of triplicates and error bars the standard deviations.

4.2.2 The role of CDC in DNA fragmentation induced by exposure of Ramos cells to rituximab and BU12-saporin

Chapter 3 showed rituximab and BU12-saporin induced DNA fragmentation in Ramos cells. The role of complement dependent mechanisms in DNA fragmentation was investigated by PI staining carried out in HI FCS. The PI staining experiment shown in figures 3.3 and 3.4 was carried out in parallel in active and HI FCS (data from the experiment carried out in normal FCS only is shown in chapter 3,) both sets of data combined are shown in figure 4.3. Ramos cells were exposed to rituximab (10μg/ml), 1F5 antibody (10μg/ml) and BU12-saporin (10μg/ml) individually and the combinations of rituximab or 1F5 antibody and BU12-saporin. Cells were also exposed to the constituent components of the immunotoxin, BU12 antibody and saporin (at equimolar concentrations to BU12-saproin). A single parameter FL3 histogram was used to determine the proportion of cells present in each stage of the cell cycle (figure 4.2). Three independent repeats of the experiment were carried out, this data are summarised in histogram form in figure 4.3.

Untreated control cells, BU12-saporin, BU12 antibody alone and saporin treated cells show little to no difference between the sub G_0/G_1 populations obtained in experiments carried out in normal and HI FCS (figure 4.2). This suggests no role for CDC in apoptosis induced by saporin, BU12 antibody and BU12-saporin. The sub G_0/G_1 populations for rituximab and 1F5 treated cells in HI FCS are reduced compared to cells treated with the same antibody in normal FCS. This indicates complement mediated mechanism may have a role in apoptosis induced by the antibodies 1F5 and rituximab.

These observations are reflected in cells treated with the combination of rituximab and BU12-saporin, and the combination of 1F5 and BU12-saporin as the sub G_0/G_1 population of cells treated with both of these combinations are reduced in experiments carried out in HI FCS. The sub G_0/G_1 populations for cells treated with the combination of saporin and rituximab, and the combination of BU12 and rituximab show only some minor increases in the presence of active complement at the earlier time points. This suggests a possible role for CDC in rituximab and 1F5 induced DNA fragmentation, but not BU12-saporin.

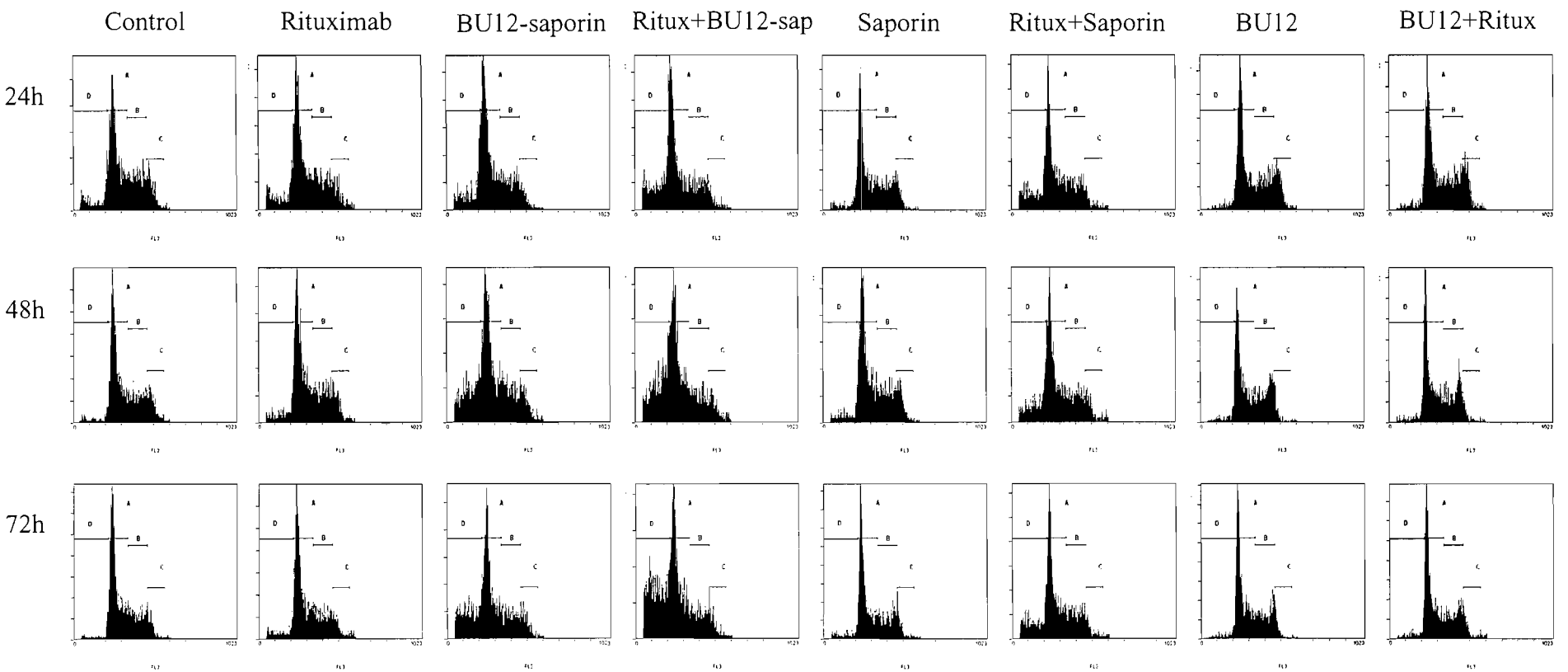

Figure 4.2
Cell cycle analysis by propidium iodide staining of Ramos cells exposed to rituximab, BU12-saporin (both at 10μg/ml), saporin and BU12 antibody (at equimolar concentration to that present in BU12-saporin) individually and in combination and stained at 24, 48 and 72 hours. Cells were exposed in media containing HI FCS. Histograms represent the amount of DNA present in the cell, gate A represent cells in G_0/G_1 phase, gate B, cells in S or M phase, gate C represents cells in G_2 or early M phase and gate D represents the sub G_0/G_1 population.

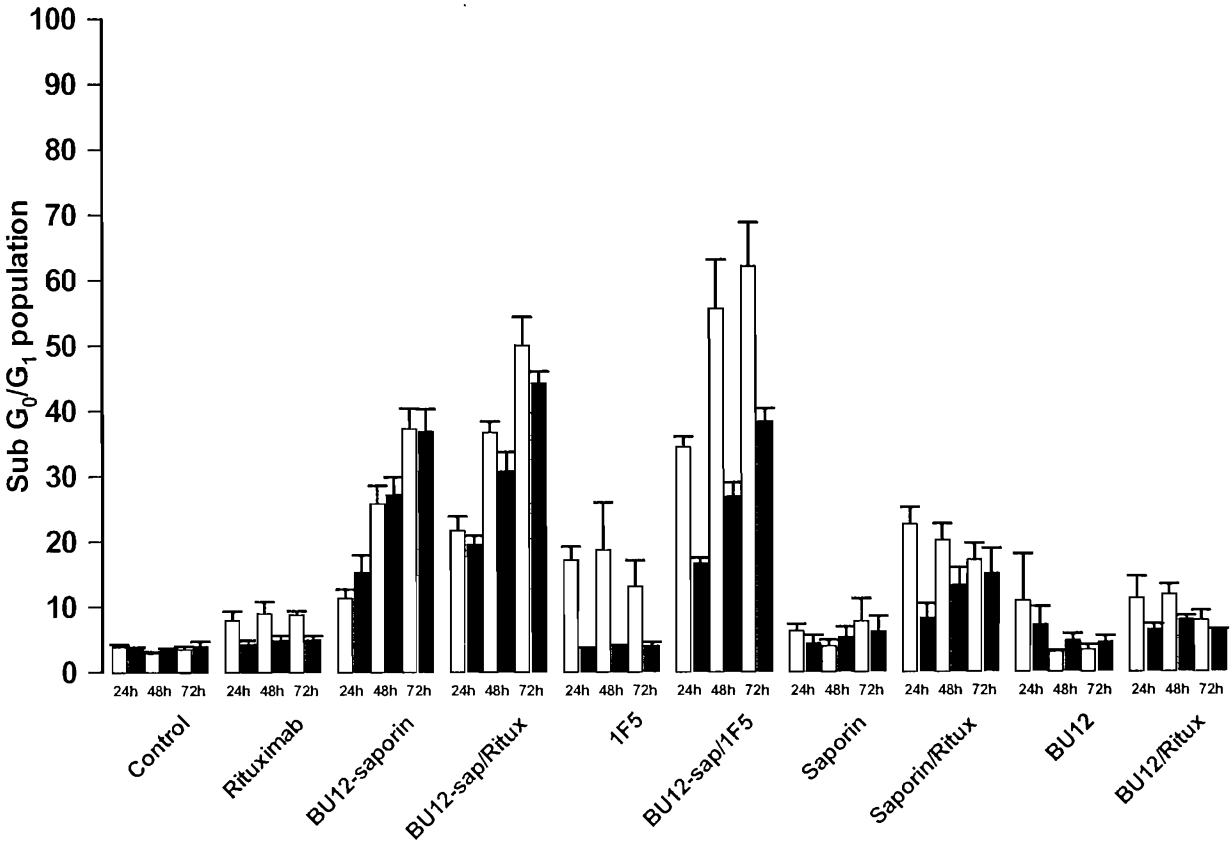

Figure 4.3
Percentage of apoptotic cells (sub G_0/G_1 population) after PI staining Ramos cells at 24, 48 and 72 hours. Cells were exposed to rituximab (10μg/ml), BU12-saporin (10μg/ml), 1F5 (10μg/ml), saporin and BU12 antibody (at equimolar concentration to BU12-saporin) individually and in combinations. The experiment was carried out in active (□) and HI FCS (■). Bars represent the mean and standard error of 3 replicate experiments.

4.2.3 Statistical analysis of DNA fragmentation data

To determine the statistical significance of the effect of HI FCS on the size of the sub G_0/G_1 population obtained by treating Ramos cells with rituximab and BU12-saporin independent t tests were carried out. The size of the sub G_0/G_1 population obtained in normal FCS was compared for significance by t test to the size of the sub G_0/G_1 population obtained in HI FCS (table 4.1). Treating cells with rituximab alone appeared to be slightly complement dependent (figure 4.3), although this observation was only statistically significant at 72 hours ($p = 0.012$) and not apparent in cells exposed to rituximab in combination. This suggests that this significant result (rituximab treated cells at 72 hours) does not reflect a pattern in these data and was due to the smaller standard error around this mean compared to standard errors calculated at other time points.

The combination of BU12 antibody and rituximab showed no significant differences between the size of the sub G_0/G_1 population in normal or HI FCS. Treating cells with the combination of saporin and rituximab showed a significant difference between the size of the sub G_0/G_1 population obtained in normal and HI FCS at 24 hours ($p = 0.026$). As is the case for the rituximab results discussed above, this significant result does not reflected a trend in the results i.e. saporin or rituximab alone treated cells do not show a CDC dependent contribution to DNA fragmentation at this time point.

The alternative murine CD20 antibody 1F5 showed large differences in the sub G_0/G_1 populations between experiments carried out in normal and HI FCS (figure 4.3). In table 4.1, 1F5 alone treated cells showed a statistically significant difference only at 24 hours between the size of the sub G_0/G_1 population in cells treated in normal FCS compared to HI FCS. The difference between the sub G_0/G_1 populations of cells treated with 1F5, for the experiments carried out in normal and HI FCS at 48 and 72 hours were not significant probably due to the large standard errors between repeats. In combination with BU12-saporin, the effect of 1F5 on the sub G_0/G_1 population in normal FCS was significant at all three time points compared to the effect in HI FCS (24h $p = 0.001$, 48h $p = 0.021$, 72h $p = 0.027$). This significant effect on the sub $G_0/G1$ population in HI FCS is likely to be due to 1F5 antibody as the effect of BU12-saporin is not affected by HI FCS.

Independent t test for equality of means		
Sample in FCS compared to sample in HI FCS	Time point	Significance at p=0.05
Control	24h	0.552
	48h	0.141
	72h	0.659
Rituximab	24h	0.067
	48h	0.110
	72h	**0.012**
BU12-saporin	24h	0.247
	48h	0.748
	72h	0.927
Rituximab and BU12-saporin	24h	0.447
	48h	0.151
	72h	0.277
1F5 antibody	**24h**	**0.003**
	48h	0.180*
	72h	0.081
BU12-saporin and 1F5	**24h**	**0.001**
	48h	**0.021**
	72h	**0.027**
Saporin	24h	0.292
	48h	0.513
	72h	0.711
Saporin and rituximab	**24h**	**0.026**
	48h	0.138
	72h	0.665
BU12 antibody	24h	0.647
	48h	0.210*
	72h	0.449
BU12 and rituximab	24h	0.221
	48h	0.083
	72h	0.340*

Table 4.1
Summary of independent t tests carried out to determine the effect of HI FCS in PI staining experiments. The experimental data used in analysis were taken from figure 4.3, bold text represents significant values at p=0.05. Statistical analysis was carried out on SPSS statistical software (LEAD technologies inc.) * Equal variances were not assumed by Levene's test.

Statistical analysis by t test of data from the experiments shown in figure 4.3 showed no patterns of significance between cells treated in normal and HI FCS for rituximab, BU12-saporin exposure either alone or in combination. Also, no patterns of significant CDC dependent contributions to DNA fragmentation are observed for the constituent components of the immunotoxin BU12 antibody and saporin alone or in combination with rituximab. Only 1F5 exposure, alone and particularly in combination with BU12-saporin showed a statistically significant decrease in DNA fragmentation activity when the experiment was carried out in HI FCS.

4.2.4 Phosphatidyl serine exposure in Ramos cells exposed to rituximab and BU12-saporin in HI FCS

By annexin V/PI staining, exposure to the combination of rituximab and BU12-saporin was shown to have slightly below additive effects on the early apoptotic and viable populations of Ramos cells (chapter 3). To determine the contribution of CDC to these effects the annexin V/PI staining experiment shown in chapter 3 (figure 3.6) was carried out in parallel in normal and HI FCS. Results from the experiments carried out in normal FCS from chapter 3 are shown with the results from the experiments carried out in HI FCS in figure 4.5. As for the previous DNA fragmentation experiment, cells were also exposed to the constituent modalities of the immunotoxin, i.e. BU12 antibody and saporin toxin, alone and in combination and stained at 24, 48, and 72 hours.

Raw flow cytometry data from a representative annexin V/PI staining experiment carried out in HI FCS are shown in figure 4.4, (equivalent raw data for a representative experiment in normal FCS is shown in figure 3.5). As described in chapter 3, dead cells which stain PI positive have lost membrane integrity and are described as primary necrotic (quadrant 1). Viable cells which stain PI negative and annexin negative appear in quadrant 3. Quadrant 2 contains the PI positive and annexin positive cells; these dead cells are described as late apoptotic and secondary necrotic. Annexin positive cells, PI negative appear in quadrant 4, this population is described as the early apoptotic cells.

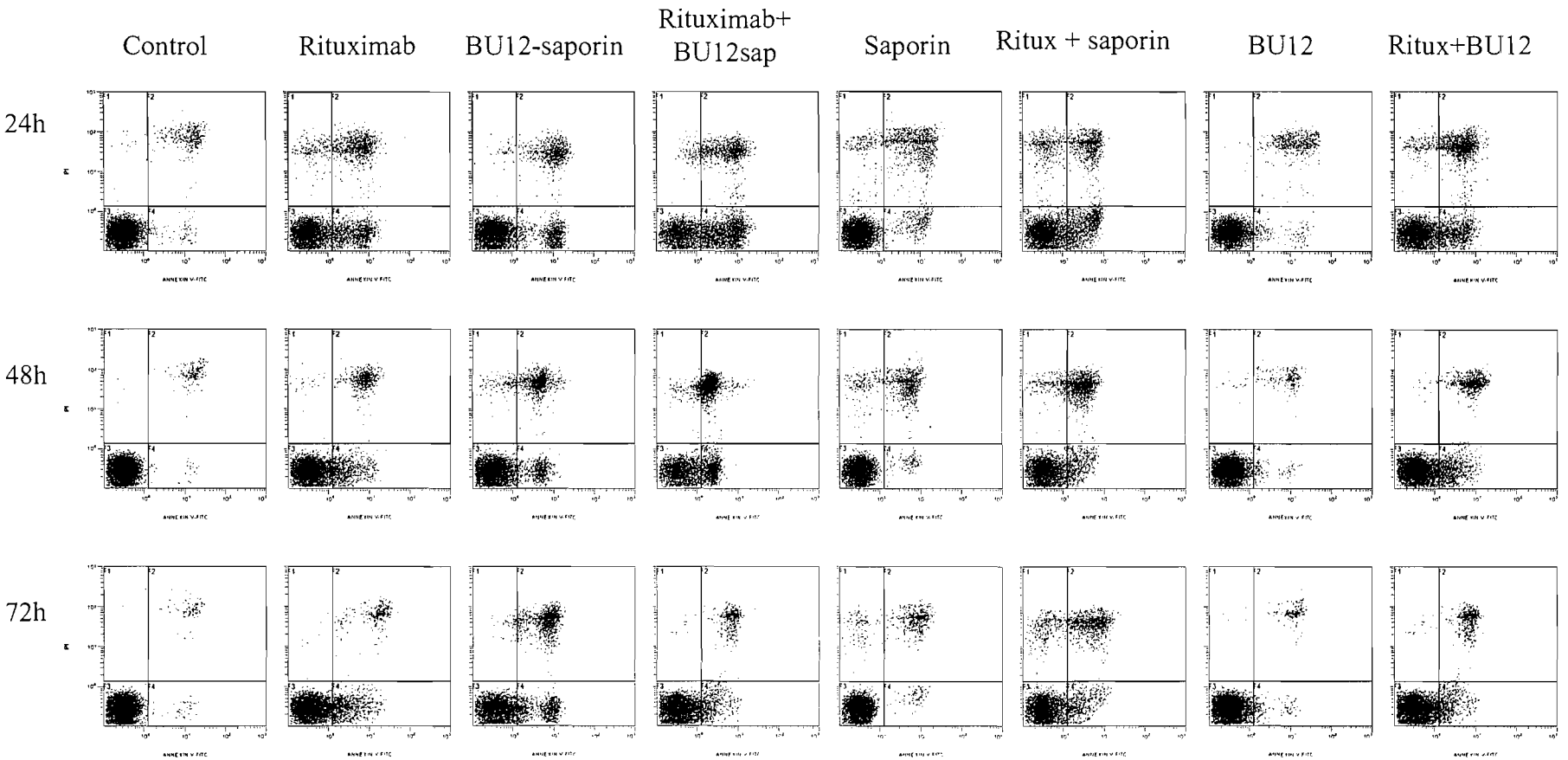

Figure 4.4

Raw data showing annexin V/PI staining of Ramos cells in HI FCS exposed to rituximab, BU12-saporin, (at 10μg/ml), saporin and BU12 antibody (at equimolar concentration to that present in BU12-saporin) individually and in combination and stained at 24, 48 and 72 hours. Annexin staining is shown on the x axis and PI staining on the y-axis. Quadrant 1 contains PI positive primary necrotic cells, quadrant 2, PI and annexin positive secondary necrotic cells, quadrant 3 viable cells and quadrant 4 PI negative annexin positive early apoptotic cells.

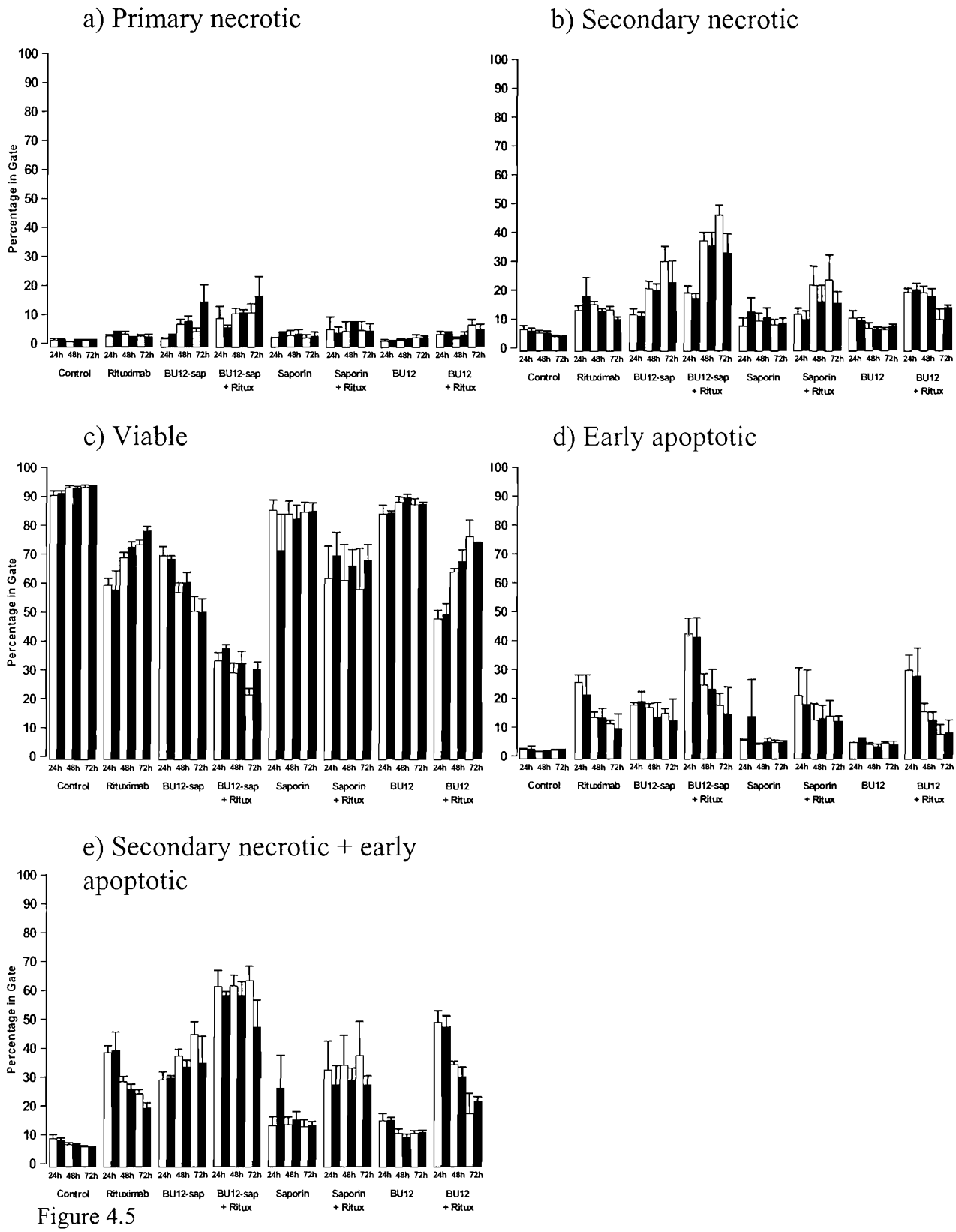

Figure 4.5

Combined annexin V/ PI staining of Ramos cells exposed to rituximab at 10µg/ml, BU12-saporin at 10µg/ml, saporin and BU12 antibody (at equimolar concentrations) individually and in combination. Staining was carried out at 24, 48 and 72 hours post exposure. Histograms represent the percentage of the cellular population determined to be; primary necrotic (PI positive) figure 4.5a, secondary necrotic (PI and annexin positive) figure 4.5b, viable (PI and annexin negative) figure 4.5c, and early apoptotic (annexin positive) figure 4.5d. Figure 4.5e represents the sum of the secondary necrotic and early apoptotic populations. The experiment was carried out in active (□) and HI FCS (■). Bars represent the mean and standard error of 6 replicate experiments.

4.2.5 Statistical analysis of phosphatidyl serine exposure data

Annexin V/PI staining experiments carried out on cells exposed to rituximab and BU12-saporin in HI FCS gave results virtually identical to experiments carried out in active FCS (figure 4.5). Over the three time points no patterns of difference are apparent between cells treated in normal and HI FCS, in general in HI FCS viability was increased slightly and slightly lower proportions of early apoptotic and secondary necrotic cells were observed (figure 4.5 b,c,d). These observations were confirmed by statistical analysis.

Statistical analyses of the annexin V/PI data from figure 4.5 by independent t test are shown in table 4.2, samples treated in normal FCS are compared to samples treated in HI FCS, for each time point and population of cells are shown. Statistical analysis showed the effect of complement was only one significant at one point, observed in the viable population with cells treated with the combination of rituximab and BU12-saporin at 72 hours ($p = 0.022$). At a 95% confidence interval, 1 in 20 tests will be significant by chance, suggesting this significant point does not represent a trend in these data. Overall complement does not play a significant role although minor, not significant effects of HI FCS are visible in the histograms of figure 4.5.

Annexin V/PI staining with the alternative CD20 antibody 1F5 in combination with BU12-saporin in normal and HI FCS is shown in figure 4.6. As shown in chapter 3, (figure 3.8) 1F5 caused cell death without increasing the early apoptotic population. Large differences were apparent between the experiment carried out in normal and HI FCS, particularly in the viable and secondary necrotic populations. Increased numbers of secondary necrotic cells were observed, reaching 65% in combination with BU12-saporin in normal FCS, whereas in HI FCS only 25% secondary necrotic cells are observed. In combination with BU12-saporin the viable population was reduced to less than 5% in normal FCS, compared to 50% for cells treated in HI FCS. No statistical tests were carried out as only two replicate experiments were performed. Low early apoptotic populations are observed in normal and HI FCS. This shows that the murine antibody 1F5 is fixing the bovine complement and causing a non-apoptotic cells death.

Sample in FCS compared to sample in HI FCS	Time point	Significance at p=0.05			
		Secondary necrotic cells	Viable cells	Early apoptotic cells	Secondary necrotic + early apoptotic
Control	24h	0.728	0.709	0.816	0.798
	48h	0.953	0.930	0.775	0.872
	72h	0.908	0.880	0.573	0.795
Rituximab	24h	0.458	0.820	0.281	0.934
	48h	0.137	0.207	0.932	0.338
	72h	0.067	0.075	0.501	0.067
BU12-saporin	24h	0.831	0.696	0.510	0.855
	48h	0.965	0.510	0.248	0.292
	72h	0.437	0.963	0.494	0.256
Rituximab + BU12-saporin	24h	0.522	0.213	0.853	0.600
	48h	0.745	0.527	0.766	0.597
	72h	0.119*	**0.022**	0.610	0.170*
Saporin	24h	0.440	0.341	0.386	0.339
	48h	0.841	0.798	0.443	0.694
	72h	0.883	0.980	0.878	0.935
Rituximab + saporin	24h	0.605	0.606	0.801	0.682
	48h	0.533	0.738	0.946	0.654
	72h	0.433	0.555	0.737	0.450
BU12	24h	0.747	0.952	0.057	0.991
	48h	0.776	0.559	0.353	0.473
	72h	0.425	0.973	0.532	0.827
BU12 + rituximab	24h	0.836	0.796	0.780	0.776
	48h	0.709	0.473	0.413	0.290
	72h	0.376	0.721*	0.938	0.603

Table 4.2
Summary of independent t tests carried out to determine the effect of HI FCS in annexin V/PI staining experiments. These data are taken from figure 4.5. Bold text represents significant values at p=0.05. Statistical analysis was carried out on SPSS statistical software (LEAD technologies inc.) * Equal variances were not assumed by Levene's test.

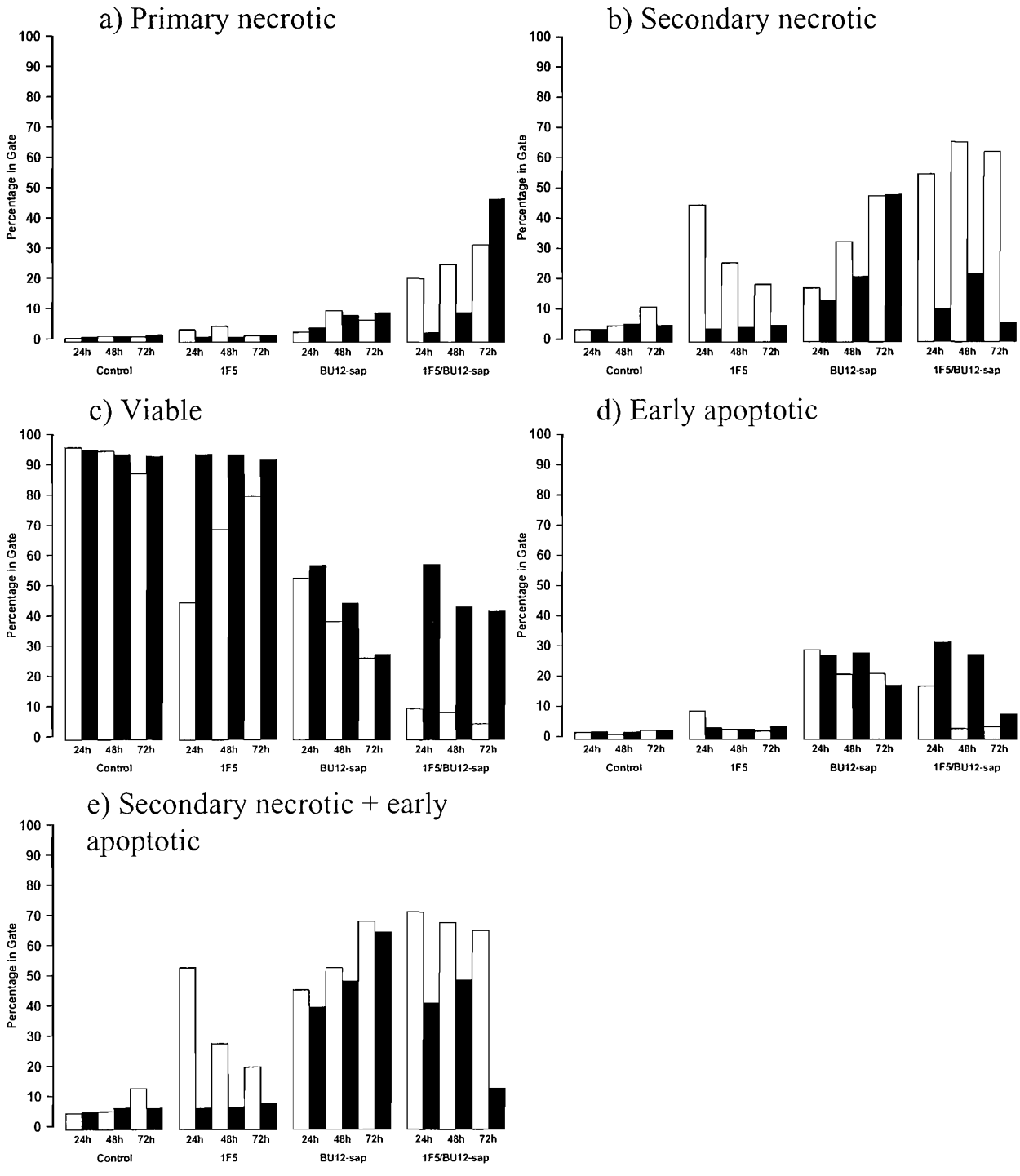

Figure 4.6
Combined annexin V/ PI staining of Ramos cells exposed to BU12-saporin (10μg/ml), and 1F5 antibody (10μg/ml), individually and in combination. Staining was carried out at 24, 48 and 72 hours post exposure. The experiment was carried out in active (□) and HI FCS (■). Histograms represent the percentage of the cellular population determined to be; primary necrotic (PI positive) figure 4.6a, secondary necrotic (PI and annexin positive) figure 4.6b, viable (PI and annexin negative) figure 4.6c, and early apoptotic (annexin positive) figure 4.6d. Figure 4.6e represents the sum of the secondary necrotic and early apoptotic populations.

4.3 Discussion

Statistical analysis of the G_0/G_1 population and annexin V/PI staining data presented in this chapter suggest cell killing by rituximab in this model is largely due to the induction of apoptosis by direct signalling. This supports the induction of apoptosis by direct signalling mechanisms proposed by several authors (Shan *et al.*, 1998, Alas *et al.*, 2001) and is contrary to the complement dependent apoptotic death described by Bellosillo (Bellosillo *et al.*, 2001). This work also contradicts the report that complement is also significant in the induction of apoptosis by rituximab (Golay *et al.*, 2000). Preliminary work in SCID mice on the effect of the combination of rituximab and BU12-saporin had also initially suggested a major role for complement mediated mechanisms (Flavell *et al.*, 2000b).

It should be taken into consideration when examining these data, these experiments were conducted with a bovine not human source of complement. Rituximab has been shown to be remarkably effective at fixing human complement (Glennie *et al.*, 2003), rituximab has also been previously shown to fix FCS (Flavell *et al.*, 2004, in press). 1F5 antibody has previously been reported to be affected by bovine complement (by ^{3}H-thymidine assay) but to only cause the effective induction of apoptosis when cross linked by a secondary antibody (Shan *et al.*, 1998). This report is partially confirmed by the results presented in this chapter; 1F5 is significantly affected by HI FCS and does not induce increases in early apoptotic population alone.

The PSI assays carried out in this chapter suggest that the protein synthesis inhibition activity of BU12-saporin alone or in combination with rituximab was not affected by de-complemented media. IC_{50} values for BU12-saporin from this chapter (figure 4.1) show the Ramos cells is be less sensitive to BU12-saporin than the data presented in chapter three (figure 3.2). This observation was noted but not thought to be critical as the IC_{50} values were consistent within this set of assays. No explanation can be proposed for the apparent increase in ^{3}H-leucine incorporation observed in the titrations carried out in HI FCS (raw data only). As this event is not reflected in the normalised data (as this increased

incorporation also occurs in the untreated control cells) it is not thought to be an important observation reflecting the action of the immunotoxin, more an artefact of the assay.

Cell cycle analysis carried out by PI staining showed the combination of BU12-saporin and rituximab caused a significant increase to the sub G_0/G_1 population compared to either used alone, which was not affected by HI FCS. Direct comparison by t test between samples treated in media containing active FCS and samples treated in media containing inactivated FCS (table 4.1), suggests no role for CDC mediated mechanisms in causing the observed increase to the sub G_0/G_1 population of cells treated with rituximab and BU12-saporin and the components of the immunotoxin.

Complement only appeared to be a significant factor when cells were exposed to the murine anti-CD20 antibody 1F5 antibody. The sub G_0/G_1 population trebled in active FCS compared to samples treated with 1F5 in heat inactivated FCS (figure 4.3), although, this effect was only statistically significant at 24 hours due to large standard errors (table 4.1). By annexin V/PI staining, at 24 hours the secondary necrotic population of 1F5 treated cells is 10 times greater in cells treated in normal FCS compared to cells treated in HI FCS (figure 4.6). Cells treated with 1F5 in combination with BU12-saporin in normal FCS showed a secondary necrotic population 5 times greater than cells treated in HI FCS.

These data suggest cell death is occurring via a complement dependent, non apoptotic cell death. The small population of early apoptotic cells and increased populations of primary and secondary necrotic cells suggest the 1F5 treated cells are staining PI positive as they have lost membrane integrity due to the action of the membrane attack complex. These effects are not apparent in experiments carried out in HI FCS as the membrane remains intact.

The lack of consistency between identical experimental repeats (particularly for the annexin V/PI staining experiments) and the resulting large standard errors may be affecting the statistics obtained. The large errors, although characteristic of these techniques, may be masking trends, as points with large standard errors are not mathematically significant. Additional replicates of each experiment were carried out to minimise this effect. This problem in particular, is suspected for the DNA fragmentation data as rituximab and 1F5 alone treated cells only show significance at 24 and 72 hours

respectively (table 4.1), although large differences are observed between the cells treated in normal and HI FCS in figure 4.2.

By annexin V/PI staining, the role of complement mediated mechanisms was not significant in the induction of apoptosis induced by rituximab and BU12-saporin (figure 4.5). The viable population of rituximab and BU12-saporin treated cells was statistically different in HI FCS at 72h ($p = 0.022$). This may represent a trend as the 24 and 48 hour data also showed a slightly decreased viable proportion of cells treated in normal FCS compared to cells treated in HI FCS (figure 4.4), but these points are not statistically significant. Also, there was no evidence of decreased viable populations in cells treated in normal FCS compared to cells treated in HI FCS, for samples exposure to rituximab or BU12-saporin alone. Suggesting this significant result does not represent a trend in these data. Large standard errors again maybe responsible for masking trends, but no other trends are apparent from these data presented as histograms (figure 4.5). Six independent repeats of this experiment were carried out in attempt to reduce these variations.

Whilst comparing the DNA fragmentation and annexin V/PI staining data it must be taken in to consideration that external exposure of phosphatidyl serine is an earlier event in the induction of apoptosis than DNA fragmentation, although both types of experiment have been carried out over the same time course. Several problems with the annexin V/PI and PI staining techniques have been observed, including increased primary necrotic populations, variation between repeats, and damage to samples during preparation (as discuss in chapter 3). Although steps were taken to minimise these problems, e.g. increased numbers of replicate experiments, there may still be an impact on the statistical analysis.

Much contradictory evidence has been presented regarding the cytotoxic mechanisms of action of rituximab. This contradiction will be due, at least in part to the different assessments of relative importance in different models, by different techniques of assessing the relative contribution of different mechanisms. Differences have also been observed in the relative importance of cellular death mechanisms between *in vitro* and *in vivo* experiments. The types of experiment conducted in this chapter which do not contain effector cells can not assess the relative contribution of ADCC and CDCC. Different

behaviour may also be observed comparing the contribution of complement from a human source rather than a bovine source.

From experiments carried out in HI FCS the results generally show slightly reduced levels of cell death for rituximab and BU12-saporin treated cells, apparent by annexin staining in the viable population (figure 4.5), statistically significant only at 72 hours, but more pronounced by PI staining although not statistically significant (figure 4.3). Taken together the data obtained from both staining techniques, (except for 1F5 antibody) indicates the effect of HI FCS in minor and is not significant overall.

4.4 Conclusions

In conclusion, the effect of exposure of Ramos cells to rituximab and BU12-saporin in de-complemented media compared to normal sera was not statistically significant. This observation was confirmed by three corroborative assays, PSI assays, DNA fragmentation studies and annexin V/PI staining. Some minor effects were observed, i.e increased viability and increased sub G_0/G_1 populations for cells exposed to rituximab and BU12-saporin in HI FCS but these effects have not been shown to be statistically significant overall. The effect of the HI FCS on the alternative CD20 antibody 1F5 was shown to be statistically significant by PI staining and apparent by annexin V/PI staining (no statistical analysis carried out). The mechanism of action of 1F5 antibody is complement dependent, though non apoptotic.

Rituximab and BU12-saporin individually and in combination showed some decreased activity in HI FCS, although this was not statistically significant overall. The constituent parts of the immunotoxin, BU12 antibody and saporin, were also shown to be affected in a minor, not statistically significant manner by HI FCS in DNA fragmentation and annexin V/PI staining techniques.

Chapter Five

Caspase activation and the effect of caspase inhibitors on Ramos cells exposed to rituximab and BU12-saporin

5.1 Introduction

Apoptosis is subject to tight positive and negative regulation by several families of intracellular proteins. Caspases are a family of cysteine aspartate proteases known to cleave and activate other members of the caspase family resulting in the proteolytic caspase cascade which activates specific enzymes and cleaves caspase substrates inducing apoptosis and cell death. Initiator caspases, such as caspases 2, 8 and 9 are activated by cleavage to initiate and convey an apoptotic signal. Effector caspases, such as caspases 3, 6 and 7 are down stream effectors which once activated by initiator caspases, cleave nuclear and cytoskeletal proteins inducing apoptosis. UV irradiation, chemotherapeutic drugs, and ligation of death inducing surface receptors result in caspase activation.

Caspase 3, often referred to as the central executioner caspase, plays a critical role in the induction of apoptosis. Caspase 3 is responsible for the cleavage of PARP, an enzyme involved in DNA repair and modification and other substrates. PARP cleavage is considered a hallmark characteristic in the induction of apoptosis. Cleavage and activation of procaspase 3 (35kDa) by initiator caspases, results in a 17kDa and a 19kDa fragment. Caspase 8 is recruited via FADD to the CD95/FAS death inducing signal complex to play an important role in the induction of death receptor mediated apoptosis. Caspase 8 shares homology with the caspase family and also contains a death domain that interacts directly with FADD. Activation of caspase 8 involves dimerisation and several autolytic cleavages, the antibody used in this chapter detects procaspase 8 as doublet of 55/50kDa which on activation is cleaved to a 40/36kDa doublet (see materials and methods for details section 2.7).

Cytochrome C released from the mitochondria during the induction of apoptosis associates with procaspase 9 and apaf 1 to form the apoptosome. This complex processes procaspase

9 into the active subunit (35kDa or 17kDa) and a smaller 10kDa subunit by cleavage at Asp^{315}. The activated form processes and activates other caspase family members, such as procaspases 3 and 7, initiating the caspase cascade resulting in apoptosis. Cleaved caspase 9 may undergo further cleavage by activated caspase 3 at Asp^{330} resulting in a 37kDa fragment. This cleavage probably serves as a positive feedback signal to amplify the signal cascade.

Rituximab has been shown to act against target CD20 positive lymphoma cells via both caspase dependent and caspase independent mechanisms. Reported work on the effect of caspase inhibitors in rituximab treated cells has shown mixed results. The peptide inhibitor of caspase 3, DEVD, has been shown to inhibit the apoptotic activity of homodimers of rituximab in Burkitt's lymphoma cell lines (Ghetie *et al.*, 2001). It has also been demonstrated previously that DEVD inhibits PARP and SP1 cleavage in BL60 lymphoma cells exposed to rituximab (Mathas *et al.*, 2000). In addition Shan reported the pan caspase inhibitor, zVAD, inhibited DNA fragmentation induced by rituximab in B-cell lines (Shan *et al.*, 2000). Although, more recently Bellosillo reported that the addition of zVAD had no effect on the viability of freshly isolated cells treated with rituximab (Bellosillo *et al.*, 2001). In B-cell lines, phosphatidylserine exposure and mitochondrial membrane permeability transition induced by rituximab were shown to be independent of caspase activation (Chan *et al.*, 2003).

The effects of peptide caspase inhibitors have been investigated in *Pseudomonas* exotoxin (PE) but not saporin containing immunotoxins. Immunotoxins containing PE have been shown to induce cell death involving caspase activation and PARP cleavage (Keppler-Hafkemeyer *et al.*, 1998). Keppler-Hafkemeyer suggests DEVD only partially inhibits apoptosis induced by a PE containing immunotoxin (Keppler-Hafkemeyer *et al.*, 1998). In contrast, immunotoxins containing the alternative ribosome inactivating protein gelonin do not appear to induce apoptosis, no DNA fragmentation was detected in treated cells by TUNEL assay (Rosenblum *et al.*, 2003). Although known to induce apoptosis, the protein synthesis inhibition activity of the ribosome inactivating protein α-sarcin was also not inhibited by zVAD (Olmo *et al.*, 2001).

To investigate the molecular events involved in apoptosis induced by saporin containing immunotoxins and rituximab series of western blots were carried out. Western blots were prepared and probed for full length and cleaved PARP in cells treated with BU12-saporin and rituximab individually and in combination. This chapter also undertakes to investigate the organisation and timing of caspase 3, 8 and 9 activation in rituximab and BU12-saporin treated cells. Thus, the pathways involved in of induction of apoptosis by saporin immunotoxins and rituximab can be proposed. Experiments with the soluble peptide caspase inhibitors DEVD and zVAD were also carried out to examine directly the role of caspase activation.

5.2 Results

5.2.1 PARP cleavage in rituximab and BU12-saporin treated Ramos cells

A series of western blots were carried out to detect PARP cleavage, a characteristic molecular hallmark of apoptosis, as a measure of caspase activation in rituximab and BU12-saporin treated cells. Ramos cells were exposed to rituximab and BU12-saporin individually and in combination for up to 9 hours, cells were then harvested, and protein lysates prepared for SDS PAGE and subsequently transferred to nitrocellulose membrane and probed with an anti-PARP antibody. The anti-PARP monoclonal antibody used in these studies (see materials and methods 2.7) detects full length (116kDa) and an 85kDa proteolytic fragment (figure 5.1.)

The combination of rituximab and BU12-saporin induced a greater degree of apoptosis in Ramos cells than rituximab or BU12-saporin alone, measured by the extent of PARP cleavage detected (figure 5.1). For example after 9 hours exposure to the combination 58% cleaved PARP was detected, cleavage induced by rituximab exposure alone achieved 24% cleaved PARP, and BU12-saporin alone produced 40% cleaved PARP (figure 5.1a). More cleaved product compared to full length PARP was detected in samples treated with the combination than when either rituximab or BU12-saporin were used individually. In turn, the amount of PARP cleavage observed in cells treated with rituximab alone is less than that observed in cells treated with BU12-saporin alone. This data is representative of several independent experiments, in some repeats the time point at which maximum PARP cleavage was detected varied by several hours, but the pattern of PARP cleavage detected was always consistent.

The work carried out in this chapter was subject to a high degree of variability within this Ramos cell model. The extent and timing of cleavages detected by western blotting varied between experimental repeats. Variation between experimental results is discussed individually for each experiment. Where several similar blots were obtained, representative data is shown and density analysis has been carried out. The variation obtained was thought likely to be a characteristic of the system. Although attempts were

a) PARP cleavage

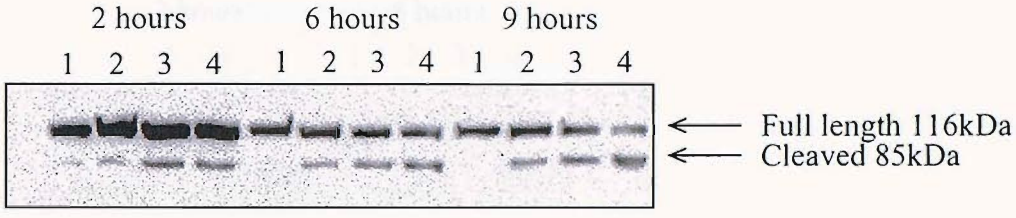

b) PCNA loading control

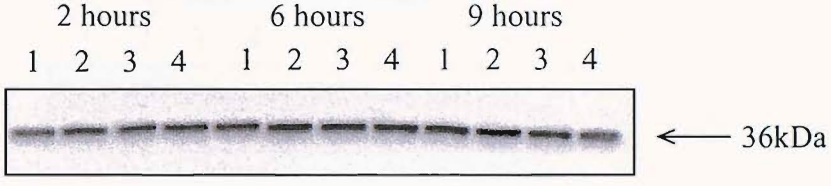

Figure 5.1
Western blots showing PARP cleavage in Ramos cells (figure 5.1a) exposed to rituximab and BU12-saporin individually and in combination for 2, 6 and 9 hours. PCNA loading control (figure 5.1b). Cell lysates were prepared for western blotting by RIPA extraction , blots were probed overnight with mouse anti-PARP (1:1000) in PBS/milk at RT, then incubated for 1 hour with secondary rabbit anti-mouse HRP (1:3000) in PBS/milk at RT and developed. Lanes show, (1) control, (2) rituximab, (3) BU12-saporin, (4) rituximab and BU12-saporin in combination (all at 10μg/ml). Figure 5.1b shows a western blot of the same samples probed for PCNA illustrating equal loading. This data is representative of 5 independent experiments (see appendix tables 1.1. and 1.2 for additional data).

Time point	2 hours				6 hours				9 hours			
Sample	Control	Rituximab	BU12-saporin	Combination	Control	Rituximab	BU12-saporin	Combination	Control	Rituximab	BU12-saporin	Combination
Cleaved PARP (%)	6	11	20	18	-	19	28	38	-	24	40	58

Table 5.1
Density analysis of the PARP western blotting cleavage data shown in the figure 5.1a. Ramos cells were exposed to rituximab and BU12-saporin individually and in combination (all at 10μg/ml) for 2, 6 and 9 hours. Data is shown as a cleaved PARP as a percentage of the total measured density of cleaved and uncleaved PARP by QuantiScan software (for details see materials and methods 2.7).

a) PARP cleavage

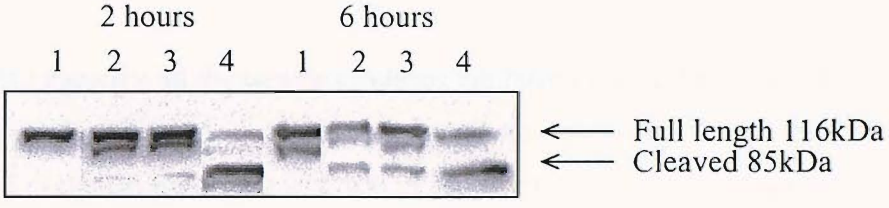

b) PCNA loading control

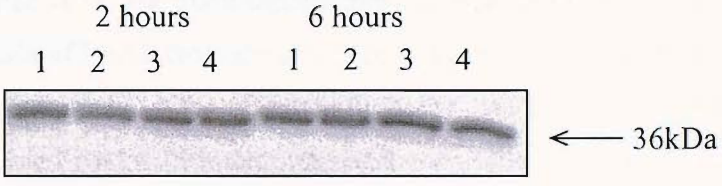

Figure 5.2
Western blots showing PARP cleavage in Ramos cells (figure 5.2a) exposed to cisplatin, saporin and cycloheximide for 2 and 6 hours. Cell lysates were prepared for western blotting by RIPA extraction, blots were probed overnight with mouse anti-PARP (1:1000) in PBS/milk at RT, then incubated for 1 hour with secondary rabbit anti-mouse HRP (1:3000) in PBS/milk at RT and developed. Lanes show, (1) control, (2) cisplatin at 1μg/ml, (3) saporin at 10μg/ml, (4) cycloheximide at 10μg/ml. Figure 5.2b shows a western blot of the same samples probed for PCNA illustrating equal loading. This data is representative of 2 independent experiments.

Time point	2 hours				6 hours			
Sample	Control	Cisplatin	Saporin	Cycloheximide	Control	Cisplatin	Saporin	Cycloheximide
Cleaved PARP (%)	-	18	14	62	-	45	22	40

Table 5.2
Density analysis of the PARP western blotting cleavage data shown in the figure 5.2a. Ramos cells were exposed to cisplatin at 1μg/ml, saporin at 10μg/ml and cycloheximide at 10μg/ml for 2 and 6 hours. Data is shown as a cleaved PARP as a percentage of the total measured density of cleaved and uncleaved PARP by QuantiScan software (for details see materials and methods 2.7).

made to standardise experiments as far as possible, the age and condition of the cells in each experiment is unlikely to identical, also small changes to culture conditions and experimental procedures beyond experimental control were unavoidable.

Ramos cells were also treated with the protein synthesis inhibitor cycloheximide which also caused PARP cleavage (figure 5.2). In this experiment maximum PARP cleavage occurred earlier with cycloheximide treatment than in cells treated with the combination of rituximab and BU12-saporin, i.e. 62% cleaved product was observed at 2 hours in cycloheximide treated cells. The toxin saporin alone also caused PARP cleavage (lane 3, figure 5.2). The levels of PARP cleavage observed with saporin were detectable (22% cleaved PARP by 9 hours), but were substantially lower than the levels detected for cisplatin (45% cleaved PARP by 9 hours) treated Ramos cells (lane 2) and lower than the levels detected for the conjugated immunotoxin, BU12-saporin (figure 5.1). These data were consistent between two individual repeats of these experiments.

Results described in this chapter occasionally show a small amount of PARP cleavage in the control lanes in several figures. This was generally only observed in the control samples at this early time point and was thought to be due to stress caused to the sample during the procedure of setting up the experiment, rather than the harvesting procedure, as cleavage is usually only apparent at the earlier time points. Bands of intermediate size (between 116 and 85kDa) are detected in figures 5.2a (also figure 5.6, 5.10), these may be due to additional PARP cleavage products as the cleavage resulting in the 85kDa fragment is not the only cleavage of PARP known to occur. Other possible explanations include non-specific bands that are not relevant to PARP cleavage. These bands were observed to change depending on the length of incubation with the secondary antibody and also, be dependent on the exposure time (data not shown).

5.2.2 Detecting caspase activation in rituximab and BU12-saporin treated Ramos cells

To determine if the apoptotic effects of rituximab and BU12-saporin described in chapter 3 were caspase dependent or independent, a series of experiments were conducted to detect caspase activation by western blotting. Cellular lysates of Ramos cells treated with

rituximab and BU12-saporin were prepared for SDS PAGE by the CHAPS method of extraction, and proteins transferred to nitrocellulose membranes for western blotting. Membranes were probed with anti-caspase antibodies (see materials and methods 2.7 for details of antibodies used) which recognised the procaspase and the cleaved form of the caspase, enabling the process of activation to be analysed over a time course. The activation of caspases 3, 8 and 9 were initially investigated after exposure to rituximab and BU12-saporin individually and in combination.

The activation of caspase 9 in Ramos cells exposed to rituximab and BU12-saporin is shown in figure 5.3. Western blots and density analysis are shown for 6, 9, and 12 hours exposure to rituximab and BU12-saporin, individually and in combination. These data were consistent between three independent repeats of this experiment. A prominent but non-specific band of approximately 32kDa is visible in all blots. Caspase 9 cleavage in response to cisplatin exposure peaks at 6 hours, caspase processed (38%) and auto-processed cleavage products (13%) were detected. (Densities are expressed as a percentage of total cleaved products and full length caspase, see materials and methods 2.7.) Also at 6 hours a small amount of caspase-processed cleavage product is also detected in the untreated control sample, probably due to stress causes to the sample during preparation.

After 9 hours, the maximum amount of caspase-processed caspase 9 cleavage product was observed in response to exposure to rituximab (43%) and BU12-saporin (42%) alone. After 9 hours, auto-processed caspase 9 cleavage product is detected in cells exposed to rituximab (15%) and BU12-saporin (too low to quantify). By 12 hours the maximum amounts of cleaved products were detected for combination treated cells (45% caspase-processed cleavage product, 17% auto-processed cleavage product).

Two caspase 3 western blots from independent experiments are shown in figure 5.4a and figure 5.4b. These two blots illustrate the variability in the timing of the activation of caspase 3 observed. Figure 5.4a shows cleavage and activation at 12 hours, and figure 5.4b shows cleavage and activation at 9 hours. The extent of cleavage also differs between the two experiments, in figure 5.4a less 19kDa cleavage product is detected (9% for both BU12-saporin and combination treated cells) (table 5.4). Whereas, in figure 5.4b, the 19kDa cleavage product (15%) is only detected in combination treated samples (table 5.4).

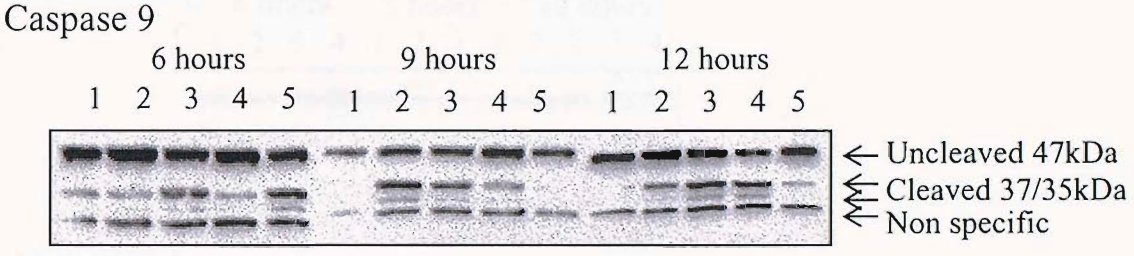

Figure 5.3
Caspase 9 western blots of Ramos cells treated with rituximab and BU12-saporin individually and combination after 2, 6, 9 and 12 hours. Cell lysates were prepared for western blotting by CHAPS extraction, blots were probed overnight with rabbit anti-caspase 9 (1:400) in TBT/milk at 4°C, then incubated for 1 hour with secondary goat anti-rabbit HRP (1:2500) in TBT/milk at RT and developed. Lanes represent cells treated as controls (1), with rituximab at 10μg/ml (2), BU12-saporin at 10μg/ml (3) the combination of rituximab and BU12-saporin at 10μg/ml (4) and cisplatin at 1μg/ml (5). Data shown is representative of 3 independent experiments (see appendix table 1.3 for additional data).

Time point	6 hours					9 hours					12 hours				
Sample	Control	Rituximab	BU12-saporin	Combination	Cisplatin	Control	Rituximab	BU12-saporin	Combination	Cisplatin	Control	Rituximab	BU12-saporin	Combination	Cisplatin
Full length (%)	76	79	64	79	49	100	41	58	76	97	100	70	49	38	83
37kDa (%)	24	21	36	21	38	-	43	42	24	3	-	30	38	45	17
35kDa (%)	-	-	-	-	13	-	15	-	-	-	-	-	13	17	-

Table 5.3
Density analysis of the caspase 9 western blotting cleavage data shown in the figure 5.3. Ramos cells were exposed to rituximab and BU12-saporin individually and in combination (all at 10μg/ml) and cisplatin at 1μg/ml for 6, 9 and 12 hours. Data is shown as a proportion of full length and cleaved caspase 9 fragments as a percentage of the total measured density by QuantiScan software.

a) Caspase 3

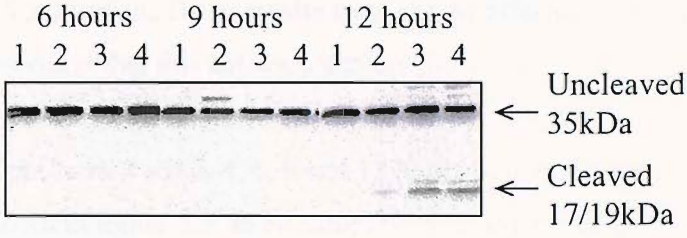

b) Caspase 3

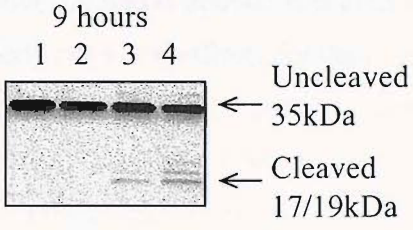

Figure 5.4
Western blots showing caspase 3 cleavage in Ramos cells exposed to rituximab and BU12-saporin. Figures 5.4a and 5.4b represent two independent experiments probed for caspase 3 cleavage at and 6, 9 and 12 hours respectively. Cell lysates were prepared for western blotting by CHAPS extraction, blots were probed overnight with rabbit anti-caspase 3 (1:400) in TBT/milk at 4°C, then incubated for 1 hour with secondary goat anti-rabbit HRP (1:2500) in TBT/milk at RT and developed. Lanes represent cells treated as controls (1), with rituximab at 10µg/ml (2), BU12-saporin at 10µg/ml (3) the combination of rituximab and BU12-saporin at 10µg/ml (4).

Time point	**12 hours (fig 5.4a)** Caspase 3 cleavage				**9 hours (fig 5.4b)** Caspase 3 cleavage			
Sample	Control	Rituximab	BU12-saporin	Combination	Control	Rituximab	BU12-saporin	Combination
Full length %	100	91	66	62	100	100	82	63
Cleaved 19kDa (%)	-	-	9	9	-	-	-	15
Cleaved 17kDa (%)	-	9	25	29	-	-	18	22

Table 5.4
Density analysis of the caspase 3 western blotting cleavage data shown in figure 5.4a and figure 5.4b. Ramos cells were exposed to rituximab and BU12-saporin individually and in combination (all at 10µg/ml) for 6, 9 and 12 hours. Data is shown as a proportion of full length and cleaved caspase 3 fragments as a percentage of the total measured density by QuantiScan software.

No caspase 3 cleavage products were detected in samples exposed to rituximab alone in the experiments shown in figure 5.4b. Caspase 3 activation has also been detected as early as 6 hours post exposure (figure 5.11). This suggests there can be up to 6 hours difference in timing of caspase 3 activation. These results may also be affected by the stability of the caspase 3 cleavage products that this antibody detects (for further discussion see 5.3.2).

Caspase 8 western blots carried out 2, 4, 6, 9 and 12 hours post exposure to rituximab and BU12-saporin are shown in figure 5.5. In all samples including the cisplatin positive control only the inactive 55/50kDa doublet was detected. This suggests either caspase 8 is inactive or this antibody has a low affinity for the cleavage products, which also may also be instable and have a short half-life. (Figure 5.12 demonstrates this antibody can detect these cleavage products.) If caspase 8 is inactive, this suggests the death receptor pathway of the induction of apoptosis was not active.

5.2.3 TRAIL and FAS receptor inhibitor studies

Western blots for caspase 8 activation have shown exposure to rituximab and BU12-saporin does not appear to induce caspase 8 activation, suggesting the death receptor pathway for the induction of apoptosis is inactive. However, the death receptor pathway may still be active as undetectable, small amounts of active caspase 8 may induce caspase 3 cleavage via the action of Bid (Borner 2003). To confirm the death receptor pathway was inactive experiments were carried out with TRAIL and FAS receptor inhibitors. These reagents were determined to be active and cause interference with FAS or TRAIL induced apoptosis induced in lymphoma cell lines (G.K.Packham, personal communication). Ramos cells were pre-treated with the FAS or TRAIL blocking agents (control samples were sham pre-treated) before exposure to rituximab and BU12-saporin. Western blots were probed for PARP cleavage (figure 5.6a) and caspase 3 cleavage (figure 5.7).

In sham pre-treated Ramos cells exposed to the combination of rituximab and BU12-saporin 42% cleaved PARP was detected. In cells exposed to the combination after pre-treatment with FAS or TRAIL blocking agents, 44% and 45% cleaved PARP was detected respectively (figure 5.6a, table 5.5). Levels of cleaved PARP detected in response to

a) Caspase 8

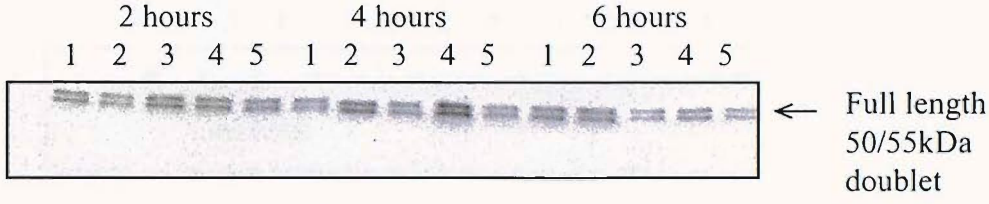

b) Caspase 8

Figure 5.5
Western blots showing caspase 8 cleavage in Ramos cells exposed to rituximab and BU12-saporin at 2, 4, 6 hours (5.5a) and 9 and 12 hours (5.5b).Data shown in 5.5a and b is representative of three experiments. Cell lysates were prepared for western blotting by CHAPS extraction, blots were probed overnight with rabbit anti-caspase 3 (1:400) in TBT/milk at 4oC, then incubated for 1 hour with secondary goat anti-rabbit HRP (1:2500) in TBT/milk at RT and developed. Lanes represent cells treated as controls (1), with rituximab at 10µg/ml (2), BU12-saporin at 10µg/ml (3), the combination of rituximab and BU12-saporin at 10µg/ml (4) and cisplatin at 1µg/ml (5).

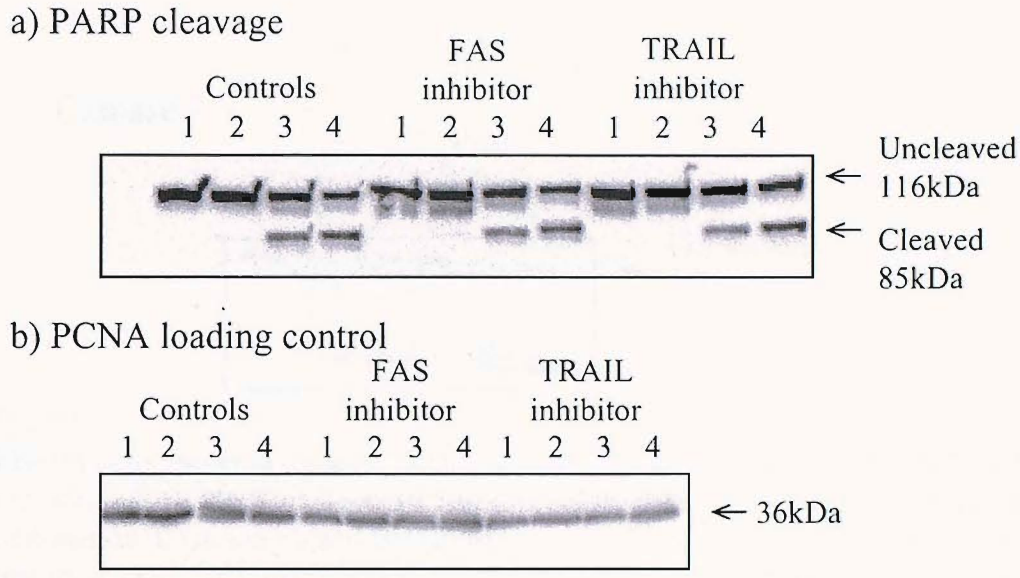

Figure 5.6
Western blots showing PARP cleavage in Ramos cells pre-treated for 1 hour with FAS blocking agent (0.5µg/ml) and anti-TRAIL (2µg/ml) blocking antibody before exposure to rituximab and BU12-saporin for 12 hours. Cell lysates were prepared for western blotting by RIPA extraction, blots were probed overnight with mouse anti-PARP (1:1000) in PBS/milk at RT, then incubated for 1 hour with secondary rabbit anti-mouse HRP (1:3000) in PBS/milk at RT. Figure 5.5a shows PARP cleavage, figure 5.5b shows a blot probed for PCNA demonstrating equal loading. Cells were pre-treated with the blocking reagent or sham treated for 1 hour before exposure to rituximab (lane 2) and BU12-saporin (lane 3) individually and in combination (lane 4) (10µg/ml). Controls are shown in lane 1.

Time point	Controls				FAS blocking agent				TRAIL blocking agent			
Sample	Control	Rituximab	BU12-saporin	Combination	Control	Rituximab	BU12-saporin	Combination	Control	Rituximab	BU12-saporin	Combination
Cleaved (%)	-	8	34	42	-	-	36	44	-	-	32	45

Table 5.5
Density analysis of the PARP western blotting cleavage data shown in figure 5.6a. Ramos cells, pre treated with a FAS or TRAIL blocking agent were exposed to rituximab and BU12-saporin individually and in combination (all at 10µg/ml) for 6, 9 and 12 hours. Data is shown as cleaved PARP as a percentage of the total measured density of cleaved and uncleaved PARP by QuantiScan software (for details see materials and methods 2.7).

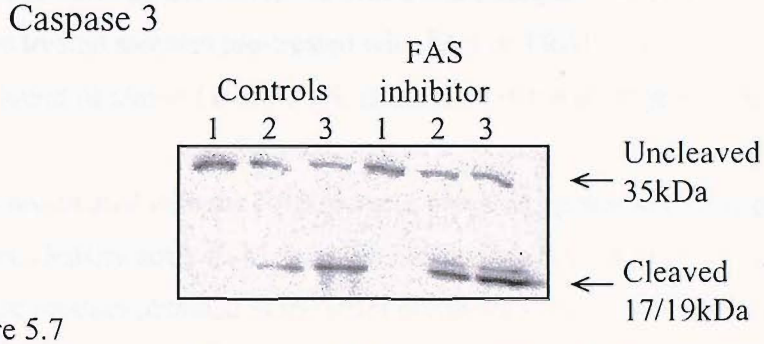

Figure 5.7
Western blots showing caspase 3 cleavage (5.6a) in Ramos cells pre-treated for 1 hour with a FAS blocking agent (0.5µg/ml) before exposure to BU12-saporin and the combination of rituximab and BU12-saporin (all at 10µg/ml) for 12 hours. Cells were pre-treated with the blocking agent for 1 hour before exposure to BU12-saporin (lane 2) individually and in combination (lane 3) (10µg/ml). Controls are shown in lane 1. Cell lysates were prepared for western blotting by CHAPS extraction, blots were probed overnight with rabbit anti-caspase 3 (1:400) in TBT/milk at 4oC, then incubated for 1 hour with secondary goat anti-rabbit HRP (1:2500) in TBT/milk at RT and developed. No repeat experiments were carried out.

Time point	Sham pre-treated			FAS blocking agent		
Sample	Control	BU12-saporin	Combination	Control	BU12-saporin	Combination
Full length (%)	100	55	32	100	27	20
Cleaved 19kDa (%)	-	-	-	-	20	15
Cleaved 17kDa (%)	-	45	68	-	53	65

Table 5.6
Density analysis of the caspase 3 western blotting cleavage data shown in figure 5.7. Ramos cells pre treated with a FAS blocking agent were exposed to rituximab and BU12-saporin individually and in combination (all at 10µg/ml) for 12 hours. Data is shown as a proportion of full length and cleaved caspase 3 fragments as a percentage of the total measured density by QuantiScan software.

BU12-saporin treatment are also approximately equal between the sham pre-treated cells (34%) and cells treated with FAS (36%) or TRAIL (32%) receptor inhibitors. The results show blocking the FAS and TRAIL receptors had no effect on the level of PARP cleavage detected in rituximab and BU12-saporin treated samples. No cleaved PARP is detected in rituximab treated samples pre-treated with FAS or TRAIL receptor inhibitor, although a minor amount of cleaved PARP, 8%, is detected in the sham pre-treated sample.

Samples pre-treated with the FAS receptor blocking agents were also probed for caspase 3 activation. Density analysis showed little difference between the amount of 17kDa caspase 3 cleavage product obtained in the sham pre-treated cells exposed to the combination (68%) compared to 65% 17kDa product obtained in the FAS receptor inhibitor treated cell exposed to the combination (table 5.6). The 19kDa cleavage product is also detected in the FAS receptor inhibitor treated cells suggesting more cleavage has occurred in the cells treated with the FAS receptor inhibitor. This observation is also apparent in cells exposed to BU12-saporin (figure 5.7). These data confirm the FAS and TRAIL receptors of the death receptor pathway for the induction of apoptosis are not active in rituximab and BU12-saporin treated Ramos cells.

5.2.4 Effect of caspase inhibitors on rituximab and BU12-saporin induced apoptosis

Experiments presented in this chapter have shown caspases 3 and 9 to be cleaved and activated in apoptotic cell death induced by rituximab and BU12-saporin individually and in combination. To quantify the proportion of caspase mediated apoptotic cell death in the response observed to rituximab and BU12-saporin, experiments were carried out with the peptide pan-caspase inhibitor zVAD. Many published reports include work with different concentrations of zVAD up to 200μM, following the report of Keppler-Hafkemeyer initially a concentration of 50μM was chosen (Keppler-Hafkemeyer *et al.*, 1998). Initially an annexin V/PI staining experiment was carried out identical to that described in chapter 3, in the presence and absence of zVAD. Figure 5.8 shows the raw data from a representative experiment, the data from three independent repeats are summarised in figure 5.9.

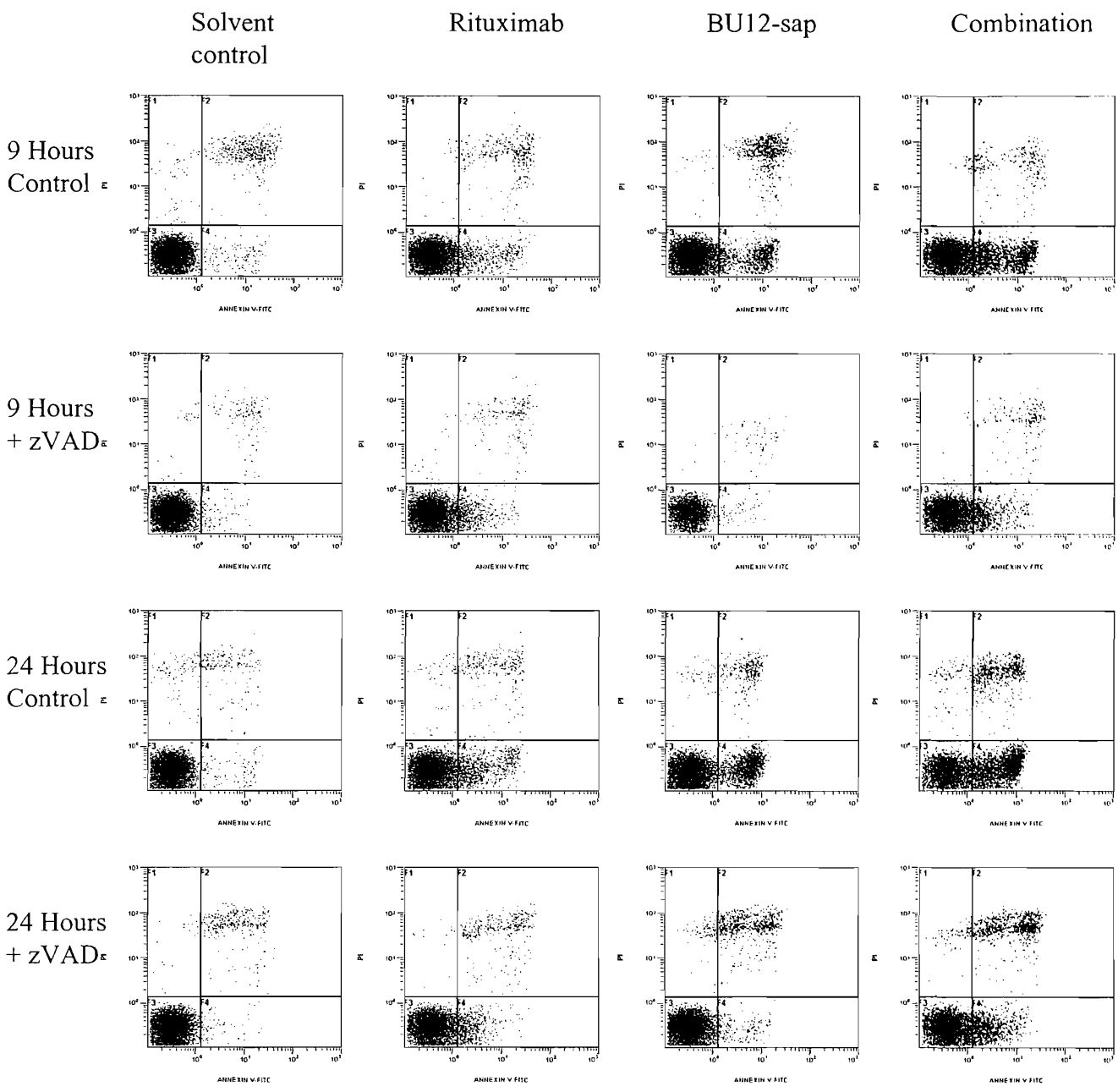

Figure 5.8
Quadrant plots representing combined annexin V/PI staining of Ramos cells treated with rituximab and BU12-saporin individually and in combination at 10µg/ml at 9 and 24 hours in the presence and absence of the peptide caspase inhibitor zVAD at 50µM.

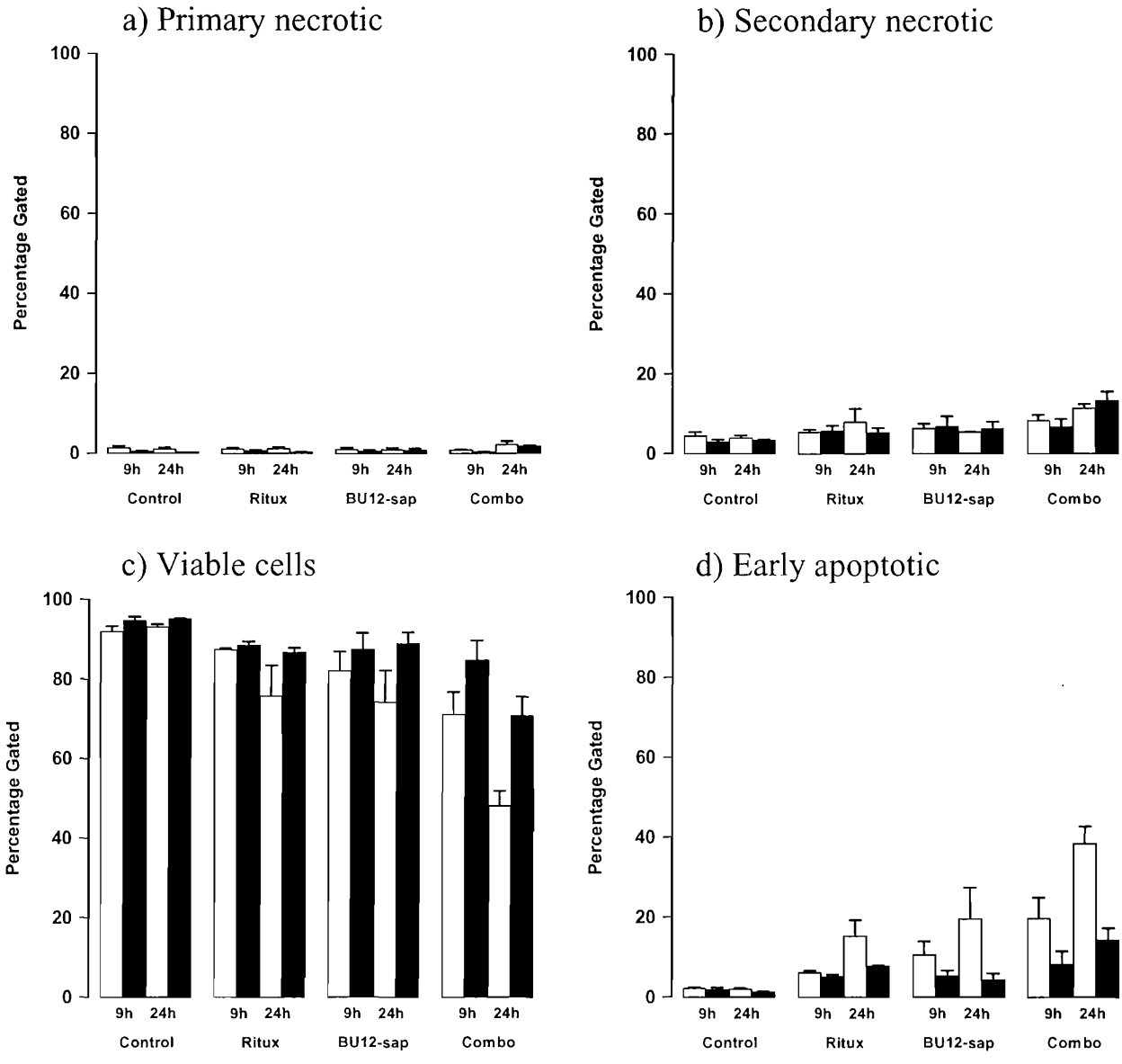

Figure 5.9
Histograms representing annexin V/PI staining of Ramos cells treated as controls, with rituximab at 10μg/ml, BU12-saporin at 10μg/ml or the combination of rituximab and BU12-saporin at 10μg/ml in the presence (■) and absence, solvent control (□) of the peptide caspase inhibitor zVAD at 50μM. Figure 5.9a shows primary necrotic cells, figure 5.9b shows secondary necrotic cells, figure 5.9c viable cells and figure 5.9d shows early apoptotic cells. Bars represent the mean of three independent experiments, error bars the standard error.

Low levels of primary necrotic and secondary necrotic cells are observed in figure 5.8, which show no marked change on addition of the caspase inhibitor (figure 5.8a and b). These raw data suggest adequate staining has been achieved as the low levels of secondary necrotic cells are probably due to these earlier time points used in this experiment compared to those shown in chapter 3. Addition of the caspase inhibitor increases the proportion of viable cells treated with rituximab or BU12-saporin, most prominently in combination treated cells. Reductions in the proportion of early apoptotic cells on addition of zVAD are also apparent in the early apoptotic population particularly in BU12-saporin and combination treated cells.

Comparison of samples treated in the presence and absence of zVAD	Time point (h)	Significance by independent t test at p = 0.05		
		Secondary necrotic	Viable cell	Early apoptotic
Control	9	0.270	0.183	0.613
	24	0.498	**0.041**	0.127
Rituximab	9	0.863	0.376	0.293
	24	0.496	0.290*	0.211*
BU12-saporin	9	0.891	0.451	0.225
	24	0.687	0.163	0.131
Rituximab + BU12-saporin	9	0.555	0.143	0.139
	24	0.509	**0.021**	**0.010**

Table 5.7
Independent t test comparison of annexin V/PI stained Ramos cell samples treated with rituximab and BU12-saporin (10μg/ml) individually and in combination in the presence and absence of the peptide caspase inhibitor zVAD (50μM) at 9 and 24 hours. Data is taken from three independent experiments shown in figure 5.9. Bold text represents data significance at p = 0.05. Statistical analysis was carried out on SPSS statistical software, LEAD technologies inc. (*Equal variances were not assumed by Levene's test.)

Independent t tests were carried out to determine if the effect of caspase inhibitors on apoptosis in rituximab and BU12-saporin treated Ramos cells was significant. The viable proportion of untreated control cells was determined to be significantly different on addition of zVAD at 24 hours. This slight, but significant, difference was probably due to the solvent added to the control samples, equivalent to that added to the zVAD treated samples. The statistical significance of this control population may also be due to the unusually small standard error between these data. At 24 hours, the combination treated viable and early apoptotic populations showed significant increase and reduction respectively on the addition of pan-caspase inhibitor (p = 0.021, p = 0.010).

5.2.5 PARP cleavage in Ramos cells treated with rituximab and BU12-saporin in the presence of caspase inhibitors

Caspase 9 and caspase 3 were shown to be active in rituximab and BU12-saporin induced apoptosis by a series of western blots (figure 5.3 and 5.4). Annexin V/PI staining showed the apoptotic affects of rituximab plus BU12-saporin on the viable and early apoptotic populations are significantly inhibited by the pan caspase inhibitor zVAD. To investigate further the effect of caspase inhibition on apoptosis induced by rituximab and BU12-saporin, a series of western blots were carried out in the presence of zVAD. Blots were probed for PARP cleavage, caspase 3, caspase 8 and caspase 9 activation in the presence of the peptide inhibitors DEVD (specific caspase 3 inhibitor) and zVAD (a pan caspase inhibitor).

PARP cleavage in Ramos cells treated with rituximab and BU12-saporin in combination was partially inhibited in the presence of caspase inhibitors (figure 5.10). PARP cleavage in Ramos cells in response to exposure to rituximab or cisplatin was completely inhibited (figure 5.10a). At 9 hours, Ramos cells treated with the combination of rituximab and BU12-saporin in the presence of zVAD showed a small proportion of cleaved PARP (16%), this was reduced several fold compared to cells treated with the combination in the absence of zVAD where 78% cleaved PARP was observed (figure 5.10a, table 5.8). In this blot two forms of PARP have been detected and included in analysis, the second form may be the ribosylated form (G.K.Packham personal communication). In the presence of zVAD, 9% cleaved PARP was detected after treatment with BU12-saporin alone compared to 67% in BU12-saporin treated solvent controls.

The effect of DEVD, the peptide inhibitor of caspase 3, on PARP cleavage in rituximab and BU12-saporin treated Ramos cells is shown in figure 5.10b. PARP cleavage by rituximab was completely inhibited in the presence of DEVD. Cleavage by BU12-saporin was almost completely inhibited, 11% cleaved PARP was detected in zVAD treated cells compared to 48% in solvent treated controls (table 5.8) PARP cleavage induced by the combination of rituximab and BU12-saporin was also partially inhibited, 21% was detected in comparison to 71% in controls.

a) PARP cleavage with zVAD

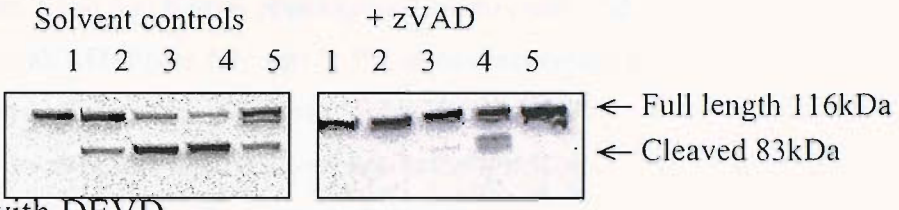

b) PARP cleavage with DEVD

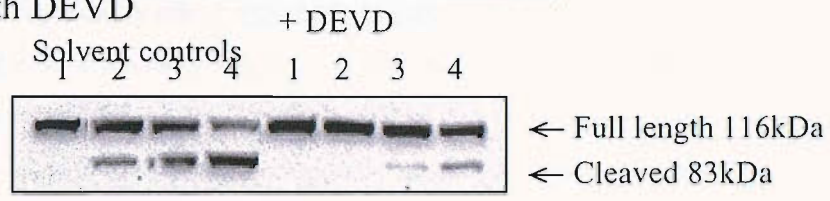

c) PCNA loading control

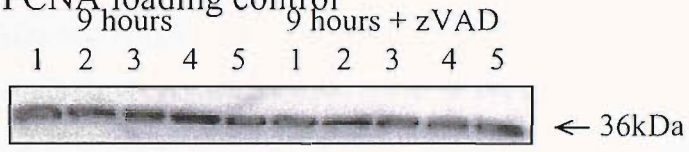

Time point	9 hours					9 hours + Inhibitor				
Sample Table 5.8	Control	Rituximab	BU12-saporin	Combination	Cisplatin	Control	Rituximab	BU12-saporin	Combination	Cisplatin
5.10a zVAD Cleaved PARP (%)	-	24	67	78	39	-	-	9	16	-
5.10b DEVD Cleaved PARP (%)	-	28	48	71	N/A	-	-	11	21	N/A

Figure 5.10
Western blots showing PARP cleavage in Ramos cells exposed to rituximab and BU12-saporin in the presence and absence of the peptide capsase inhibitor zVAD at 50μM. Figure 5.7b shows PCNA loading controls. Controls are shown in lane 1, rituximab at 10μg/ml (lane 2) and BU12-saporin at 10μg/ml(lane 3) individually and in combination at 10μg/ml(lane 4) and cisplatin at 1μg/ml lane 5.

5.2.6 Caspase activation in Ramos cells treated with rituximab and BU12-saporin in the presence of caspase inhibitors

To determine the extent of caspase inhibition western blots were probed for cleavage of procaspases 3 and 8 in Ramos cells exposed to rituximab and BU12-saporin in the presence of zVAD (figure 5.11 and 5.12). In this experiment caspase activation has occurred at an earlier time point than shown in figure 5.3 and 5.4. This change in sensitivity to rituximab and BU12-saporin is thought likely to be due to the condition of the cells, although every effort was made to standardise this variability. Cleaved caspase 3 was detected after 6 hours of exposure to rituximab and BU12-saporin (figure 5.11) compared to 9 or 12 hours previously described (figure 5.4). The extent of cleavage in this experiment was also greater than previously observed (figure 5.11 and 5.4).

These caspase 3 western blots (figure 5.11) show more bands of intermediate size (between 35kDa and 17kDa) than were detected previously. These bands are likely to be the result of antibody cross reactivity with other active caspases (personal communication G.Packham). Due to the quantity of these additional bands, figure 5.11 has not quantified. Full length procaspase 3 was detected in all caspase inhibitor treated samples, unlike for the samples treated in the absence of zVAD. Some 19kDa caspase 3 cleavage product, but no 17kDa product, were detected in the BU12-saporin, combination and cisplatin treated samples in the presence of zVAD at all time points. This may be a result of the solvent added, as these products are also present in the solvent treated controls.

Caspase 8 shows cleavage and activation by 9 hours (figure 5.12). This series of blots (figure 5.11 and 5.12) shows the most extensive caspase activation, suggesting caspase 8 activation is a result of feedback rather than a role in the initiation of apoptosis This was the only blot that caspase 8 activation with rituximab and BU12-saporin exposure was detected. Activation of caspase 8 in FAS independent apoptosis has previously been detected downstream of caspase 3 activation in BJAB cells (Wieder *et al.*, 2001). Caspase 8 activation may have not been previously detected in other blots due to low levels of cleaved products. It is thought the same order of caspase activation was occurring, although at an earlier time point in this experiment as discussed previously.

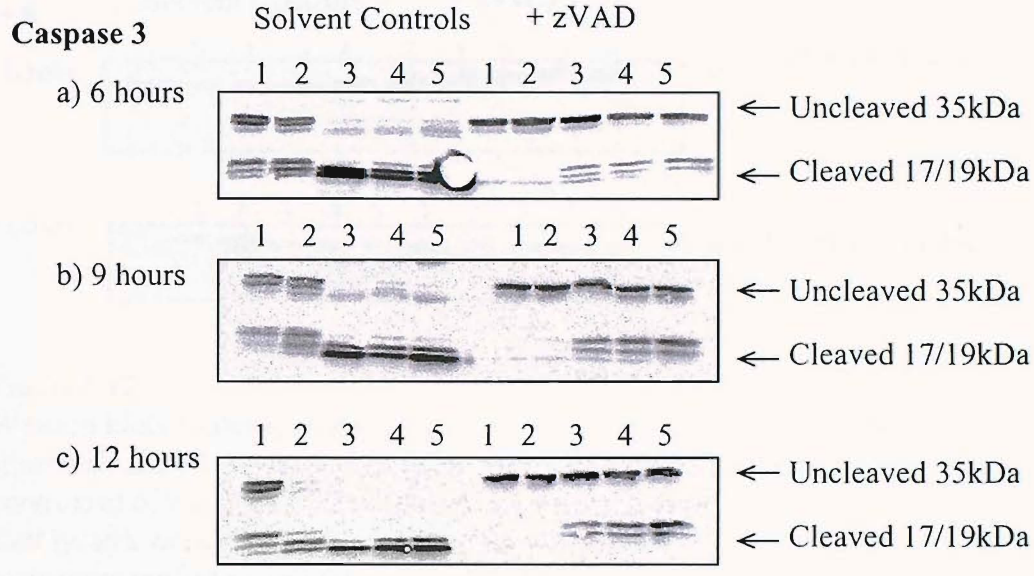

Figure 5.11
Western blots showing caspase 3 cleavage in Ramos cells exposed to rituximab and BU12-saporin in the presence and absence of zVAD at 50μM. Figures 5.11a, b and c represent samples taken at 6, 9 and 12 hours post exposure respectively. Cell lysates were prepared for western blotting by CHAPS extraction, blots were probed overnight with rabbit anti-caspase 3 (1:400) in TBT/milk at 4oC, then incubated for 1 hour with secondary goat anti-rabbit HRP (1:2500) in TBT/milk at RT and developed. Lanes represent cells treated as controls (1), with rituximab at 10μg/ml (2), BU12-saporin at 10μg/ml (3) the combination of rituximab and BU12-saporin at 10μg/ml (4) and cisplatin at 1μg/ml (5).

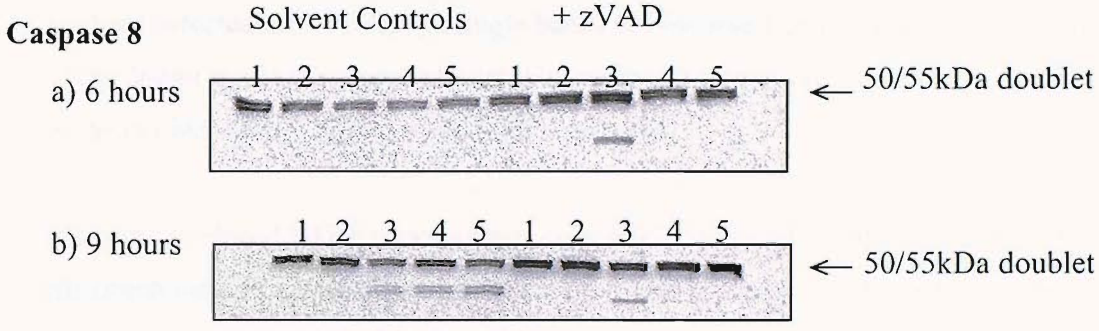

Figure 5.12
Western blots showing caspase 8 cleavage in Ramos cells exposed to rituximab and BU12-saporin in the presence of zVAD or as solvent controls at 6, 9 and 12 hours exposure (figures a, b and c respectively). Cell lysates were prepared for western blotting by CHAPS extraction, blots were probed overnight with rabbit anti-caspase 3 (1:400) in TBT/milk at 4oC, then incubated for 1 hour with secondary goat anti-rabbit HRP (1:2500) in TBT/milk at RT and developed. Lanes represent cells treated as controls (1), with rituximab at 10µg/ml (2), BU12-saporin at 10µg/ml (3), the combination of rituximab and BU12-saporin at 10µg/ml (4) and cisplatin at 1µg/ml (5).

Uncleaved caspase 8 (%) / cleaved (%)	Solvent controls					+ zVAD				
	Control	Rituximab	BU12-saporin	Combination	Cisplatin	Control	Rituximab	BU12-saporin	Combination	Cisplatin
9 hours	-	-	25	26	35	-	-	-	-	-

Table 5.9
Density analysis of the caspase 8 western blotting cleavage data shown in figure 5.12. Ramos cells exposed to rituximab and BU12-saporin in the presence and absence of the peptide caspase inhibitor zVAD at 50µM. Data is shown as a proportion of full length and cleaved caspase 8 fragments as a percentage of the total measured density by QuantiScan software.

Caspase 8 was inactive at 6 hours, in both the samples treated in the presence and absence of zVAD (figure 5.12). By 9 hours, cleaved caspase 8 doublets were detected in BU12-saporin (25%), combination (26%) and cisplatin (35%) treated samples. No active caspase doublets were detected in the samples treated in the presence of zVAD at 9 hours. Density analysis detected the doublets as single bands so only one figure is quoted for the density of the doublets. zVAD completely inhibits caspase 8 activation in the late stages of apoptosis induced by rituximab and BU12-saporin.

Rituximab induced PARP cleavage was completely inhibited by DEVD and zVAD. rituximab induced caspase 3 and 8 activation is also completely inhibited by zVAD. BU12-saporin induced PARP cleaved is almost completely inhibited by DEVD and zVAD, and caspase 8 cleavage by BU12-saporin is inhibited by zVAD. The effect of the combination is similar to that of BU12-saporin alone. Partial PARP cleavage is observed with zVAD and DEVD treatment, caspase cleaved is inhibited. Statistically significant inhibition of the effect of the combination on Ramos cells was detected by statistical analysis of annexin VPI staining data. Exposing Ramos cells to cisplatin in the presence of zVAD inhibits PARP, caspase 8 and partially inhibits caspase 3 cleavage.

5.3 Discussion

5.3.1 PARP cleavage in rituximab and BU12-saporin treated Ramos cells

Western blots of cell lysates exposed to rituximab and BU12-saporin were probed for the hallmark of apoptosis, PARP cleavage to begin investigation of these apoptotic effects at the molecular level. The results described in this chapter demonstrate that rituximab and BU12-saporin, individually and in combination induce PARP cleavage in Ramos cells. Although the timing and extent of PARP cleavage varied between experiments, consistently the combination of rituximab and BU12-saporin induced a greater degree of PARP cleavage than either rituximab or BU12-saporin alone. BU12-saporin alone also consistently induced greater PARP cleavage than rituximab alone at the same time point. Cleaved PARP fragments could be detected between two hours and twelve hours after exposure to rituximab and BU12-saporin.

Rituximab alone has been shown to induce PARP cleavage *in vitro* in two lymphoma models, cell lines with the t(14,18) translocation and human Burkitt's lymphoma cell lines (Mathas *et al.*, 2000). PARP cleavage in response to rituximab was also detected in freshly isolated cells from CLL patients (Byrd *et al.*, 2002). In this chapter exposing Ramos cells to rituximab alone has also been shown to induce PARP cleavage. Several authors have failed to detect PARP cleavage in cells treated with rituximab alone (Alas *et al.*, 2001a). In these reports PARP cleavage was been reported in cells treated with rituximab and a secondary cross linking antibody (Shan *et al.*, 2000) or when cells are treated with rituximab in combination with another agent, such as retinoids or glucocorticoids (Shan *et al.*, 2001, Rose *et al.*, 2002). No PARP cleavage was detected when the AIDS related lymphoma cells line, 2F7 were exposed to rituximab (20μg/ml) or cisplatin alone, however, when used in combination cleavage was observed by 24 hours (Alas *et al.*, 2002).

Rituximab mediated complement dependent cytotoxicity (CDC) has also been shown to act independently of PARP cleavage (Bellosillo *et al.*, 2001). The cytotoxic effect of rituximab was concluded by Bellosillo to be mediated at least in part by CDC, a

mechanism which is CD59 regulated, and a caspase independent and involving the generation of superoxide radicals (O_2^-)(Bellosillo *et al.*, 2001). The generation of reactive oxygen species could only detected by Bellosillo and co-workers in experiments carried out normal human serum, thus may not be detected in experiments using FCS as a source of complement, as in this chapter.

The ribosome inactivating protein, saporin and the protein synthesis inhibitor cycloheximide were also shown to induce PARP cleavage but with different kinetics (figure 5.2). Inhibition of protein synthesis by cycloheximide involves a different mechanism than that employed by ribosome inactivating proteins. Cycloheximide inhibits protein synthesis by inhibiting the sequence involved in the transfer of amino acids from of tRNA to the new peptide (Obrig *et al.*, 1971). Cycloheximide has been previously reported not to induce PARP cleavage (Keppler-Hafkemeyer *et al.*, 1998). Other reports have shown PARP cleavage by cycloheximide is induced via a FAS associated death domain dependent mechanism (Tang *et al.*, 1999). Exposure of Jurkat T-cells to cycloheximide for 8 hours (at 20μg/ml) resulted in PARP cleavage and the release of cytochrome c, and the activation of caspases 3 and 8.

In addition to their rRNA glycosidase activity, ribosome inactivating proteins including saporin have previously also been shown to cause DNA fragmentation by PI staining and DNA laddering assays (Bolognesi et al., 1998, Bergamaschi *et al.*, 1996). Immunotoxins containing PE, and PE alone have been previously shown to cause PARP cleavage (Keppler-Hafkemeyer *et al.*, 1998). Additionally, saporin has been shown to depurinate poly(ADP-ribosyl)ated polymerase PARP (auto modified PARP) also involved in DNA repair. The effects of this DNA depurination is not clear, at a sub toxic level saporin induces transformation in fibroblasts (Barbieri *et al.*, 2003).

Taken together this evidence shows that protein synthesis inhibition and apoptosis may not be mutually exclusive events although no general correlation can be described. Protein synthesis inhibition may eventually lead to apoptosis. An apoptotic cell death rather than a necrotic cell death was observed in response to the ribosome inactivating protein α-sarcin in a human rhabdomyosarcoma cell line (Olmo *et al.*, 2001). Olmo suggest α-sarcin induces PARP cleavage and caspase activation as a downstream event after 28S rRNA catalytic cleavage and protein synthesis inhibition (Olmo *et al.*, 2001). Cycloheximide

which employs an alternative mechanism of protein synthesis inhibition as described above has in some studies been shown not to induce PARP cleavage and caspase 3 activation. DNA degradation was observed in lymphoma cells lines after protein synthesis was reduced to less than 10% by ricin, PE and diphtheria toxins, but not cycloheximide (Kochi and Collier 1993)

The alternative hypothesis proposes that protein synthesis inhibition and apoptosis have are the result of two separate catalytic activities of ribosome activating proteins. In this view, apoptosis and protein synthesis inhibition are two separate mechanisms, induced by different regions of the molecule. In the case of the ribosome inactivating protein, ricin a motif in a portion of the molecule away from active site involved in protein synthesis inhibition was proposed to be responsible for apoptosis (Baluna *et al.*, 2000). Supporting this hypothesis although implicating a different site for the DNA fragmentation catalytic activity, different residues have been identified in saporin associated with each catalytic activity. There is some overlap in the required residues and it appears saporin binds DNA and rRNA at the same active site, although the local positioning of the two substrates could be different (Bagga *et al.*, 2003).

This suggests BU12-saporin may induce protein synthesis inhibition, with PARP cleavage and apoptosis as a subsequent downstream event. Or, BU12-saporin may have two separate catalytic activities, DNA fragmentation and RNA glycosidase activity which both contribute to the cytotoxic activity of saporin.

5.3.2 Caspase 3, 8 and 9 activation in rituximab and BU12-saporin treated Ramos cells

To determine the apoptotic pathways involved in the response to rituximab and BU12-saporin the timing and extent of caspase activation was investigated by western blotting. In this chapter, rituximab and BU12-saporin alone and in combination were shown to induce caspase 3 and caspase 9 activation (figure 5.3 and 5.4). The timing and extent of caspase cleavage was observed to vary between experiments in this system. Hence, the

timing of caspase activation relative to time of exposure to rituximab and BU12-saporin can not be determined, although the order of caspase activation can be deduced.

In response to rituximab and BU12-saporin alone or in combination, caspase 9 was consistently cleaved before cleaved caspase 3 was detected (figure 5.3 and 5.4). These results suggest the mitochondrial pathway of activation of apoptosis and the release of cytochrome C via formation of the apoptosome by signalling upstream of caspase 3 activation. In contradiction, figure 5.3 shows the caspase-processed cleavage product of caspase 9 (37kDa) was detected before the auto–processed cleavage product (35kDa), suggesting caspase 9 was not in fact the first caspase to undergo cleavage and activation. Instead suggesting activation of caspase 9 was the result of the positive feedback loop, as the auto-processed cleaved product was detected after the caspase-processed cleavage product.

The affinity of the antibody used for these cleavage products and the stability of these products must also be taken into consideration. The caspase 9 auto processed product is thought to have a shorter half life and be degraded. The auto processed product may have a lower affinity for this antibody or be only low levels may be present. Although equally, small amount of caspase 9 auto-processed product is required for the formation of small amounts of apoptosome may have formed first, which were not present in large enough quantities to be detected, resulting in a larger quantity of caspase 3 cleavage down stream. In the same way the affinity and stability of the caspase 3 cleavage products must also be considered. In this manner, the results suggest the caspase 8 antibody used in this chapter has a low affinity for the caspase 8 cleavage products as they have only been detected is samples showing large amount of caspase 3 and 9 cleavage.

The reported behaviour of caspases after treatment with rituximab, individually and in combination with a cytotoxic drug, or with a secondary cross linking antibody varies between reports. Several reports state caspase activation can not be detected in CD20 positive cells treated with rituximab alone with out a cross linking antibody. PARP cleavage and caspase 3 activation was only detected on the addition of a secondary cross linking antibody (Mathas *et al.*, 2000). Another study also detected activated caspase 3 (by colourimetric assay) only on clustering of CD20 molecules on cross linking (Hofmeister *et al.*, 2000). This is supported by a another study showing only cross linking anti-CD20

resulted in apoptosis involving loss of mitochondrial membrane potential release of cytochrome c and the activation of caspases 3 and 9 (van der Kolk *et al.*, 2002).

Evidence for caspase 3 and 9 activation and PARP cleavage in cells from rituximab treated CLL patients has been shown (Byrd *et al.*, 2002). *In vivo* cross linking of bound rituximab may occur via cells bearing Fc receptors. Byrd shows no evidence for caspase 8 activation, which is consistent with the results described in this chapter. Caspase 3, or a caspase 3-like enzyme has been shown to be activated in cells treated with a PE containing immunotoxin by 4 hours of exposure (Keppler-Hafkemeyer *et al.*, 1998). No caspase 1 or 2 activation was detected (Keppler-Hafkemeyer *et al.*, 1998). In contradiction, caspases 1 and 3 have been shown to be involved in the cytotoxic activity of the RNA glycosidase ricin (Hu *et al.*, 2001).

In experiments similar to those performed in this chapter, no evidence of caspase 3, 9 or 8 cleavage or PARP cleavage was found when 2F7 (an AIDS related lymphoma cell line) cells were exposed to rituximab at 20μg/ml (double the concentration used in this chapter) or cisplatin (1μg/ml) alone at 3, 6, 12 and 24 hours. When used in combination rituximab and cisplatin result in cleavage of PARP and caspases 3 and 9 activation by 24 hours, but not caspase 8 (Alas *et al.*, 2002). The results obtained when rituximab and cisplatin are used in combination show some similarity to the results obtained in this chapter, although the results obtained when either are used alone oppose the findings from this chapter. In this chapter rituximab and cisplatin alone were shown to induce PARP cleavage, caspase 3 and caspase 9 activation, but to a lesser degree than in combination.

5.3.3 The death receptor pathway in rituximab and BU12-saporin induced apoptosis

Experiments conducted in this chapter with TRAIL and FAS receptor blocking reagents showed no decrease in PARP cleavage and caspase 3 cleavage in cells exposed to rituximab and BU12-saporin, compared to sham treated samples (figure 5.6 and 5.7). This corroborated previous evidence showing inactive caspase 8 (figure 5.5), and confirms these receptors as examples of the death receptor pathway of apoptosis were not involved in the induction of apoptosis by rituximab and BU12-saporin. FAS receptor and FAS

ligand expression has been previously shown to be unchanged by rituximab treatment (Alas *et al.*, 2002), inactive caspase 8 has also been confirmed in several studies (Alas *et al.*, 2002, Byrd *et al.*, 2002).

Ideally the experiments presented in this chapter would have included more positive controls (e.g. FAS ligand) to confirm the blocking activity of the anti-TRAIL and anti-FAS antibodies used. As material was extremely limited, no anti-TRAIL treated samples were available for a caspase 3 western blot and there was no rituximab treated sample for the anti-FAS treated cells on the western blot probed for caspase 3 activation, also no replicate experiments were performed.

Studies blocking FAS receptors in Ramos cells have previously also shown no reduction in rituximab induced apoptosis (Shan *et al.*, 2000). No other studies on the death receptor pathway with the ribosome inactivating protein saporin are known to have been undertaken. Olmo has shown the caspase 8 and death receptor pathway is not involved in sarcin induced apoptosis (Olmo *et al.*, 2001). These two studies appear to confirm the results shown in this chapter.

5.3.4 Caspase inhibitors in rituximab and BU12-saporin induced apoptosis

Western blotting for caspase activation in response to rituximab and BU12-saporin was carried out in the presence of peptide caspase inhibitors to determine the contribution of caspase mediated effects. Apoptosis induced by rituximab and BU12-saporin in combination was partially inhibited by the peptide pan-caspase inhibitor zVAD. This was demonstrated by combined annexin V/PI staining studies in the presence of zVAD, (figure 5.9), and western blots probed for caspase 3 and 9 activation and PARP cleavage in the presence of DEVD and zVAD (figures 5.10, 5.11, 5.12). The effect of rituximab alone on PARP cleavage was completely inhibited by zVAD, whereas the effect of BU12-saporin was almost completely inhibited, and the combination was partially inhibited. These effects were also apparent with the caspase 3 specific inhibitor DEVD (figures 5.10b).

In this chapter, PARP cleavage in rituximab treated Burkitt's lymphoma Ramos cells was completely inhibited at 50μM by DEVD and zVAD. Although the effect of zVAD on annexin V/PI stained rituximab treated cells was apparent but not statistically significant. This apparent contradiction between the morphological and molecular level observations has also been observed by other investigators. DEVD was shown to completely inhibit caspase 3 and the activity of a caspase 3-like enzyme, although the morphological changes associated with apoptosis were only partially inhibited (Keppler Hafkemeyer *et al.,* 1998). In freshly isolated B-cells zVAD was shown to have no effect on rituximab alone mediated phosphatidylserine exposure, DNA fragmentation, cell shrinkage, or loss of mitochondrial membrane potential (Bellosillo *et al.,* 2001). A study using cross linked rituximab also showed zVAD blocks caspase 3, 9 and PARP cleavage but not apoptosis measured by annexin V/PI staining and DNA fragmentation in Ramos cells (van der Kolk *et al.,* 2002).

The partial inhibition observed maybe due to a limitation of these reagents rather than due to the involvement of caspase independent mechanisms. A caspase independent mechanism for the induction of apoptosis involving the generation of reactive oxygen species has been proposed (Bellosillo *et al.,* 2001), although no cleaved PARP was detected by Bellosillo and no alternative mechanisms for caspase independent cleavage of PARP are currently known. If the poor permeability of zVAD and DEVD was causing partial caspase inhibition, partial inhibition would also be observed as partially inhibited PARP cleavage in the cisplatin treated positive controls (figure 5.10). No partial PARP cleavage is observed, but in the caspase 3 and 8 blots with zVAD cisplatin treated cells show results similar to the behaviour of combination treated cells, suggesting partial cleavage is the result of partial caspase inhibition by the peptide inhibitors (figure 5.11, 5.12).

Previous work with peptide caspase inhibitors has been criticised for the use of these inhibitors at high concentrations to combat low permeability. At higher concentrations the effects of the peptide inhibitor are less specific, cathepsins and calpains are also inhibited. zVAD is also a poor inhibitor of some caspases such as caspase 2 (Chan *et al.,* 2003). In this chapter, caspase inhibitors were used at 50μM, in line with the work carried out by Keppler-Hafkemeyer (Keppler-Hafkemeyer *et al.,* 1998, 2000). In some of the other studies discussed here have been used as high as 200μM. This may account for some of

the discrepancy between the observations reported. Dose dependent inhibition of apoptosis was demonstrated (by acridine orange staining) by DEVD used at concentrations up to 200μM in rituximab and cross linking antibody treated lymphoma cells (Mathas *et al.*, 2000).

Additional studies have included work with alternative peptide caspase inhibitors to implicate other caspases in rituximab and ribosome inactivating protein induced apoptosis. Mathas showed the interleukin 1β-converting enzyme inhibitor, YVAD had no effect on rituximab induced apoptosis in cell lines with the t(14,18) translocation and human Burkitt's lymphoma cell lines, suggesting caspase 1 was not involved (Mathas *et al.*, 2000). Also in a Burkitt's lymphoma cell line, PARP cleavage induced by homdimers of rituximab was completely inhibited by DEVD and zVAD at 50μM but only partial inhibited by the inhibitor YVAD, suggesting in contradiction, a possible role for caspase 1 (Ghetie *et al.*, 2001).

Previously, PARP cleavage has been inhibited by DEVD, zVAD and IETD (a caspase 8 inhibitor) in cells treated with a PE containing immunotoxin by 4 hours of exposure (Keppler Hafkemeyer *et al.*, 1998). Keppler Hafkemeyer and co workers also failed to detect caspase 1 and 2 suggesting they are unlikely to be involved. On treatment with zVAD cells were shown to become 2 to 3 fold more resistant to the PE containing immunotoxin, this is likely to be due to the fact zVAD has not been shown not to effect the ADP ribosylation activity of the toxin PE (^{3}H-leucine incorporation activity was unaffected, Keppler-Hefkeymer *et al.*, 1998). The effect of caspase inhibitors on the protein synthesis activity of saporin has not been investigated in this chapter.

5.5 Conclusions

Rituximab and BU12-saporin individually induced PARP cleavage, the hallmark characteristic of apoptosis which was detected by western blotting. In combination, rituximab and BU12-saporin induced greater PARP cleavage than either reagent alone. Individually rituximab and BU12-saporin also induced caspase 3 and caspase 9 cleavage, increased caspase 3 and 9 cleavage was observed in cells exposed to the combination of

rituximab and BU12-saporin. In this model the extent and timing of PARP and caspase cleavage varies between experiments thus the kinetics involved can not be further described. As examples of the death receptor pathway, FAS and TRAIL receptors has been shown not to be involved in apoptotic death induced by rituximab and BU12-saporin in studies using FAS and TRAIL receptor blocking agents.

The effects of caspase inhibitors in cells exposed to rituximab and BU12-saporin was also investigated. The pan caspase inhibitor zVAD and the caspase inhibitor DEVD completely inhibited PARP cleavage in rituximab treated cells. PARP cleavage in BU12-saporin treated cells was almost completely inhibited, whereas PARP cleavage induced by the combination was only partially inhibited. Since the 85kDa cleavage product of PARP is characteristic of caspase activity, these results suggest that caspase inhibition was only partial. These partial inhibition effects were also apparent by annexin V/PI staining, and are likely to be due to the low permeability of the peptide inhibitors. Although, it cannot be excluded that the partial inhibition observed may be due to alternative caspase independent mechanisms or downstream effects of protein synthesis inhibition which is thought not to be affected by peptide caspase inhibitors (Keppler-Hefkeymer *et al.*, 1998, Olmo *et al.*, 2001). This possibility would involve a non caspase protease with the ability to cleave PARP at approximately the same site.

Chapter Six

Role of Bcl-2 family proteins in apoptosis induced by rituximab and BU12-saporin exposure in Ramos cells

6.1 Introduction

The pathways of apoptosis are subject to both positive and negative regulation. The relative abundance of pro-apoptotic and anti-apoptotic Bcl-2 family proteins contribute to determining the susceptibility of a cell to apoptosis. Bcl-2 is a pro-apoptotic member of the family, over expression of Bcl-2 has been linked to a variety of different malignancies including lymphomas, bowel, breast, lung, and skin cancers (Baliga *et al.*, 2002). Bcl-2 family proteins are characterised by the presence of one or more Bcl-2 homology domains and control the permeability of the outer mitochondrial membrane. The t(14;18) translocation in B-cell follicular lymphomas results in the constitutive over expression of Bcl-2, as the *bcl-2* gene is repositioned next to the constitutively expressed immunoglobin heavy chain gene promoting cell survival and inhibiting apoptosis.

Dysregulation of Bcl-2 family protein expression is not only implicated in the development of malignancies, but influences the cellular response to treatment as an inability to induce apoptosis contributes to resistance to chemotherapy regimens. Anti-apoptotic members of the Bcl-2 family of proteins include Bcl-2, Bcl-X_L and Mcl-1. Anti-apoptotic proteins protect the integrity of the mitochondria by preventing cytochrome c release and the activation of caspase 9. Pro-apoptotic proteins include Bax, Bad, Bid, and Bak. Some pro-apoptotic Bcl-2 family members, such as Bax and Bid translocate from the cytosol to the mitochondria, undergo conformational change and insert into the mitochondrial membrane to disrupt mitochondrial transmembrane potential. Pro-apoptotic member of the Bcl-2 family such as Bim contain BH3 death domains which are know to bind the BH3 binding pocket of Bcl-2 and Bcl-X_L to form heterodimers which block the survival promoting activity of Bcl-2 and Bcl-X_L (Borner 2003).

The advantage of using rituximab against malignant cells over expressing Bcl-2 has been proven in clinical trials. Treating B lymphoma cell lines with rituximab has been shown to overcome resistance to apoptosis mediated by Bcl-2 over expression (Mathas *et al.*, 2000). Rituximab and CHOP chemotherapy significantly improved event free survival in Bcl-2 positive diffuse large B cell lymphoma patients (58%±10% versus 32%±10%, p = 0.001) (Mounier *et al.*, 2003). Cell samples from patients with low grade or follicular non Hodgkin's B cell lymphoma converted from Bcl-2 positive to Bcl-2 negative (detected by PCR) on treatment with rituximab suggesting a role for rituximab in the clearing of residual disease (Czuczman *et al.*, 1999).

Few studies have been carried out to determine the role of Bcl-2 family proteins in ribosome inactivating protein mediated cell death. PARP cleavage induced by a PE containing immunotoxin is inhibited by over expression of Bcl-2 (Keppler-Hafkemeyer *et al.*, 1998). Over expression of Bcl-2 partially inhibited apoptosis induced by ricin, also detected by PARP cleavage (Hu *et al.*, 2001). The effect of saporin on Bcl-2 over expressing cells is unknown.

This chapter aims to investigate the role of Bcl-2 family proteins in Ramos cells exposed to rituximab and BU12-saporin. In cell lines over expressing Bcl-2 or Bcl-X_L annexin V/PI staining and protein synthesis inhibition assays were carried out in response to rituximab and BU12-saporin exposure. The effect of Bcl-2 and Bcl-X_L over expression was also explored at the molecular level by western blotting for changes in expression levels of other Bcl-2 protein family members, PARP cleavage and caspase 3 cleavage in response to rituximab and BU12-saporin. Investigating the role of Bcl-2 family proteins will determine whether the combination of rituximab and BU12-saporin could play a role in treating cells resistant to apoptosis conferred by over expression of Bcl-2.

6.2 Results

6.2.1 Expression levels of selected Bcl-2 family proteins in Ramos cells exposed to rituximab and BU12-saporin

To determine the role Bcl-2 family proteins in the apoptotic effects of rituximab and BU12-saporin, western blots were carried out to determine the expression levels of specific anti-apoptotic and pro-apoptotic members of the Bcl-2 family. Figure 6.1 shows the expression level of Bcl-X_L, Bak, Mcl-1 and Bax in Ramos cells after 2, 4, and 6 hours exposure to rituximab and BU12-saporin alone and in combination. Blots for PARP cleavage (figure 6.1a) are shown as positive controls to illustrate the induction of apoptosis (discussed in chapter 5 in more detail). As expected the combination gave a greater degree of PARP cleavage. A western blot probed for the antigen PCNA (shown in figure 6.1b) demonstrates equal loading.

These samples were also probed for Bcl-2 expression but Ramos cells only express constitutive Bcl-2 at a low, undetectable level thus no Bcl-2 was detected in control samples. No changes in expression of Bcl-2 were detected on exposure to rituximab and BU12-saporin (data not shown, but see figure 6.2). Ramos cells show consistent Bcl-X_L expression over the 6 hour time period which is not affected by exposure to rituximab or BU12-saporin (figure 6.1c). Figures 6.1d and 6.1e show the expression of Bax and Bak in Ramos cells in response to rituximab and BU12-saporin treatment. Although variable, no consistent pattern of change could be determined for Bak and Bax expression. These data, confirmed by identical repeats of these experiments, suggested expression of Bak and Bax do not consistently change in response to rituximab and BU12-saporin exposure. Expression levels of Mcl-1 in Ramos cells also appeared to be unaltered in cells treated with rituximab and BU12-saporin.

The experiments shown in figures 6.1 suggest no change in expression of Bcl-2, Bcl-X_L, Bak, Bax or Mcl-1 occurs with the induction of rituximab and BU12-saporin mediated apoptosis. However it is possible these western blots may have failed to detect small

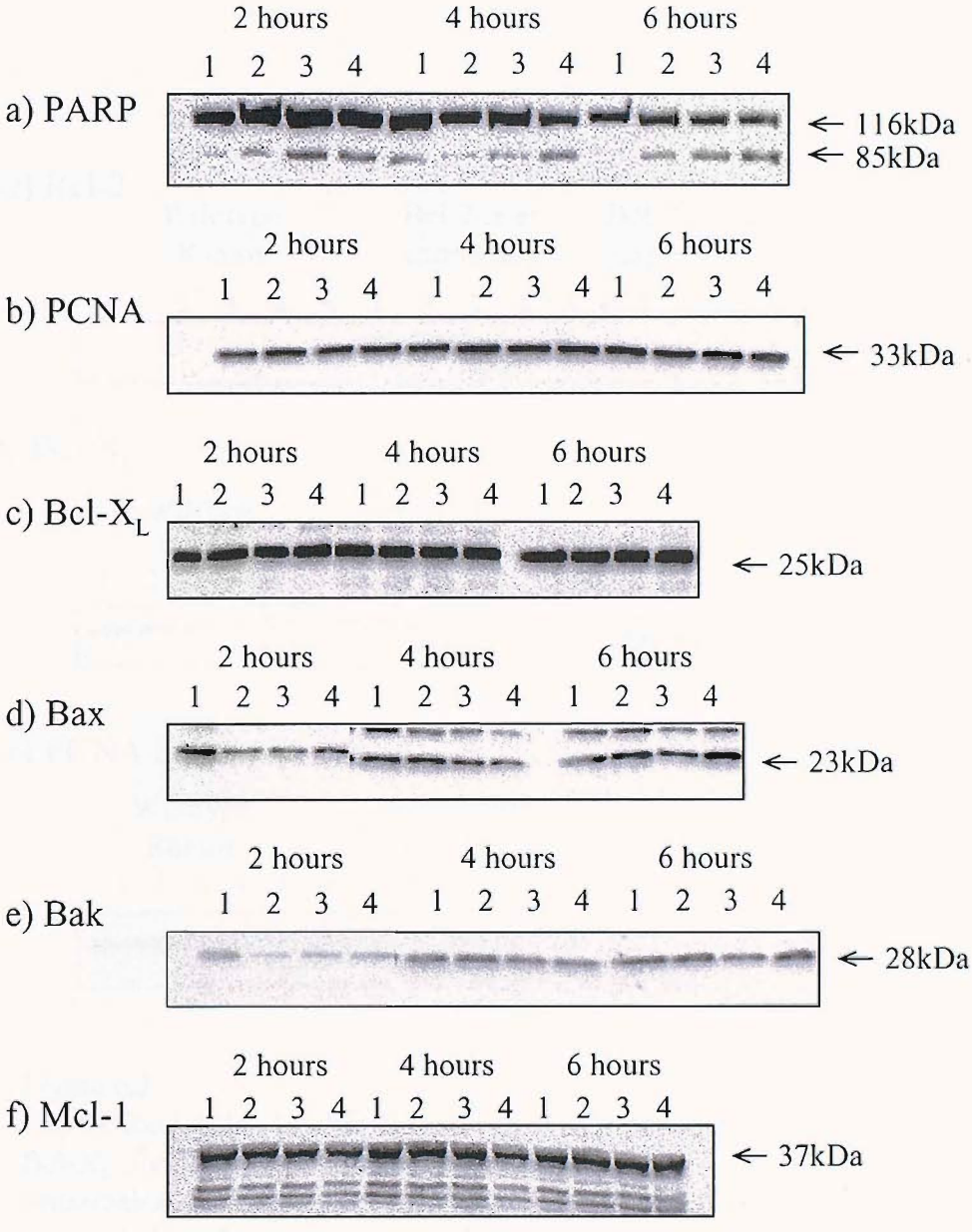

Figure 6.1
Western blots showing changes in expression levels of Bcl-2 family proteins, Bcl-X_L (c), Bax (d), Bak (e) and Mcl-1 (f) over a 6 hour time course after exposure of Ramos cells to rituximab and BU12-saporin alone or in combination. As controls PCNA, to demonstrate equal loading and PARP to demonstrate the onset of apoptosis are also shown (figure 6.1a and 6.b). Cell lysates were prepared for western blotting by RIPA extraction, blots were probed overnight with appropriate primary antibody, then incubated for 1 hour with appropriate secondary HRP conjugated antibody at 4°C and developed (for full details see materials and methods). Cells were treated as controls (lane 1) with rituximab (lane 2) or BU12-saporin (lane 3) or the combination of rituximab and BU12-saporin, lane 4 (all at 10µg/ml). Blots 6.1 c, d, e, and f are representative of 2 independent experiments.

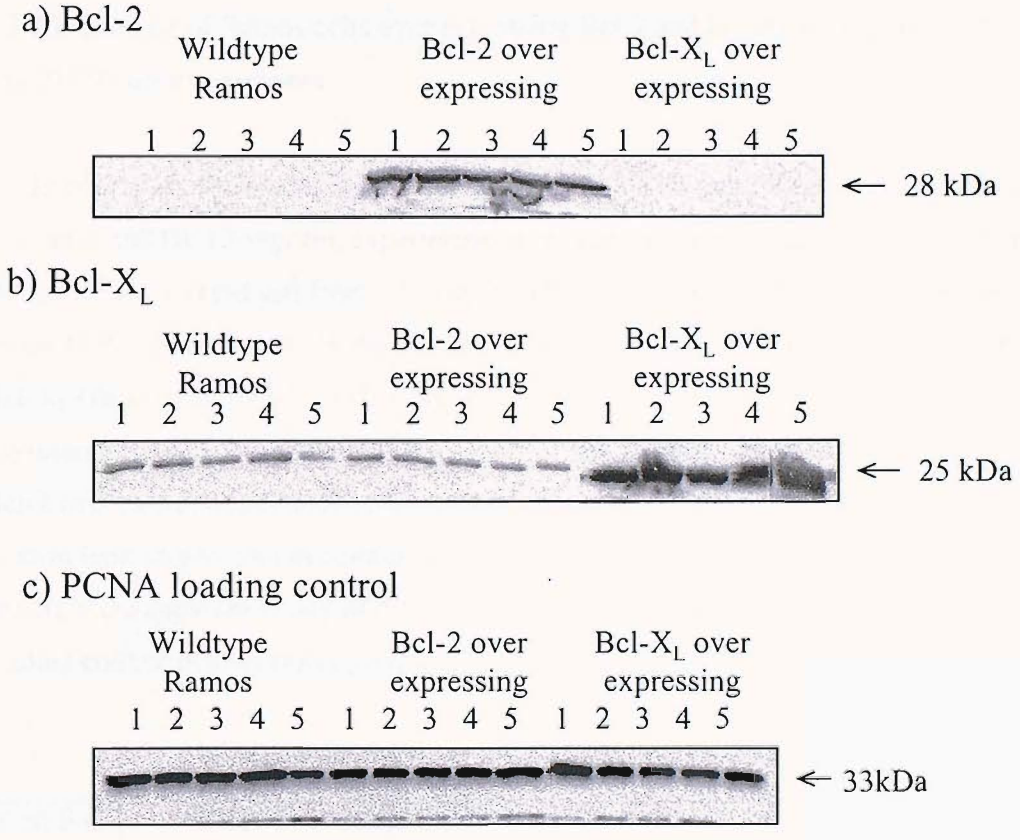

Figure 6.2
Expression levels of Bcl-2 and Bcl-X_L in wildtype and Bcl-2 (fig 6.2a) and Bcl-X_L (fig 6.2b) over expressing Ramos cells after 12 hours exposure to rituximab and BU12-saporin individually and in combination. Figure 6.2c shows PCNA, demonstrating equal loading. Cell lysates were prepared for western blotting by RIPA extraction , blots were probed overnight with appropriate primary antibody at 4°C, then incubated for 1 hour with secondary HRP conjugated antibody at RT and developed (for full details see materials and methods). Cells were treated as controls (lane 1) with rituximab at 10μg/ml (lane 2) or BU12-saporin at 10μg/ml (lane 3), the combination of rituximab and BU12-saporin at 10μg/ml (lane 4) or cisplatin at 1μg/ml. Blots are representative of 2 independent experiments.

changes in Bcl-2 family proteins expression, due to small undetectable changes in expression level.

6.2.2 Behaviour of Ramos cells over expressing Bcl-2 and Bcl-X_L in response to rituximab and BU12-saporin exposure

To determine if over expression of Bcl-2 or Bcl-X_L could promote resistance against rituximab and BU12-saporin, experiments were carried out in Ramos cells over expressing Bcl-2 or Bcl-X_L (kind gift from J.J.Murphy.) Western blots confirmed the expression levels of Bcl-2 and Bcl-X_L in the two Ramos cell lines transfected to over express Bcl-2 or Bcl-X_L (figure 6.2). Bcl-2 levels were not detectable in the wildtype or Bcl-X_L over expressing Ramos cells, although low levels of Bcl-X_L were detected in the wildtype and Bcl-2 over expressing Ramos cells. After 12 hours exposure to rituximab and BU12-saporin individually and in combination no changes to the expression levels of Bcl-2 or Bcl-X_L were apparent in any of the treated cells or cisplatin treated controls. The PCNA loading control demonstrates samples were loaded in equal amounts (figure 6.2c).

Cell line	Wildtype Ramos					Bcl-2 over expressing Ramos					Bcl-X_L over expressing Ramos				
Sample (Density arbitrary units)	Control	Rituximab	BU12-saporin	Combination	Cisplatin	Control	Rituximab	BU12-saporin	Combination	Cisplatin	Control	Rituximab	BU12-saporin	Combination	Cisplatin
Bcl-2 fig6.2a	-	-	-	-	-	145	144	139	138	143	-	-	-	-	-
Bcl-X_L fig6.2b	101	103	84	110	63	92	84	84	81	82	232	228	213	210	221

Table 6.1
Density analysis of the expression levels of Bcl-2 and Bcl-X_L in wildtype and Bcl-2 and Bcl-X_L over expressing Ramos cell lines from the western blots shown in figure 6.2. Ramos cells were exposed to rituximab and BU12-saporin individually and in combination (all at 10μg/ml) for 2, 6 and 9 hours. Data is shown as arbitrary units measured by QuantiScan density analysis software (for details see materials and methods 2.7).

To determine the sensitivity of the Bcl-2 and Bcl-X_L over expressing Ramos cell lines to BU12-saporin and rituximab induced apoptosis annexin V/PI staining experiments were performed. Wildtype Ramos and the Ramos cells over expressing Bcl-2 and Bcl-X_L were exposed to rituximab and BU12-saporin individually and in combination for 24 and 48 hours and stained with annexin V/PI. Figure 6.3 shows a histogram summary of data from three independent experiments. The most striking difference in behaviour between these cells is observed comparing the effect of wildtype to Bcl-X_L over expressing Ramos cells. The Bcl-X_L over expressing cells show greater resistance to rituximab and BU12-saporin than the Bcl-2 over expressing cell line.

6.2.3 Statistical analysis of phosphatidyl serine exposure

Independent t-tests were carried out on these data (figure 6.3) to determine any statistically significant differences in the behaviour of the cell lines in response to rituximab and BU12-saporin. The results of the t-test for the comparison of the Bcl-X_L over expressing cell line compared to wildtype Ramos cells are shown in table 6.1. As no significant values were determined in a similar t-test comparison of the Bcl-2 over expressing Ramos cells compared to wildtype Ramos these data are not shown.

By annexin V/PI staining both Bcl-2 and Bcl-X_L over expressing cell lines showed a degree of resistance to rituximab and BU12-saporin alone and in combination and also cisplatin. Compared to the annexin V/PI staining experiment carried out in chapter 3 (figure 3.6) overall less secondary necrotic and early apoptotic cells and more viable cells were stained in these experiments. This could be attributed to reduced sensitivity of these cells to rituximab and BU12-saporin (reflecting the variable sensitivity observed in chapter 5, discussed further in section 5.2.1) or variability in staining performance between different batches of annexin V/FITC.

The statistics show the effect of rituximab on Bcl-X_L over expressing cells compared to the response of wildtype Ramos cells is significant in the viable and secondary necrotic cellular stained populations at 24 and 48 hours respectively. The effect of BU12-saporin is more distinct, a statistically significant difference was observed in all stained populations

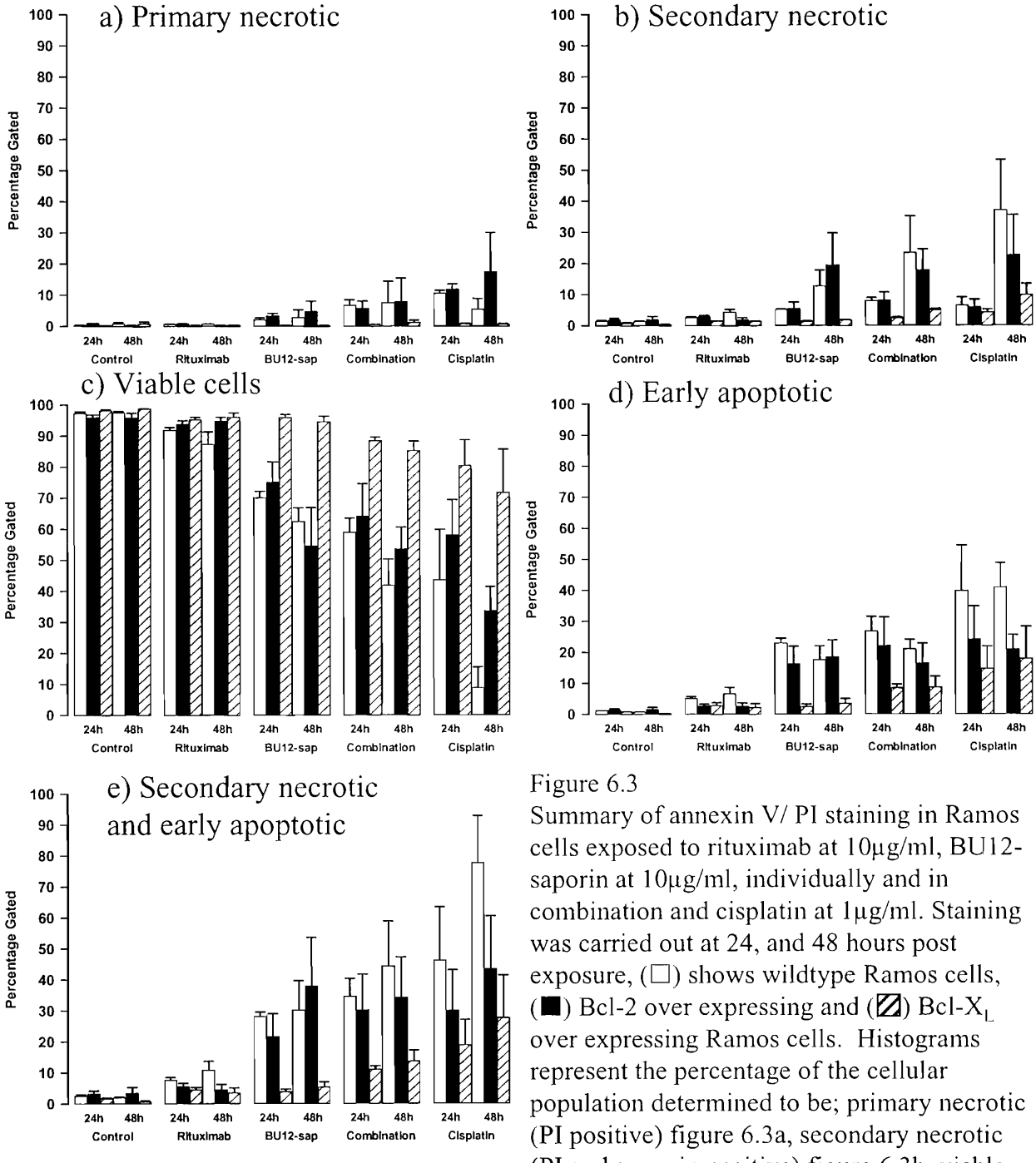

Figure 6.3
Summary of annexin V/ PI staining in Ramos cells exposed to rituximab at 10μg/ml, BU12-saporin at 10μg/ml, individually and in combination and cisplatin at 1μg/ml. Staining was carried out at 24, and 48 hours post exposure, (□) shows wildtype Ramos cells, (■) Bcl-2 over expressing and (▨) Bcl-X_L over expressing Ramos cells. Histograms represent the percentage of the cellular population determined to be; primary necrotic (PI positive) figure 6.3a, secondary necrotic (PI and annexin positive) figure 6.3b, viable (PI and annexin negative) figure 6.3c, and early apoptotic (annexin positive) figure 6.3d. Figure 6.3e represents the sum of the secondary necrotic and early apoptotic populations. Bars represent the mean and standard error of 3 replicate experiments.

at 24 and 48 hours except the secondary necrotic population at 48 hours. The combination of rituximab and BU12-saporin has a statistically significant effect on each of the stained population of Bcl-X_L over expressing cells compared to wildtype Ramos at 24 hours, but only the viable population at 48 hours. This suggests that over expressing Bcl-X_L provided more significant protection against BU12-saporin than rituximab, which is reflected in the results obtained for the combination of rituximab and BU12-saporin.

Treating cells over expressing Bcl-X_L with cisplatin significantly increased the viable proportion of cells, but the trends observed in the other stained populations were not statistically significant, probably due to large standard errors between repeats. Over expressing Bcl-2 is not statistically significantly effective against cisplatin but figures 6.3c and d suggest a possible trend of protection. This suggests a possible mechanistic difference between the over expression of Bcl-2 and Bcl-X_L as Bcl-2 provides some protection against the cytotoxic mechanism of cisplatin but not the antibody based drugs.

Sample	Time (h)	Secondary necrotic	Viable cells	Early apoptotic	Secondary necrotic + apoptotic
Control	24	0.227	0.237	0.202	0.192
	48	0.087	0.125*	0.110	**0.016**
Rituximab	24	0.080*	**0.054**	0.077	0.069
	48	**0.053**	0.11	0.312	0.094
BU12-saporin	24	**0.0004**	**0.0004**	**0.0004**	**0.0002**
	48	0.181*	**0.001**	**0.003**	0.062
Combination	24	**0.030**	**0.003**	**0.021**	**0.051***
	48	0.260*	**0.009**	0.061	0.166*
Cisplatin	24	0.477	0.114	0.200	0.227
	48	0.233*	**0.020***	0.153	0.072

Table 6.2
Results of independent t tests showing the statistical significance of the effect of rituximab and BU12-saporin on wildtype Ramos cells compared to Bcl-X_L over expressing Ramos cells. Bold text shows data significant at p = 0.05. * Equal variances not assumed (Levene's test)

Titrations of rituximab and BU12-saporin against the over expressing cells in a protein synthesis inhibition assay gave highly variable results. Figure 6.4 shows representative

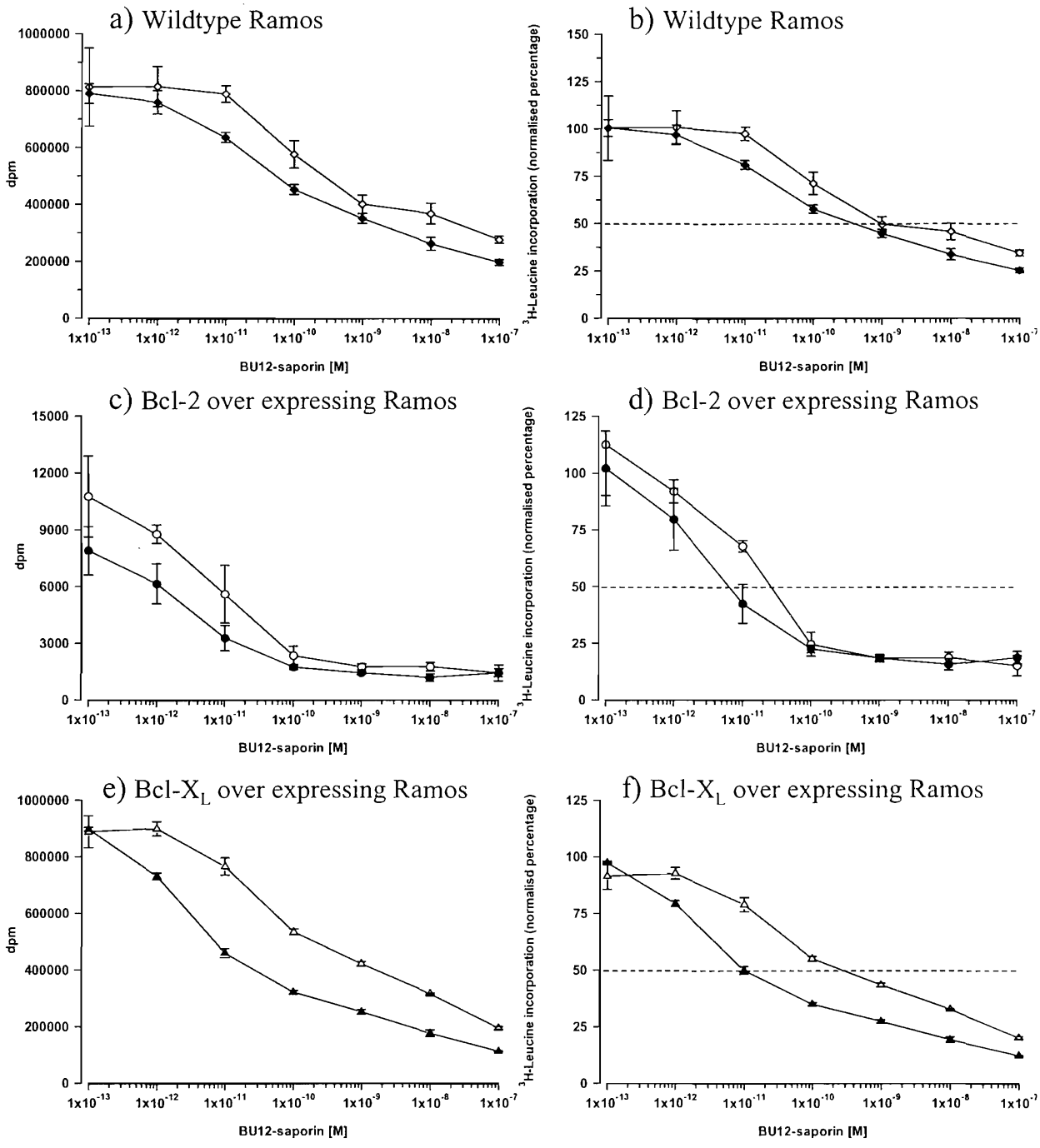

Figure 6.4

Dose response curves from a PSI assay showing the effect of BU12-saporin titrated in the presence and absence of rituximab on wildtype (◇), Bcl-2 (○) and Bcl-X_L (△) over expressing Ramos cells. Cells were exposed to the drug combinations for 24 hours then pulsed with 1μCi 3H-leucine for 16 hours and harvested. Open symbols represent a titration of BU12-saporin, solid symbols represent the addition of rituximab. Points represent the mean of triplicate cultures, error bars represent the standard deviation Sd(n-1) between triplicates. Figures 6.4a, 6.4c and 6.4e show raw data as decays per minute, figures 6.4b, 6.4d and 6.4f represents normalised data expressed as a percentage of ^{3}H-leucine uptake by control cells or uptake by cells treated with rituximab alone. Data shown represents one of four identical repeats carried out.

data from four independent experiments. Results are treated with caution due to the wide variations in these data obtained. A large difference in the amount of ^{3}H-leucine incorporation was observed between the cell lines. The raw data for the Bcl-2 over expressing cells show low counts, around 4 000 to 1 500 dpm. For the wildtype and Bcl-X_L over expressing cells counts were in the range of 800 000 to 200 000 dpm. This explains why small standard deviations are apparent in figure 6.4b and f, but large standard deviations appear in figure 6.4d.

The IC_{50} values obtained for BU12-saporin in the wildtpye and Bcl-2 and Bcl-X_L over expressing cell lines in the presence and absence of rituximab were also subject to wide variation. Compared to the protein synthesis inhibition data shown in chapter 3, the wildtype Ramos are approximately 1 log less sensitive to BU12-saporin (figure 6.4). This could be due to variability in between batches of BU12-saporin or due to variation in the condition of the cells or clonal artefacts. These protein synthesis inhibition assays also show large differences in the amount of leucine incorporation between the cell lines over the same time period. This suggests these cell lines have different rates of protein synthesis, which may affect the effect of BU12-saporin.

An augmentation effect was observed in each of the cell lines on the addition of rituximab, although the magnitude of augmentation was also subject to some variation (figure 6.4).This experiment showed over expression of Bcl-2 and Bcl-X_L did not result in resistance to protein synthesis inhibition induced by BU12-saporin. Whereas by annexin V/PI staining, cells over expressing Bcl-X_L were significantly more resistant to BU12-saporin than wildtype Ramos cells.

6.2.4 PARP cleavage and caspase 3 activation in Bcl-2 and Bcl-X_L over expressing Ramos cells exposed to rituximab and BU12-saporin.

Bcl-X_L over expressing cells were shown to be significantly resistant to the apoptotic effects of rituximab and BU12-saporin by annexin V/PI staining. By annexin V/PI staining, Ramos cells over expressing Bcl-2 showed slight but not significant resistance to apoptosis induced by rituximab and BU12-saporin. This effect was not as evident as that

observed in Bcl-X_L over expressing cells. To compare the resistance effects of Bcl-2 and Bcl-X_L over expression on apoptosis at the molecular level, western blots for PARP cleavage and caspase 3 cleavage in response to rituximab and BU12-saporin exposure were performed.

PARP cleavage induced by rituximab and BU12-saporin individually and in combination and also cisplatin after 12 hours exposure in Bcl-2 and Bcl-X_L over expressing cells is shown in figure 6.5. The pattern of PARP cleavage obtained in the wildtype Ramos treated with rituximab and BU12-saporin was consistent with that described in chapter 5. Density analysis showed in Bcl-2 over expressing cells rituximab mediated PARP cleavage was inhibited. Cleavage induced by BU12-saporin in Bcl-2 over expressing cells, the combination of rituximab and BU12-saporin (42% cleaved PARP) and PARP cleavage mediated by cisplatin was partially inhibited (56% cleaved PARP) (figure 6.5, table 6.3). In Bcl-X_L over expressing cells, figure 6.5 shows PARP cleavage was completely inhibited in rituximab, BU12-saporin and cisplatin treated cells, but partially inhibited in cells treated with the combination (32% cleaved PARP) (figure 6.5, table 6.3). This reflects the results from the annexin V/PI staining experiments, Bcl-2 over expression provides a degree of protection against rituximab and BU12-saporin individually and in combination, but greater protection was afforded by Bcl-X_L over expressing cells.

Western blotting was carried out to determine caspase 3 activation in Bcl-2 and Bcl-X_L over expressing Ramos cells (figure 6.6). The pattern of caspase 3 activation in wildtype Ramos cells exposed to rituximab and BU12-saporin, as expected was consistent with that described previously in chapter 5. Activated caspase 3 was detected in combination and cisplatin treated Bcl-2 over expressing Ramos cells, although at a reduced level compared to that detected in wildtype Ramos cells. No 19kDa cleavage product was detected in the combination treated Bcl-2 over expressing cells. Full length caspase 3 was detected in the cisplatin treated Bcl-2 over expressing cells unlike with wildtype Ramos cells. No cleaved caspase 3 fragments are detected in any of the Bcl-X_L over expressing treated cells. This confirms the results obtained by annexin V/PI staining and the PARP cleavage blots.

These data showed resistance to caspase mediated apoptosis by Bcl-2 over expression can be partially over come by treatment with rituximab and BU12-saporin in combination. This was demonstrated by annexin V/PI staining experiments, PARP cleavage and caspase

a) PARP cleavage

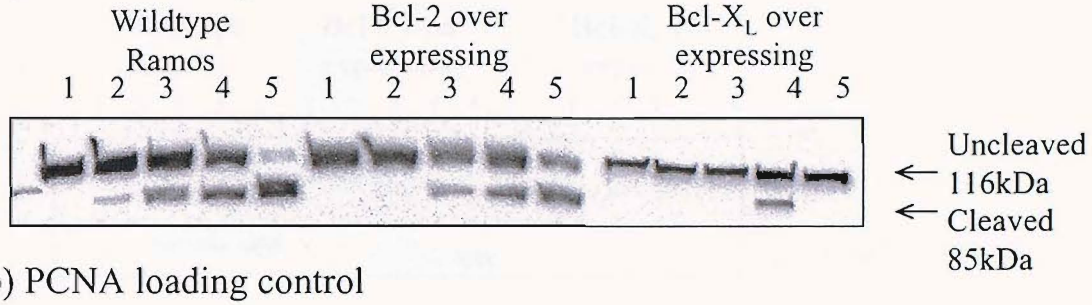

b) PCNA loading control

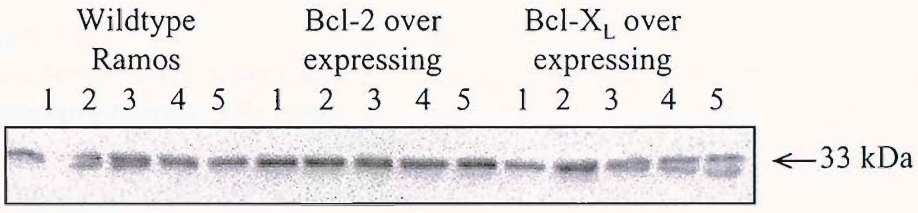

Figure 6.5

Western blots showing PARP cleavage (fig 6.5a) in wildtype and Bcl-2 and Bcl-X_L over expressing Ramos cells after 12 hours exposure to rituximab and BU12-saporin individually and in combination. Cells were treated as controls (lane 1) with rituximab at 10µg/ml (lane 2) or BU12-saporin at 10µg/ml (lane 3), the combination of rituximab and BU12-saporin at 10µg/ml (lane 4) or cisplatin at 1µg/ml. Cell lysates were prepared for western blotting by RIPA extraction , blots were probed overnight with mouse anti-PARP (1:1000) in PBS/milk at RT, then incubated for 1 hour with secondary rabbit anti-mouse HRP (1:3000) in PBS/milk at RT and developed. Figures 6.5b shows a western blot probed with PCNA to demonstrate equal loading. Data shown is representative of two identical experiments carried out.

Cell line	Wildtype Ramos					Bcl-2 over expressing Ramos					Bcl-X_L over expressing Ramos				
Sample	Control	Rituximab	BU12-saporin	Combination	Cisplatin	Control	Rituximab	BU12-saporin	Combination	Cisplatin	Control	Rituximab	BU12-saporin	Combination	Cisplatin
Cleaved PARP (%)	0	18	35	46	77	0	0	37	42	56	0	0	0	32	0

Table 6.3

Density analysis of the levels of cleaved and uncleaved PARP detected in wildtype, Bcl-2 and Bcl-X_L over expressing Ramos cell lines from the western blots shown in figure 6.5. Ramos cells were exposed to rituximab and BU12-saporin individually and in combination (all at 10µg/ml), and cisplatin (1µg/ml) for 12 hours. Data is shown as a ratio of uncleaved and cleaved PARP as a percentage of the total measured density by QuantiScan software (for details see materials and methods 2.7).

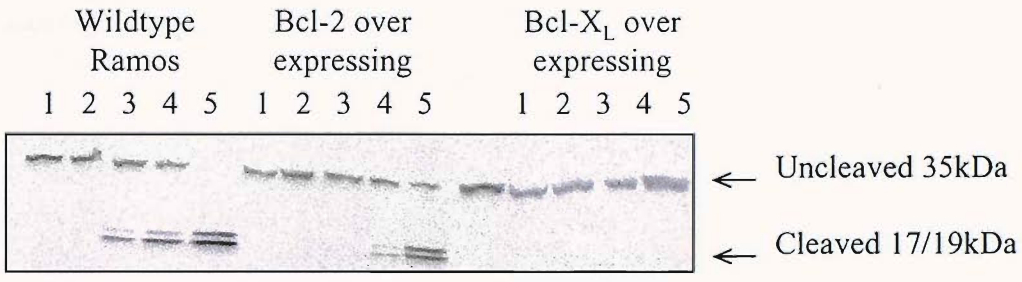

Figure 6.6
A western blot showing caspase 3 cleavage in wildtype and Bcl-2 and Bcl-X_L over expressing Ramos cells exposed to rituximab and BU12-saporin. Cells were treated as controls (lane 1) with rituximab at 10μg/ml (lane 2) or BU12-saporin at 10μg/ml (lane 3), the combination of rituximab and BU12-saporin at 10μg/ml (lane 4) or cisplatin at 1μg/ml for 12 hours. Cell lysates were prepared for western blotting by CHAPS extraction, blots were probed overnight with rabbit anti-caspase 3 (1:400) in TBT/milk at 4°C, then incubated for 1 hour with an HRP conjugated secondary goat anti-rabbit antibody (1:2500) in TBT/milk at RT and developed.

Time point	Wildtype Ramos					Bcl-2 over expressing Ramos					Bcl-X_L over expressing Ramos				
Sample	Control	Rituximab	BU12-saporin	Combination	Cisplatin	Control	Rituximab	BU12-saporin	Combination	Cisplatin	Control	Rituximab	BU12-saporin	Combination	Cisplatin
Uncleaved (%)	100	100	50	32	-	100	100	100	72	17	100	100	100	100	100
Cleaved 19kDa(%)	-	-	12	19	40	-	-	-	-	40	-	-	-	-	-
Cleaved 17kDa(%)	-	-	38	49	60	-	-	-	28	43	-	-	-	-	-

Table 6.4
Density analysis of the caspase 3 western blotting cleavage data shown in figure 6.6. Wildtype, Bcl-2 and Bcl-X_L over expressing Ramos cells were exposed to rituximab and BU12-saporin individually and in combination (all at 10μg/ml) or cisplatin at 1μg/ml for 12 hours. Data is shown as a proportion of full length and cleaved caspase 3 fragments as a percentage of the total measured density by QuantiScan software.

3 cleavage western blots. Cells over expressing of Bcl-X_L were significantly resistant to rituximab and BU12-saporin individually and to a lesser extent in combination. This was demonstrated by annexin V/PI staining experiments and western blotting for PARP and caspase 3 cleavage.

6.3 Discussion

Bcl-2 family proteins play a critical role in the regulation of apoptosis. Bcl-2 has anti-apoptotic and chemo-protective effects associated with the failure of treatment regimens in lymphoma patients. Bcl-2 is also upregulated by Epstein Barr virus (EBV) in the majority of EBV associated lymphoproliferative disease (Loomis *et al.*, 2003). The role of Bcl-2 family proteins, such as Bcl-2 and Bcl-X_L, in the induction of apoptosis by rituximab and BU12-saporin were important to determine if rituximab and BU12-saporin can be employed against this form of chemo-resistant disease.

Previous studies have reported over expression of Bcl-2 does not confer resistant to rituximab. Two independent reports showed Ramos cells over expressing Bcl-2 were not resistant to apoptosis mediated by cross linking CD20 (Shan *et al.*, 2002, van der Kolk *et al.*, 2002). A B lymphoma cell line over expressing Bcl-2 containing the t(14;18) translocation, SU-DHL4, was also sensitive to apoptosis mediated by CD20 cross linking (Shan *et al.*, 2000). Although slower induction of apoptosis in response to cross linking CD20 was detected in t(14;18) positive lymphoma lines, compared to Burkitt's lymphoma cell lines (Mathas *et al.*, 2000), suggesting in this case the over expression of Bcl-2 may have conferred slight resistance to rituximab.

The experiments presented in this chapter showed the level of expression of Bcl-2, Bcl-X_L, Bax, Bak, and Mcl-1 are unchanged after exposure to rituximab and BU12-saporin individually and in combination. Significant up regulation of Bax on induction of apoptosis by CD20 (cross linked) which decreased after 6 to 8 hours has been reported, associated with no change in Bcl-2, Bcl-X_L or Bad expression in Burkitt's lymphoma cell lines (Mathas *et al.*, 2000). Over expression of Bax in the human B lymphoma cell line BL-41 was previously shown to sensitise Burkitt's lymphoma cells to apoptosis (Weinmann *et al.*, 1997). Mathas suggested CD20 induced apoptosis involves a similar pathway to BCR mediated apoptosis, where Bcl-2 and Bcl-X_L levels remain unaltered and Bax levels are up regulated (Mathas *et al.*, 2000). In this chapter, Bcl-2 and Bcl-X_L levels were not observed to change in response to rituximab exposure, partially corroborating this theory, however no Bax up-regulation was detected.

Primary CLL cells showed decreased expression of Mcl-1 and XIAP after rituximab treatment but no changed Bcl-2 or Bax expression was observed (Byrd *et al.*, 2002). These observations were thought to reflect a favourable clinical result (Byrd *et al.*, 2002). Mcl-1 is an essential survival molecule for B lymphoma cells and is cleaved by caspases to a death promoting molecule during apoptosis (Michels *et al.*, 2004). In this chapter expression of Mcl-1 in Ramos cells was unchanged after rituximab or BU12-saporin treatment. This suggests, contrary to the evidence proposed by Byrd, down regulation of Mcl-1 may not be involved in the induction of apoptosis by rituximab in this system.

In an AIDS related lymphoma model exposure to rituximab inhibited expression of Bcl-2, but no change was observed in the expression level of Bad, Bax or Apaf-1 (Alas *et al.*, 2002). Expression levels of Bcl-X_L were not affected by rituximab exposure in AIDS related lymphoma (2F7) cells (Alas *et al.*, 2001a). Down regulation of Bcl-2 by rituximab was shown sensitise cells to cytotoxic drugs by decreasing activation of signal transducer and activator of transcription 3 (STAT3), known to be constituently activated in non Hodgkin's lymphoma (Alas *et al.*, 2001b). Downregulation of STAT3 was achieved by inhibiting the autocrine/paracrine signalling loops of the anti apoptotic cytokine IL10, via Janus associated kinase (JAK) 1 (Alas *et al.*, 2001a and 2003). Daudi and Ramos cells have been shown to be not sensitised in this manner, as no changes in their Bcl-2 or IL10 levels were detected (Alas *et al.*, 2001a).

In a recent study rituximab was shown to down regulate Bcl-X_L expression and up regulate Apaf-1 in Ramos cells (Jazirehi *et al.*, 2003). In combination with paclitaxel, rituximab induced tBid formation, release of cytochrome c and caspase activation resulting in synergistic apoptosis in NHL cells that were resistant to the apoptotic effects of paclitaxel or rituximab alone (Jazirehi *et al.*, 2003). Suggesting in Bcl-2 deficient cells, the homologue Bcl-X_L is a novel intracellular target of rituximab responsible for sensitization to paclitaxel induced apoptosis. In this chapter no down regulation of Bcl-X_L was detected, although western blots to detect Apaf-1 and Bid were not carried out. A concentration of rituximab double that used in this chapter was used, also observations were made at much later time points (up to 48 hours) suggesting possible reasons for the discrepancies between the results presented in this chapter (Jazirehi *et al.*, 2003).

Cells over expressing Bcl-2 were not resistant to the effects of rituximab and BU12-saporin exposure as detected by annexin V/PI staining, PARP cleavage, caspase 3 cleavage and PSI assays. By annexin V/PI staining Bcl-2 over expressing Ramos cells did not behave significantly differently to wildtype cells. Resistance to rituximab alone, but not BU12-saporin or the combination was observed in western blots for PARP cleavage. Western blots for caspase 3 cleavage showed resistance to rituximab and more resistance to BU12-saporin and combination than observed by other techniques. Although PSI assays showed dose response curves for BU12-saporin and the combination of rituximab and BU12-saporin similar to those obtained for wildtype cells. Taken together these data suggest the combination of rituximab and BU12-saporin is effective against Bcl-2 over expressing Ramos cells.

The ribosome inactivating protein abrin showed results similar to those obtained in this chapter on Jurkat cells and Jurkat cells over expressing Bcl-2. Bcl-2 over expressing Jurkat cells were resistant to abrin mediated apoptosis, but protein synthesis inhibition was unaffected (by PSI assay) (Narayanan *et al.*, 2004). In the Bcl-2 over expressing cells no changes to mitochondrial membrane permeability or reactive oxygen species were detected, as in the wildtype cells. Narayanan suggests the mitochondrial pathway of apoptosis is activated as a down stream effect of protein synthesis inhibition due to mitochondrial damage and increased reactive oxygen species production (Narayanan *et al.*, 2004).

In the experiments presented in this chapter over expression of Bcl-X_L did confer resistance to rituximab and BU12-saporin, and cisplatin determined by annexin V/PI staining, PARP cleavage, and caspase 3 cleavage. By PSI assay, a dose response curve was obtained in response to BU12-saporin comparable to that obtained in wildtype cells, which showed augmentation on addition of rituximab. This suggested the protein synthesis inhibition activity of saporin was not disrupted by over expression of Bcl-X_L. This does not explain why the effect of BU12-saporin in a PSI assay can be augmented by rituximab in Bcl-X_L over expressing cells. It is unlikely that complement mediated mechanisms without apoptosis are responsible for such a large augmentation effect (see chapter 4).

PARP cleavage induced by a PE containing immunotoxin was inhibited by over expression of Bcl-2 (Keppler-Hafkemeyer *et al.*, 1998). Also overexpression of Bcl-2 partially inhibited apoptosis induced by ricin, only minimal amounts of PARP cleavage were obtained (Hu *et al.*, 2001). Ricin has previously been shown to modulate the expression level of several members of the Bcl-2 family of proteins. Bcl-X_L and Bcl-2 expression levels decreased with prolonged ricin exposure (Hu *et al.*, 2001). Bax also decreased early in apoptosis to a level hardly detectable by late apoptosis and Bak expression increased with ricin induced apoptosis (Hu *et al.*, 2001). Overexpression of Bcl-2 partially inhibited apoptosis induced by BU12-saporin, reduced PARP cleavage was observed although modulation of Bcl-X_L, Bcl-2, Bax and Bak was not observed in the experiment s carried out in this chapter in cells treated with a saporin based immunotoxin. This suggests the apoptotic effects of saporin and ricin show significant differences.

The apoptotic effects of the protein synthesis inhibitor cycloheximide are inhibited by over expression of Bcl-2 (Hu *et al.*, 2001). Hu observed little to no additivity when cycloheximide and ricin (type II RIP), which alone was partially inhibited by over expression of Bcl-2, were used in combination against Bcl-2 over expressing cells (Hu *et al.*, 2001). The apoptotic effects of abrin (type II RIP), PE and PE containing immunotoxins are inhibited by Bcl-2 over expression, but not the protein synthesis inhibition activity (Narayanan *et al.*, 2004, Keppler-Hafkemeyer *et al.*, 1998). The apoptotic effects of BU12-saporin (saporin is a type I RIP) were only slightly inhibited by over expression of Bcl-2 and inhibited by the over expression of Bcl-X_L, whilst the protein synthesis inhibition activity was not affected. Previously this Bcl-X_L over expressing cell line was also shown not to be resistant to the apoptotic effects of cycloheximide, but to protect against FAS mediated apoptosis (Alam *et al.*, 1997). This suggests protein synthesis inhibitors which induced apoptosis and inhibit protein synthesis via different mechanisms respond differently compared to ribosome inactivating proteins in Bcl-2 and Bcl-X_L over expressing cells.

6.4 Conclusions

These results showed Ramos cells over expressing Bcl-2 were not resistant to the effects of rituximab and BU12-saporin exposure, as detected by annexin V/PI staining, PARP cleavage, caspase 3 cleavage and PSI assays. Overexpression of Bcl-X_L did confer resistance to rituximab and BU12-saporin individually and in combination, and cisplatin determined by annexin V/PI staining, PARP and caspase 3 cleavage. The protein synthesis inhibition activity of saporin appeared to be unaltered in PSI assays carried out on Bcl-2 and Bcl-X_L over expressing cells. The difference observed between the effect of rituximab and BU12-saporin on Bcl-2 or Bcl-X_L over expressing cells, maybe due to the magnitude of overexpression of Bcl-2 or Bcl-X_L or fundamental differences in the behaviour of Bcl-2 and Bcl-X_L. The results show rituximab and BU12-saporin could play a role in treating cells resistant to apoptosis conferred by over expression of Bcl-2, but that elevated levels of Bcl-X_L may interfere with effective cell killing.

Chapter Seven

General Discussion and Conclusions

Antibody based therapies have the potential to treat cancer in a selective manner. Existing cancer therapies treat the disease in a non selective manner, also causing damage to normal cells. Using cocktails of current anti cancer drugs has proven more effective than individual drugs used alone. Similarly, cocktails of different antibody drugs are also proving more effective. This thesis describes the use of two different antibody-type drugs against human B cell lymphoma cell lines. The results showed when the two are used in combination their efficacy at killing lymphoma cells is significantly improved.

Chapter three describes the effect of rituximab and BU12-saporin on protein synthesis inhibition and follows several charactistic features of the induction of apoptosis in B cell lymphoma cell lines. The PSI assays, described in chapter three, showed that BU12-saporin and rituximab individually caused protein synthesis inhibition. The CD19 targeted immunotoxin BU12-saporin showed a 4 log increase in potency compared to the toxin saporin alone. The combination of rituximab and BU12-saporin caused protein synthesis inhibition in an additive manner, and causing a 5-fold increase to potency as compared to BU12-saporin (data normalised against a rituximab alone treated control). This suggests that in Ramos cells rituximab augments the protein synthesis inhibition activity of BU12-saporin.

A panel of B cell lymphoma cell lines showed an augmentation effect between the effects of rituximab and BU12-saporin that was detectable but less pronounced. A wide range of sensitivities to BU12-saporin was observed which may be related to the level of CD19 expression. Also in protein synthesis inhibition assays, cycloheximide did not show any augmentation effects when used in combination with rituximab against Ramos cells. Cycloheximide is known to inhibit protein synthesis via inhibition of peptidyl-transferase reactions during peptide extension processes, rather than acting as a RNA glycosidase (Obrig *et al.*, 1971). This suggests the augmentation effects between rituximab and BU12-

saporin may be related to the specific RNA glycosidase activity of the ribosome inactivating protein component.

Analysis of data obtained from PI staining experiments shows that the induction of apoptosis (inferred from DNA fragmentation) by rituximab and BU12-saporin was greater than additive when compared to their effects alone. The combination of the murine CD20 antibody (1F5) and BU12-saporin also had an additive effect. The sub G_0/G_1 population increase in cells treated with saporin or BU12 antibody alone or in combination with rituximab was minor. By annexin V/PI staining the effect of rituximab and BU12-saporin in combination was also seen to be additive in the early apoptotic populations at the early time points and in the viable and secondary necrotic populations at later time points. These data suggest both rituximab and BU12-saporin induce apoptosis alone and also have additive apoptotic effects when used in combination.

In this thesis low levels of apoptosis were detected in cells treated with rituximab alone by all techniques. This low level is thought likely to be due to the absence of cross linking via a cross linking antibody or Fc receptor bearing cells. Cross linking has been shown to upregulate signalling pathways, significantly increasing the levels of apoptosis detected (Shan *et al.,* 1998).

The experiments conducted out in chapter 3 and 4 were carried out over several time points which highlighted differences in the timing of the cellular response to rituximab and BU12-saporin. Rituximab is proposed to mediate a more rapid response, hence the appearance of a peak of early apoptotic cells at 24 hours which stabilises at 48 and 72 hours (figure 3.4). This early effect of rituximab accounts for the initial large drop in viability, the undamaged cells are then able to continue replicating by 48 and 72 hours causing the steady increase in viability observed. The PI data however, suggests that the level of DNA fragmentation induced by rituximab is fairly consistent over the 72 hour time period (figure 3.3). BU12-saporin induces maximal protein synthesis inhibition by 48 hours, at this time point the greatest decrease is observed in the viable population and greater increases are observed in the secondary necrotic populations (figure 3.4). The PI data confirms the largest increase to the sub G_0/G_1 population in cells treated with BU12-saporin occurs at 48 hours (figure 3.2).

The molecular data from the western blotting analysis carried out in chapter 5 shows a different pattern in the timing of the effects of rituximab and BU12-saporin compared to the observations from annexin V/PI staining. PARP and caspase cleavage by rituximab or BU12-saporin is detected at similar time points (to within 3 hours). Although this is not initially apparent as BU12-saporin generally induces a greater response than rituximab. The observed difference between the timing of the molecular and morphological observations is thought to reflect the two different mechanism of action of saporin, the DNA and RNA glycosidase activity.

The temporally unsynchronised activity may account for some of the insignificant values observed in the statistical comparisons of the effects on the combination compared to BU12-saporin or rituximab alone. The effect of rituximab may be significant at 24, but not 48 and 72 hours, whereas BU12-saporin is not significant at 24 hours, but causes a significant effect by 48 and 72 hours (tables 4.1, 4.2). This difference in time taken for the maximal effect of rituximab and BU12-saporin to be observed, and the large standard deviations, together may contribute to distorting the statistical significance of data.

Previously in a SCID mouse Ramos/lymphoma model, the combination of rituximab and BU12-saporin was shown to significantly prolong survival compared to either reagent used alone (Flavell *et al.*, 2000a). Cell death via a complement mediated mechanism was proposed. However, the experiments described in chapter 4 show no significant requirement for complement in rituximab, BU12-saporin, saporin or BU12 antibody induced apoptosis or protein synthesis inhibition used alone or in combination. Interestingly the murine antibody 1F5 showed a significantly different pattern of activity in heat inactivated complement. In 1F5 treated cells low early apoptotic populations were detected, suggesting the main mechanism of action is the formation of the membrane attack complex, causing the loss of membrane integrity resulting in the majority of cells staining PI positive accounting for the higher, non apoptotic primary and secondary necrotic populations.

Molecular events involved in the induction of apoptosis by rituximab and BU12-saporin were initially investigated by western blotting. PARP cleavage detected in Ramos cells treated with the combination of rituximab and BU12-saporin was greater than that detected in rituximab or BU12-saporin treated cells alone. Minor PARP cleavage was

detected in saporin treated cells. Caspase cleavage was also detected by western blotting. Experiments detecting caspase activation by cleavage are limited by the large variability between results from identical experimental replicates. The variability in the timing and extent of cleavage in this system was too great to determine the order and extent of caspase cleavage and activation precisely. The variation is thought to be clonal artefact, or due changes in the culture conditions beyond experimental control affecting the sensitivity of cells. Thus the exact timing of caspase cleavage can not be determined.

Cleavage was detected between 2 and 6 hours for caspase 9, and between 9 and 12 hours for caspase 3. Caspase 8 was only found to be cleaved in cells in the later stages of apoptosis. The timing of caspase cleavages and the appearance of caspase-processed and auto-processed caspase 9 fragments suggests caspase 9 is activated before caspase 3 suggesting the mitochondrial pathway for the induction of apoptosis. Experiments with FAS and TRAIL inhibitors confirm that FAS and TRAIL receptors, as examples of the death receptor pathway for the induction of apoptosis, are not active in rituximab and BU12-saporin mediated apoptosis.

The results obtained from the experiments carried out with the peptide caspase inhibitors can be interpreted in two ways. The pan caspase inhibitor zVAD was shown to partially inhibit PARP cleavage in cells exposed to the combination of rituximab and BU12-saporin. This may either be due to the poor permeability of zVAD, thus it only causes partial caspase inhibition, resulting in some residual PARP cleavage. As no residual PARP cleavage was observed in positive controls (e.g. cisplatin and cycloheximide) this suggests complete caspase inhibition could be assumed, which leads to the suggestion that cell death by rituximab and BU12-saporin may involve a caspase independent mechanism. The pattern of results from the caspase cleavage experiments carried out in the presence of zVAD suggest that only partial inhibition of caspases has been achieved by zVAD.

The role of selected Bcl-2 family proteins has been investigated in apoptosis induced by rituximab and BU12-saporin. No changes in expression levels of Mcl-1, Bcl-X_L, Bak, or Bax were detected in response to rituximab and BU12-saporin. In Ramos cells Bcl-2 was undetectable, both before and during exposure to rituximab and BU12-saporin. In chapter 6 experiments carried out on Ramos cells over expressing Bcl-2 and Bcl-X_L are described,

in order to determine if over expression of these proteins provided protection against exposure to rituximab and BU12-saporin.

In chapter 6, annexin V/PI staining and western blotting for PARP and caspase 3 cleavage showed that over expression of Bcl-X_L provided protection against exposure to rituximab and BU12-saporin. Over expression of Bcl-2 provided a degree of protection against rituximab and BU12-saporin, although less than Bcl-X_L. The over expressing cells used in protein synthesis inhibition assays showed mixed results. Leucine incorporation by the Bcl-2 and Bcl-X_L cells was different from wildtype cells suggesting the cells had different rate of growth and metabolism. Also the sensitivity for these cells types to BU12-saporin by PSI assay differed to wildtype Ramos, although an augmentation of BU12-saporin by rituximab was observed in each.

Over expression of Bcl-2 has been previously shown not to protect again the action of rituximab (van der Kolk *et al.*, 2002). Ribosome inactivating proteins, such as ricin have also been shown to be partially affected by over expression of Bcl-2 (Hu *et al.*, 2001), whereas the action of abrin was completely inhibited by the over expression of Bcl-2 (Narayanan *et al.*, 2004). The difference between the level of protection afforded against rituximab and BU12-saporin may be due to the level of over expression of Bcl-2 and Bcl-X_L. The degree of expression of Bcl-2 and Bcl-X_L has not been determined in this study. The difference in the level of protection afforded by these anti-apoptotic proteins may be due to expression levels or unknown fundamental differences in the properties of Bcl-2 and Bcl-X_L.

Ribosome inactivating proteins were initially thought to act as RNA glycosidases, although evidence now points to an additional role as a DNA glycosidases. Cell death via the inhibition of protein synthesis and the induction of apoptosis initially appeared to involve conflicting mechanisms, as protein synthesis was thought to be required for apoptosis (Wyllie *et al.*, 1984). However studies with the protein synthesis inhibitors gliotoxin and cycloheximide were later found to contest this view (Waring 1990, Geier *et al.*, 1996). Cells exposed to saporin die showing the morphological and molecular characteristics of apoptosis (Bergamaschi *et al.*, 1996). Thus the relationship between protein synthesis inhibition and apoptosis is of significant interest.

Apoptosis and protein synthesis inhibition may be separate events initiated in the case of protein toxins by different parts of the molecule. The motif in ricin responsible for vascular leak syndrome has been proposed to be responsible for the induction of apoptosis in human umbilical vein endothelial cells (Baluna *et al.*, 2000). This suggests that the activity of ricin is due to two separate catalytic activities mediated by different parts of the molecule. Although this vascular leak motif is not present in saporin, an as yet unidentified motif may be responsible for vascular leak syndrome and also possibly apoptosis in this manner. Residues have been identified associated with the DNA fragmentation activity of saporin, which show some overlap with residues involved in protein synthesis inhibition suggesting saporin possesses two catalytic activities which are both required for complete cytotoxic activity, although suggesting binding of DNA and rRNA by saporin occurs through the same active site (Bagga *et al.*, 2003).

Alternatively protein synthesis inhibition may lead to apoptotic cell death. In the lymphoma cell line U937, after ribosome inactivating protein exposure the morphological features of apoptosis were observed after protein synthesis was reduced to 10% of normal levels (Kochi *et al.*, 1993). This suggests protein synthesis inhibition results in apoptosis. This idea is also supported by Olmo and co-workers who showed α-sarcin induced caspase activation as a process downstream of 28S rRNA catalytic cleavage and protein synthesis inhibition (Olmo *et al.*, 2001). Caspase activation occurred when protein synthesis was reduced to 50% of normal levels in target cells.

Investigation of the kinetics of the two catalytic activities of abrin showed the signal for apoptosis is triggered at a time point later than the inhibition of protein synthesis (Narayanan *et al.*, 2004). The apoptotic pathway induced by abrin involves caspase 3, but is caspase 8 independent and involves mitochondrial membrane potential damage and reactive oxygen species production. Protein synthesis inhibition may result in the inhibition of translation of a constitutive protein continuously required to maintain the mitochondrial membrane transition pore in closed position (Narayanan *et al.*, 2004).

Ricin induced apoptosis has been shown to involve increased expression of Bak and decreased expression of Bcl-X_L and Bax (Hu *et al.*, 2001). This suggests apoptosis in response to protein synthesis inhibition may be a result of changes to expression of pro and anti apoptotic factors, oxidative stress and mitochondrial damage leading to increased

reactive oxygen species production. Proteins in mammalian tissues have recently been found to possess adenine glycosylase activity similar to that of ribosome inactivating proteins (Berbieri *et al.*, 2001). This suggests that ribosome inactivating proteins may exploit an existing mechanism of cell death triggered by cellular stress (mitochondrial stress and the production of reactive oxygen species) in response to protein synthesis inhibition (Narayanan *et al.*, 2004).

Experiments with peptide caspase inhibitors have proven no more conclusive in this debate. The effect of zVAD on cell lines exposed to PE and α-sarcin is the inhibition of DNA fragmentation catalytic activity but not the RNA glycosidase catalytic activity (Keppler-Hafkemeyer *et al.*, 2000, Olmo *et al.*, 2001). Keppler-Hafkemeyer and co-workers suggest this shows the two separate catalytic activities of PE. Although, Olmo and co-workers interpret this result as evidence for both caspase dependent and caspase independent forms of apoptosis or non-apoptotic death, suggesting these mechanisms always act as a consequence of the proteins synthesis inhibition activity of α-sarcin.

The observed timing of the apoptotic events detected in these chapters tentatively suggest that apoptosis is initiated before the action of the immunotoxin. The initiation of apoptosis can be detected by PARP cleavage by 2 and 6 hours exposure to rituximab and BU12-saporin whereas protein synthesis inhibition was detected after 48 hours by leucine incorporation assay. However, protein synthesis assays were not carried out to detect inhibition at earlier time points. Although work on other saporin containing immunotoxins on the T cell line, HSB, suggests 50% of normal protein synthesis inhibition is achieved 10 to 20 hours post exposure (Field 2002). In Jurkat cells, 50% of control protein synthesis was detected within 1-2 hours of abrin exposure (Narayanan *et al.*, 2004). Although, Kochi (1993) proposed a 10% decrease in proteins synthesis inhibition was sufficient for apoptosis, which suggests from the amount of protein synthesis inhibition observed previously, apoptosis in the present study may result from protein synthesis inhibtion by BU12-saporin exposure.

It is likely the variability previously observed in this system, regarding the extent and timing of PARP and caspase cleavages would prevent further analysis of the relative timing of these events. Understanding the timing of protein synthesis inhibition and the induction of apoptosis in cells exposed to BU12-saporin may determine a specific time

point for the addition of rituximab to achieve the maximum augmentation effects. However, early studies conducted as part of this works showed no increased protein synthesis inhibition in Ramos cells exposed to rituximab for one 1 hour pre or post BU12-saporin exposure (data not shown).

Taken together the evidence presented in these chapters provides the rationale for the use of rituximab and BU12-saporin in combination. The immunotoxin BU12-saporin induces cells death via protein synthesis inhibition and apoptosis. These effects can be augmented by the use of BU12-saporin in combination with rituximab. By protein synthesis inhibition assay a 5 fold increase in potency was observed. The combination of rituximab and BU12-saporin in a DNA fragmentation assay showed a statistically significant , greater than additive, increase in the sub G_0/G_1 population. Similarly annexin V/PI staining of Ramos cells exposed the combination also showed additive statistically significant results.

In Ramos cells exposed to the combination of rituximab and BU12-saporin greater cleavage of the caspase substrate PARP was detected by western blot than in cells exposed to rituximab or BU12-saporin alone. Caspase 3 and caspase 9 cleavage was detected in response to rituximab and BU12-saporin with no caspase 8 cleavage detected, except in late apoptotic cells. As examples of the death receptor pathway, blocking TRAIL or FAS receptors did not reduce the level of PARP cleavage detected, or caspase 3 cleavage. This suggested induction of apoptosis by rituximab and BU12-saporin involved the mitochondrial pathway rather than the death receptor pathway. Further work is required to determine the precise pathways involved.

The caspase inhibitor zVAD completely inhibited PARP cleavage by rituximab, almost completely inhibited PARP cleavage by BU12-saporin. Caspase 3 cleavage was also partially inhibited. This suggests rituximab and BU12-saporin induced caspase dependent apoptosis; the partial cleavage observed was likely to be a result of partial caspase inhibition by this type of inhibitor. No changes in the expression levels of Mcl-1, Bax, Bak, Bcl-2 or Bcl-X_L were detected in response to rituximab and BU12-saporin. Over expression of Bcl-X_L but not Bcl-2 significantly protected Ramos cells from rituximab and BU12-saporin induced apoptosis, suggesting a possible use of this combination against cells over expressing Bcl-2.

Rituximab and BU12-saporin induce apoptosis and work together in an additive and possibly synergistic manner. These findings emphasize the value of the complementation approach. The immunotoxin BU12-saporin induces cells death via protein synthesis inhibition and apoptosis. Apoptosis appears to be induced as a consequence of RNA glycosidase activity and subsequent protein synthesis inhibition, the exact mechanism by which saporin results in caspase activation remains to be determined. The elucidation and quantification of these mechanisms and their interaction may be important to the therapeutic application of immunotoxins; particularly with reference to cancer cells showing resistance to some apoptotic mechanisms (for example cells over expressing Bcl-2). This provides the rationale for further investigation to determine the relationship between pathways of apoptosis and protein synthesis involved for future therapeutic use.

Appendix

Chapter 5: Additional data

Sample	6h	9h	12h
Control	3(±4.24)	0(±0)	0(±0)
Rituximab	15(±5.66)	19.2(±11.1)	15(±6.08)
BU12-saporin	24(±5.66)	48.1(±12.1)	32.3(±3.79)
Combination	28(±14.14)	65.6(±11.87)	40.3(±6.66)

Appendix table 1.1

Mean and standard deviation of cleaved PARP band density obtained from 5 repeat western blots of Ramos cell samples treated with rituximab and BU12-saporin individually and in combination at 6, 9 and 12 hours (see figure 5.1).

	Independent t-test comparison of:	
Time point	Rituximab to Combination treated cells	BU12-saporin to combination treated cells
6 hours	p = 0.35	p = 0.75
9 hours	**p = 0.0002**	**p = 0.05**
12 hours	**p = 0.008**	p = 0.14

Appendix table 1.2

Independent t-test comparison of PARP cleavage in rituximab or BU12-saporin treated Ramos cells compared to combination treated cells at 6, 9 and 12 hours. Significance at p = 0.05 is shown in bold text (see figure 5.1).

Sample	Time point	Time point		
		6 hours	9 hours	12 hours
Control	Full length	76(±11)	100(±0)	100(±0)
	37kDa	24(±11)	-	-
	35kDa	-	-	-
Rituximab	Full length	69.67(±9.5)	47.67(±15.2)	65(±12.6)
	37kDa	30.33(±9.5)	36(±7.2)	35(±12.6)
	35kDa	-	16(±5.6)	
BU12-saporin	Full length	64.6(±11.8)	56(±5.3)	49.0(±1.0)
	37kDa	35.33(±11.8)	44(±5.3)	38.67(±1.5)
	35kDa	-	-	12.33(±2.08)
Combination	Full length	76.33(±13.5)	73.67(±3.2)	34.33(±4.9)
	37kDa	23.7(±13.5)	17(±10.1)	42.33(±6.8)
	35kDa	-	10(±0)	19.0(±12.4)
Cisplatin	Full length	43.33(±26.4)	90.67(±8.0)	86(±19.9)
	37kDa	13.67(±26.4)	9.33(±12.5)	11(±3.6)
	35kDa	-	-	4(±0)

Appendix table 1.3

Mean and standard deviation of caspase 9 cleavage product band density obtained from 3 repeat western blots of Ramos cell samples treated with rituximab and BU12-saporin individually and in combination at 6, 9 and 12 hours (see figure 5.3).

References

Alam, M.K, Davison, S., Siddiqui, N., Norton, J.D. and Murphy, J.J. (1997). Ectopic expression of Bcl-2 but not Bcl-X_L rescues Ramos B-cells from FAS mediated apoptosis. *European Journal of Immunology,* **27,** pp3485-3491.

Alas. S., Emmanouilides, C. and Bonavida, B. (2001a). Inhibition of IL10 by rituximab results in down-regulation of Bcl-2 and sensitization of B-cell non Hodgkin's lymphoma to apoptosis. *Clinical Cancer Research,* **7,** pp709-723.

Alas. S. and Bonavida, B. (2001b). Rituximab induces STAT3 activity in NHL through inhibition of IL10 autocrine and paracrine loop and results in down-regulation of Bcl-2 and sensitization to cytotoxic drugs. *Cancer Research,* **61,** pp5137-5144.

Alas. S., Ng, C.P. and Bonavida, B. (2002). Rituximab modifies the cisplatin mitochondrial signaling pathway, resulting in apoptosis in cisplatin resistant non Hodgkin's lymphoma. *Clinical Cancer Research,* **8,** pp836-845.

Alas. S. and Bonavida, B. (2003). Inhibition of constitutive STAT3 activity sensitises resistant non Hodgkin's lymphoma and multiple myeloma to chemotherapeutic drug mediated apoptosis. *Clinical Cancer Research,* **9,** pp316-326.

Ansall. S. (2003). Adding cytokines to monoclonal antibody therapy: Does the concurrent administration of IL2 add to the efficacy of rituximab in B-cell NHL? *Leukemia and Lymphoma,* **44,** pp1309-1315.

Auer, R.L., Corbo, M., Fegan, C.D., Frankel, S.R. and Cotter, F. (2001). Bcl-2 anti-sense induces apoptosis and potentiates activity of both cytotoxic chemotherapy and rituximab in primary CLL cells. **Blood,** *96,* abstract 3358.

Bagga, S., Seth, D. and Batra, J.K. (2003). The cytotoxic activity of the ribosome inactivating protein saporin is attributed to it's rRNA glycosidase and DNA fragmentation activities. *Journal of Biological Chemistry*, **278,** pp4813-4820.

Bagga, S., Hosur, M.V. and Batra, J.K. (2003). Cytotoxicity of the ribosome inactivating protein saporin is not mediated through macroglobulin receptor. *FEBS letters,* **541,** pp16-20.

Baliga, B.C. and Kumar, S. (2002). Role of Bcl-2 family of proteins in malignancy. *Haematological Oncology,* **20,** pp63-74.

Baluna, R., Rizo, J., Gordon, B.E., Ghetie, V. and Vitette, E.S. (1999). Evidence for a structural motif in toxins and interleukin-2 that may be responsible for binding to endothelial cells and initiating vascular leak syndrome. *Proceedings of the National Academy of Sciences,* **96,** pp3957-3962.

Baluna, R., Coleman, E., Jones, C., Ghetie, V and Vitetta, E.S. (2000). The effect of a monoclonal antibody coupled to ricin A chain-derived peptides on endothelial cells in vitro: In sights into toxin mediated vascular damage. *Experimental Cell Research,* **258,** pp417-424.

Baluna, R., Sausville, E.A., Stone, M.J., Stetler-Stevenson, M.A., Uhr, J., and Vitetta, E.S. (1996). Decreases in levels of serum fibronectin predict the severity of vascular leak syndrome in patients treated with ricin A chain containing immunotoxins. *Clinical Cancer Research,* **2,** pp1705-1712.

Baluna, R. and Vitetta, E.S. (1997). Vascular leak syndrome: A side effect of immunotherapy. *Immunopharmacology,* **37,** pp117-132.

Barbieri, L and Stirpe, F. (1982). Ribosome-inactivating proteins from plants: Properties and possible uses. *Cancer Surveys,* **1,** pp490-514.

Barbieri, L., Brigotti, M., Perocco, P., Carnicelli, D., Ciani, M., Mercatali, L. and Stirpe, F. (1996). Polynucleotide adenosine glycosidase activity of saporin-L1: Effect on DNA, RNA and poly(A). *Biochemical Journal,* **319,** pp507-513.

Barbieri, L., Brigotti, M., Perocco, P., Carnicelli, D., Ciani, M., Mercatali, L. and Stirpe, F. (2003). Ribosome inactivating proteins depurinate poly ADP ribosylated poly ADP ribosylated polymerase and have transforming activity. *FEBS letters,* **538,** pp178-182.

Bellosillo, B., Villamor, N., Lopez-Guillermo, A., Esteve, J., Campo, E., Colomer, D. and Montserrat, E. (2001). Complement mediated cell death induced by rituximab in B-cell lymphoproliferative disorders is mediated in vitro by a caspase-independent mechanism involving the generation of reactive oxygen species. *Blood,* **98,** pp2771-2777.

Bergamashi, G., Perfetti, V., Tonon, L., Novella, A., Lucotti, C., Danova, M., Glennie, M.J., Merlini, G. and Cazzola, M. (1996). Saporin a ribosome inactivating protein used to prepare immunotoxins induces cell death via apoptosis. *British Journal of Haematology,* **93**, pp789-794.

Berkower, I. (1996). The promise and pitfalls of monoclonal antibody therapeutics. *Current Opinion in Biotechnology,* **7**, pp622-628.

Bohen, S.P., Troyanskaya, O.G., Alter, O., Warnke, R., Botstein, D., Brown,P.O. and Levy, R. (2002). Variation in gene expression pattern in follicular lymphoma and the response to rituximab. *Proceedings of the National Academy of Sciences,* **100,** pp1926-1930.

Boirivant, M., Pica, R., DeMaria, R., Testi, R., Pallone, F and Strober, W. (1996). Stimulated Human lamina propria T cells manifest enhanced FAS mediated apoptosis. *The American Society for Clinical Investigation*, **98,** pp2616-2622.

Bolognesi, A., Tazzari, P.L., Olivieri, F., Polito, L., Falini, B. and Stirpe, F. (1996). Induction of apoptosis by ribosome-inactivating proteins and related immunotoxins. *International Journal of Cancer,* **68**, pp349-355.

Bolognesi, A., Tazzari, P.L., Olivieri, F., Polito, L., Lemoli, R.M., Terenzi, A., Pasqualucci, L., Falini, B. and Stirpe, F. (1998). Evaluation of immunotoxins containing single-chain ribosome inactivating proteins and an anti-CD22 monoclonal antibody (OM124) in vitro and in vivo studies. *British Journal of Haematology,* **101,** pp179-188.

Bolognesi, A., Polito, L., Tazzari, P.L., Lemoli, R.M., Lubelli, C., Fogli, M., Boon, L., de Boer, M. and Stirpe, F. (2000). In vitro anti-tumour activity of anti-CD80 and anti-CD86 immunotoxins containing type 1 ribosome inactivating proteins. *British Journal of Haematology,* **110,** pp351-361.

Borner, C. (2003). The Bcl-2 family: sensors and checkpoints for life-or-death decisions. *Molecular Immunology,* **39,** pp615-647.

Boughton. B. (2003). Rituximab for Bcl-2 positive cancers. *The Lancet*, **4,** p69.

Brenner. C. and Kroemer, G. (1999). The mitochondrion: Decisive for cell death control? In *Signalling Pathways in Apoptosis* edited by D. Walters and M.Laven pp207-226. Harwood

Byrd. J.C., Kitada, S., Flinn, I.W., Aron, J.L., Pearson, M., Lucas, D. and Reed, J.C. (2002). The mechanism of tumour cell clearance by rituximab in vivo patients with B CLL: evidence of caspase induction and apoptosis induction. *Blood*, **99,** pp1038-43.

Cardarelli, P.M., Quinn, M., Buckman, D., Fang, Y., Colcher, D., King, D.J. Bebbington, C. and Yarranton, G. (2002). Binding to CD20 by anti-B1 antibody or Fab2 is sufficient for induction of apoptosis in B cell lines. *Cancer Immunology Immunotherapy,* **51,** pp15-24.

Carter, P. (2001). Improving the efficacy of antibody based cancer therapies. *Nature Reviews Cancer,* **1,** pp118-129.

Cartron, G., Dacheux, L., Salles, G., Solal-Celigny, P., Bardos, P., colombat, P. and Watier, H. (2002). Therapeutic activity of humanized anti-CD20 monoclonal antibody and polymorphism of the IgG Fc receptor gene. *Blood,* **99,** pp754-758.

Chan. H.T.C., Hughes, D., French, R.R., Tutt, A.L., Walshe, C.A., Teeling, J.L., Glennie, M.J. and Cragg, M.S. (2003). CD20 induced lymphoma cell death is independent of both caspases and it's redistribution into Triton x-100 insoluble membrane rafts. *Cancer Research,* **63,** pp5480-5489.

Cheson, B.D. (2002). CHOP plus rituximab balancing facts and opinion. *The New Englamd Journal of Medicine,* **346,** pp280-281.

Clynes, R.A., Towers, T.L., Prestra, L.G. and Ravetech, J.V. (2000). Inhibitory Fc receptors modulate in vivo cytotoxicity against tumour targets. *Nature Medicine,* **6,** pp443-446.

Cohn, E.E. and Rudin, C.M. (2001) Onyx pharmaceuticals *Current Opinion Investigation Drugs,* **2,** 1770-1775

Coiffer, B., Lepage, E., Briere, J., Herbrecht, R., Tilly, H., Bouardallah, R., Morel, P., van den Neste, E., Salles, G., Gaulard, P., Reyes, F. and Gisselbrecht, C. (2002). CHOP chemotherapy plus rituximab compared with CHOP alone in elderly patients with diffuse large cell lymphoma. *New England Journal of Medicine,* **346,** pp235-242.

Coiffier, B., Haioun, C., Ketterer, N., Engert, A., Tilly, H., Ma, D., Johnson, P., Lister, A., Feuring-Buske, M., Radford, J.A., Capdeville, R., Diehl, V. and Reyes, F. (1998). Rituximab (anti-CD20 monoclonal antibody) for the treatment of patients with relapsing or refractory aggressive lymphoma: a multicenter phase II study. *Blood,* **92,** pp1927-32.

Colombat, P., Salles, G., Brousse, N., Eftekhari, P., Soubeyraon, P., Delwail, V., Haioun, C., Foussard, C., Sebban, C., Stamatoullas, A., Milipied, N., Boue, F., Tailan, B., Lederlin, P., Najman, A., Thieblemont, C., Montestruc, F., Mathieu-Boue, A., Benzohra, A., and Solal-Celigny, P. (2001). Rituximab as a single first line therapy for patients with follicular lymphoma with a low tumour burden: clinical and molecular evaluation. *Blood,* **97,** pp101-106.

Cragg, M.S., French, R.R. and Glennies, M.J. (1999). Signaling antibodies in cancer therapy. *Current Opinion in Immunology,* **11,** pp541-547.

Cragg, M.S., Morgan, S.M., Chan, H.T.C., Morgan, B.P., Filatov, A.V., Johnson, P.W.M., French, R.R., and Glennie, M.J. (2003). Complement mediated lysis by anti-CD20

monoclonal antibody correlates with segregation into lipid rafts. *Blood,* **101,** pp1045-1052.

Czuczman, M.S. (1999). CHOP plus rituximab chemoimmunotherapy of indolent B-cell lymphoma. *Seminars in Oncology,* **26,** pp88-96.

Czuczman, M., Jonas, C., Stephan, M., Scarpace, A., Rack, M., Kunkel, L., Grillo-Lopez, A. and Steven, B. (1999). Pilot study of Rituxan in combination with fludarabine in chemotherapy in patients with low grade or follicular non Hodgkin's lymphoma. *Proceedings of the American Society of Clinical Oncology,* **18,** p61

Czuczman, M.S., Grillo-Lopez, A.J., White, C.A., Saleh, M., Gordon, L., LoBuglio, A.F., Jonas, C., Klippenstein, D., Dallaire, B. and Varns, C. (1999). Treatment of patients with low-grade B-cell lymphoma with the combination of chimeric anti-CD20 monoclonal antibody and CHOP chemotherapy. *Journal of Clinical Oncology,* **17,** pp268-76.

Dales, J.P., Palmerinin, F., Devilard, E., Hassoun, J., Birg, F. and Xerri, L. (2001). Caspases: Conductors of the cell death machinery in lymphoma cells. *Leukaemia and Lymphoma,* **41,** pp247-253.

Darzynkiewicz, Z., Juan, G., Li, X., Gorczyca, W., Murakami, T. and Traganos, F. (1997). Cytometry in cell necrobiology: analysis of apoptosis and accidental cell death (necrosis). *Cytometry,* **27,** pp1-20.

Day, P.J., Lord, M. and Roberts, L.M. (1998). The deoxyribonuclease activity attributed to ribosome inactivating proteins is due to contamination. *European Journal of Biochemistry,* **258,** pp540-545.

Deans, J.P., Robbins, S.M., Polyak, M.J. and Savage, J.A. (1998). Rapid redistribution of CD20 to a low density detergent insoluble membrane compartment. *Journal of Biological Chemistry,* **273,** pp344-348.

Demidem, A., Lam, T., Alas, S., Hariharan, K., Hanna, N. and Bonavida, B. (1997). Chimeric anti-CD20 (IDEC-C2B8) monoclonal antibody sensitizes a B-cell lymphoma cell line to cell killing by cytotoxic drugs. *Cancer Biotherapy and Radiopharmaceuticals,* **12,** pp177-186.

Dempsey, P.W., Doyle, S.E., He, J.Q. and Cheng, G. (2003). The signaling adaptors activated by TNF superfamily. *Cytokine and Growth Factor Reviews,* **14,** pp193-209.

Dermine, S., Armstrong, A., Hawkins, R.E. and Stern, P.L. (2002). Cancer vaccines and immunotherapy. *British Medical Bulletin,* **62,** pp149-162.

Dillman, R.O. (2001). Monoclonal antibody therapy for lymphoma. *Cancer Practice,* **9,** pp71-80.

Emmanouilides, C., Jazirehi, A.R. and Bonavida, B. (2002). Rituximab mediated sensitization of B-non Hodgkin's lymphoma to the cytotoxicity induced by paclitaxel

gemcitabine and vinorelbine. *Cancer Biotherapy and Radiopharmaceuticals,* **17,** pp621-630.

Emmanouilides, C., Jazirehi, A.R., Gan, X.H., and Bonavida, B. (2003). Selective down regulation of Bcl-xl and upregulation of Apaf-1 expression in Ramos NHL by rituximab: Sensitization to paclitaxel mediated apoptosis. *Blood,* **11,** abstract 2255.

Endo, Y., Mitsui, K., Motizuki, M. and Tsurgi, K. (1987). The mechanism of action of ricin and related toxic lectins on eukaryotic ribosomes. The site and characteristics of the modification in 28S ribosomal RNA caused by the toxins. *Journal of Biological Chemistry,* **262,** pp5908-5912.

Endo, Y. and Tsurugi, K. (1988). The RNA N-glycosidase activity of ricin A-chain. The characteristics of the enzymatic activity of ricin A-chain with ribosomes and with rRNA. *Journal of Biological Chemistry,* **263,** pp8735-8739.

Endo, Y., Tsurugi, K. and Lambert, J.M. (1988a). The site of action of six different ribosome inactivating proteins from plants on eukaryotic ribosome: the RNA N-glycosidase activity of the proteins. *Biochemical and Biophysical Research Communications,* **150,** pp1032-1036.

Erickson, H.A., Reinhardt, R.L., Hermanson, J.B., Panoskaltsis-Mortari, A. and Pennell, C.A. (2001). Visualization of Immunotoxin mediated tumour cell death. *Clinical Cancer Research,* **7,** pp890s-894s.

Evans, L.S. and Hancock, B.W. (2003). Non Hodgkin Lymphoma. *The Lancet,* **362,** pp139-146.

Fiers, W., Beyaert, R., Declercq, W. and Vandenabeele, P. (1999). More than one way to die: apoptosis, necrosis and reactive oxygen damage. *Oncogene,* **18,** 7719-7730.

Fitzgerald, D. (1996). Why toxins! *Seminars in Cancer Biology,* **7,** pp87-95.

Flavell, D.J., Boehm, D.A., Emery, L., Noss, A., Ramsay, A. and Flavell, S.U. (1995a). Therapy of human B cell lymphoma bearing SCID mice is more effective with anti CD19 and anti CD38 saporin immunotoxins used in combination than alone. *International Journal of Cancer,* **62,** pp337-344.

Flavell. D.J., Flavell, S.U., Boehm, D.A., Emery, L., Noss, A., Ling, N.R., Richardson, P.R., Hardie, D. and Wright, D.H. (1995b). Pre-clinical studies with the anti-CD19 immunotoxin BU12-saporin for the treatment of human B cell tumours. *British Journal of Cancer,* **72,** pp1373-1379.

Flavell. D.J., Warnes, S., Noss, A. and Flavell, S.U. (1998). Host-mediated antibody dependent cellular cytotoxicity contributes to the in vivo therapeutic efficacy of anti CD7 saporin immunotoxin. *Cancer Research,* **58,** pp5787-5794.

Flavell. D.J. (1998). Saporin Immunotoxins. *Current Topics in Microbiology,* **234,** pp57-61.

Flavell. D.J., Warnes, S., Noss, A. and Flavell, S.U. (2000). Anti-CD7 antibody and immunotoxin treatment of human CD7+ T cell leukaemia is significantly less effective in NOD/LtSz-scid mice than in CB.17 scid mice. *British Journal of Cancer,* **83,** pp1755-1761.

Flavell. D.J., Warnes, S., Noss, A. and Flavell, S.U. (2000a). Co-operative therapeutic effects between anti CD20 antibodies and an anti CD19 immunotoxin in a SCID mouse model of human B-cell lymphoma. *Proceeding of the American Association of Cancer Research,* **41,** abstract 523.

Flavell. D.J., Warnes, S., Symons, M., Noss, A. and Flavell, S.U. (2000b). Augmentation of the anti lymphoma activity of an anti CD19 immunotoxin by anti CD20 antibody is mediated via a complement dependent mechanism. *Blood,* **11,** abstract 342.

Flavell. D.J., Warnes, S., Noss, A. and Flavell, S.U. (2001). Delineation of the cytotoxic mechanisms operating in SCID mice zenografted with human B cell lymphoma following treatment with a combination of anti CD20 antibody plus anti CD19 immunotoxin. *American Association of Cancer Research* ***46***

Flieger, D., Renoth, S., Beier, I., Sauerbruch, T. and Schmidt-Wolf, I. (2000). Mechanisms of cytotoxicity induced by chimeric mouse human monoclonal antibody IDEC-C2B8 in CD20 expressing lymphoma cell lines. *Cellular Immunology,* **204,** pp55-63.

Fu, T., Burbage, C., Tagge, E.P., Brothers, T., Willingham, M.C. and Frankel, A.E. (1996). Ricin toxin contains three lectin sites which contribute to its in vivo toxicity. *International Journal of Immunopharmacology,* **18,** pp685-692.

Fujimoto, M., Poe, J.C., Hasegawa, M. and Tedder, T.F. (2001). CD19 amplification of B lymphocyte Ca response. *Journal of Biological Chemistry,* **276,** pp44820-44827.

Funakoshi, S., Longo, D.L and Murphy, W.J. (1996). Differential in vitro anti-tumour effects mediated by anti-CD40 and anti-CD20 monclonal antibodies against human B-cell lymphomas. *Journal of Immunotherapy,* **2,** pp93-101.

Geier, A., Bar-Shalom, I., Beery, R., Haimsohn, M., Hemi, R., Malik, Z., Lunenfeld, B. and Karasik, A. (1996). Induction of apoptosis in MDA-231 cells by protein synthesis inhibitors is suppressed by multiple agents. *Cancer Investigations,* **14,** pp435-444.

Ghetie, M.A., Tucker, K., Richardson, J., Uher, J.W. and Vitetta, E.S. (1992). The anti-tumour activity of an anti-CD22 immunotoxin in SCID mice with disseminated Daudi lymphomas enhanced by either an anti-CD19 antibody or an anti-CD19 immunotoxin. *Blood,* **80,** pp2315-2320.

Ghetie, M.A., Picker, L.J., Richardson, J.A., Tucker, K., Uher, J.W. and Vitetta, E.S. (1994). Anti-CD19 inhibits the growth of human B-cell tumor lines in vitro and of Daudi cells in SCID mice by inducing cell cycle arrest. *Blood,* **83,** pp1329-1336.

Ghetie, M.A., Podar, E.M., Ilgen, A., Gordon, B.E., Uher, J.W. and Vitetta, E.S. (1997). Homodimerization of tumour-reactive monoclonal antibodies markedly increases their ability to induce growth arrest or apoptosis of tumour cells. *Proceedings of the National Academy of Sciences USA,* **94,** pp7509-7514.

Ghetie. M.A., Bright, H. and Vitetta, E.S. (2001). Homodimers but not monomers of rituxan induce apoptosis in human B lymphoma cells synergize with a chemotherapeutic agent and an immunotoxin. *Blood,* **97,** pp1392-1398.

Ghia, P., Boussiotis, V.A., Schultze, J.L., Cardoso, A.A., Dorfman, D.M., Gribben, J.G., Freedman, A.S. and Nadles, L.M. (1998). Unbalanced expression of Bcl-2 family proteins in follicular lymphoma: Contribution of CD40 signaling in promoting survival. *Blood,* **91,** pp244-251.

Glennie, M., Morgan, S., Chan, C., Trench, R., Tutt, A., Johnson,P. and Cragg, M. (2003). Understanding how anti-CD20 antibodies work. *British Journal of Cancer,* **88**, S2-S2 July sup. 1

Golay, J., Facchinetti, V., Gramigna, R., Lazzari, M., Dastoli, G., Barbui, T., Rambaldi, A. and Introna, M. (2001 a). Rituximab kills freshly isolated BNHL and BCLL more efficiently by complement than ADCC in vitro. *Blood,* **96,** abstract 633.

Golay, J., Lazzari, M., Facchinetti, V., Bernasconi, S., Borleri, G.M., Barbui, T., Rambaldi, A. and Introna, M. (2001b). CD20 levels determine the in vitro susceptibility to

rituximab and complement of B-cell CLL: further regulation by CD55 and CD59. *Blood,* **98,** pp3383-3389.

Golay, J., Manganini, M., Facchinetti, V., Gramigna, R., Broady, R., Borleri, G.M., Rambaldi, A. and Introna, M. (2003). Rituximab mediated antibody dependent cellular cytotoxicity against neoplastic B cells is stimulated strongly by interleukin-2. *Journal of Hematology,* **88,** pp1002-1012.

Golay, J., Zaffaroni, L., Vaccari, T., Lazzari, M., Borleri, G.M., Bernasconi, S., Tedesco, F., Rambaldi, A. and Introna, M. (2000). Biologic response of B lymphoma cells to anti-CD20 monoclonal antibody rituximab in vitro: CD55 and CD59 regulate complement-mediated cell lysis. *Blood,* **95,** pp3900-3908.

Gottlieb, R. (2000). Mitochondria: execution central. *FEBS letters,* **482**, pp6-12.

Grillo-Lopez, A.J, White, C., Varns, C., Shen, D., Wei, A., McClure, A. and Dallaire, B.K. (1999). Overview of the first clinical developments of Rituximab. *Seminars in Oncology,* **26,** pp66-73.

Grossbard, M.L., Freedman, A.S., Ritz, J., Coral, F. Goldmacher, V.S., Elisea, L., Spector, N., Dear, K., Lambert, J.M. and Blattler, W.A. (1992). Serotherapy of B cell neoplasms with anti B4 blocked ricin: a phase I trial of daily bolus infusion. *Blood,* **79,** pp576-585.

Haider, J.H., Shamseddines, A., Salem, Z., Abou Mard, Y., Nasr, M.R., Zaatari, G. and Bazarbachi, A. (2003). Loss of CD20 expression in relapsed lymphoma after rituximab therapy. *European journal of Haematology,* **70,** pp330-332.

Hariharan, K., Anderson, D., Leigh, B., Berquist, L.G., Murphy, T., Leonard, J.B., Braslawsky, G.R. and Hanna, N. (2001). Therapeutic activity of IDEC 114 (anti CD80) and rituximab in B cell lymphoma. *Blood,* **96,** abstract 2549.

Harjunpaa, A., Wiklund, T., Collan, J., Janes, R., Rosenberg, J., Lee, D., Grillo-Lopez, A. and and Meri, S. (2001). Complement activation in circulation and central nervous system after rituximab (anti CD20) treatment of B-cell lymphoma. *Leukaemia and Lypmphoma,* **42,** pp731-738.

Harjunpaa, A., Junnikkala, S. and Meri, S. (2000). Rituximab (anti-CD20) therapy of B-cell lymphomas: direct complement killing is superior to cellular effector mechanisms. *Scandinavian Journal of Immunology,* **51,** pp634-41.

Hekman, A., Honselaar, A, Vuist, W.M.J., Sein, J.J., Rodenhuis, S., Huinink, W.W.T., Somers, R., Rumke, P, and Melief, C.J.M. (1991). Initial experience with treatment of human B-cell lymphoma with anti-CD19 monoclonal antibody. *Cancer Immunology Immunotherapy,* **32,** pp364-372.

Herrera, L. Yarbrough, S. Ghetie, V., Aquino, D.B. and Vitetta, E.S. (2003). Treatment of SCID/human B cell precursor ALL with anti-CD19 and anti CD22 immunotoxin. *Leukemia,* **17,** pp334-338.

Hirsch, T., Marchetii, P., Susin, S.A., Dallaporta, B., Zamzami, N., Marzo, I., Geuskens, M. and Kroemer, G. (1997). The apoptosis necrosis paradox. Apoptogenic proteases activated after the mitochondrial permeability transition determine the mode of cell death. *Oncogene,* **15,** pp1573-1581.

Hofmeister, J.K., Cooney, D. and Coggeshall, K.M. (2000). Clustered CD20 induced apoptosis: src-family kinase, the proximal regulator of tyrosine phosphorylation, calcium influx, and caspase 3- dependent apoptosis. *Blood Cells Molecules and Diseases,* **26,** pp133-43.

Holland, G. and Zlotnik, A. (1993) Interleukin 10 and cancer. *Cancer Investigation,* **11,** pp751-758

Horssen, V. Preijers, F.W.M.B., van Oosterhout, Y.V.J.M., Eling, W.M.C. and de Witte, T (2000). Relationship of the CD22 immunotoxin dose and the tumour establishment in a SCID mice model. *Leukemia and Lymphoma,* **39,** pp591-599.

Houchins, J.P. (2000). Immunotoxin induced apoptosis. *Stem Cells,* **18,** pp383-385.

Hu, R., Zhai, Q., Liu, W. and Liu, X. (2001). An insight into the mechanism of cytotoxicity of ricin to hepatoma cell: Roles of Bcl-2 family proteins, caspases, Ca2+ dependent proteases and protein kinase C. *Journal of Cellular Biochemistry,* **81,** pp583-593.

Hu, W. and Kavanagh, J.J. (2003) Anticancer therapy targeting the apoptotic pathway. *The Lancet Oncology,* **4,** pp721-729

Huard, B., Schneider, P, Mauri, D., Tschopp, J. and French, L.E. (2001). T cell costimulation by the TNF ligand BAFF. *The Journal of Immunology,* **167,** pp6225-6231.

Iordanov, M.S, Ryabinina, O.P., Wong, J., Dinh, T.H., Newton, D.L., Rybak, S.M. and Magun, B.E. (2000). Molecular determinants of apoptosis induced by the cytoxic ribonuclease onconase. *Cancer Research,* **60,** pp1983-1994.

Jain, R.K and Baxter, L.T. (1998) Mechanisms of heterogeneous distribution of monoclonal antibodies and other macromolecules in tumours: significance of elevated interstitial pressure. *Cancer Research* **48,** pp7022-7032

Jazirehi. A.R., Gan, X., de Vos, S., Emmanouilides, C. and Bonavida, B. (2003). Rituximab (anti-CD20) selectively modifies Bcl-XL and apoptosis protease activating factor expression and sensitises human non Hodgkin's lymphoma B cell lines to paclitaxel induced apoptosis. *Molecular Cancer Therapeutics,* **2,** pp1183-1193.

Jimenez, A. and Vazquez, D. (1985). Plant and fungal proteins and glycoprotein toxins inhibiting eukaryote proteins synthesis. *Annual Review of Microbiology,* **39,** pp649-72.

Jo, M., Kim, T.H and Seol, D.W. Apoptosis induced in normal human hepatocytes by tumour necrosis factor relating apoptosis inducing ligand. *Nature Medicine*, **6,** pp564-567.

Junnikkala, S., Harjunpaa, A. and Meri, S (2003). Establishment of a CD59 deficient follicular lymphoma cell line: a tool for a studying the role of complement in rituximab mediated killing of lymphoma cells. *Molecular Immunology,* **40,** pp218-219.

Kanzaki. M., Shibata, H., Mogami, H. and Kojima, I. (1995). Expression of calcium-permeable cation channel CD20 accelerates progression through the G1 phase in Balb/c 3T3 cells. *Journal of Biological Chemistry,* **270,** pp13099-13104.

Karin, M. and Ben-Neriah, Y. (2000). Phosphorylation meets ubiquitination: The control of NF-κB activity. *Annual Review of Immuology,* **18,** pp621-663.

Kennedy, A.D. and Solga, M.D., Schuman, T.H., Chi, A.W., Lindorfer, M.A., Sutherland, W.M., Foley, P.L. and Taylor, R.P. (2003). An anti C3bi mAb enhances complement activation C3bi deposition and killing of CD20 cells by rituximab. *Blood,* **101,** pp1071-1079.

Keppler-Hafkemeyer, A., Kreitman, R.J. and Pastan, I. (2000). Apoptosis induced by immunotoxins used in the treatment of hematologic malignancies. *International Journal of Cancer,* **87,** pp86-94.

Keppler-Hafkemeyer, A., Brinkmann, U. and Pastan, I. (1998). Role of caspases in immunotoxin-induced apoptosis of cancer cells. *Biochemistry*, **37,** pp16934-16942.

King, M.A. (2000). Detection of dead cells and measurement of cell killing by flow cytometry. *Journal of Immunological Methods,* **243,** pp155-166.

Kinloch, R.A., Treherne, J.M., Furness, L.M., Hajimohamadreza, I. (1999). The Pharmacology of Apoptosis. *Trends in Pharmacolgical Sciences,* **20,** pp35-42.

Kitada, S., Pederson, I.M., Schimmer, A.D. and Reed, J.C. (2002). Dysregulation of apoptosis genes in hematological malignancy. *Oncogene,* **21,** pp3459-3474.

Kochi, S.K. and Collier, R.J. (1993). DNA fragmentation and cytolysis in U937 cells treated with Diphtheria toxin or other inhibitors of protein synthesis. *Experimental Cell Research,* **208,** pp296-302.

van der Kolk, L.E., Evers, L.M., Omene, C., Lens, S.M.A., Lederman, S., van Lier, R.A.W., van Oers, M.H.J. and Eldering E. (2002). CD20 induced B cell death can bypass mitochondria and caspase activation. *Leukemia,* **16,** pp1735-1744.

Kreitman, R.J. and Pastan, I. (1998). Accumulation of recombinant immunotoxin in a tumor in vivo: fewer than 1000 molecules per cells are sufficient for complete responses. *Cancer Research,* **58,** pp968-975.

Kreitman, R.J., (1999). Immunotoxins in cancer therapy. *Current Opinion in Immunology,* **11,** pp570-578.

Linenberger, M.L., Malony, D.G. and Bernstein, I.D. (2002). Antibody directed therapies for hematological malignancies. *Trends in Molecular Medicine,* **8,** pp69-76.

Lord, J.M and Roberts, L.M. (1998). Toxin entry: Reterograde transport through the secretory pathway. *The Journal of Cell Biology,* **140,** pp733-736.

Los, M., Burek, C.J and Stroh, C. (2003) Anti cancer drugs of tomorrow: apoptotic pathways as targets for drug design. *Drug discovery today,* **8,** pp67-77.

Lutter, M., Fang, M., Luo, X., Nishijima, M., Xie, X. and Wang, X. (2000). Cardiolipin provides specificity for targeting of tBid to mitochondria, *Nature Cell Biology,* **2,** pp754-762

Mack, A., Furmann, C. and Hacker, G. (2000). Detection of caspase activation in intact lymphoid cells using standard caspase substrates and inhibitors. *Immunological Methods,* **241,** pp19-31.

Magni, M., Di Nicola, M., Devizzi, L., Matteucci, P., Lombardi, F., Gandola, L., Ravagnani, F., Giardini, R., Dastoli, G., Tarela, C., Pileri, A., Bonadonna, G. and Gianni, A.M. (2000). Successful in vivo purging of CD34 containg peripheral blood harvests. Evidence for a role of both chemotherapy and rituximab infusion. *Blood,* **96,** pp864-869.

Manches, O., Lui, G., Chaperot, L., Gressin, R., Molens, J.P., Jacob, M.C., Sotto, J.J., Leroux, D., Bensa, J.C., and Plumas, J. (2003). In vitro mechanisms of action of rituximab on primary non Hodgkin's lymphomas. *Blood,* **101,** pp949-954

di,Maro, A., Ferranti, P., Mastronicola, M., Polito, L., Bolognesi, A., Stirpe, F., Malorni, A. and Parente, A. (2001). Reliable sequence determination of ribosome inactivating proteins by combination electrospray mass spectrometry and Edman degradation. *Journal of Mass Spectrometry,* **36,** pp38-46.

Mateo, V., Brown, E.J., Biron, G., Rubio, M., Fischer, A., Le Deist, F. and Sarfati, M. (2002). Mechanisms of CD47 induced caspase independent cell death in normal and leukaemic cells. *Blood,* **100,** pp2882-2890.

Mathas. S., Rickers, A., Bommert, K., Dorken, B. and Mapara, M.Y. (2000). Anti CD20 and B cell receptor mediated apoptosis: Evidence for shared intracellular signaling pathways. *Cancer research,* **60,** pp7170-7176.

von Mehren, M., Adams, G.P. and Weiner, L.M. (2003) Monoclonal antibody therapy for cancer. *Annual Review of Medicine,* **54,** pp343-369

von Mehren, A., Adams, G.P and Weiner, L.M. (2003). Monoclonal antibody therapy for cancer. *Annual Review of Medicine,* **54,** pp343-369

McGrath, M., Rosenblum, M.G., Phillips, M.R. and Scheinberg, D.A. (2003). Immunotoxin resistance in multidrug resistant cells. *Cancer Research,* **63,** pp72-79.

Michel, R.B. and Mattes, M.J. (2002). Intracellular accumulation of the anti-CD20 antibody 1F5 in B lymphoma cells. *Clinical Cancer Research,* **8,** pp2701-2713.

Michels , J., O-Neill, J.W., Dallman, C.L., Mouzakiti, A., Haben, F., Brimmell, M., Zhang, K.Y.J., Craig, R.W., Marcusson, E.G., Johnson, P.W.M. & Packham, G.P. (2004). Mcl-1 is required for Akata B-lymphoma cell survival and is converted to a cell death molecule by efficient caspase mediated cleavage. *Oncogene. in press*

Mounier, N., Briere, J., Gisselbrecht, C., Emile, J., Lederlin, P., Sebban, C., Berger, F., Bosly, A., Morel, P., Tilly, H., Bouabdallah, R., Reyes, F., Gaulard, P. and Coiffer, B. (2003). Rituximab plus CHOP overcomes Bcl-2 associated resistance to chemotherapy in elderly patients with diffuse large cell lymphoma. *Blood,* **101,** pp4279-4284.

Muhlenbeck. K (2000). The TNF-related apoptosis inducing ligand receptors TRAIL R1 and TRAIL R2 have distinct cross linking requirements for initiation of apoptosis and are non redundant in JNK activation. *The Journal of Biological Chemistry,* **275,** pp32208-32213.

Myers, D.E., Jun, X., Waddick, K.G., Forsyth, C., Chelstrom, L.M., Gunther, R.L., Tumer, J. and Uckun, F.M. (1995) Membrane associated CD19-lyn complex is an endogenous p53 independent and Bcl-2 independent regulator of apoptosis in human B lineage lymphoma cells. *Proceedings of the National Academy of Sciences,* **92,** pp9575-9579

Nagy, Z.A., Hubbner, B., Lohning, C., Rauchenberger, R., Reiffert, S., Thomassen=Wolf, E., Zahn, S., Leyer, S., Schier, E.M., Zahradnik, A., Brunner, C., Lobenwein, K., Rattel, B., Stranglmaier, M., Hallek, M., Wing, M., Anderson, S., Dunn, M., Kretzschmar, T. and Tesar, M. (2002). Fully human, HLA-DR specific monoclonal antibodies efficiently

induce programmed cell death of malignant lymphoid cells. *Nature Medicine,* **8**, pp801-807.

Narayanan, S., Surolia, A. and Karande, A.A. (2004). Ribosome inactivating proteins and apoptosis: Abrin causes cell death via mitochondrial pathway in Jurkat cells. *Biochemical Journal,* **377,** pp233-240.

Nauta, A.J., Daha, M.R., Tijsma, O., Water, B., Tedesco, F and Roos, A. (2002). The membrane attach complex of complement induces caspase activation and apoptosis. *European Journal of Immunology,* **32,** 783-792.

Ning, Z., Norton, J.D., Johnson, D. and Murphy, J.J. (1995). Early gene signalling dependent and independent induction of apoptosis in Ramos human B cells can be inherited by over expression of bcl-2. *Biochemical and Biophysical Research Communications,* **215,** pp23-29.

Obrig. T.G., Culp, W.J, McKeehan, W.L. and Hardesty, B. (1971). The mechanism by which cycloheximide and related glutarimide antibiotics inhibit peptide synthesis on reticulocyte ribosome. *Journal of Biological Chemistry,* **246,** pp174-181.

O'Keefe, T.L., Williams, G.T., Davies, S.L. and Neuberger, M.S. (1998). Mice carrying a CD20 gene disruption. *Immunogenetics,* **48,** pp125-132.

Olmo, N., Turnay, J., de Buitrago, G.G., de Silanes, I.L., Gavilanes, J.G. and Lizarbe, M.A (2001). Cytotoxic mechanism of the ribotoxin α-sarcin. *European Journal of Biochemistry,* **268,** pp2113-2124.

Otero, D.C., Anzelon, A.N. and Rickert, R.C. (2003). CD19 function in early and late B-cell development. *Journal of Immunology,* **170,** pp73-83.

Pastan, I. (1997). Targeted therapy of cancer with recombinant immunotoxins. *Biochimica Biophysica Acta,* **1333**, C1-6.

Pedersen. I.M., Buhl, A.M., Klausen, P., Geisler, C.H. and Jurlander, J. (2002). The chimeric anti-CD20 antibody rituximab induces apoptosis in B cell CLL through a p38 mitogen activated protein kinase dependent mechansim. *Blood,* **99,** pp1314-1319.

Pennell, C.A. and Erickson, H.A. (2002). Designing Immunotoxins for Cancer Therapy. *Immunologic Research,* **25,** pp177-191.

Petrie, R.J. and Deans, J.P. (2002). Colocalization of the B cell receptor and Cd20 followed by activation dependent dissociation in distinct lipid rafts. *The Journal of Immunology,* **169,** pp2886-2891.

Pierce, S.K. (2002). Lipid rafts and B cell activation. *Nature Reviews Immunology,* **2,** pp96-105.

Piro, L.D., White, C.A., Grillo-Lopez, A.J., Janakiraman, N., Saven, A., Beck, T.M., Varns, C., Shuey, S., Czuczman, M., Lynch, J.W., Kolitz, J.E. and Jain, V. (1999). Extended Rituximab (anti Cd20 monoclonal antibody) therapy for relapsed or refractory low-grade or follicular NHL. *Annals of Oncology,* **10,** 655-661.

Polunovsky, V.A.W., C.H. Ingbar, D.H. Peterson, M.S. and Bitterman, P.B. (1994). Induction of endothelial cell apoptosis by TNF-alpha: Modulation by inhibitors of protein synthesis. *Experimental Cell Research,* **49,** pp584-594.

Polyak, M.J. and Deans, J.P. (2002). Alanine and proline are critical determinants for extracellular CD20 epitopes; heterogeneity in the fine specificity of CD20 monoclonal antibodies is defined by additional requirements imposed by both amino acid sequence and quaternary structure. *Blood,* **99,** pp3256-3262.

Reed, J.C. (1997) Double identity for proteins of the Bcl-2 family. *Nature,* **387,** pp773-776

Reed, J.C (1999). Bcl-2 family proteins. In *Apoptosis and Cancer chemotherapy*, editors Hickman and Dive, chapter 7. Humana press,

Rehwald, U., Schulz, H., Reiser, M., Sieber, M., Staak, J.O., Morschhuser, F., Driessen, C., Rudiger, T., Muller-Hermelink, K., Diehl, V. and Engert, A. (2003). Treatment of relapsed CD20 Hodgkin lymphoma with the monoclonal antibody rituximab is effective and well tolerated: results of a phase 2 trial of the German Hodgkin lymphoma study group. *Blood,* **101,** pp420-424.

Reiser, M. and Diehl, V. (2002). Current Treatment of follicular non Hodgkin's lymphoma. *European Journal of Cancer,* **38,** pp1167-1172.

Rigley, K. and Callard, R. (1991). Inhibition of B-cell proliferation with anti-CD19 monoclonal antibodies: Anti-CD19 antibodies do not interfere with early signalling events triggered by anti-IgM or interleukin-4. *European Journal of Immunology,* **21,** pp535-540.

Roche (2000). Rituximab product monograph.

Roncuzzi, L. and Gasperi-Campani, A. (1996). DNA nuclease activity of the single chain ribosome inactivating proteins dianthin 30, saporin 6, and gelonin. *FEBS letters*, **392,** pp16-20.

Rose, A.L., Smith, B.E. and Malony D.G. (2002). Glucocorticoids and rituximab in vitro: synergistic antiproliferative and apoptotic effects. *Blood,* **100,** pp1765-1773.

Rosenblum. M., Cheung, L.H., Liu, Y. and Marks, J.W III (2003). Design, expression, purification and characterisation in vitro and in vivo of an anti melanoma single chain fv antibody fused to the toxin gelonin. *Cancer Research,* **63,** pp3995-4002.

Salvatore, G., Beers, R., Margulies, I., Kreitman, R.J. and Pastan, I. (2002). Improved cytotoxic activity towards cell lines and fresh leukemia cells of a mutant antiCd22 IT obtained by antibody phage display. *Clinical Cancer Research,* **8,** pp995 1002.

Sanchez-Beato, M., Sanchez Aguilera, A. and Piris, M.A. (2003). Cell cycle regulation in B-cell lymphoma. *Blood,* **101,** pp1220-1235.

Sandvig, K. and van Deurs, B. (2002). Membrane traffic exploited by protein toxins. *Annual Review of Cell and Developmental Biology,* **18,** pp1-24.

Sandvig, K. and van Deurs, B. (2002). Transport of protein toxins into cells: pathways used by ricin, cholera toxin and Shiga toxin. *FEBS letters,* **529,** pp49-53.

Santanche, S., Bellelli, A. and Brunori, M. (1997). The unusual stability of saporin. *Biochemical Biophysical Research Communications,* **234,** pp129-132.

Sartorius, U., Schmitz and Krammer, P.H. (2001). Molecular mechanisms of death receptor mediated apoptosis. *Chemistry and Biochemistry,* **2,** pp20-29.

Sato, S., Steeber, D.A. and Tedder, T.F. (1995). The CD19 signal transduction molecule is a response regulator of B-lymphocyte differentiation. *Proceedings of the National Academy of Sciences,* **92,** pp11558-11562.

Sato, S., Miller, A.S., Howard, M.C. and Tedder, T.F. (1997). Regulation of B lymphocyte development and activation by the CD19/CD21/CD81/Leu13 complex requires the cytoplasmic domain of CD19. The *Journal of Immunology,* **159,** pp3278-3287.

Savino, C., Federici, L., Ippoliti, R., Lendaro, E. and Tsernoglou, D. (2000). The crystal structure of saporin SO6 from *Saponaria officinalis* and it's interation with the ribosome. *FEBS letters,* **470,** pp239-243.

Scaffidi, C., Kirchhoff, S., Krammer, P.H. and Peter, M.E. (1999). Apoptosis signaling in lymphocytes. *Current opinion immunology,* **11,** pp277-285.

Schattner, E.J. Mascarenhas, J., Reyman, I., Koshy, M., Woo, C., Friedman, S.M. and Crow, M.K. (1998). Chronic lymphocytic leukaemia B cells can express CD40 ligand and demonstrate T-cell type costimulatory capacity. *Blood,* **91,** pp2689-2697.

von Schilling, C. (2003). Immunotherapy with antiCD20 compounds. *Seminars in Cancer Biology,* **13,** pp211-222.

Semac. I., Palomba, C., Kulangara, K., Klages, N., van Echten-Ceckert, G., Borisch, B. and Hoessli D.C. (2003). Anti-CD20 therapeutic antibody rituximab modifies the functional organisation of raft microdomains of B lymphoma cells. *Cancer Research,* **63,** pp534-540.

Shan. D., Gopal, A.K., Press, O.W. (2001). Synergistic effects of fenretinide and anti-CD20 antibodies on apoptosisinduction of malignant B-cells. *Clinical Cancer Research,* **7,** pp2490-2495.

Shan, D., Ledbetter, J.A. and Press, O.W. (1998). Apoptosis of malignant human B-cells by ligation of CD20 with monoclonal antibodies. *Blood,* **91,** pp1644-52.

Shan, D., Ledbetter, J.A. and Press, O.W. (2000). Signaling events involved in anti-CD20-induced apoptosis of malignant human B cells. *Cancer Immunology and Immunotherapy,* **48,** pp673-83.

Sieber, T., Schoeler, D., Ringel, F., Pascu, M. and Schriever, F. (2003). Selective internalisation of monclonal antibodies by B cell chronic lymphocytic leukaemia cells. *British Journal of Haematology,* **121,** pp485-461.

Simpson, J.C., Roberts, L.M., Romisch, K., Davey, J., Wolf, D.H. and Lord, J.M. (1999). Ricin A chain utilises the endoplasmic reticulum-associated protein degradation pathway to enter the cytosol of yeast. *FEBS letters,* **459,** pp80-84.

Smallshaw. J.E., Ghetie, V., Rizo, J., Fulmer, J.R., Trahan, L.L., Ghetie, M.A. and Vitettta, E.S. (2003). Genetic engineering of an immunotoxin to eliminate pulmonary vascular leak in mice. *Nature Biotechnology,* **21,** pp387-391.

Stepczynska, S., Lauder, K., Engels, I.H., Janssen, O., Kabelitz, D., Wesselborg, S and Schulze-Osthoff, K. (2001). Staurosporin and conventional anticancer drugs induce overlapping, yet distinct pathways of apoptosis and caspase activation. *Oncogene,* **20,** pp1193-1202.

Stockmeyer, B., Dechant, M., van Egmond, M., Tutt, A.L., Sundarapandiyan, K., Graziano, R.F., Repp, R., Kalden, J.R., Gramatzki, M., Glennie, M.J. van de Winkel, J.G.J. and Valerius, T. (2000). Triggering FCα-Receptor 1 (CD89) Recruits neutrophils as

effector cells for CD20 directed antibody therapy. *Journal of Immunology,* **165,** pp5954-5961.

Tallman, M.S. (2002). Monoclonal Antibody Therapy in Leukemias. *Seminars in Hematology,* **39,** pp12-19.

Tang, D.T., Lahti, J.M., Grenet, J. and Kidd, V.J. (1999). Cycloheximide induced T cell death is mediated by a Fas assoicated death domain dependent mechanism. *The Journal of Biological Chemistry,* **274,** pp7245-7252.

Tazzari, P.L., Polito, L., Bolognesi, A., Pistillo, M.P., Capanni, P., Palmisano, G.L., Lemoli, R.M., Curti, A., Biancone, L., Camussi, G., Conte, R., Ferrara, G.B. and Stripe, F. (2001). Immunotoxins containing recombinant anti CTLA 4 single chain fragment variable antibodies and saporin: In vitro results and in vivo effects in an acute rejection model. *Journal of Immunology,* **167,** pp4222-4229.

Tedder, T.F. and Engel, P. (1994). CD20: A regualator of cell cycle progression of B lymphocytes. *Immunology today,* **15,** pp450-454.

Tedder, T.F., Haas, K.M. and Poe, J.C. (2002). CD19-CD21 complex regulates an intrinsic src family kinase amplification loop that links innate immunity with B lymphocyte intracellular calcium response. *Biochemical Society Transactions,* **30,** pp807-810.

Thrush., G.R., Lark, L.R., Clinchy, B.C., Vitetta, E.S. (1996). Immunotoxins an update. *Annual Review of Immunology,* **14,** pp49-71.

Tsujimoto, Y. (2003) Cell death regulation by the Bcl-2 protein family in mitochondria *Journal of Cellular Physiology,* **195,** pp158-167

Vermes, I., Haanen, C. and Reutelingsperger, C. (2000). Flow cytometry of apoptotic cell death. *Journal of Immunological Methods,* **243,** pp167-190.

Vilpo, J.A., Koski, T., and Vilpo, L.M. (2000). selective toxicity of vincristine against chronic lymphocytic cells in vitro. *European Journal of Haematology,* **65,** pp370-378.

Voso, M.T., Pantel, G., Rutella, S., Weis, M., D'Alo, F., Urbano, R., Leone, G., Haas, R., and Hohaus, S. (2002). Rituximab reduces the number of peripheral blood b-cells in vitro mainly by effector cell mediated mechanisms. *Haematologica,* **87,** pp918-925.

Wang, S. and El Deiry, S. (2003). TRAIL and apoptosis induction by TNF-family death receptors. *Oncogene,* **22,** pp8628-8633

Waring , P. (1990). DNA fragmentation induced in macrophages by gliotoxin does not require protein synthesis and is preceded by raised inositol triphosphate levels. *Journal of Biological Chemistry,* **265,** pp14476-14480.

Weinmann, P., Bommert, K., Mapara, M.Y., Dorken, B. and Bargou, R.C. (1997). Over expression of the death-promoting gene Bax-alpha sensitizes human BL-41 Burkitt

lymphoma cells for surface IgM mediated apoptosis. *European journal of Immunology,* **9,** pp2466-2468.

Weng, W.K., and Levy, R. (2001). Rituximab induced annexin V staining of tumour cells does not predict clinical outcome following rituximab treatment. *Blood,* **96,** abstract 1430.

Wesche, J., Rapak, A. and Olsnes, S. (1999). Dependence of ricin toxicity on translocation of the toxin A-chion from the endoplasmic reticulum to the cytosol. *Journal of Biological Chemistry,* **274,** pp34443-34449.

White, C.A., Weaver, R.L. and Grillo-Lopez, A.J. (2001). Antibody targeted immunotherapy for treatment of malignancy. *Annual Review of Medicine,* **52,** pp125-145.

Wieder, T., Essmann, F., Prokop, A., Schmelz, K., Schulze-Osthoff, K., Beyaert, R., Dorken, B. and Daniel, P.T. (2001). Activation of caspase-8 in drug induced apoptosis of B lyphoid cells is independent of CD95/FAS receptor interaction and occurs downstream of caspase -3. *Blood,* **97**, pp1378-1387.

Wyllie, A.H. Morris, R.G. Smith, A.L. and Dunlop, D. (1984). Chromatin cleavage in apoptosis: Association with condensed chromatin morphology and dependence on macromolecular synthesis. *Journal of Pathology,* **142,** pp67-77.

Yamaizumi, M., Mekada, E., Uchida, T. and Okada, Y. (1978). One molecule of Diphtheria toxin fragment A introduced in to a cell can kill the cell. *Cell,* **15,** pp245-250.

Yazawa, N., Fujimoto, M., Sato, S., Miyake, K., Asano, N., Nagai, Y., Takeuchi, O., Takeda. K., Okochi, H., Akira, S., Tedder, T.F. and Tamaki, K. (2003). CD19 regulates innate immunity by the toll like receptor RP105 signaling in B lymphocyes. *Blood,* **102,** pp1374-1380.

Zimmermann. K.C., Bonzon, C. and Green, D.R. (2001). The machinery of programmed cell death. *Pharmacology and Therapeutics,* **92,** pp57-70.